Year : 2023

Understanding HIV permissiveness landscape at population and single-cell level

Brandt Ludivine

Brandt Ludivine, 2023, Understanding HIV permissiveness landscape at population and single-cell level

Originally published at : Thesis, University of Lausanne

Posted at the University of Lausanne Open Archive http://serval.unil.ch
Document URN : urn:nbn:ch:serval-BIB_63C2B1767F687

UNIL | Université de Lausanne
Faculté de biologie
et de médecine

Institut de Microbiologie, Centre Hospitalier Universitaire Vaudois

Understanding HIV permissiveness landscape at population and single-cell level

Thèse de doctorat ès sciences de la vie (PhD)

présentée à la

Faculté de biologie et de médecine
de l'Université de Lausanne

par

Ludivine BRANDT

Master de l'Université de Lausanne

Jury

Prof. Olaia Naveiras, Présidente
Prof. Angela Ciuffi, Directrice de thèse
DrSc. Jérôme Gouttenoire, MER1-PD, Expert
Prof. Matthieu Perreau, Expert
Prof. David Gfeller, Expert
Prof. Carine Van Lint, Experte

Lausanne
2023

UNIL | Université de Lausanne
Faculté de biologie
et de médecine

Institut de Microbiologie, Centre Hospitalier Universitaire Vaudois

Understanding HIV permissiveness landscape at population and single-cell level

Thèse de doctorat ès sciences de la vie (PhD)

présentée à la

Faculté de biologie et de médecine
de l'Université de Lausanne

par

Ludivine BRANDT

Master de l'Université de Lausanne

Jury

Prof. Olaia Naveiras, Présidente
Prof. Angela Ciuffi, Directrice de thèse
DrSc. Jérôme Gouttenoire, MER1-PD, Expert
Prof. Matthieu Perreau, Expert
Prof. David Gfeller, Expert
Prof. Carine Van Lint, Experte

Lausanne
2023

UNIL | Université de Lausanne
Faculté de biologie
et de médecine

Ecole Doctorale
Doctorat ès sciences de la vie

Imprimatur

Vu le rapport présenté par le jury d'examen, composé de

Président·e	Madame	Prof.	Olaia	**Naveiras**
Directeur·trice de thèse	Madame	Prof.	Angela	**Ciuffi**
Expert·e·s	Monsieur	Dr	Jérôme	**Gouttenoire**
	Monsieur	Prof.	Matthieu	**Perreau**
	Monsieur	Prof.	David	**Gfeller**
	Madame	Prof.	Carine	**Van Lint**

le Conseil de Faculté autorise l'impression de la thèse de

Ludivine Marie Salomé Brandt

Maîtrise universitaire ès Sciences en sciences moléculaires du vivant, Université de Lausanne

intitulée

Understanding HIV permissiveness landscape at population and single-cell level

Lausanne, le 3 novembre 2023

pour le Doyen
de la Faculté de biologie et de médecine

Olaia Naveiras

Prof. Olaia Naveiras

Acknowledgements

First, I would like to thank Prof. Angela Ciuffi for accepting me as a PhD student. I truly appreciated her patience throughout the 4 years I worked under her supervision, as well as her almost constant good mood and enthusiasm. I am especially thankful for everything I learned under her guidance, like strong scientific rigor and great communication skills.

I thank my thesis committee for their availability and their insightful comments.

I am grateful to Sara and Raquel for their precious help and advice in the lab. In particular, I thank Sara for always being available whenever I needed a second opinion, and Raquel for her attention to details and for showing me what a meticulous organization is.

I also thank all of the collaborators that helped in the project, especially Paolo for taking care of the bioinformatic analyses and in particular for his swiftness and patience in the last couple of months to set up the final data.

A big thank to all the 4th floor team for the time spent and activities done together, like in the beer science or the factory visit of our favorite food. Also, for the incredible efficiency in the writing of a highly scientific paper (aka the birthday card)!

A special mention to Beril, Maliki and Noémie without whom this thesis would not have been the same, especially in the last months: their support and friendship was priceless! I will miss our philosophical discussions around a coffee or a glass of wine.

I would also like to thank my parents and my sister Lorraine that were always caring and supporting me.

Last but not least, a special thanks to Xavier for his support during weird experimental schedules and for happily enduring the reading of the following hundred pages. Most importantly, for always believing in this adventure, sometimes even more than I did and for reminding it to me whenever I needed it.

Abstract

The large CD4+ T cell diversity is a major determinant of HIV infection success. On top of that, individual sex and age shape the immune response as well as the immune cell type distribution. Importantly, *ex vivo* experiments showed that sex affected HIV replication in people living with HIV (PWH), with viral transcription being reduced in women. Although novel technologies enabling to explore cellular heterogeneity at the single-cell level allowed for further comprehensive understanding of HIV biology, precise view of cellular features needed in a permissive cell is still lacking. To this aim, we analyzed this permissiveness spectrum from individual and cellular angle.

We investigated sex- and age-based differences in permissiveness and identified molecular determinants associated with cell activation potency. For this, we stimulated primary CD4+ T cells from 20 HIV-negative blood donors over a total period of 6 days and infected them every 24h with HIV-based vectors pseudotyped with VSV-G or native HIV envelopes. Infection levels were assessed by flow cytometry and identified an increased susceptibility to HIV between 24 and 72h post-stimulation. Sex- and age-based analyses at these time points showed an increased susceptibility to HIV in males and in donors aged 50 years or more. Parallel assessment of surface marker expression revealed expression in increased cell numbers of activation markers and immune check point inhibitors in donor cells displaying increased permissiveness to HIV, as well as a positive correlation between marker expression and infection kinetics. Transcriptomic analyses further highlighted genes involved in activation and cell cycle in male and older donor cells, consistent with a role for cell stimulation in these differences.

In the second approach, we took advantage of single-cell RNA-Seq to investigate evolution of CD4+ T cell subtype distribution upon activation and compare it with HIV susceptibility assessed by flow cytometry. Our data suggest that most cells were permissive in early activation, when the frequency of activated/proliferating cells was the lowest. Assessment of HIV RNA expression allowed to identify infected cells: in early activation time, all proliferating cells were HIV+ while naïve, central memory and regulatory T cells were heterogeneously infected. Projection of their transcriptomic signature on HIV non-exposed cells enabled the identification of a signature of 53 genes, that are downregulated in permissive cells and highly expressed in non-permissive cells, consistent with a role in antiviral response, innate immunity and response to IFN-γ.

Altogether, this work shows that addressing cellular and individual-linked heterogeneity allows refining our understanding of HIV biology. Identification of features characterizing permissive cells linked to cellular activation may help uncover novel players involved in viral latency and their association with reactivation potency, and hopefully ultimately leading to specific reservoir eradication strategies.

Résumé

L'importante diversité des cellules T CD4+ a été démontrée comme étant un facteur majeur du succès d'infection du VIH. De plus, le sexe et l'âge d'un individu influent sur la distribution des cellules immunitaires et la réponse engendrée. Notamment, le sexe a été montré comme impactant la réplication du VIH chez les personnes vivant avec le VIH dans des expériences *ex vivo*, avec une transcription virale réduite chez les femmes. Bien que de nouvelles technologies aient permis d'explorer l'hétérogénéité cellulaire sur des cellules uniques, nous rapprochant ainsi d'une compréhension globale de la biologie du VIH, une image complète et précise des caractéristiques cellulaires nécessaires à la cellule permissive manque toujours. Pour cela, nous avons analysé le spectre de permissivité du point de vue de l'individu et de la cellule.

Nous avons étudié les différences de permissivité au VIH basées sur le sexe et l'âge et exploré le lien avec la capacité d'activation cellulaire. Pour cela, chaque 24h pendant six jours, nous avons infecté des cellules T CD4+ provenant de donneurs négatifs au VIH, en utilisant des vecteurs viraux basés sur le VIH, pseudotypés avec une enveloppe VSV-G ou native du VIH, et avons mesuré le niveau d'infection par cytométrie de flux. Nous avons pu observer que les cellules étaient les plus permissives entre 24 et 72h après stimulation et que celles provenant d'hommes et d'individus âgés de 50 ans ou plus montraient une susceptibilité au VIH supérieure durant cette fenêtre temporelle. En parallèle, la mesure de marqueurs de surface a montré une plus grande expression de marqueurs d'activation et d'épuisement dans les cellules de donneurs les plus permissives, ainsi qu'une corrélation entre les cinétiques d'expression et d'infection. Des analyses transcriptomiques ont souligné le rôle de l'activation dans ces différences, du fait de l'enrichissement de groupes de gènes liés à l'activation et au cycle cellulaire chez les catégories de donneurs les plus permissives.

Avec la deuxième approche, nous avons utilisé du séquençage d'ARN sur cellules uniques pour étudier l'évolution de la composition de cellules T CD4+ au cours de l'activation, que nous avons comparé à des données de susceptibilité au VIH obtenues par cytométrie de flux. Nous avons vu que la plupart des cellules étaient permissives au début de l'activation, au moment où la fréquence de cellules activées/proliférantes était la plus basse. En mesurant la production d'ARN du VIH au début de l'activation, toutes les cellules proliférantes comportaient le VIH alors que les naïves, mémoires centrale et régulatrices présentaient des niveaux d'infection hétérogènes. Projeter leur signature transcriptomique sur des cellules non-exposées au VIH a permis l'identification d'une signature de 53 gènes, peu exprimés dans les cellules permissives et plus fortement dans les cellules résistantes, qui sont impliqués dans la réponse antivirale, l'immunité innée et la réponse à l'IFN-γ.

En conclusion, ce travail montre qu'approcher l'hétérogénéité au niveau de la distribution de sous-types cellulaires liée à l'individu permet d'affiner notre compréhension de la biologie du VIH. Identifier les caractéristiques des cellules permissives associées à l'activation pourrait permettre de révéler de nouveaux acteurs impliqués dans les mécanismes de latence ou de réactivation, et mener à terme à l'élimination ciblée du réservoir.

Table of contents

I. Introduction

A. HIV identification

In December 1981, the New England Journal of Medicine reported multiple cases of young men having sex with men (MSM) diagnosed with *Pneumocystis jirovecii* pneumonia or Kaposi sarcoma, which are diseases usually limited to immunocompromised individuals [1-5]. In 1982, the term acquired immunodeficiency syndrome (AIDS) was used for the first time as there was enough evidence to describe the new illness, characterized by impaired immunity and opportunistic infections without known cause [6]. At the same time, the multiplication of young MSM presenting marked CD4+ T cell depletion across the USA, in New York and in California, argued for an infectious etiology.

In 1983, Françoise Barré-Sinoussi from Luc Montagnier's lab at Pasteur Institute (Paris, FR) identified the presence of viral particles budding from infected lymphocytes from a young homosexual man presenting pre-AIDS symptoms [7]. The same study also evidenced reverse transcriptase in the lymph node biopsy, hinting at infection with a retrovirus. The lack of cross-reactivity with human T cell leukemia virus type 1 (HTLV-1, another human retrovirus) antiserum led to the hypothesis that AIDS was caused by a distinct retroviral agent, which was named lymphadenopathy-associated virus (LAV). In the same Science issue, Robert Gallo's team also reported the isolation of an HTLV-related virus from an AIDS individual that he called human T cell leukemia virus type 3 (HTLV-III) [8]. One year later, an independent study by Levy and colleagues at the California Department of Health Services (Berkeley, US-CA), outlined the presence of a virus that cross-reacted with LAV antiserum in 22 individuals diagnosed with AIDS, that was named AIDS-associated retrovirus (ARV) [9]. As LAV, HTLV-III and ARV were later recognized as being the same virus, the International Committee on Taxonomy of Viruses adopted in 1986 the name of human immunodeficiency virus (HIV) to refer to the AIDS etiological agent, as suggested by a consensus of scientists [10].

Since the start of the epidemic, and in absence of a sterilizing cure, HIV has infected 85.6 million people and 40.4 million people have died of AIDS-related illnesses [11].

B. HIV pathogenesis

HIV transmission occurs through body fluids, either horizontally via sexual contact or direct blood contamination via infected material, or vertically from mother-to-child. Sexual transmission route accounts for most HIV acquisitions, with heterosexual contact estimated to account for 70% of HIV cases worldwide despite its low efficiency. Indeed, in absence of antiretroviral therapy (ART), male-to-female and female-to-male transmission rates are estimated to be 0.08-0.38% and 0.04-0.3% per contact, respectively [12]. Homosexual contacts present higher rates of HIV acquisition with up to 1.43% for receptive anal intercourse and 0.62% for the insertive one [13]. Risk factors such as pre-existing coinfection, pro-inflammatory environment, hormone levels and microbiota composition can increase transmission likelihood, with male-to-female

transmission reaching up to 10% and insertive homosexual contact up to 33% [14]. HIV can also be acquired via direct exposure of bloodstream to contaminated material such as needles, syringes or other drug injection equipment, with a risk estimated to be around 0.63% [15]. Finally, HIV can be transmitted from a mother to her baby during pregnancy, at birth or by breastfeeding, with an estimated risk of 15-30% [16].

Mucosae are the main HIV transmission sites, as reproductive or gastrointestinal tracts are the main acquisition routes [17]. HIV directly reaches submucosa by disrupting tight junctions between epithelial cells and targets a subset of dendritic cells (DCs) specifically present in the epithelium of the skin and mucosa (Langerhans cells, LCs) (*Fig.1A*) [14, 18]. LCs can either (i) internalize virions via langerin, partially degrading them or (ii) undergo productive infection, through CD4- and CCR5-mediated entry [14, 18]. HIV is subsequently transmitted to DCs present at the submucosa, which migrate into lymphoid organs that are naturally enriched with CD4+ T cells and macrophages, where HIV is disseminated. HIV cell transmission occurs either via productive infection, as in vaginal DCs that can sustain HIV replication, or via recipient cell through virion attachment to C-type lectin surface receptors, such as monocyte-derived DCs that harbor a high antiviral cellular environment, which then bring it in close proximity from susceptible cells [14]. Of note, cell-associated transmission by virological synapses is a more efficient mechanism than cell free-virion.

The clinical course of HIV infection varies between individuals but typically starts with flu-like symptoms for up to three months after primary infection and is the result of viral replication and high viral load (*Fig. 1B*) [19]. The peak of viremia is associated with a first rapid decay in CD4+ T cell counts, as they are the main cell type supporting HIV replication. This stage corresponds to the acute phase of infection and is also the phase where HIV widely disseminates across the lymphoid organs. During the second stage of infection, the chronic phase, viremia is somehow stabilized to a viral load setpoint, while CD4+ T cell counts progressively decline. This phase lasts for up to ten years after primary infection and corresponds to clinical latency. AIDS occurs at the last stage of infection when CD4+ T cell counts are lower than 200 cells/µL, marking severe immunosuppression, resulting in increased viremia and infections by opportunistic pathogens, ultimately leading to death of the infected individual.

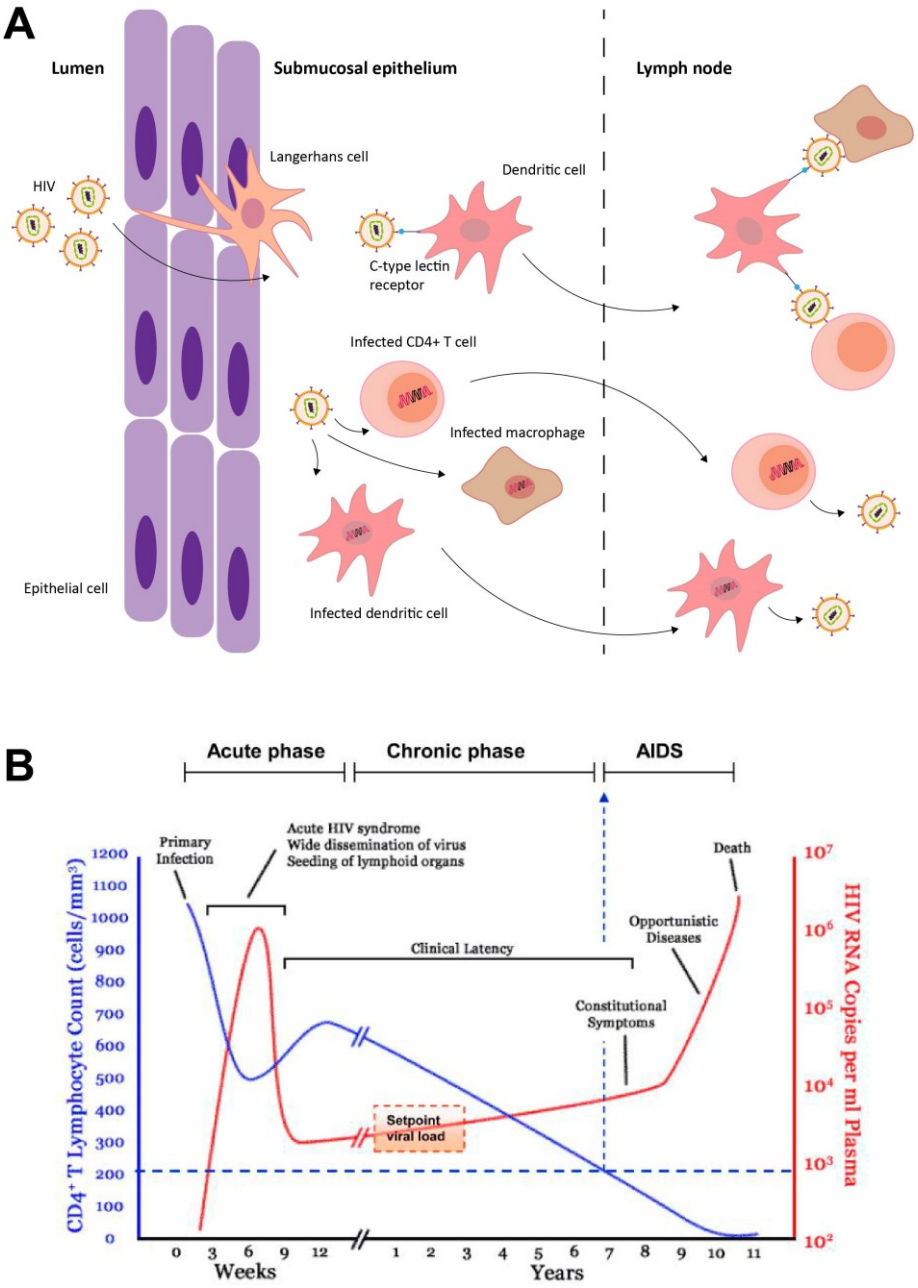

Figure 1: HIV infection. (A) HIV sexual transmission: HIV crosses the epithelial barrier of the mucosa to target LCs, DCs, CD4+ T cells or macrophages at the submucosal epithelium level, where it can establish a productive infection or bind C-type lectin receptor from DC. It further disseminates to the lymph nodes by DC carriage or migration of infected cells. Adapted from Wu and Kewalramani [20]. (B) HIV clinical progression: plasma HIV RNA levels (red) rapidly peak upon HIV acquisition, causing a first drop in CD4+ T cell counts (blue) during the acute phase, typically occurring in the first 9-12 weeks. In the chronic phase, the viremia is controlled to a stable level, corresponding to the setpoint viral load. This results in the progressive decline of CD4+ T cells. After 7-10 years on average, CD4+ T cell counts are < 200 cells/µL, triggering AIDS onset and leading to opportunistic pathogen infections, ultimately resulting in death of the individual. From An and Winkler [21]. LC, Langerhans cell; DC, dendritic cell; AIDS, acquired immunodeficiency syndrome.

C. HIV therapy and epidemiology

The first treatment for HIV infection, zidovudine (or AZT), was approved by the Food and Drug Administration (FDA) in 1987 and was directed against one of the three virus enzymes. It is a thymidine analog and functions as nucleoside reverse transcriptase inhibitor (NRTI) that blocks synthesis of proviral DNA by competitive inhibition and chain termination, therefore preventing DNA integration into the host genome and subsequent generation of novel viral particles. Since then, other NRTIs were approved, but none were able to stop HIV infection in the long term, resulting in viremia rebound and emergence of resistance mutations. In 1995, saquinavir, the first protease inhibitor (PI) entered the market [22]. This latter restricts cleavage of the viral polyprotein and therefore maturation into infectious viral particles. However, mutations conferring drug resistance emerged as well, indicating that monotherapies were ineffective. To overcome this issue, a higher selection pressure needed to be exerted by antivirals on HIV, hence the idea in 1997 of a combined antiretroviral therapy (cART, or now simply ART) targeting concomitantly both viral enzymes (reverse transcriptase and protease) with three antiviral inhibitors. The introduction of cART completely transformed the pandemic evolution, changing from an ultimately lethal condition to a chronic disease with survival of people with HIV (PWH) [22]. cART was originally composed of a combination of three antiviral drugs, such as two NRTIs and one PI. Today, there are additional classes of inhibitors that can be included in ART, with improved tolerability and allowing for personalized and adapted treatment. These include non-nucleoside reverse transcriptase inhibitors (NNRTIs), entry inhibitors (EIs) and integrase strand transfer inhibitors (INSTIs) [22].

However, despite its efficiency, ART does not provide a sterilizing cure and must thus be taken life-long to guarantee viral suppression (< 50 RNA copies/mL plasma). Indeed, if antiretroviral treatment is interrupted, viral rebound is observed, suggesting the persistence of HIV-infected cells in the body of PWH [23]. As of today, ART is still the gold standard treatment and current research efforts are being made to further reduce toxicity and develop long-acting drugs. For example, in 2021, Cabenuva, which consists of a combination of cabotegravir (INSTI) and rilpivirine (NNRTI), became the first FDA-approved intramuscular antiretroviral drug only requiring a monthly injection [24].

Forty years after its discovery, and in absence of a sterilizing cure, HIV is still an important public health concern, with 39 million people currently living with HIV and 1.3 million novel infections as of 2022 [11]. Moreover, 25% of infected people do not have access to ART and 15% are not even aware of their seropositive status. Although significant efforts have been undertaken in HIV prevention, detection and care, AIDS still accounted for 630,000 deaths in 2022. To end the pandemic by 2030, the United Nation adopted in 2021 the Global AIDS Strategy 2021-2026 [25]. The heart of the program is ending inequalities by enlarging equitable access to people-centered HIV services, diminishing societal barriers preventing HIV goals and providing more financial means towards response to HIV regarding health, social protection and human rights. In addition, the current strategy aims at achieving the 95-95-95 targets by 2025, *i.e.* 95% of

PWH being aware of seropositivity, 95% of PWH aware of their status being under ART and 95% of PWH under ART displaying suppressed viral loads [26].

Two types of HIV exist, HIV-1 (hereafter abbreviated HIV), which is responsible for the pandemic infection, and HIV-2 that accounts for one to two million PWH, mainly in West Africa [27]. Both types induce a similar disease, although HIV-2 results in slower progression and lower viral loads. HIV is divided into groups M, N, O and P, that are thought to result from independent zoonotic transmissions, with more than 90% cases caused by group M, which is itself composed of distinct subtypes A, B, C, D, F, G, H, J, K and L, whose prevalence differs worldwide [28, 29]. The highest genetic diversity is found in West Africa, where subtypes A, C and D are dominant. Subtype B predominates in Europe, North America and Australia, while subtype A is most prevalent in East Africa and Russia, and subtype C in Southern Africa and India.

D. HIV structure and life cycle

HIV is an enveloped virus of the genus *Lentivirinae* belonging to the *Retroviridae* family. It harbors two copies of single-stranded positive-sense RNA genome that are protected by a capsid. The 9.2 kb-long HIV genomic RNA organization consists of 9 sense open reading frames (ORFs) that code for 15 proteins (*Fig. 2*). Although less understood, the viral genome can also produce an antisense protein (ASP), generated from the 3' long terminal repeat (LTR) [30]. The three main ORFs code for structural proteins and enzymes that are essential to produce infectious particles and hence establish productive infection: group-specific antigens (*gag*), polymerase (*pol*) and envelope (*env*) [31]. Gag (Pr55) polyprotein is incorporated into the budding particle and cleaved by the viral protease into matrix (MA/p17), capsid (CA/p24), nucleocapsid (NC/p7) and p6, while Gag-Pol (Pr160) polyprotein also produces protease (PR), reverse transcriptase (RT) and integrase (IN) upon cleavage. Env (gp160) is cleaved by the cellular furin into surface glycoprotein (SU/gp120) and transmembrane protein (TM/gp41) before reaching the cell membrane. The remaining ORFs code for two regulatory proteins and four accessory ones. The regulatory proteins are trans-activator of transcription (Tat) and regulator of expression of virion proteins (Rev), which enhances viral transcription and promotes nuclear export of transcripts, respectively. The four accessory proteins, viral infectivity factor (Vif), virus protein U (Vpu), virus protein R (Vpr) and negative factor (Nef) increase virus infectivity and help escape host cellular immune response [32]. LTR present at both 5' and 3' ends of the viral genome are direct identical sequences that contain regulatory promoter regions, as well as sequences necessary for reverse transcription and subsequent integration of viral genome into the host chromosome [33]. Finally, the genome also contains a packaging signal (ψ) sequence which is a cis-acting RNA element interacting with NC to incorporate the viral RNA genome into newly formed virions [34].

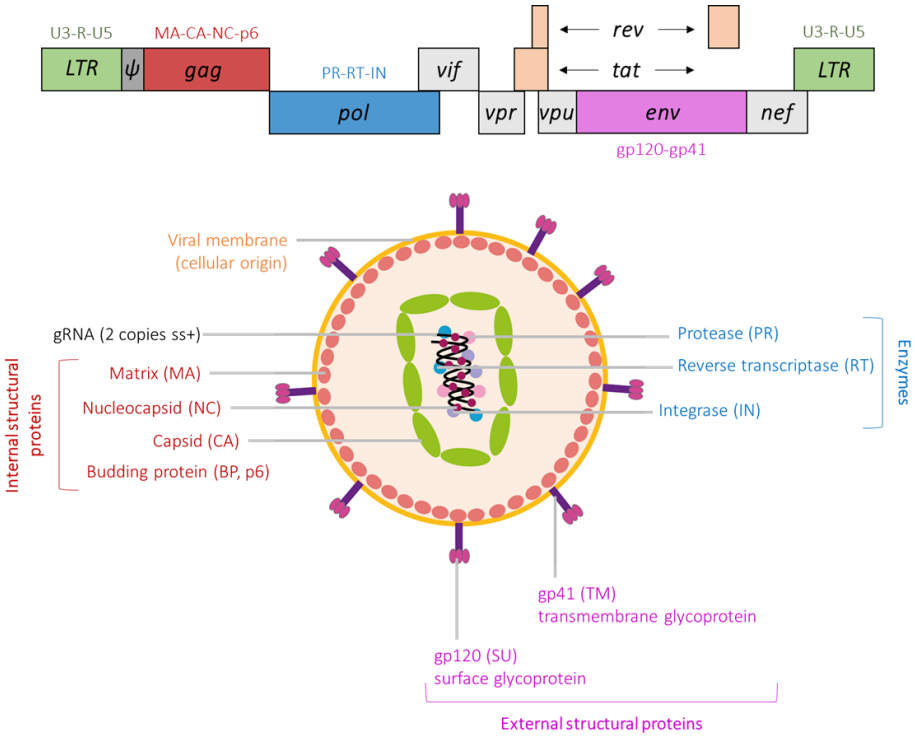

Figure 2: HIV genomic and structural composition. The proviral genome is composed of 9 sense ORFs (upper panel). *Gag*, *pol* and *env* code for essential proteins involved in HIV replication that are cleaved before or after virion incorporation (lower panel): *gag* for MA, CA, NC and p6; *pol* for PR, RT and IN; and *env* for gp120 and gp41. *Tat* and *rev* code for regulatory proteins involved in transcription enhancement and export. *Vif, vpr, vpu* and *nef* code for accessory proteins that are not essential for viral replication but are involved in viral pathogenesis. The LTR sequences are subdivided into unique 3' (U3), repeated (R) and unique 5' (U5) regions, and contain transcription factor binding sites, transcription initiation site, enhancer and regulatory regions. Ψ sequence allows encapsidation of two viral RNA genome copies into nascent viral particles. ORF, open reading frame; MA, matrix; CA, capsid; NC, nucleocapsid; BP, budding protein; PR, protease; RT, reverse transcriptase; IN, integrase; LTR, long terminal repeat.

The presence of the cluster of differentiation 4 (CD4) receptor on CD4+ T cells, DCs and macrophages designates them as primary cellular targets for HIV infection. Binding of the docking glycoprotein (gp120) to CD4 initiates gp120 conformational change, enabling subsequent binding to a chemokine co-receptor, mainly CC chemokine receptor type 5 (CCR5) or CXC chemokine receptor type 4 (CXCR4). This latter triggers a second conformational change that allows gp41 exposure and ultimately the fusion of the viral envelope with cell membrane (*Fig. 3A*) [35].

Subsequently, the capsid is delivered into the cytoplasm of the host cell, where the genomic RNA starts to be reverse transcribed into dsDNA. Upon complete extension, the so-formed viral linear dsDNA (vDNA) is longer than the RNA genome: indeed, RNA has two distinct ends (U3-R in 3' and R-U5 in 5'), which are duplicated during reverse transcription to become U3-R-U5 at both ends of vDNA, forming the LTRs [36].The vDNA associates with viral and host proteins, including IN to compose pre-integration complex (PIC), which is followed by nuclear importation of the capsid to the nucleus through nuclear pore [37, 38]. There, the capsid disassembles and vDNA integrates into the host

genome [39]. This step is crucial for productive replication, *i.e.* enabling transcription and expression of all viral products.

Viral transcription occurs as a two-step process relying on a positive-feedback loop (*Fig. 3B*). HIV mRNAs are produced by alternative splicing and exist under three major forms: unspliced (US) transcripts which are ~9 kb long and consist of the viral genome as well as encoding *gag-pol* ORFs, incompletely or singly spliced (SS) transcripts which are ~4 kb long and contain, *env, vif, vpr* and *vpu* genes, and completely or multiply spliced MS transcripts which are ~1.8/2 kb long and contain *tat, rev* and *nef* genes. During the early phase, only the 1.8/2 kb MS variants can exit the nucleus, allowing the synthesis of Tat and Rev: Tat enhances HIV transcription by binding to transactivation-responsive region (TAR, located downstream of 5' LTR), and Rev promotes export to the cytoplasm of 4 and 9 kb transcripts by binding to Rev-responsive element (RRE). This biphasic process ensures that all viral proteins are synthesized during the late phase, and that the RNA genome is exported to the cytoplasm [40, 41].

Viral transcription and translation rely on host cell machineries. Viral protein assembly and RNA genome incorporation take place at the surface of the host cell, where viral particles bud and are released [42]. Maturation occurs through cleavage of polyprotein precursors by the viral protease, resulting in fully mature and infectious virions.

The complete replication cycle typically lasts 24 to 48h, with release of viral particles starting as early as 18h post-infection (p.-i.) [43].

As for all viruses, infection success relies on virus-host interactions. These will be essential for viral tropism determination, for cellular factors hijacked and exploited by the virus to promote its own replication, and for the capacity of the virus to overcome innate immune defense of the target cell. The following chapters will provide a few insights on these topics and a better understanding of cell permissiveness to HIV infection.

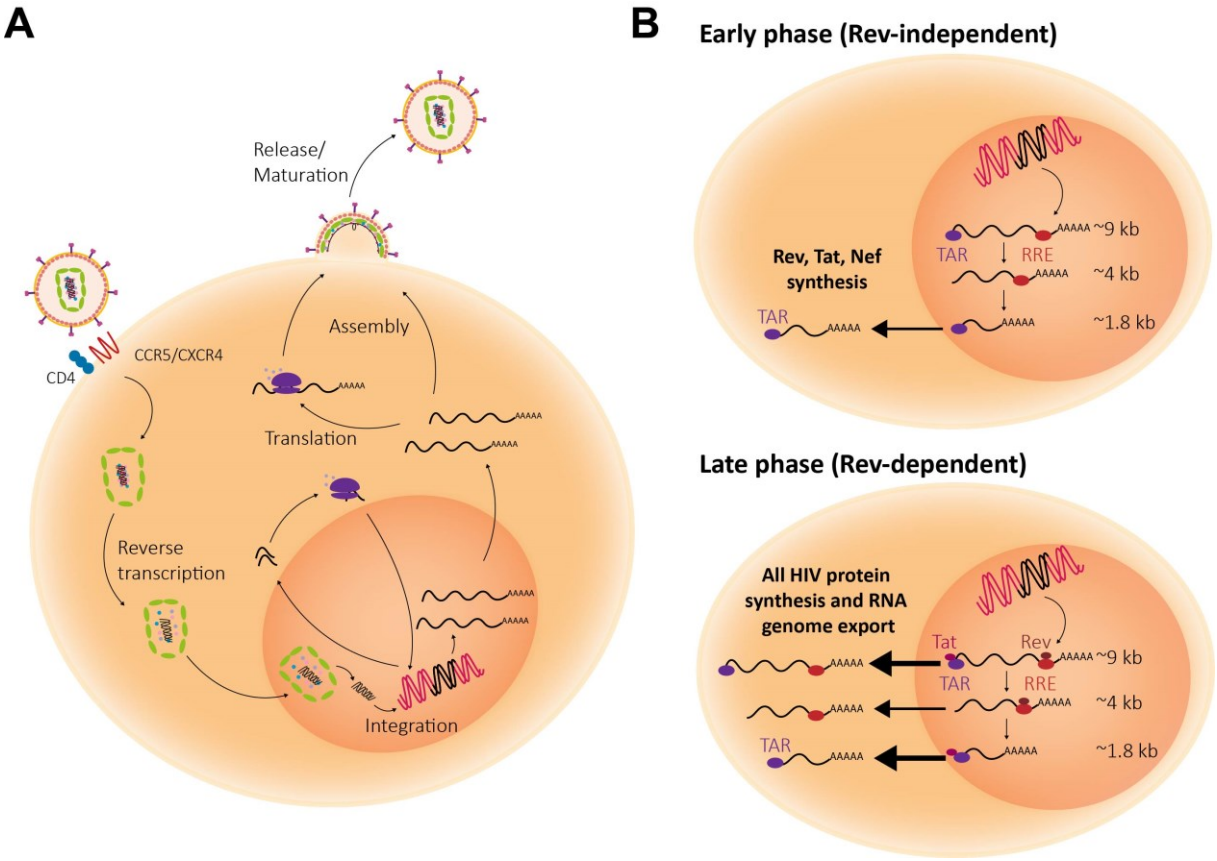

Figure 3: HIV life cycle. (A) Binding of HIV gp120 to CD4 and CCR5 or CXCR4 co-receptor allows fusion between viral and cellular membranes via consecutive conformational rearrangements of gp120 and gp41. This enables viral core entry into the cytoplasm. On its way to the nucleus, viral RNA undergoes reverse transcription into viral double-stranded DNA, which will be integrated into the host genome through the action of integrase. Host cell machinery is then exploited to produce viral mRNAs and proteins. Viral proteins and RNA genome assemble and bud at the cell membrane. Precursor Gag and Gag-Pol proteins are then processed by the protease during the maturation step in order to form infectious particles. (B) Viral transcript regulation occurs as a positive-feedback loop. HIV transcripts exist under three forms: US, (~9 kb), SS, (~4 kb) and MS, (~1.8/2 kb). Only the MS transcript can exit the nucleus during the early phase, which leads to Rev, Tat and Nef synthesis. Tat enhances transcription rate through TAR binding and Rev binding to RRE allows exit of the two other alternative splice forms during the late phase. At this stage, all HIV proteins can therefore be synthesized, and the US RNA genome can be exported to the cytoplasm. Adapted from Karn and Stoltzfus [40]. US, unspliced; SS, singly spliced; MS, multiply spliced; TAR, Trans-Activating Region; RRE, Rev-Responsive Element.

E. HIV tropism and envelope specificity

HIV entry mechanism is a dynamic process that evolves over the course of clinical progression. HIV entry is mediated by primary engagement of CD4 receptor that is expressed on T cells, monocytes, macrophages and DCs. At the protein level, the main determinant of HIV tropism is gp120, as it plays a critical role in receptor and co-receptor binding. It is composed of five conserved domains (C1-C5) and five variable loops (V1-V5). Gp120 attaches CD4 through CD4 binding site (CD4bs) domain, inducing V3 exposure through conformational change, which is essential in engaging co-receptor and is therefore a critical element in tropism determination [44]. Indeed, the sole modification of 1-3 critical residues of V3 results in a tropism switch, with mainly

substitution from glutamic acid to charged residues, such as lysine or arginine at position 25 [45, 46].

HIV entry also requires the presence of a chemokine co-receptor, generally CCR5 or CXCR4. They are expressed differentially regarding cell types: CCR5 can be found on memory CD4+ T cells, macrophages and DCs, while CXCR4 is expressed on both naïve and memory CD4+ T cells [47]. Before the discovery of the molecular mechanisms of entry, HIV tropism was historically categorized into macrophage tropism (M-tropic) and T cell tropism (T-tropic). It was later termed depending on co-receptor usage, R5- or X4-tropic, for CCR5 or CXCR4 use, respectively, which define the cell types in which the virus can enter (*Fig. 4*) [48]. Importantly, X4-tropic strains require increased density of CD4 receptors due to different stoichiometry compared to R5-tropic strains, making them less successful in infecting low CD4-expressing cells like macrophages and DCs [49]. HIV isolates typically use one or the other co-receptor, but some of them display affinity for both, and therefore are termed R5X4-tropic. Although CCR5 and CXCR4 are exploited by the majority of strains, alternative co-receptors can be used as well, such as CCR6 or CCR8 [50]. Despite the possible presence of multiple HIV variants, only one virion is transmitted during sexual intercourse, referred as transmitted founder (T/F). This founder virus has been shown to be R5-tropic [12, 51] and displays a selective advantage, as it is resistant to interferons (IFNs) and defensins secreted by epithelial cells [52]. Upon transmission, the first cells encountering the virus in genital mucosa are DCs and macrophages, which express both CD4 and CCR5. These cells play a crucial role in infection establishment by transmitting the virus to CD4+ T cells that are enriched in CCR5 in the mucosa [53, 54]. As the virus needs CD4 and CCR5 to establish the infection, individuals lacking CCR5 (*CCR5Δ32*) are resistant to HIV infection transmitted via sexual contact [55]. Selective advantage for R5-tropic strains has not only been shown for mucosal entry route, but also for parenteral one, which may be due to the presence of one gp120 epitope enabling neutralization of X4-tropic strains, that is absent from R5-tropic ones [56, 57].

During most of the chronic infection phase, R5-tropic viruses are dominant, but eventually, X4-tropic viruses prevail over R5-tropic ones in half of untreated patients [58]. It is worth noting that this co-receptor switch is subtype dependent: it has been typically observed in subtype B, but not in subtype A or C, that favor CCR5 all over infection [59]. Alternatively, subtype D generally uses CXCR4, or both CXCR4 and CCR5. Tropism switch is associated with disease progression and CD4+ T cell pool reduction due to increased cytopathic effects of X4-tropic strains [48, 60]. Indeed, X4-tropic strains were shown to exhibit specific mutations in Tat, Vpr and LTR, suggesting a coexerting selection pressure together with gp120, resulting in a faster replication rate and increased pathogenesis. Recently, this switch was demonstrated to be a consequence of immune activation, as it is linked to T cell differentiation and depletion [61].

In addition to entry mode, R5- and X4-tropic strains were shown differentially impact signaling cascades in post-fusion step: both induce expression of mitogen-activated protein kinase (MAPK) pathway that regulates growth, proliferation, and genes involved in initiation of TCR activation, but R5-tropic strains generates an enhanced upregulation, which may facilitate viral replication [62, 63]. Both strain types also present differences

in necessary post-entry environment, with R5-tropic viruses requiring uracil DNA glycosylase (UNG2) for reverse transcription, which is not the case of X4-tropic viruses [64]. UNG2 expression in primary T cells is low, and therefore might account for a lower T cell infection by R5- compared to X4-tropic viruses [65]. The differences in cellular environment requirements are further supported by the fact that specific cellular subtype enriched in CCR5 are restricting R5- but not X4-tropic virus infection [66].

Altogether, both expression of cellular receptors to HIV and cellular environment influence susceptibility to HIV depending on viral tropism, which can impact cellular activation signaling.

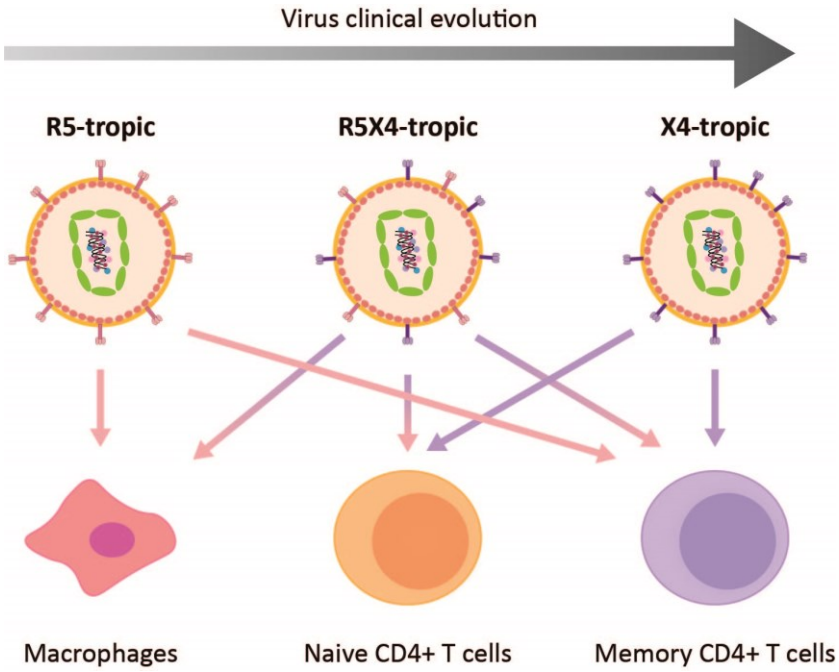

Figure 4: HIV tropism switch during clinical progression. R5-tropic viruses are dominant in early disease stage, as they infect CCR5+ cells, such as macrophages or memory CD4+ T cells, present in the mucosa. With disease progression and CCR5-target cell depletion, a tropism switch toward X4-tropic viruses, which are able to infect naïve and memory CD4+ T cells, can be observed. Typically, viruses displaying dual tropism can be found as the switch occurs. Adapted from Este and Telenti [67].

F. HIV restriction factors

Restriction factors represent the first line of defense against HIV infection and are usually induced upon IFN expression. Indeed, upon cell entry, HIV is recognized by a series of host proteins aiming at blocking infection by interfering with specific steps of viral life cycle (*Fig. 5*). Infection success will thus result from HIV ability to overcome these blocks. Typical examples include apolipoprotein B mRNA editing enzyme, catalytic subunit 3G (APOBEC3G), SAM domain and HD domain-containing protein 1 (SAMHD1), bone marrow stromal antigen 2 (BST-2/Tetherin) and tripartite motif-containing protein 5 (TRIM5α). Their discovery was initially attributed to their interaction with

viral accessory proteins that are able to counteract their restriction activity, often occurring through their degradation [68].

APOBEC3G is the most widely characterized HIV restriction factor. It is encapsidated into newly formed virions and blocks viral reverse transcription by deamination of cytidines to uridines, which consequently leads to hypermutation and premature stop of vDNA synthesis [69]. Vif binds APOBEC3G and antagonizes it by recruiting E3 ubiquitin ligase complex to target it to proteasome for degradation [70]. SAMHD1 impairs reverse transcription by hydrolyzing cellular dNTPs, making them unavailable for vDNA synthesis [71]. It can be counteracted by HIV-2 Vpx, that targets it to the proteasome. BST-2 prevents the release of newly formed virions by tethering budding particles to the cellular membrane [72]. HIV thwarts its action through Vpu accessory protein, that elicits proteasomal or lysosomal degradation. Last, TRIM proteins represent a large family displaying antiretroviral activity, among which TRIM5α being the strongest [68]. Its activity is exerted by binding viral capsid and accelerating disassembly, which undermines nuclear import of vDNA [73]. Of note, TRIM5α is poorly active against retrovirus hosted by the same species but is potent against retroviruses infecting other species. It is therefore an effective cellular defense mechanism, allowing prevention of cross-species transmission.

Within the last decade, novel cellular factors have been identified as displaying antiretroviral activity, broadening our understanding of the cellular arsenal against HIV, although the restriction mechanism and the counteracting viral protein involved remain to be identified for many of them. Interferon-induced transmembrane (IFITM) proteins and serine incorporator 3 and 5 (SERINC3/5) can be incorporated in newly formed viral particles and subsequently impair the fusion of the virion envelope with the host cell membrane [74, 75]. In addition, IFITM can also restrain viral protein translation by favoring translation of cellular mRNAs. It was shown that Nef overcomes both IFITM and SERINC3/5, but the mechanisms are not fully understood yet. After effective viral entry, PIC nuclear import can be avoided through interaction of MX2 with the capsid [76]. At the transcriptional level, zinc-finger antiviral protein (ZAP) specifically targets MS viral mRNAs to induce their exosomal degradation [77]. A variety of cellular factors were shown to act during late viral replication steps, in particular by targeting Env: membrane-associated RING-CH 2 and 8 (MARCH2/8) and Schlafen 11 (Slfn11) prevent viral particle formation through Env downregulation via lysosomal degradation thanks to ubiquitin ligase activity [78, 79], and selectively block translation of viral proteins [80], respectively. Restriction factors were also evidenced to operate on Env protein folding: accumulation of misfolded Env proteins due to translocator protein (TSPO) overexpression results in recognition by endoplasmic reticulum class I α-mannosidase (ERManI), leading to their degradation by endoplasmic reticulum-associated protein degradation pathway [81]. In macrophages, the IFN-induced guanylate binding protein 5 (GBP5) interferes with Env incorporation into virions, resulting in decreased infectivity. Mutations in Vpu lead to increased Env expression, resulting in insufficient GBP5 levels to inhibit Env incorporation into virions [82]. Recently, it was observed in macrophages that mannose receptor binds mannose residues found on Env to target it for lysosomal

degradation, which can be counteracted by the combined action of Vpr, especially enriched in macrophages, and Nef by unknown mechanisms [83].

Overall, expression of IFN-induced genes and HIV restriction factors are thus likely to protect cells from viral infection, while cells devoid of these protective factors are highly permissive to HIV infection [84, 85].

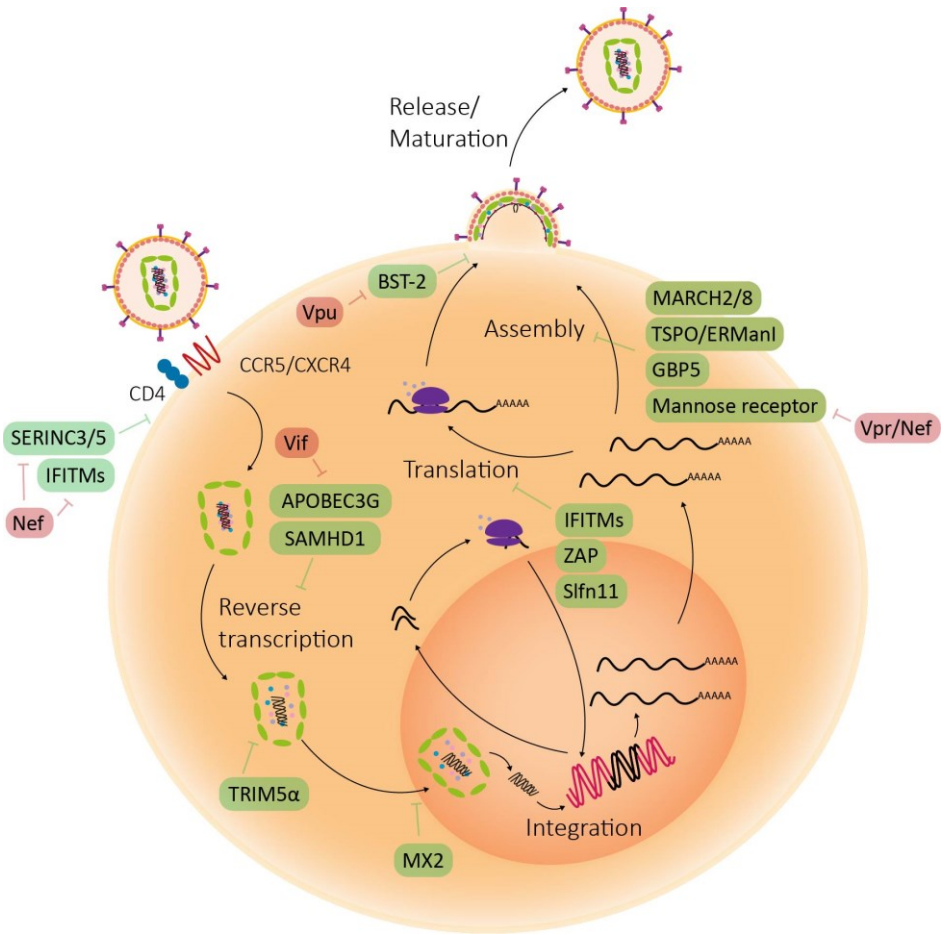

Figure 5: HIV restriction factors and associated viral counterparts. Cells are equipped with diverse factors enabling repression of HIV replication at diverse HIV life cycle steps (indicated in green boxes). Viral envelope fusion with cellular membrane can be prevented by SERINC3/5 and IFITMs. Reverse transcription is impaired by APOBEC3G and SAMHD1, while TRIM5α accelerates capsid disassembly. Nuclear import of vDNA may be inhibited by MX2. IFITMs, ZAP and Slfn11 impede translation of viral proteins. Assembly is prevented by MARCH2/8, TSPO/ERManI, GBP5 and mannose receptor that target Env processing. Finally, BST-2 compromises virion release. Viral accessory proteins (indicated in red boxes) can thwart some of these restriction factors to restore efficient viral replication. Nef counteracts SERINC3/5, IFITMs and together with Vpr, mannose receptor. Vif and Vpu induce degradation of APOBEC3G and BST-2, respectively. SERINC3/5, serine incorporator 3 and 5; IFITM, Interferon-induced transmembrane; SAMHD1, SAM domain and HD domain-containing protein 1; TRIM5α, tripartite motif-containing protein 5; ZAP, zinc-finger antiviral protein; Slfn11, Schlafen 11; MARCH2/8, membrane-associated RING-CH 2 and 8; TSPO, translocator protein; ERManI, endoplasmic reticulum class I α-mannosidase; GBP5, guanylate binding protein 5; BST-2, bone marrow stromal antigen 2; APOBEC3G, apolipoprotein B mRNA editing enzyme, catalytic subunit 3G.

G. The diversity of CD4+ T cells and permissiveness to HIV

The intricate interplay of various cellular factors, coupled with the diversity of target cells expressing distinct biomarkers, underscores the spectrum of permissiveness to HIV infection. This permissiveness is essentially a measure of virus success in establishing infection within a specific host cell. In simpler terms, a fully permissive cell enables HIV to go through the entire replication cycle, including entry, reverse transcription of its genome, integration into the host genome, and the exploitation of the host cellular machinery to actively produce viral proteins and release new viral particles. Conversely, a less permissive cell falls short of achieving complete viral replication.

It is therefore crucial to deepen our understanding of the cellular features that either promote or impede HIV infection. This knowledge is instrumental in deciphering the factors that determine whether a particular cell can be fully exploited by the virus or not.

It is well known that cell permissiveness to HIV is influenced by distinctive features of CD4+ T cells, which dictate viral entry and expression efficiency [85, 86]. The heterogeneity of CD4+ T cells originate from (i) their activation status, *i.e.* resting *vs* activated and proliferating, (ii) multiple lineages or subsets, *i.e.* T helper-1 (Th1), T helper-2 (Th2), T helper-9 (Th9), T helper-17 (Th17), T helper-22 (Th22), T follicular helper (Tfh) or T regulatory (Treg) [87] and (iii) the multiple differentiation stages, *i.e.* naïve, effector, memory, terminally differentiated and exhausted [88]. This cellular heterogeneity is expressed at the transcriptome and proteome levels and is translated functionally at the immune response level. Understanding the complex correlations between cell heterogeneity and susceptibility to viral infection is still quite challenging and a clear picture is still missing.

CD4+ T cell activation is defined as a cascade of events initiated by T cell receptor (TCR) stimulation, which triggers expression of cell surface molecules shaping the immune response (including cytokine receptors), and cytokine secretion (*Fig. 6*). TCR is mounted on CD3, a complex of membrane proteins that is responsible to propagate the signal induced by antigen binding when presented by major histocompatibility complex class II (MHC II)-expressing antigen-presenting cell (APC), such as DC or macrophage. Briefly, this results in immunoreceptor tyrosine-based activation motif (ITAM) phosphorylation by lymphocyte-specific protein tyrosine kinase (LCK), enabling the recruitment of zeta-chain-associated protein kinase 70 (Zap70), which is then also phosphorylated by LCK [89]. Phosphorylated Zap70 is released to phosphorylate linker for activation of T cells (LAT), triggering signaling cascades of phosphoinositide 3-kinase (PI3K), protein kinase B (PKB, or AKT), interleukine-2-inducible T cell kinase (ITK) and protein kinase C (PKC). PI3K induces nuclear import of nuclear factor κ-light-chain-enhancer of activated B cells (NF-κB) through pyruvate dehydrogenase lipoamide kinase isozyme 1 (PDK-1), and activation of mammalian target of rapamycin complex 1 (mTORC1) through AKT, which regulates effector function and promotes proliferation and differentiation, respectively. ITK pathway leads to generation of inositol triphosphate (IP_3) and diglyceride (DAG) molecules through cleavage of phosphatidylinositol biphosphate (PIP_2). IP_3 subsequently provokes calcium excretion, resulting in nuclear factor of activated T cells

(NFAT) nuclear import by calcineurin, which drives cytokine production and cell differentiation. DAG activates MAPK/extracellular signal-regulated kinase (ERK) pathway to recruit activator protein 1 (AP-1), a transcription factor contributing to interleukine-2 (IL-2) gene transcription. To properly induce activation, CD3 stimulation does not suffice, but binding of the T cell costimulatory molecule CD28 to CD80 or CD86 on APC is necessary to efficiently conduct the signal, as lack of costimulation results in an anergic state and makes the cell unresponsive [90]. More precisely, it further activates the PI3K pathway, reinforcing its signal [89]. Importantly, strength and length of stimulation are critical parameters towards the fate of cellular differentiation. Notably, a strong signal is known to favor Th1 differentiation over Th2, while a prolonged signal is associated with Tfh differentiation [91, 92].

Expression of specific surface markers that differentially upregulate over the course of activation discriminate activated cells from resting ones. These markers are involved in cellular survival and proliferation, and include notably CD69 (early stage), CD25 (late stage) and human leukocyte antigen DR isotype (HLA-DR) (very late stage) [93]. Furthermore, CD69 is involved with differentiation to effector or regulatory phenotype, and in tissue retention [94]. As the subunit A of IL-2 receptor (IL-2RA), CD25 responds to IL-2 and enhances its production by positive feedback loop in order to help monitor subtype differentiation, in particular controlling the appropriate amount of Treg differentiation [95]. As for HLA-DR, it is documented as being part of the class II MHC complex normally expressed on APC, but its function on lymphocytes is not fully understood yet [96]. Efficient activation process is precisely balanced with the triggering of coinhibitory pathways in order to prevent autoimmunity. More precisely, immune check point inhibitors (ICIs) such as programmed cell death protein 1 (PD-1), cytotoxic T lymphocyte-associated protein 4 (CTLA-4), T cell immunoglobulin and mucin containing protein 3 (TIM-3), T cell immunoreceptor with Ig and ITIM domains (TIGIT) and lymphocyte activation gene 3 (LAG-3) are upregulated together with activation markers upon physiological conditions to restrict TCR-induced signaling cascade at different steps. Among the mechanisms that are characterized, PD-1 action results in limitation of Zap70 phosphorylation induced by LCK and inhibition of PI3K, while TIGIT blocks PI3K, only but also downregulates T cell activation by promoting tolerogenic DCs [97, 98]. Similar to PD-1, TIM-3 and CTLA-4 also prevent LCK and PI3K signaling, respectively, although CTLA-4 does not directly inhibit PI3K but acts through AKT blockade [97, 99].

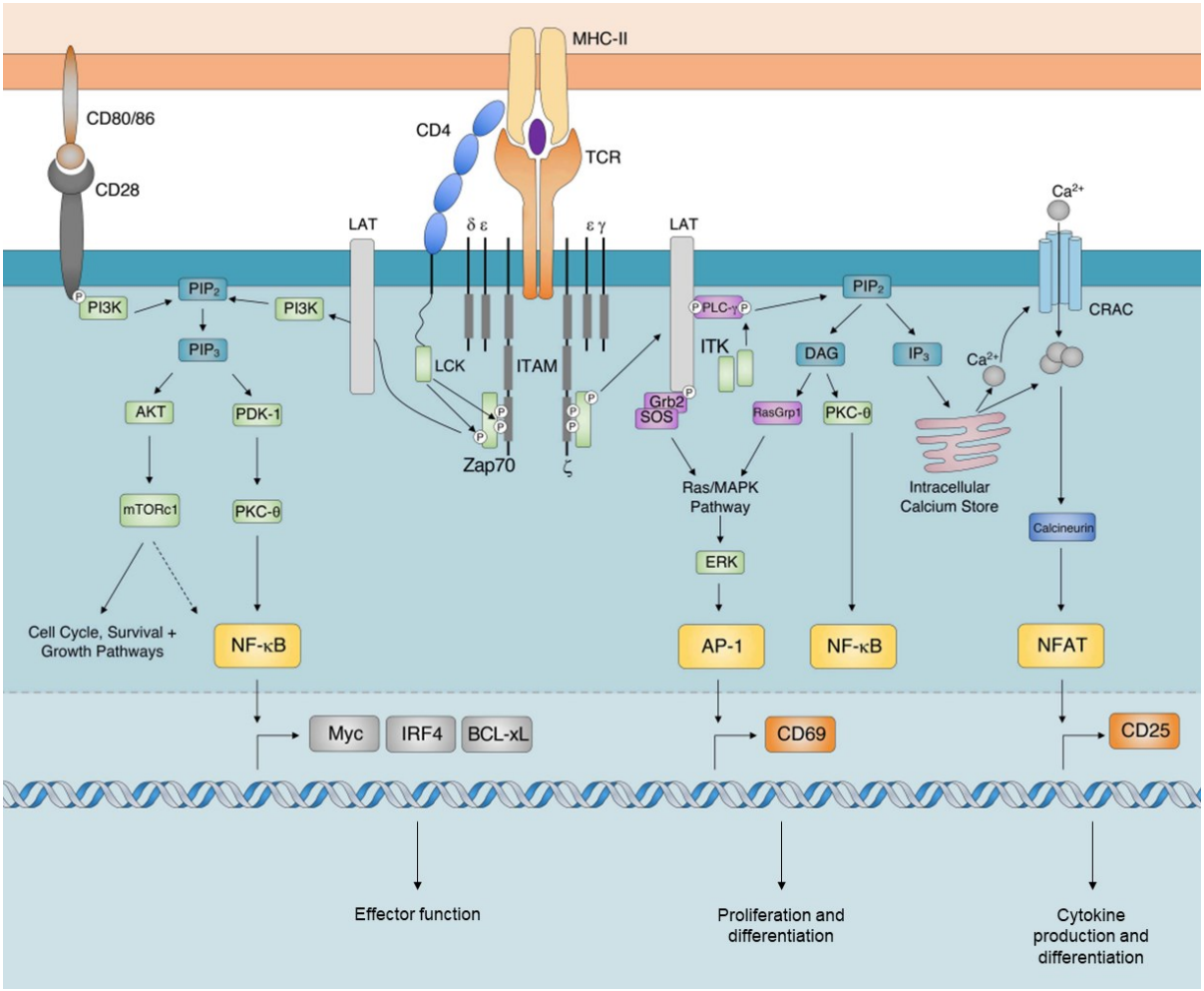

Figure 6: T cell receptor (TCR) stimulation signaling cascade in CD4+ T cells. The figure depicts the interaction between the antigen presenting cell (top cell, orange) and the CD4+ T cell (bottom cell, blue). Antigen (purple) presentation through MHC II to TCR, which is mounted on CD3 (represented by subunits δε and εγ). Through a complex signaling cascade, different pathways are triggered to induce effector function, proliferation, differentiation and cytokine production. mTORC1 metabolism induces cell proliferation and survival, NF-κB regulates transcription to promote effector function by enhancing transcription of Myc, IRF4 and BCL-XL. MAPK controls cell proliferation and differentiation by AP-1 and upregulation of CD69. Calcineurin metabolism provokes CD25 upregulation via NFAT, resulting in cytokine production and differentiation. NF-κB and mTORC1 signaling are further reinforced by CD28 costimulation. Adapted from Bhattacharyya and Feng [89]. MHCII, major histocompatibility complex class II; TCR, T cell receptor; mTORC1, mammalian target of rapamycin complex 1; NF-κB, nuclear factor κ-light-chain-enhancer of activated B cells; Myc, myelocytomatosis; IRF4, interferon regulatory factor 4; BCL-xL, B cell lymphoma extra-large; MAPK, mitogen-activated protein kinase; AP-1, activator protein 1; NFAT, nuclear factor of activated T cells.

Over the course of activation, naïve CD4+ T cells differentiate into effector cells and act by producing cytokines and chemokines to activate specific immune cells or recruit them to the hazard location (*Fig. 7A*). Depending on the source and strength of immune activation, as well as cytokine environment, CD4+ T cells differentiate into different types of effector T cells to respond appropriately: Th1, Th2, Th9, Th17, Th22, Tfh and Treg, mainly [87, 90]. If needed these cells can switch subtype, as they are highly plastic to the environment. Intracellular pathogens, such as viruses or mycobacteria induce Th1 cells differentiation, which respond by attracting macrophages and stimulating phagocytosis. Th2 cells counteract extracellular parasites, such as helminthes by recruiting eosinophils, basophils and mast cells. Moreover, they activate B cell proliferation and antibody production to enhance humoral response. Similar to Th2, Th9

response also aims at parasite neutralization, but displays an enhanced mast cell stimulating effectiveness and proliferating capacity. Other extracellular pathogens such as bacteria and fungi promote Th17 induction, which fights them back by recruiting neutrophils that release reactive oxygen species. Initially thought to be derived from Th17, Th22 cells play a role in autoimmunity and were recently identified as being an independent subtype [100]. Unlike the previously described T helper cells, Tfh are not specific to one pathogen type but command naïve CD4+ T cells to migrate to B cell follicle, in the spleen and tonsils. There, these newly differentiated Tfh help strengthen B cell response and produce high-affinity antibodies. Last, Treg harbor the capacity to dampen immunity in order to prevent an over efficient immune response, which can lead to autoimmune disorders. They are also involved in self-tolerance and restoring immune homeostasis after pathogen clearance [90]. Recently, it has been evidenced that CD4+ T cell could also exhibit cytotoxic functions, referred as cytotoxic CD4+ T cells (CTL). Those latter originate from the different effector subtypes previously described, and can secrete granzyme B and perforin to directly kill their target [101]. It must be taken into consideration that those Th cell subtypes are defined by their cytokine secretion profile and a dominant regulating transcription factor. Indeed, surface markers can somehow be used to discriminate them, but with the limitation to have varying expression depending on the anatomical distribution [102]. In addition, the frequency of the different subtypes varies across the tissues, with for example, an enrichment of Th17 in the gastrointestinal tract as compared to peripheral blood [102].

CD4+ T cell diversity is also supplied by the pool of memory cells, comprised of different discrete types, which harbor distinctive surface markers (*Fig. 7B*). Although still debated, the most probable model of differentiation into memory cells is the progressive model, which involves that the majority of them originates directly from naïve cells and that the cells pass through every stage of differentiation [103]. While a minor part of memory cells originates from effector cells, the majority of them starts their differentiation directly from naïve cells following antigen priming. Indeed, 90% of activated cells die by apoptosis following activation [104]. Memory cells further differentiate after novel stimulation in the following order: stem cell memory (T_{SCM}), central memory (T_{CM}), effector memory (T_{EM}) and terminal effector (T_{TE}). Less differentiated types have an enhanced proliferative and persistence capacity, with T_{SCM} and T_{CM} taking part in most of differentiated memory cell pool regeneration after novel antigen stimulation. However, they are mostly confined to secondary lymphoid organs and display poor effector functions. Conversely, the more the memory cells are differentiated, like T_{EM} or T_{TE}, the more they develop trafficking abilities and effector functions, such as those described above. In return, they have a limited potential for proliferation and eventually tend to die or become exhausted [105]. These so-called exhausted cells present a sustained expression of ICIs (or exhaustion markers), such as the aforementioned PD-1, TIGIT, LAG-3, CTLA-4 or TIM-3, and are notably the result of chronic infection, when a pathogen cannot be cleared [106]. Consequently, exhausted cells characterized by the expression of multiple of these markers, fail to respond to activation due to enhanced expression of ICIs and are thus unable to complete their immune function.

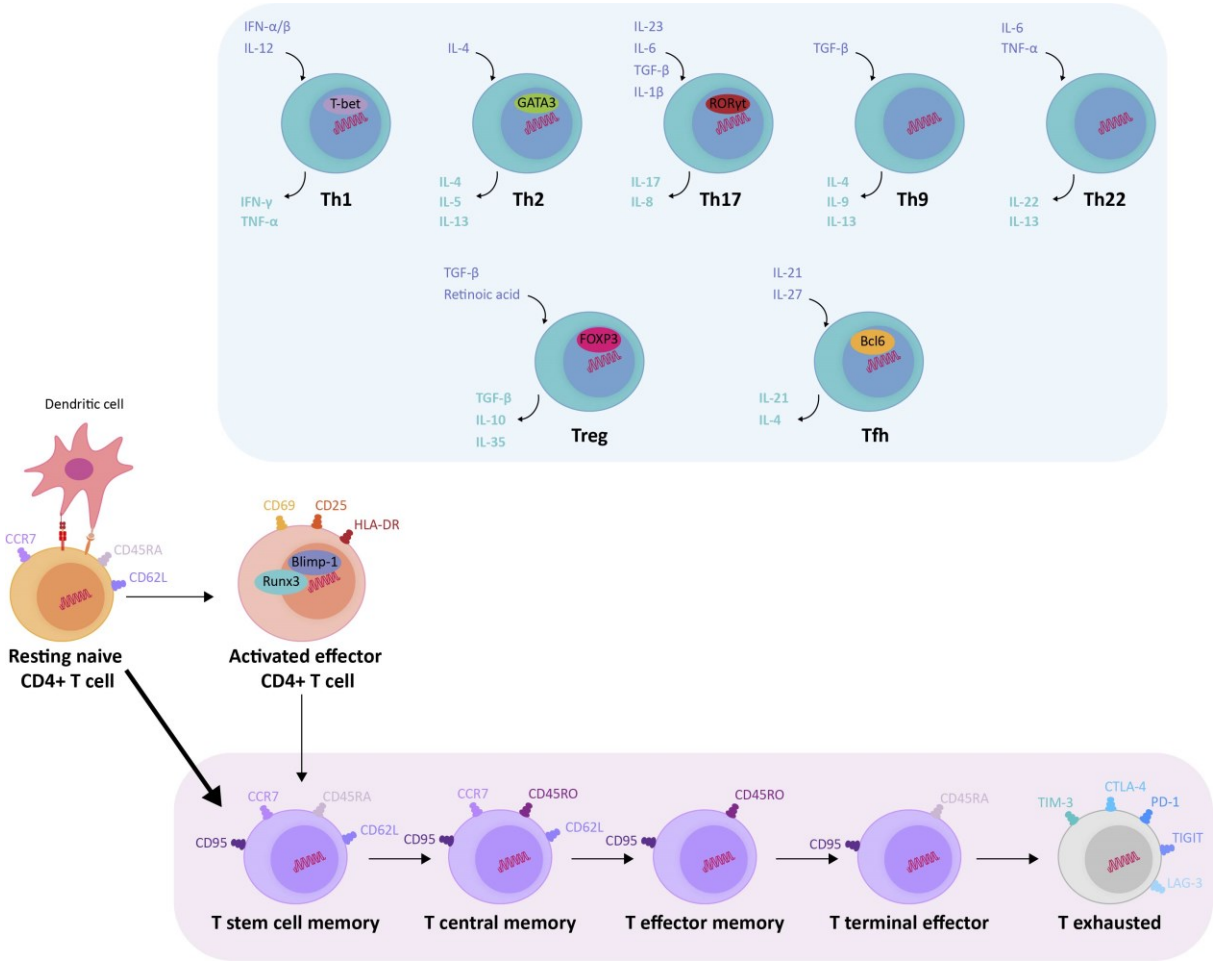

Figure 7: Overview of CD4+ T cell diversity. (A) The diversity is fueled by the different subtypes (in blue), which can be differentiated by a master transcription factor regulator (indicated in the nuclei), the polarizing cytokines in the environment (dark blue) and the cytokines they secrete (light blue). (B) After antigen priming, naïve CD4+ T cells activate and engage their differentiation process by either becoming effector cells, or directly becoming stem cell memory, which is the first stage of memory cell differentiation (in purple). After each round of re-stimulation, memory cells further differentiate in central memory, then in effector memory and finally in terminal effector. At some point, they are not able to differentiate anymore and die, or become exhausted. Every type of memory cell that reactivated can be of one or the other subtype indicated in A.

In the HIV field, specific subtypes of CD4+ T cells were evidenced as favoring viral replication or being enriched with HIV DNA. In particular, Cavrois *et al.* evidenced all types of memory CD4+ T cells as enabling HIV entry, and Th17 and Tfh subtypes as revealing an increased permissiveness to viral replication as compared to other tonsillar CD4+ T cells [107]. They further characterized these cells, which displayed high expression of CD69, CD38, PD-1, CD57, and low CD127. Another study by Rato *et al.* showed that cellular activation state was the main driver of transcriptional heterogeneity and identified highly permissive cells as expressing increased levels of CD25, CD298, CD63 and CD317 [85]. In PWH, TIM-3 was identified as enriched in cells prone to viral rebound in patients undergoing treatment interruption, while PD-1 was demonstrated to be enriched at the surface of latently infected cells [108, 109]. Interestingly, cells harboring integrated HIV DNA from ART-treated patients were shown to be enriched for PD-1, TIGIT and LAG-3, and corresponding inducible reservoir to harbor at least one of these markers [110]. Finally, studies evidenced CTLA-4 as being enriched in HIV specific-CD4+ T cells [111] and in the latent reservoir of Simian

Immunodeficiency Virus (SIV)-infected macaques [112]. Nevertheless, it is not fully understood whether these markers are upregulated following HIV infection or are expressed on cell types favoring HIV infection and thereafter surviving. Indeed, *ex vivo* studies on cells derived from PWH do not permit the understanding of cellular pool and state at the time of primary infection.

Therefore, CD4+ T cell diversity is a key element in HIV studies, as it is well established that subpopulations are not equally permissive to HIV and display discrepancies to viral pathogenesis and reactivation (*Fig. 8*). However, the cellular players present in each subpopulation, that are responsible to drive permissiveness or resistance to HIV, are yet to be comprehensively identified. Furthermore, understanding the dynamics of expression of these cellular factors has to consider CD4+ T cell dynamics (activation status, subset and differentiation).

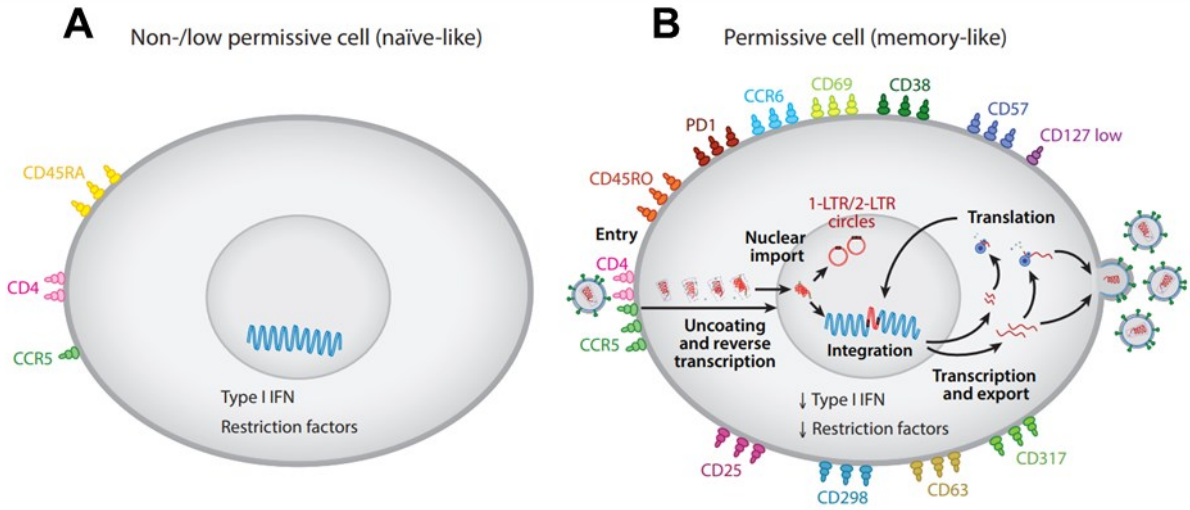

Figure 8: Distinctive features of permissive cells to HIV. (A) Non-permissive cells are typically naïve CD4+ T cells due to their cellular environment and display low CCR5 expression. (B) Alternatively, permissive cells are mostly memory CD4+ T cells, Th17 (CCR6+CCR4+) or Tfh (PD-1+CXCR5+) cells expressing activation markers. Adapted from Brandt *et al.* [113].

H. Sex and age differences in immunity and impact on HIV

Besides cellular composition, HIV replication success can be influenced by individual-specific features, such as sex or age. Indeed, growing amounts of evidence show that sex can shape the immune response (*Fig. 9*), and consequently susceptibility to autoimmune or infectious diseases, cancers, as well as vaccine response [114-116]. Taken together, women experience a higher incidence in multiple sclerosis, type I diabetes or rheumatoid arthritis, for example and account for 80% of autoimmune disease cases in the US [117]. Conversely, prevalence is higher in men for most cancers that are not associated with reproductive organs and suffer higher related mortality [118]. Regarding infectious diseases, women are globally less susceptible to viral infections and present lower viral loads compared to men, such as for severe acute respiratory syndrome coronavirus 2 (SARS-CoV-2), hepatitis B (HBV) or C (HCV), which can be attributed to enhanced IFN-I responses, notably [115]. However, it is worth noting that

some viruses display increased pathogenicity in women, such as herpes simplex virus (HSV) or Influenza A virus (IAV). Finally, women globally produce a more potent antibody response following administration of most available vaccines, but also experience greater adverse effects thereafter [119].

These discrepancies can be attributed to both hormonal regulation and genetic factors (*Fig. 9A*). Lymphocytes, macrophages and DCs are hormone-sensitive due to their expression of estrogen or progesterone receptor, and their activity was found to be influenced by estrogen. Interestingly, the opposite effect can be obtained depending on high or low estrogen concentration: low estrogen favors Th1 and cell-mediated response, while high concentrations result more likely in Th2 response coupled to humoral immunity [114]. As for progesterone, its activity globally results in lower immune activation and response, with for example decreasing IFN-γ in natural killer (NK) cells [120]. Androgens, that circulate in higher concentrations in adult men than women, display an immune suppressive action, notably by enhancing expression of peroxisome proliferator-activated receptor α (PPARα), which consequently inhibits NF-κB and JUN signaling and dampens cellular activation [121]. Sex-specific immune discrepancies are also outlined at a pre-pubertal age, highlighting a causality that cannot be attributed to steroid hormones, with for example male children displaying greater pro-inflammatory response following lipopolysaccharide (LPS) stimulation [122]. Indeed, X chromosome encodes numerous genes involved in immune response, such as *Toll Like receptor 7* (*TLR7*) and *8*, receptors to IL-2 and 13, transcription factors regulating cellular differentiation fate, such as *forkead box P3* (*FOXP3*), as well as miRNAs involved in immune response. This has considerable implications for sex-based immune differences: in women, 15% of X-encoded genes escape X inactivation and are consequently enriched as compared to men [123].

Overall, women display stronger innate and adaptive immune responses compared to men. In lymphocytes specifically, many differences were highlighted (*Fig. 9B*). First, women have higher CD4+ T cell counts, as well as increased CD4+/CD8+ T cell ratio, whereas it is the opposite for men, who have higher CD8+ T cell frequencies and counts [124-126]. These frequency differences are about 2% for both cell types [127]. Second, female lymphocytes were reported to better respond to phytohemagglutinin (PHA) activation, by displaying higher levels of CD69+ cells [127], and to exhibit upregulated activation signaling in unstimulated peripheral blood mononuclear cells (PBMCs) [128], which may account for stronger adaptive response. Finally, CD4+ T cell subset composition differs with sex, with women mounting increased Th1 and Th2 responses, while men usually produce higher Th17 levels [114, 129].

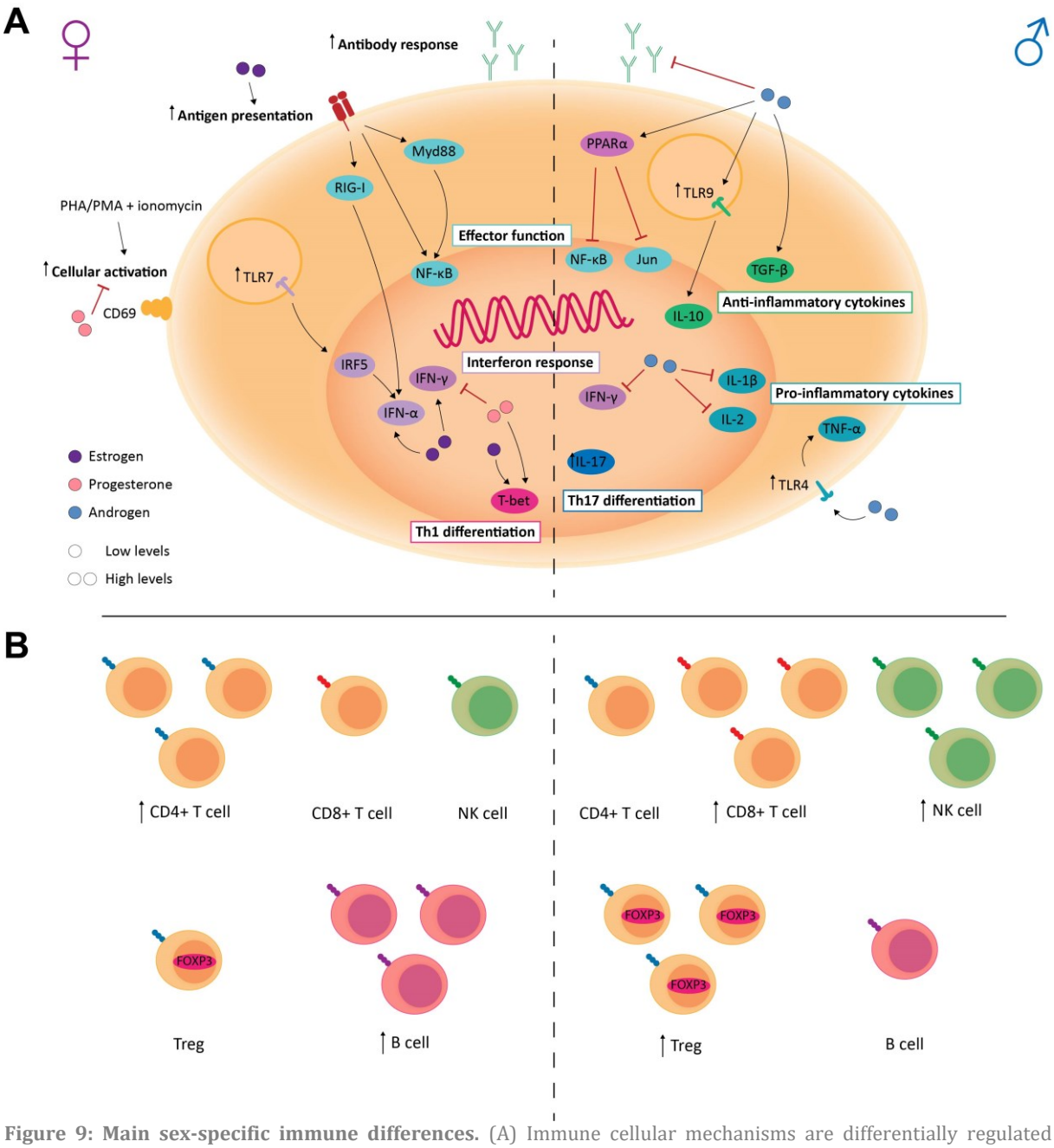

Figure 9: Main sex-specific immune differences. (A) Immune cellular mechanisms are differentially regulated between men and women. These differences are the results of steroid hormones (represented in circles) that can enhance or inhibit a specific function, with estrogen (purple) and progesterone (pink) being dominant in women, while androgens (blue) are dominant in men. Remaining differences result from genetic factors. In women, antibody response is more potent as it is not dampened by androgens. They present an enhanced antigen presentation capacity, resulting in increased NF-κB expression, which promotes effector function. Additionally, RIG-I expression is promoted, which positively regulates IFN-α response. This is further supported by enhanced TLR7 signaling as well as positive estrogen regulation. Th1 differentiation is more important in women due to positive T-bet regulation by estrogen and progesterone. Conversely, androgens stimulate PPARα, which reduces activation by NF-κB and Jun inhibition. In addition, androgens promote anti-inflammatory cytokine expression, such as IL-10 and TGF-β, and inhibit IFN-γ response and pro-inflammatory cytokines IL-1β and IL-2. Conversely, TLR4 function is promoted by androgen, which results in enhanced TNF-α production. Male cells express increased levels of IL-17, promoting Th17 differentiation. (B) Immune cell counts and frequencies vary with sex. PHA, phytohemagglutinin; PMA, phorbol myristate acetate; NF-κB, nuclear factor κ-light-chain-enhancer of activated B cells; RIG-I, retinoic acid-inducible gene I; IFN, interferon; TLR, Toll like receptor; PPARα, peroxisome proliferator-activated receptor α; IL, interleukin; TGF-β, transforming growth factor β; TNF-α, tumor necrosis factor α.

Immunity evolves with age, which is therefore another major contributor to individual-linked immune discrepancies, and consequently increases susceptibility to infectious diseases or decreases vaccine response [130]. First alterations are visible from the age of 50 years old, but clinical manifestations start to appear from the age of 65. Innate immune differences include a peripheral NK cell count increase with age [131]. Regarding lymphocytes, the frequency of T_N logically diminishes with age to the profit of memory populations, which appears to be more pronounced in CD8+ T cells as the immune system is continuously fed with novel antigens. In addition, thymus involution with ageing results in reduced T_N generation [132]. Although all memory subtypes are concerned, the increase is more important towards late-stage differentiation memory subtypes, displaying enhanced effector function with reduced proliferation capacity. Of note, decline of naïve lymphocytes is more pronounced in men than women [133]. Besides, response strength of CD4+ T_N to TCR signaling is reduced in elderly individuals due to miRNA regulation and their CD4+ T_N tend to favor effector differentiation compared to memory generation, contributing to a greater production of pro-inflammatory cytokines, which was recently attributed to earlier CD25 upregulation upon activation [134-136]. Epigenetic studies outlined that PBMCs from people older than 65 years old show sexual dimorphism of genomic activity, with a higher activity in B and T cells from female donors, and a higher activity in monocytes from male donors. Furthermore age-associated alterations in lymphocytes are relatively sparse in CD4+ T cells, while they tend to favor later differentiation and effector phenotypes in CD8+ T cells [137, 138]. Additionally, as individuals age, there is a decline in the CD4+/CD8+ T cell ratio, which appears to be more pronounced in men. Age-induced progressive downregulation of TCR signaling potentially compensates for increase of APC activation. Nevertheless, costimulation results in a higher transcriptional activity [130]. Finally, Botafogo *et al.* addressed CD4+ subset distribution in ageing and found that counts of Th1, Th2, Th17, Th22 and Tfh increase with age [139].

These immune divergences raise the question on whether they also reflect differences in HIV infection susceptibility and pathogenicity. The latest epidemiological statistics show that women represent 54% of infected people and are more susceptible to HIV seroconversion by a two-fold factor compared to men through heterosexual intercourse [11, 140]. This preferential HIV acquisition is attributed to hormone exposure and to local inflammations, which affect the mucosa barrier and render it more permissive [141]. Use of progesterone-based contraceptives induce an increase in CCR5+ CD4+ T cells in the cervix and therefore enhance HIV acquisition risk [142]. Although both sexes experience a similar AIDS progression rate [143], women progress with initially lower viral loads [144]. Alternatively, at a given viral load, women progress faster and with a steeper CD4+ T cell decline [145]. However, HIV replication was shown to be less efficient in women by measurement of viral activity and reactivation potential: a recent study by Scully *et al.* evidenced that despite similar HIV DNA loads in CD4+ T cells of both ART-treated women and men, women displayed a 77% reduction of residual plasma viremia by Gag RNA measurement, as well as a reduction of both multiply spliced (4-fold) and unspliced (35%) RNA [146]. In addition, they showed by measuring Tat/Rev transcripts following CD4+ T cell activation that women displayed a 2-fold reduction of inducible HIV RNA relatively to HIV DNA levels. Multiple reasons can be at

the origin of this phenomenon. First, CD8+ T cell activation diverge between men and women: plasmacytoid DC in women produce significantly more IFN-α in response to HIV ligand binding to TLR7, resulting in enhanced CD8+ T cell activation [147]. This increase in IFN-α additionally results in higher expression of interferon-stimulated genes (ISGs) in CD4+, CD8+ T cells and DC from untreated women when compared to the levels observed in men [148]. Second, a study on primary macrophages showed that male cells are more susceptible to HIV infection due to reduced SAMHD1 activity [149]. Finally, the estrogen receptor is a potent regulator of HIV latency: estrogen binding represses viral reactivation, while receptor blockade promotes it, outlining the key role of sex hormones in HIV biology [150]. Recently, Gianella *et al.* outlined that women post-menopause undergo higher provirus reactivation as compared to younger women, which is possibly caused by estrogen decline [151]. Although a significant part of these sex-specific differences can be attributed to hormonal regulation, other evidence demonstrate lower viral loads in prepubescent women compared to men of same age, suggesting the involvement of other factors such as genetic differences [152]. As an example, certain pivotal pathogen sensor genes and regulatory miRNAs are encoded on X chromosome. In women, these genes could confer a selective advantage due to incomplete X chromosome inactivation, resulting in bi-allelic expression [141].

Regarding age, a recent model has demonstrated a positive correlation between the case fatality rate of AIDS and increasing age, though the exact cause of this correlation remains unclear. It could be due to increased HIV severity because of acquisition at an older age, or result from a higher susceptibility to opportunistic pathogens caused by accentuated biological ageing driven by chronic inflammation [153]. Indeed, most studies exploring the relationship between HIV and age tend to focus on comorbidities and ageing with HIV in order to improve treatments of PWH, and do not investigate the direct impact of HIV on cells from older individuals, likely because of social behavior that favors HIV acquisition during the reproductive age [154].

Consequently, heterogeneity at individual level must be considered in HIV studies, as it is now clear that individual features, such as sex and age affect immunity, and that their impact on HIV response is not fully understood yet.

I. Single-cell technologies and HIV studies

Population analyses play a pivotal role in the field of virus-host interactions and allowed the identification of many cellular patterns linked to infection. However, measurements performed at population level lack the ability to decipher cellular heterogeneity and identify rare cell phenotypes. Therefore, due to their high cellular diversity and heterogeneity, population studies on CD4+ T cells provide only limited information. Over the past decade, significant technological progress led to the development of novel techniques, launching the era of single-cell analyses. These cutting-edge methods allowed for the one-by-one characterization of a complex cell population. Single-cell analyses quickly encountered successful applications in many fields of biology, such as embryology, oncology, immunology or even plant breeding [155].

Tang *et al.* published the first single-cell RNA-Seq (sc-RNA-Seq) study in 2009, by sequencing the whole transcriptome of a single mouse blastomere by manual isolation using a modified microarray protocol [156]. Since then, an ever-growing range of new techniques for sc-RNA-Seq are being developed, enabling the processing of more and more cells, that differ between methods and applications. Mainly, there are three varying parameters between workflows: (i) cell isolation, (ii) amplification method and (iii) sequencing method (*Table 1*). The first cell isolation methods that were developed enabled the sequencing of around 100 cells and relied on physical cell separation that was achieved by manual microdilution or fluorescence-assisted cell sorting (FACS), such as single-cell tagged reverse transcription (STRT-Seq) and massively parallel RNA single-cell (MARS-Seq), respectively [157, 158]. Advances in microfluidics enabled the rise of integrated circuits, such as the commercialized Fluidigm C1, which allows automation of cell isolation by physical separation. Drop-Seq, which is the reference for the first droplet-based technologies further improved throughput to more than 10,000 cells [159]. Briefly, cells are encapsulated into nanoliter-sized droplets containing a different barcode for each cell RNA, which enable pooled PCR amplification after reverse transcription and therefore reduces experimental cost. On the contrary, methods like STRT-Seq or switching mechanism at the 5' end of RNA template (SMART-Seq)/SMART-Seq2 require individual reverse transcription and PCR amplification for each cell that is sequenced, which is labor intensive and can introduce technical artifacts [160, 161]. Today, the most commonly used technologies incorporate unique molecular identifier (UMI) to tag each transcript, thereby reducing amplification bias. Finally, sequencing can be carried either for a short transcript sequence at either end of the transcript (*i.e.* 3’ or 5’ capture protocol), or for full-length, depending on the downstream application. The first approach enables to quantify transcript expression and reduces sequencing cost, while the second one is necessary to detect transcript variants. SMART-Seq/SMART-Seq2 or Fluidigm C1 relies on full-length amplification, while Drop-Seq or MARS-Seq only amplifies 3’ end. Currently, the droplet-based Chromium Controller from the company 10X Genomics thrives as the most widely used platform, which is the result of high cell throughput at a reasonable cost, and sensitivity in detecting rare cell types (*Figure 10*). However, it presents the limitation of reduced sensitivity for detection of lowly-expressed transcripts. Conversely, SMART-Seq2 is more adapted in rare transcripts detection, but to the trade-off of a high cost [162].

Table 1: Comparison of different sc-RNA-Seq protocols. Adapted from Jovic *et al.* [163]. SMART-Seq, switching mechanism at the 5' end of RNA template; MATQ-Seq, multiple annealing and dC-tailing-based quantitative single-cell RNA-seq; CEL-Seq, cell expression by linear amplification and sequencing; MARS-Seq, massively parallel RNA single-cell; inDrop-Seq, indexing droplets; UMI, unique molecular identifiers.

Method	Single cell isolation	Cell throughput	UMI	Sequencing	Publication year
SMART-Seq	FACS	>100	No	Full-length	2012
CEL-Seq	FACS	>100	Yes	3' end	2012
SMART-Seq2	FACS	>100	No	Full-length	2013
Fluidigm C1	Microfluidics	>100	No	Full-length	2013
MARS-Seq	FACS	>100	Yes	3' end	2014
Drop-Seq	Microdroplets	>10,000	Yes	3' end	2015
inDrop-Seq	Microdroplets	>10,000	Yes	3' end	2015
10X Genomics	Microdroplets	>10,000	Yes	3'/5' end	2016
MATQ-Seq	FACS	>100	Yes	Full-length	2017
Seq-Well	Microfluidics	>1,000	Yes	3' end	2017

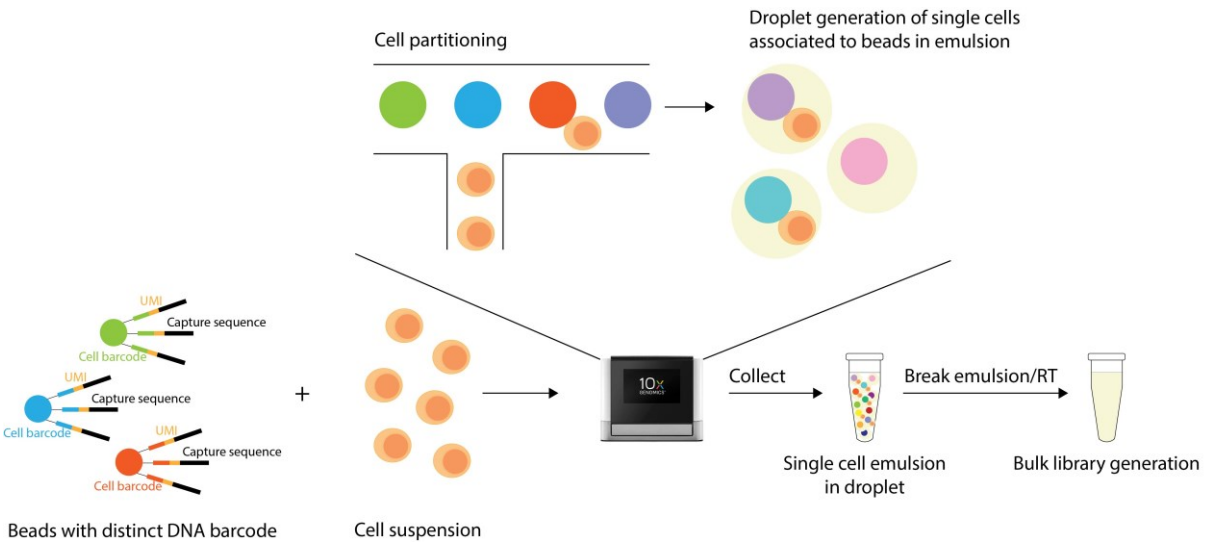

Figure 10: 10X Genomics technology. Beads barcoded with distinct DNA barcode containing (i) cell barcode for individual cell identification, (ii) UMI for transcript identification and (iii) capture sequence for subsequent library construction, as well as cell suspension are processed in the 10X Chromium controller machine. Briefly, cells and beads transit through microfluidic circuit in order to make droplets containing a single cell associated to a single bead and recover them in emulsion. Emulsions are then processed for single-cell mRNA reverse transcription, which breaks the emulsion and allows for bulk library generation. UMI, unique molecular identifier; RT, reverse transcription.

The advent of single-cell technologies is not limited to sc-RNA-Seq, but allows nowadays to characterize diverse molecular features, such as single-cell transposase-accessible chromatin followed by sequencing (sc-ATAC-Seq) for epigenetic regulation study, and can also combine multiple techniques simultaneously, which is referred to as multiomics [164].

Having multimodal analyses presents the perk of obtaining complementary information of the same exact cell, thereby providing an increased precision in cell type and phenotype identification. For example, genome and transcriptome sequencing (G&T-Seq) and gDNA-mRNA sequencing (DR-Seq) allow deciphering simultaneously genomic DNA and mRNA in order to identify single nucleotide polymorphism (SNP) at molecular levels [165, 166]. Epigenetic regulation analysis takes advantage of chromatin accessibility methods and is studied at single-cell resolution using single nucleus assay for transposase-accessible chromatin followed by sequencing (sn-ATAC-Seq) [167], and mapping of chromatin proteins bound to DNA by single-cell cleavage under targets and tagmentation (scCUT&Tag) [168], or cytosine methylations by single-cell bisulfite sequencing (scBS-Seq) [169]. It can now be combined to sc-RNA-Seq to associate a cell type with chromatin accessibility on different platforms, such as simultaneous high-throughput ATAC and RNA expression with sequencing (SHARE-Seq) or 10X Genomics Single Cell Multiome ATAC + Gene Expression assay [170]. In parallel to the first sc-RNA-Seq protocols, protein expression at single-cell resolution was investigated, giving rise to methods like cytometry time-of-flight (CyTOF) [171]. This method is based on mass cytometry coupled to antibodies conjugated with isotopes, enabling the measurement of up to 100 parameters. Yet, as this can be insufficient to fully characterize a cell, and RNA levels do not always reflect protein expression, multimodal methods like cellular indexing of transcriptomes and epitopes by sequencing (CITE-Seq) were developed to overcome this issue [172]. Briefly, proteins are measured by DNA barcoded-conjugated antibodies that are incubated with cell suspensions before droplet-based single-cell isolation. Therefore, protein quantification can be performed by sequencing the DNA barcode of an antibody. A commercialized version was set up by 10X Genomics that enables simultaneous profiling of transcriptome, cell surface proteins and TCR sequence. The latest innovation in single-cell technologies provides valuable benefits for tissue analyses as they provide spatial coordinates of a cell within the system. This is achieved by barcoding spatial localization of a cell within a tissue that can be coupled to an array to capture mRNA, such as with Visium platform from 10X Genomics [164].

Since 2012, the field of HIV already benefited of such advances, mainly with studies characterizing host response to infection, viral latency and reactivation, as well as cellular permissiveness to HIV replication (*Table 2*) [113]. These studies reveal that addressing cellular heterogeneity in HIV studies is essential as cellular distribution affects HIV response.

Table 2: Summary of HIV research advances achieved with single-cell technologies.

HIV-related aim	Approach	Outcomes	References
Infection outcome	Sc-RNA-Seq, ECCITE-Seq (surface protein, transcriptome, HIV RNA and TCR)	Infection induces loss of T_N, signature of inflammation and response to IFN-α, persistent TNF response and upregulation of oxidative phosphorylation metabolism	[173-175]
Inducible reservoir	Single-provirus sequencing, sc multiplex PCR, sc-RNA-Seq, ECCITE-Seq (surface protein, transcriptome, HIV RNA and TCR), STIP-Seq (TCR, integration site and proviral sequence), HIV-Flow (p24+ cell sorting), FISH-Flow (HIV RNA)	Reservoir cells are mainly expanded clones and display phenotypic heterogeneity. Cells harboring inducible provirus are preferentially Th1, T_{EM} and enriched for VLA-4, ICIs, HLA-DR, granzymes, BCL2 and SERPIN9, and are resistant to killing. Translation-competent reservoir consists of provirus with short 5' deletions integrated in cancer-related genes and are clones with pathogen-specificity.	[174, 176-182]
Reactivation	Microarray sc imaging, combined sc RNA FISH to p24, cell phenotype and vDNA, single-cell-in-droplet PCR, sc-RNA-Seq	Cellular heterogeneity in extent and time of viral latency reactivation. Reactivation mostly in T_{EM} and mediated by ADAP1	[86, 183-186]
Latency	Sc-RNA-Seq, sc vRNA quantification, GERDA (Gag+ and Env+, proviral sequence, polyA-RNA)	Latent cells are enriched with HIST-1 and IL-32 and are preferentially T_N, or T_{CM} with lymphoid homing properties	[187-189]
Viral transcription	DOGMA-Seq (chromatin and vRNA), sc-RNA-Seq	HIV transcription is linked to chromatin accessibility and depends on T cell signaling	[186, 190]
Permissiveness	Combined sc TCR and vDNA, CyTOF/CyTOF coupled to sugar detection, sc-RNA-Seq	Cells more susceptible to infection are Th17, Tfh, memory CD4+ T cell CCR5*hi,* cells enriched for fucose and sialic acid, T_{EM}, cells with activated and exhausted phenotype and cells displaying low IFN-I response. Phenotype of susceptible cells is dependent on infection stage	[85, 107, 191-193]
HIV-induced cell death	Sc-RNA-Seq	Cells killed by HIV express CXCR5 and CXCR4	[193]

J. The latent reservoir

The current ART contains in most cases a combination of three inhibitors, targeting different enzymatic steps of viral replication. Although ART leads to successful reduction of viremia down to undetectable levels, complete eradication of the virus cannot be achieved due to the presence of a latent reservoir, *i.e.* infected cells that are transcriptionally silent, or that do not express viral proteins, and hence do not produce viral particles. Indeed, this viral reservoir is responsible for a viremia rebound in case of treatment interruption [194], thereby representing the major barrier towards cure.

Viral reservoir(s) can be defined as cell types or anatomical sites where replication-competent provirus persists despite ART [195, 196]. The major reservoir consists of long-lived infected memory CD4+ T cells, mostly T_{CM} and T_{EM} [197]. Despite T_{CM} accounting for an increased part of the reservoir, T_{EM} are responsible for most of clonal expansion [198]. Alternatively, naïve and effector CD4+ T cells only contribute modestly to the reservoir. By harboring high levels of HIV DNA and undergoing slow decay, T_{SCM} might play a significant part in the viral reservoir [199]. In addition, there are increasing amounts of evidence supporting the fact that macrophages, DCs and microglia can also contribute to the viral reservoir, although likely to a lesser extent [200, 201]. The majority of these reservoir cells dwells in anatomical reservoirs, such as lymph nodes and the gut mucosa, as measured by the frequency of infected cells and viral RNA load in ART-treated patients [202, 203], but it has been evidenced that persistently infected cells can also be found in central nervous system, lungs, bone marrow and genital tract [204]. Indeed, HIV is able to target a wide range of tissues, which results in site-specific properties of viral persistence induced by different pools of reservoir cells. In B cell follicles, Tfh represent another long-lived reservoir, as it is an immune-restricted site, where CD8+ T cells cannot access [205, 206].

The occurrence of direct HIV infection of quiescent cells exist but seems to be limited due to several blocks of HIV replication [204]. The formation of the latent reservoir is hypothesized to be closely linked to CD4+ T cell activation, *i.e.* activated CD4+ T cells are more permissive to HIV infection, which then either die or return to resting memory (*Fig. 11*). Latency establishment seems to be increased when the activated cell is transitioning back to a resting state. Blood analysis demonstrated that inducible replication-competent proviruses were present in 1 out of 1 million CD4+ T cells [196], although intact proviruses are present in 60 out of 1 million CD4+ T cells [207]. In addition, between 95 and 98% of quiescent cells harbor defective provirus (induced by genomic deletion or APOBEC-mediated hypermutations) and can therefore still produce viral RNA or proteins [208]. Although these cells do not produce infectious particles, they may nonetheless play a role in sustained inflammation and T cell activation by partly synthetizing viral components [204]. Investigations on these quiescent cells outlined that they rarely lead to protein translation, as transcripts are incomplete or not suited for alternative splicing [209]. Upon circumstances that are up to now only partially understood, latently infected cells harboring replication-competent provirus can somewhat spontaneously reactivate, thus transitioning back to a productive infection state and initiating a novel round of infection. As this is regulated by a myriad

of factors, HIV reactivation likelihood varies at both cellular and individual levels and depends on latency depth [210].

Latently infected cells can persist in a diverse panel of dormancy depth [211], depending on the mechanisms involved for each cell that are not mutually exclusive. The determinant factors include (i) provirus integration site and sense, (ii) epigenetic control of viral transcription, (iii) bioavailability of transcription and elongation factors, (iv) post-transcriptional blocks and (v) miRNA regulation [204]. Studies outlined that provirus integrates preferentially into actively transcribed genes thanks to cleavage and polyadenylation specific factor 6 (CPSF6)-mediated nuclear import of the core and to lens epithelium-derived growth factor (LEDGF)/p75-bound integrase [212, 213]. On the contrary, quiescent cells were more likely to harbor provirus in intergenic regions [214]. Integration orientation also plays a role on HIV transcription activity: antisense integration results in transcriptional interference, inhibiting expression, while sense integration enhances viral transcription [215]. Moreover, epigenetic regulation of chromatin surrounding the integration site influences the level of viral transcription, as HIV genome must be accessible to transcription factors and transcriptional machinery. HIV takes advantage of NF-κB cellular transcription factor to bind to the LTR and initiate the transcription [216]. Besides, NF-κB plays a second role by recruiting positive transcription elongation factor (P-TEFb), working similarly as Tat elongation process [217]. In addition, the absence of viral particle production can also be caused by post-transcriptional blocks with for example, splicing impairment leading to lack of viral proteins, or RNA export blockade [218, 219]. Finally, cellular miRNA can either enhance viral production by silencing proteins involved in transcriptional regulation [220], or inhibit it by targeting the 3' end of HIV transcripts [221] or *nef* RNA [222]. Although the mentioned factors provide valuable knowledge about latency mechanisms, these are not observed extensively in latency models, highlighting the heterogeneity of relevant cells and the fact that much remains to be deciphered.

Currently, one of the explored solutions to purge the latent reservoir is the "shock and kill" strategy. This strategy aims at both reactivation of latently infected cells and their subsequent neutralization by the immune system, as a result of novel viral component production, or cell death due to viral cytopathic effects. However, the multiplicity of latency mechanisms, and therefore, the heterogeneity of latently infected cells, makes it difficult to achieve universal reactivation. Indeed, a complete reactivation would require targeting all mechanisms involved in latency, reaching the reservoir cells that dwell in different anatomical compartments, and being well tolerated. So far, maximal reactivation has been observed on cells isolated from ART-treated patients using anti-CD3/anti-CD28 combined to IL-2, mimicking antigen activation, but at the cost of a high toxicity [223]. Ever since, many latency-reversing agents (LRAs) have been developed that can be used either alone, or in combination. Those are not specific to HIV and impact different pathways of cellular metabolism. These include notably histone deacetylase inhibitor (HDACi), agonists of PKC, agonists of P-TEFb, second mitochondria-derived activator of caspase (SMAC) mimetics or immunomodulatory molecules such as IL-15, TLR agonists or ICIs [224, 225]. Unfortunately, none of them proved successful in global reactivation of all latently infected cells isolated from ART-treated individuals up to now. Recently, a study showed that only 16.28% of the viral

reservoir could be reverted to a transcriptionally active state using various LRAs, with only 10.1% being translationally competent [226]. As shock and kill cure strategies so far result in a limited success, other approaches have been explored. Notably, the other strategy that paved the way to HIV cure is to prevent reactivation of the latent reservoir and is referred to as "block and lock" [227]. More precisely, it aims at lastingly preventing viral transcription, even after treatment interruption. The involvement of many proteins in viral transcription and silencing provides the opportunity to achieve silencing through different avenues, that are currently under investigation and include notably: (i) Tat inhibition, (ii) LEDGF inhibitors (LEDGINs), (iii) siRNA targeting transcription factor binding sites in LTR, (iv) inhibition of HIV transcription complex facilitator (FACT) and (v) inhibition of mTOR. So far, these approaches led to significant reduction of viral transcription and of reactivation in presence of LRAs in experimental setups, but still lack evidence of success in clinical trials [227].

The main obstacle to these approaches resides in the large heterogeneity of latently infected cells, regarding cell type and dominant molecular mechanisms of latency exploited, rendering difficult the one-for-all therapeutic approach. Further analyses of these cells should inform about the determinants responsible for this heterogeneity. Indeed, the identification of novel factors in rare subtypes of latently infected cells may help design improved targeted treatments to increase the proportion of reactivated cells in a shock and kill strategy or to provide novel inhibitors aiming at eradicating HIV.

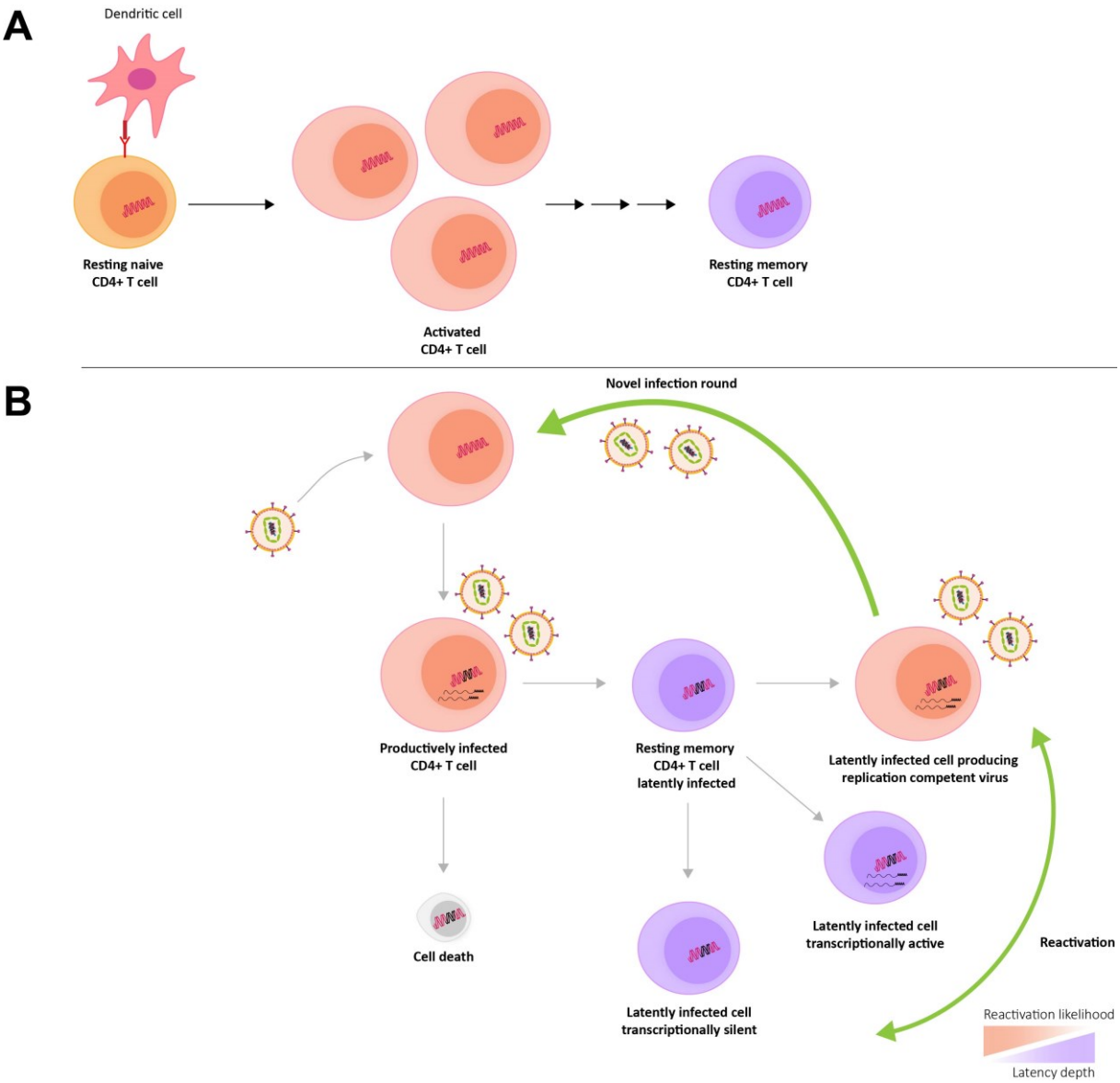

Figure 11: HIV in CD4+ T cell. (A) Naïve CD4+ T cells are in a resting state until their TCR binds to MHC-associated antigenic peptide by an APC (*i.e.* DC or macrophage). This triggers their transition to an activated state, and their proliferation, allowing the completion of their effector immune functions. After this, most cells die, but surviving effector CD4+ T cells differentiate to memory cells and return to a resting state. (B) CD4+ T cells are mostly permissive to HIV infection when they are in an activated state. The initial step of infection involves a productive infection state, where HIV is actively replicating within the cell, leading mostly to cell death. A minority of infected cells can however transition back to a resting state, and therefore becoming latently infected (that can harbor either a complete or a defective provirus). Latently infected cells can be either transcriptionally silent or produce viral transcripts and/or proteins to a basal level. Part of transcriptionally silent cells harbor replication-competent provirus that can somehow reactivate to initiate a novel round of infection. Reactivation likelihood differs between the cells and usually depends on latency depth. Adapted from Murray *et al.* [228]. TCR, T cell receptor; MHC, major histocompatibility complex; APC, antigen-presenting cell; DC, dendritic cell.

II. Aims

The large CD4+ T cell diversity is a major determinant of HIV infection success, as permissiveness to HIV is cell-type dependent. On top of that, individual sex and age shape the immune response and the distribution of immune cells and may thus further affect HIV replication. Indeed, sex was shown to affect HIV replication in PWH in *ex vivo* experiments, with women displaying lower plasma viremia and reduced viral reactivation. Regarding age, most studies investigate comorbidities and ageing with HIV but do not address the cellular impact of HIV on cells from ageing individuals. Thus, we hypothesized that sex effects are imprinted at the cellular level and could be recapitulated *in vitro*, and that age-related immune changes could impact HIV replication *in vitro*. The activation status being a major contributing factor of HIV infection success, we investigated cell permissiveness to HIV in correlation with CD4+ T cell activation kinetics and cell distribution. We also performed transcriptomic analyses at bulk and single-cell levels to identify and refine the specific gene signature allowing distinction of permissive from resistant cells.

Main project: Sex and age impact CD4+ T cell susceptibility to HIV *in vitro* through cell activation dynamics

This work aimed at characterizing how individual sex and age affect CD4+ T cell permissiveness to HIV and investigating the correlation with cellular activation by T-cell receptor-mediated stimulation.

Manuscript in preparation:

- Ludivine Brandt, Paolo Angelino, Raquel Martinez, Sara Cristinelli, Angela Ciuffi, Sex and age impact CD4+ T cell susceptibility to HIV *in vitro* through cell activation dynamics, 2023. (In preparation).

Additional project: Single-cell analysis identified novel determinants of CD4+ T cell permissiveness to HIV

This work aimed at understanding how T-cell receptor-mediated stimulation affects CD4+ T cell pool composition and at identifying cellular factors accounting for cell permissiveness to HIV.

Manuscript in preparation and published review:

- Paolo Angelino, Ludivine Brandt, Raquel Martinez, Sara Cristinelli, Angela Ciuffi, Single-cell analysis identified novel determinants of CD4+ T cell permissiveness to HIV, 2023. (In preparation).
- Ludivine Brandt, Sara Cristinelli, Angela Ciuffi, Single-Cell Analysis Reveals Heterogeneity of Virus Infection, Pathogenicity, and Host Responses: HIV as a Pioneering Example, Annual Review of Virology, Volume 7, 2020.

III. Results and discussion

A. Main project: Sex and age impact CD4+ T cell susceptibility to HIV *in vitro* through cell activation dynamics

During my PhD, I mainly worked on understanding differences between individuals regarding HIV infection success by addressing sex- and age-based differences. After optimization of cell culture and infection workflow, we successfully addressed the effect of these factors upon HIV infection in correlation with CD4+ T cell activation kinetics and studied their cellular composition by transcriptomic analyses.

Summary

This study aimed at investigating sex- and age-based differences at cellular level and their impact on cell permissiveness to HIV through a kinetics of CD4+ T cell activation, in order to correlate individual permissiveness to HIV to cell activation ability. To this aim, we used primary CD4+ T cells from 20 HIV-negative blood donors and stimulated them for 6 days. We collected cells every 24h and infected them with HIV-based vectors pseudotyped with VSV-G or native HIV envelopes and assessed infection success by flow cytometry. Cell activation status was measured by parallel staining of surface markers of activation, immune checkpoint inhibitors, as well as HIV entry receptors. We performed bulk RNA-Seq on cells from all studied donors to investigate their cellular transcriptome 24 and 72h p.-s. prior to HIV infection. Finally, we performed sc-RNA-Seq on selected donors to explore CD4+ T cell pool composition.

Contribution

- Conceptualization of experiments was made in collaboration with AC and SC.
- Performing experiments: optimization of cell culture for activation, infection, surface marker staining, RNA extraction and preparation of cell suspensions for sc-RNA-Seq. Single-cell Chromium loading and library preparation were performed by RM.
- Data analysis: flow cytometry data. Bulk and sc-RNA-Seq experiments were analyzed by PA.
- Writing of manuscript was performed with AC.
- Figure design and formatting.

The manuscript is currently in preparation and is enclosed hereafter.

Sex and age impact CD4+ T cell susceptibility to HIV *in vitro* through cell activation dynamics

Ludivine Brandt[1], Paolo Angelino[1,2], Raquel Martinez[1], Sara Cristinelli[1], Angela Ciuffi[1]

[1] *Institute of Microbiology, Lausanne University Hospital and University of Lausanne, Switzerland*
[2] *DS-facility, AGORA Cancer Research Center, Swiss Institute of Bioinformatics, Lausanne, Switzerland*

Abstract

Cellular composition and responsiveness of immune system evolve upon ageing and are influenced by biological sex. CD4+ T cells from women living with HIV exhibit decreased viral replication *ex vivo* compared to men. We thus hypothesized that these findings could be recapitulated *in vitro*, and infected primary CD4+ T cells with HIV-based vectors pseudotyped with VSV-G or HIV envelopes. We used cells isolated from 20 donors to interrogate the effect of sex and age on permissiveness over a 144h activation kinetics. Our data identified an increased permissiveness to HIV between 24 and 72h post-stimulation. Sex- and age-based analysis at these time points showed increased susceptibility to HIV of cells isolated from males and from donors over 50 years old, respectively. Parallel assessment of surface marker expression revealed expression of activation (CD69, CD25, HLA-DR) and immune checkpoint inhibitors (PD-1 and CTLA-4) markers in increased cell numbers from donors displaying increased permissiveness to HIV. Furthermore, positive correlations were identified between CD69, PD-1 and CTLA-4 expression kinetics and HIV expression kinetics. Cell population heterogeneity was assessed by single-cell RNA-Seq analysis and no cell subtype enrichment was identified according to sex. Finally, transcriptomic analyses further highlighted the role of activation in those differences with enriched activation and cell cycle gene sets in men and in older women cells. Altogether, this study brought further evidence about individual features affecting HIV replication at the cellular level and should be considered in latency reactivation studies for HIV cure.

Introduction

Virus success to establish infection depends on the expression of surface receptors for viral entry and on a cellular permissive environment favoring viral replication. Within a cell population, susceptible cells to human immunodeficiency virus type 1 (HIV-1, hereafter abbreviated HIV) have to express the CD4 entry receptor as well as CCR5 or CXCR4 coreceptor. Moreover, the majority of these cells display a restrictive cellular environment, making them initially refractory and non-permissive to viral infection, unless exposed to specific activation stimuli: over activation, the cell population diversifies, increasing heterogeneity. Consequently, the varying intracellular composition results in heterogeneous response to viral infection. The diversity of CD4+ T cells, the main targets of HIV, is fueled by (i) activation status, (ii) cell subset and (iii) differentiation stage. Multiple studies aimed at identifying molecular determinants associated with increasing permissiveness to HIV. Examples include cell types and features such as enhanced CCR5 expression [1], all types of memory CD4+ T cells,

especially effector memory cells, T helper (Th) 17 and T follicular helper (Tfh) subtypes [2, 3], and cells displaying an activated or exhausted phenotype displaying a low type I interferon response [4].

Besides cellular composition, HIV replication success can be influenced by individual-specific features, such as gender or age. Indeed, growing amounts of evidence show that sex can shape the immune response [5-7]. Sex-related differences can be explained by differential steroid hormone regulation as well as genetic factors [5]. The latest epidemiological statistics reveal that women represent 54% of people with HIV (PWH) and are more susceptible to HIV seroconversion by a two-fold factor compared to men through heterosexual intercourse [8, 9]. Although both sexes experience similar AIDS progression rate [10], women progress with initially lower viral loads [11]. Moreover, Scully *et al.* showed that HIV replication is less efficient in women under antiretroviral therapy (ART) upon measurement of viral transcriptional activity and reactivation potential [12]. This observed lower replication may be the result of plasmacytoid dendritic cells in women that produce more type I interferon in response to HIV ligand binding to TLR7, enhancing CD8+ T cell activation, provoking higher expression of interferon-stimulated genes in CD4+, CD8+ T cells and dendritic cells from untreated women when compared to the levels observed in men [13, 14]. Last, estrogen receptor was shown to be a strong regulator of HIV latency: estrogen binding to its receptor can repress viral reactivation, while receptor blockade can promote it, outlining a key role for sex hormones in HIV biology [15]. Recently, Gianella *et al.* outlined that women post-menopause undergo higher provirus reactivation as compared to younger women, which is possibly caused by estrogen decline [16]. Although a significant part of these gender-specific differences can be attributed to hormonal regulation, evidence demonstrate lower viral loads in prepubescent women compared to men of same age, suggesting the involvement of other factors, such as genetic differences due to incomplete X inactivation [17, 18].

Age is another major contributor to immune differences, with first alterations being visible at the age of 50 years old, with thymic involution leading to reduced T cell generation [19]. With age, naïve/memory cell balance shifts towards increased memory cell frequencies, that is more pronounced in late-stage differentiation memory subtypes, displaying enhanced effector function and reduced proliferation capacity. In the HIV field, most studies address the effect of ageing with HIV in order to improve older patient care without investigating a potential direct impact of HIV on cells from older individuals [20].

Here, we addressed whether these sex-based differences could be recapitulated *in vitro,* without hormonal influence and biases caused by a prolonged HIV infection. In addition, we interrogated the effect of age on cellular permissiveness to HIV. To this aim, we isolated CD4+ T cells from 20 HIV-negative individuals, activated them over a period of 6 days, and infected them every day with three HIV-based vectors pseudotyped with VSV-G, CCR5- (R5-) or CXCR4- (X4-) tropic envelopes, and harboring two fluorescent reporters, one LTR-driven GFP reporter and one constitutive EF1α-driven mKO2 reporter (HIV GKO [21]) that were monitored by flow cytometry. We compared reporter expression by flow cytometry and by sex and age to reflect permissiveness over time

post-TCR stimulation. We found that viral infection peaked at 24h-72h post-stimulation (p.-s.), as expected. During these times, cells derived from men and individuals older than 50 years old displayed enhanced cell susceptibility to HIV, correlating with increased activation markers and immune check point inhibitors (ICIs) expression. Transcriptomic analysis revealed enrichment of activation and cell cycle gene sets in men and in ageing individuals, supporting a major role for activation in the permissiveness phenotype. Finally, we identified differential regulation in sex-linked genes that may impact permissiveness to HIV.

Results

Cell permissiveness to HIV evolves with cell activation dynamics

To explore individual permissiveness to HIV in CD4+ T cells, we studied a cohort of 20 HIV-negative blood donors varying in sex and age (22 to 72 years old) through TCR-induced activation dynamics (*Fig. 1A*). Resting CD4+ T cells from each donor were stimulated for a total of 144h (*Fig. 1B*). Every 24h, cells were collected and assessed for selected surface marker expression (*Supplementary Fig. 1A*) and HIV infection as reported by HIV GKO (*Supplementary Fig. 1B and C*) by flow cytometry. Our results showed a stable expression over time p.-s. of HIV entry markers, with ubiquitous expression of CD4 and CXCR4, but limited expression of CCR5 (present only on 12% of CD4+ T cells on average) (*Supplementary Fig. 2A*). The relative expression of these markers, as reflected by mean fluorescence intensity (MFI) outlined increasing levels of CD4 but decreasing levels of CXCR4 and CCR5 over stimulation (*Supplementary Fig. 2B*). In parallel, expression of cell surface proteins related to activation, *i.e.,* CD69, CD25 and HLA-DR, as well as ICIs, *i.e.,* PD-1, CTLA-4 and TIM-3 were measured to monitor cell activation status. As expected, activation marker expression increased with time p.-s. with differential kinetics. The early CD69 activation marker increased and peaked at 72h p.-s. with an average of 74% positive cells before decreasing, while CD25 was progressively upregulated over TCR-mediated stimulation until being expressed at the surface of most cells (93% on average at 144h) (*Supplementary Fig. 2A*). The late HLA-DR activation marker showed progressive upregulation, reaching 47% HLA-DR+ cells at 144h on average. Relative MFI of activation markers showed a peak of CD69 levels 24h p.-s. before a steep decline (*Supplementary Fig. 2B*). CD25 levels peaked 96h p.-s. and HLA-DR increased progressively in time. Following activation kinetics, ICIs are upregulated simultaneously with activation mark-ers in order to constrain cell proliferation, as a control feedback loop. The three selected ICIs displayed increased expression over time, but with different proportions: PD-1 ex-pressing cells peaked at 120h with 81%, CTLA-4+ cells reached 45% at 96h and TIM-3+ cells 78% cells at 144h (*Supplementary Fig. 2A*). Consistently, expression levels of the three markers increased with stimulation and decreased in late time points, at 96h for PD-1 and CTLA-4, and 144h for TIM-3 (*Supplementary Fig. 2B*).

Infection was carried out with an HIV GKO (HIV_LTR-GFP-EF1α-mKO2) dual reporter vector, pseudotyped with three different envelopes: VSV-G for amphotropic viral entry, and natural HIV envelopes, LAI for CXCR4 tropism and BaL for CCR5 tropism. Expression

level of GFP and mKO2 was assessed at 47h post-infection (p.-i.) (*Supplementary Fig. 1A*). HIV infection success was evaluated in three ways to assess susceptibility, population permissiveness and intracellular permissiveness (*Fig. 1C-E*). The proportion of susceptible cells to HIV was assessed by the number of cells expressing the constitutively EF-1α-driven mKO2 reporter. Data revealed an increasing proportion of susceptible cells, peaking at 72h p.-s. for HIV GKO/VSV-G (26.4%) and LAI (8.6%) and between 24h and 48h p.-s. for HIV GKO/BaL (1.1%) (*Fig. 1C*). The analysis of the relative GFP MFI reflected the level of LTR-driven GFP production in the total population and thus assessed the global cell permissiveness to HIV, *i.e.* the combination of cell susceptibility to HIV (from entry to integration) and successful viral expression (*Fig. 1D*). Data mirrored cell susceptibility kinetics, suggesting that susceptible cells are similarly permissive, *i.e.* enabling productive HIV infection. Finally, in order to discriminate the impact of entry from determinants of intracellular permissiveness, we investigated GFP expression in GFP+ cells (*i.e.* productively infected cells) and observed higher amounts of GFP expression at 24h p.-s., suggesting that the intracellular environment favoring permissive infection is rapidly established upon TCR-mediated stimulation (*Fig. 1E*). Data also showed a progressive decline of LTR-driven GFP expression over time p.-s., which could not be explained by the direct establishment of latent infection, as the proportion of mKO2+GFP- infected cells was stable or declining over time (*Supplementary Fig. 3A*). In addition, the stability of the LTR promoter in driving GFP expression over time p.-i. was assessed by infecting cells 24h p.-s. and monitoring fluorescent reporter expression at 23h, 47h, 71h, 95h, 119h and 143h p.-i. (*Supplementary Fig. 3B-D*). In this context, GFP expression accumulated to peak at 47h p.-i. and then tended to decline with time, in particular with HIV envelopes, likely due to death of infected cells.

As expected, our data showed that CD4+ T cell permissiveness to HIV was higher upon TCR-mediated stimulation, in particular between 24 and 72h p.-s. Despite permissiveness differences among donor cells, similar kinetics were overall observed.

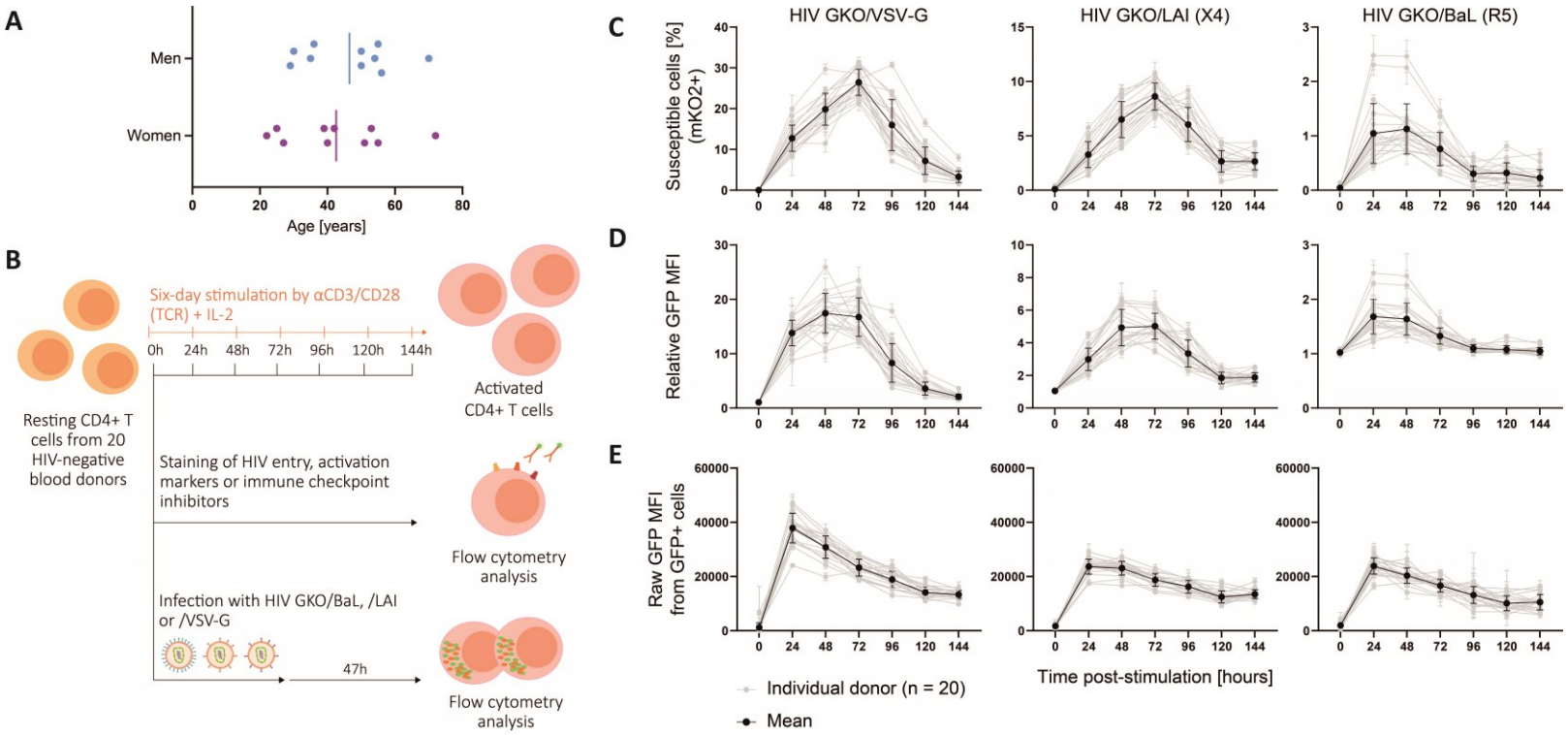

Figure 1: Cell permissiveness to HIV evolves with cell activation dynamics. (A) Panel of 20 HIV-negative blood donors included 10 men and 10 women of age ranging from 22 to 72 years old. The vertical bar represents the mean age for men and women respectively. (B) Resting CD4+ T cells from 20 HIV-negative blood donors were stimulated with αCD3/CD28 in presence of IL-2 during 144h. Each 24h, cells were collected and were either stained for cell surface proteins or infected with the HIV GKO dual reporter vector. Activation state was tracked by measuring cell surface protein expression of activation and ICIs as well as HIV entry receptors by fluorophore-conjugated antibody staining. Each staining was performed in duplicates and assessed by flow cytometry. In parallel, cells were infected with HIV GKO harboring distinct viral envelopes (VSV-G, X4-tropic LAI, R5-tropic BaL) in biological duplicates. Cell permissiveness to HIV was assessed 47h p.-i. by flow cytometry. (C-E) Infection success over time p.-s. for the three HIV GKO vectors harboring distinctive envelopes (VSV-G, LAI, BaL). Grey lines represent infection kinetics obtained for each individual donor and is the mean of biological duplicates. Black line represents the mean of all donors. Error bars represent the SD. (C) Proportion of cells susceptible to HIV infection was assessed by cells expressing EF1α-driven mKO2. (D) Global cell population permissiveness to HIV was assessed as relative GFP MFI, normalized by the corresponding mock-infected control, informing success of entry, integration and productive LTR-driven GFP expression (E) Intracellular permissiveness level was assessed by measuring the raw GFP MFI in GFP+ cells. p.-i., post-infection; p.-s., post-simulation; SD, standard deviation; MFI, Mean Fluorescence Intensity.

Sex and age impact CD4+ T cell susceptibility to HIV infection

To study the impact of specific features such as sex and age on CD4+ T cell permissiveness to HIV, data were re-analyzed according to these parameters. Comparison of HIV infection kinetics between women and men cells revealed that infection kinetics were similar between both sexes, but that men harbored increased numbers of susceptible cells compared to women between 24-72h p.-s., in the time window where cells were previously identified as being most permissive (*Fig. 2A*). This difference was significant for both VSV-G- and LAI-mediated entry (*, $p = 0.01$), but not for BaL-mediated entry ($p = 0.87$), whose interpretation is complicated by the low level of infection success. Permissiveness as reflected by GFP revealed increased levels in men cells and showed significance for VSV-G-mediated entry and a trend for LAI-mediated entry (HIV GKO/VSV-G, * $p = 0.02$; HIV GKO/LAI, $p = 0.05$; HIV GKO/BaL, $p = 0.07$) (*Supplementary Fig. 4A*). However, intracellular GFP levels were similar between sexes (HIV GKO/VSV-G, $p = 0.26$; HIV GKO/LAI, $p = 0.17$; HIV GKO/BaL, $p = 0.55$) (*Supplementary Fig. 4B*).

The impact of age on cell susceptibility to HIV was evaluated by analyzing the proportion of mKO2+ susceptible cells in young (< 50 years old) and old donors (≥ 50 years old) (*Fig. 2B*). As for sex impact analysis, the kinetics of susceptibility displayed by each age category was comparable over time. However, when focusing on the 24-72h window p.-s., older donors exhibited an increased susceptibility to infection compared to younger ones. Although significant for LAI (X4)-using virus (*, $p = 0.01$), only a non-significant trend can be observed for BaL (R5)-tropic virus ($p = 0.14$), and no impact is visible for viruses entering via the VSV-G route ($p = 0.15$). Consistently, permissiveness levels were increased upon LAI (X4)-tropic infection (*, $p = 0.03$) but not for BaL- ($p = 0.12$) or VSV-G- ($p = 0.09$) mediated entry (*Supplementary Fig. 4C*). Intracellular GFP levels were similar between young and old donors with each virus (HIV GKO/VSV-G, $p = 0.27$; HIV GKO/LAI, $p = 0.37$; HIV GKO/BaL, $p = 0.76$) (*Supplementary Fig. 4D*). Similar results were obtained when age was treated as a continuous variable (*Supplementary Fig. 5A-C*). For both sex and age impact, our results suggest that the difference occurs during entry, integration and productive LTR-driven GFP expression.

Data were further dissected to interrogate the impact of sex and age combination, looking at the area under the curve (AUC) displayed by susceptible cells during the relevant 24h-72h p.-s. window (*Fig. 2C*). At first, single previous results were recapitulated, *i.e.* male cells displaying increased susceptibility to VSV-G-mediated HIV entry as compared to female cells (**, $p = 0.004$), and cells isolated from older donors showing enhanced susceptibility to LAI (X4)-mediated HIV entry (*, $p = 0.03$). Analysis of HIV GKO/LAI (X4) infection was particularly interesting. Indeed, although male cells only tended to display enhanced susceptibility to viral infection compared to female cells ($p = 0.07$), combination of sex and age revealed gradual susceptibility to HIV GKO/LAI infection with the lowest AUC displayed by younger women and the highest by older men (*, $p = 0.02$). This effect could not be observed when using HIV GKO/BaL (R5) potentially because of the low infection success rate in this setting.

The effect of sex and age was investigated similarly on latency establishment by assessing the AUC corresponding to the proportion of latently infected cells (mKO2+ GFP-) over total infected cells (mKO2+) in the 24h-72h p.-s. window (*Fig. 2D*). Although sex did not appear to affect latent infection mediated by VSV-G entry, data suggest that age impacted the proportion of latently infected cells, with younger donors displaying higher AUC upon VSV-G- and LAI-mediated HIV entry (*, $p = 0.003$ and *, $p = 0.002$, respectively), but not upon BaL-mediated HIV entry ($p = 0.65$).

Sex and age impact on GFP expression stability was also controlled in p.-i. settings. Male cells displayed an enhanced GFP production over total time of infection, with all three vectors (HIV GKO/VSV-G, * $p = 0.03$; HIV GKO/LAI, ** $p = 0.003$; HIV GKO/BaL, ** $p = 0.004$), reflecting an increased HIV protein production (*Supplementary Fig. 6A*). This was shown as well for older donor cells, except upon HIV GKO/VSV-G infection (HIV GKO/VSV-G, $p = 0.34$; HIV GKO/LAI, ** $p = 0.001$; HIV GKO/BaL, ** $p = 0.001$) (*Supplementary Fig. 6B*). Finally, AUC of latent cell rate in time p.-i. (as reflected by rate of mKO2+ GFP- cells over total mKO2+ cell population) was significantly increased in younger donors upon infection with the three vectors (HIV GKO/VSV-G, ** $p = 0.002$; HIV GKO/LAI, ** $p = 0.003$; HIV GKO/BaL, ** $p = 0.01$) (*Supplementary Fig. 6C*). Overall, these data are complementary to the infection success measured as the proportion of susceptible cells (mKO2+) or global permissiveness (mKO2+ GFP+).

Altogether, these data suggest that sex and age impact cell permissiveness to HIV infection *in vitro*, depending on the viral entry route. Globally, male and old donor cells displayed increased susceptibility and showed increased permissiveness to HIV infection (VSV-G- and/or LAI-mediated entry), reflecting a more favorable environment for HIV entry, integration and viral protein production. Consistently, young donor cells appear to favor latent infection.

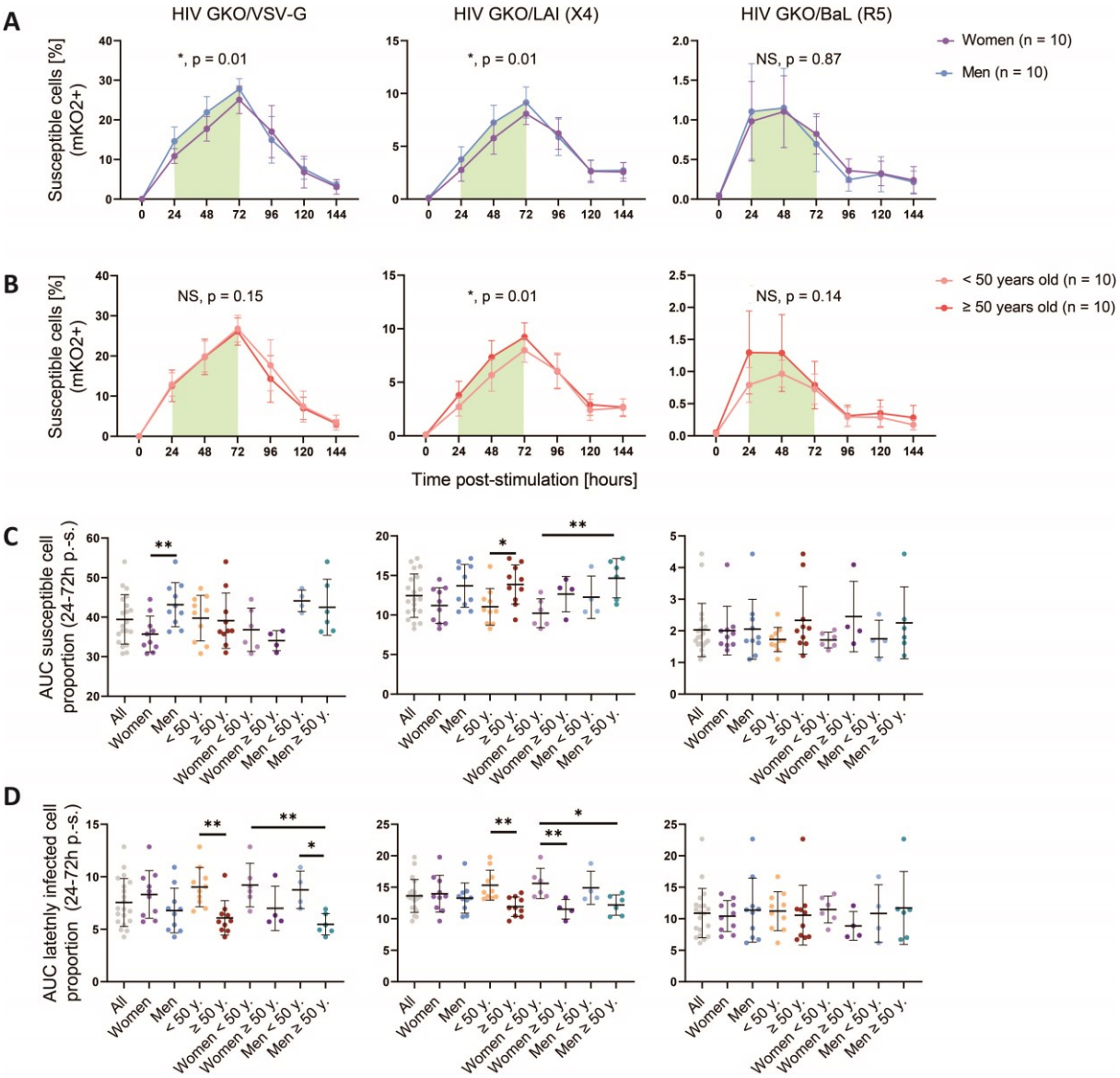

Figure 2: Sex and age impact CD4+ T cell susceptibility to HIV infection. (A, B) Proportion of susceptible cells (mKO2+) over time p.-s. for the three HIV GKO reporters (VSV-G, LAI (X4), BaL (R5)), separated according to sex (women: purple; men: blue) (A) or according to age (<50 years old: pale orange; ≥50 years old: red) (B). Lines represent the mean of each category per time point. Error bars represent SD. Statistical differences were calculated between 24 and 72h p.-s. (indicated by the green box) using paired t-test. (C, D) Proportion of susceptible (mKO2+) cells (C) or latently infected cells (mKO2+ GFP- over mKO2+ population) (D) to HIV, calculated as AUC between 24 and 72h p.-s., and according to multiple donor categories. Infection was performed with the three HIV GKO vectors (VSV-G, LAI (X4), BaL (R5)). Each dot represents the mean of biological duplicates of one donor. Statistical differences between sex and age were calculated by two-way ANOVA. * $p < 0.05$, ** $p < 0.01$. p.-s., post-stimulation; SD, standard deviation; AUC, area under curve; ANOVA, analysis of variance.

Activation-induced marker expression is biased by sex and age and correlate with cell permissiveness to HIV

Cellular activation is a pivotal parameter in cell permissiveness to HIV infection. To address whether cell activation features might explain sex- and age-specific differences observed in cell permissiveness to HIV, we monitored the expression of selected activation markers (CD69, CD25 and HLA-DR) and ICIs (PD-1, CTLA-4 and TIM-3), as well as HIV entry receptors (CD4, CXCR4 and CCR5) over time. Cell rate of expression of

HIV entry receptors showed no sex-specific bias (CD4, $p = 0.99$; CXCR4, $p = 0.86$; CCR5, $p = 0.46$) (*Fig. 3A*), suggesting that they do not account for the observed differences. Analysis of activation markers showed that male cells expressed significantly more CD69+ and CD25+ cells upon TCR-mediated stimulation than female cells (CD69 *, $p = 0.003$; CD25 *, $p = 0.03$). However, HLA-DR displayed no sex-specific bias ($p = 0.16$). Consistent with activation marker data, the three ICIs were expressed on a significantly larger proportion of cells in men (PD-1, **, $p < 0.0001$; CTLA-4, **, $p = 0.003$; TIM-3, *, $p = 0.02$). Similarly, age-differentiated analysis of activation kinetics showed a significant higher proportion of cells from older donors expressing activation markers and ICIs CD25 (*, $p = 0.02$), HLA-DR (***, $p = 0.0002$) and CTLA-4 (**, $p = 0.007$) (*Fig. 3B*). Importantly, CD4 and CXCR4 were present in a larger proportion of cells derived from older donors (CD4, *, $p = 0.01$); CXCR4, *, $p = 0.02$), and it cannot be excluded that they might account for the HIV susceptibility difference, they were expressed by >95% cells, resulting in a quasi-ubiquitous availability of HIV receptors.

To assess whether expression of these markers was linked to cell permissiveness to HIV, we correlated relative cell surface protein expression with relative GFP expression of HIV-infected cells over time p.-s. for all three HIV GKO viruses for each donor separately and found positive correlations with activation markers and ICIs (*Fig. 3C*). CTLA-4 expression kinetics correlated well with infection kinetics from HIV GKO/VSV-G ($p < 0.05$ in 20/20 donors, mean R-square = 0.86) and HIV GKO/LAI ($p < 0.05$ in 18/20 donors, mean R-square = 0.74), whereas the correlation was only partial with HIV GKO/BaL ($p < 0.05$ in 12/20 donors, mean R-square = 0.75). PD-1 relative expression displayed a high correlation with infection through LAI-mediated entry ($p < 0.05$ in 17/20 donors, mean R-square = 0.80), and a milder one through VSV-G-mediated entry ($p < 0.05$ in 10/20 donors, mean R-square = 0.65). CD69 was only found to exhibit a significant correlation with virus infection using BaL-mediated entry ($p < 0.05$ in 18/20 donors, mean R-square = 0.86); potentially highlighting a higher dependence of R5-tropic viruses to cells in early activation.

In summary, these data identified sex- and age-specific differences on activation kinetics, as revealed through expression of selected activation markers and ICIs. In particular, male and older donor cells shown to display higher cell permissiveness also displayed higher marker expression levels. Moreover, we highlighted that relative expression kinetics of CD69, PD-1 and CTLA-4 correlated with permissiveness to HIV on an entry-dependent mode.

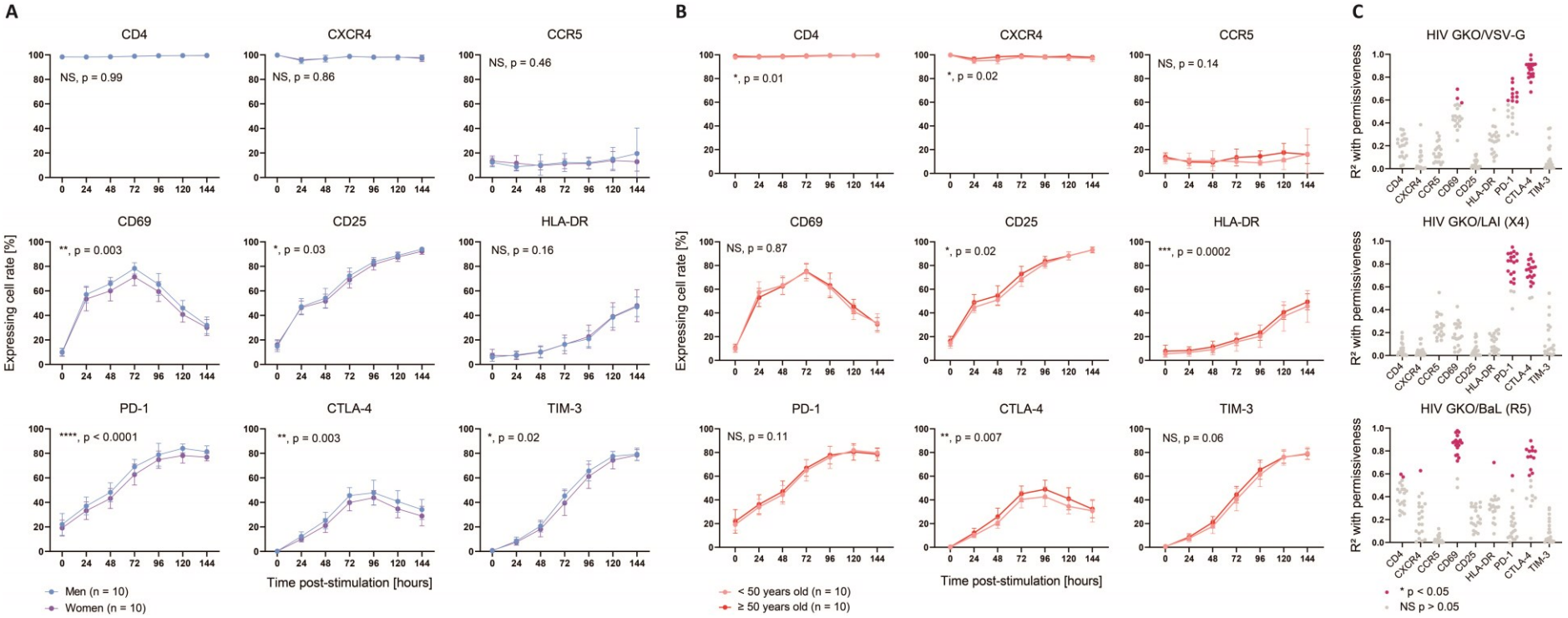

Figure 3: Activation-induced marker expression is biased by sex and age and correlate with permissiveness to HIV. (A, B) Proportion of cells expressing selected cell surface proteins over time p.-s. Proteins analyzed include HIV entry markers (CD4, CXCR4 and CCR54; upper graphs), activation markers (CD69, CD25 and HLA-DR; middle graphs) and ICIs (PD-1, CTLA-4 and TIM-3; lower graphs). Lines represent the mean of each category per time point. Error bars represent SD. Statistical differences were calculated using paired t-test. (A) Surface maker expression according to sex. Women are represented in purple and men in blue. (B) Surface marker expression according to age. Donors younger than 50 years old are represented in pale orange and donors being 50 years old or older in red. (C) Correlation analysis between protein surface expression (MFI of stained sample normalized to corresponding non-stained sample) and permissiveness to HIV (relative GFP MFI, normalized to corresponding mock-infected sample) for the three HIV GKO vectors (top: VSV-G; middle: LAI (X4); bottom: BaL (R5)) throughout activation kinetics. Each dot represents R-square value calculated by linear regression for one donor with the mean of infection duplicates and staining duplicates. Non-significant correlations ($p > 0.05$) are represented in grey and significant ones (*, $p < 0.05$) in pink. p.-s., post-stimulation; SD, standard deviation; MFI, Mean Fluorescence Intensity.

CD4+ T cell pool composition is not biased by sex

To address whether sex bias in permissiveness to HIV could be linked to CD4+ T cell subpopulation composition, we stimulated cells from two female and two male donors for 24h and performed single-cell-RNA-Seq (sc-RNA-Seq). We investigated a total of 24,626 single cells and mapped them against three different references (*i.e.* DICE [22], Monaco [23] and Seurat [24]) (*Fig. 4A, Supplementary Table 1*). As each database was constructed using different experimental protocols and addressed different layers of CD4+ T cell subpopulations, it allows to have a comprehensive understanding of the subpopulation distribution, at the subtype and differentiation stage levels. DICE annotation did not identify any sex-specific subpopulation enrichment and revealed that naïve stimulated T cells represented more than 65% of cells in both sexes (*Fig. 4B*). Other cell types including memory T regulatory (Treg), naïve, naïve Treg, Tfh, Th1, Th1/Th17, Th17 and Th2 accounted only for minor cell fractions. Consistently, annotation with Monaco reference did not reveal any sex bias either. This latter dataset showed an enrichment of Treg and Th1/Th17, followed by naïve and Th1. The remaining cells were split between Tfh, T terminal effector (Tte), Th17 and Th2. Finally, Seurat annotation showed comparable enrichment of CD4+ T cell subpopulations between men and women, with T central memory (Tcm) representing more than 70% of cells in both, and the rest being divided between cytotoxic T lymphocytes (CTL), naïve, proliferating, T effector memory (Tem) and Treg.

Overall, comparison of our four donors with the three reference databases and the 23 annotated subtypes did not reveal sex-specific cell subtype distribution, suggesting that the differential permissiveness to HIV between male and female cells cannot be explained by cellular subpopulation composition.

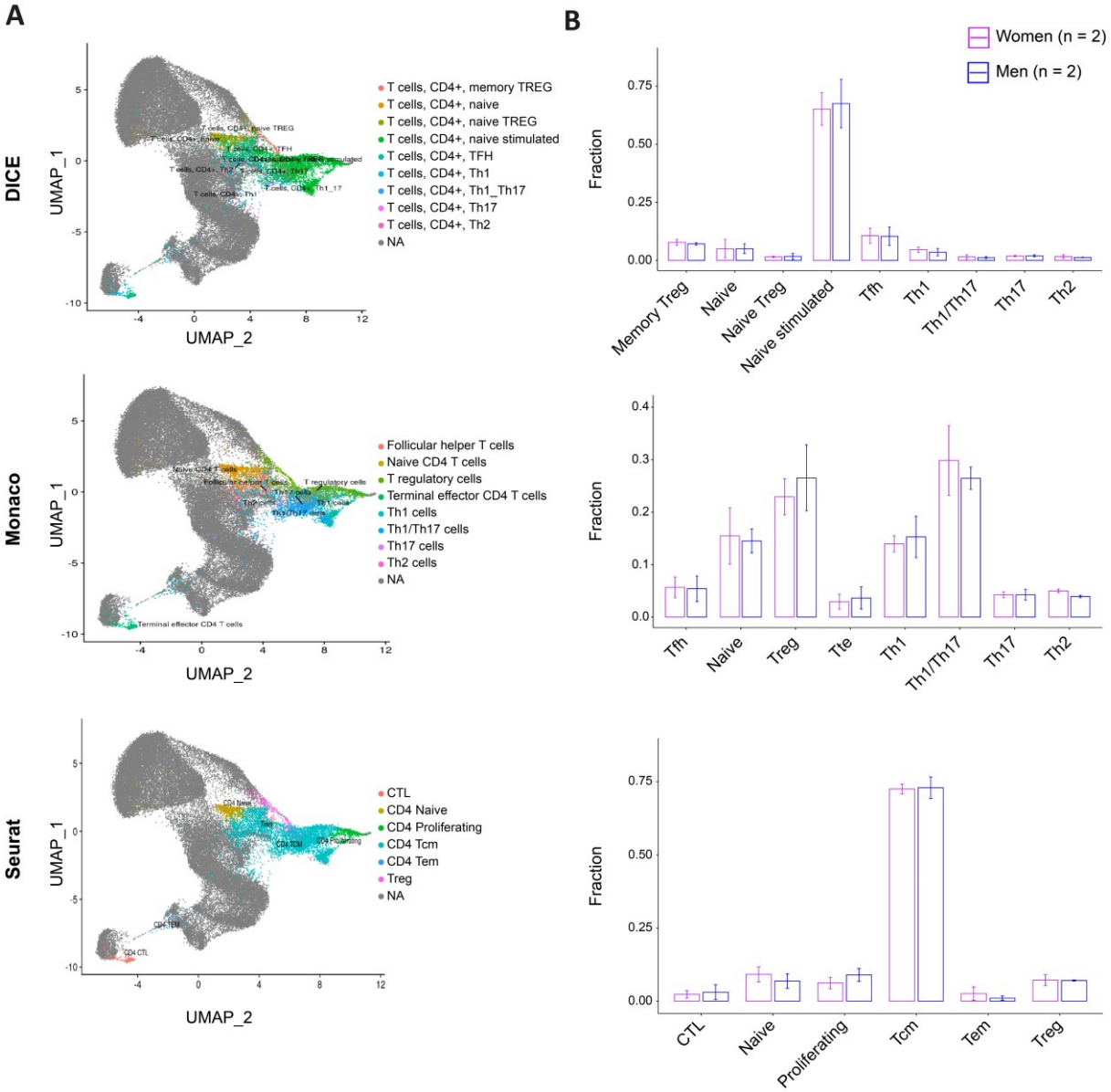

Figure 4: CD4+ T cell pool composition is not biased by sex. Single-cell distribution was assessed by three reference datasets: DICE (top), Monaco (middle) and Seurat (bottom). (A) UMAP projections of our four-donor cell distribution pattern (colored) on reference datasets (grey). (B) Cell subtype fraction by sex, and according to corresponding database annotation (top: DICE; middle: Monaco; bottom: Seurat). Women are represented in purple and men in blue, Error bars represent SD. Statistics were calculated using t-test, which reported no significant p-value for all comparisons. UMAP, uniform manifold approximation and projection; SD, standard deviation; Treg, regulatory T cells; Tfh, T follicular helper; Th1, T helper 1; Th17, T helper 17; Th2, T helper 2; Tte, T terminally differentiated; CTL, cytotoxic T lymphocyte; Tcm, T central memory; Tem, T effector memory.

Identification of sex-specific gene expression and of sex and age impact on activation-linked pathways

To further investigate and identify the cellular determinants responsible for donor-related permissiveness to HIV, we stimulated CD4+ T cells from each donor for 24 or 72h hours and performed transcriptomic analyses. Principal component analysis (PCA) revealed that 71% of variance between samples was linked to activation as expected, while 4% was attributed to sex (*Fig. 5A*). Interestingly, samples derived from men were grouped independently of age, while those derived from women tended to cluster by age

categories. Over a total of 13,154 detected genes, differential gene expression analysis (DGEA) between men and women cells at 24h p.-s. outlined 28 differentially expressed genes (DEG). Top DEG genes were mostly linked to X and Y chromosomes, with X-linked genes enriched in women, and Y-linked genes enriched in men and absent in women as expected (*Fig. 5B*). To ensure a balanced biological function between sexes, most X- and Y-linked genes unrelated to reproductive functions harbor a corresponding paralog on the other chromosome. As most DEG between men and women are linked to sex chromosomes, we interrogated the combined expression of corresponding paralogs in both sexes (*Fig. 5C*). At 24h p.-s., 5 out of the 9 gene pairs presented a differential average expression in function of sex, with EIF1AY/EIF1AX (p = 1.4 x 10^{-10}), RPS4Y1/RPS4X (p = 6.3 x 10^{-6}), DDX3Y/DDX3X (p = 7.8 x 10^{-6}) and PRKY/PRKX (p = 0.0065) that were enriched in women, while USP9Y/USP9X (p = 2.9 x 10^{-7}) were enriched in men. The translation of differential gene expression on functional pathway regulation was then assessed by hallmark gene set enrichment analysis (GSEA) (*Fig. 5D and E*). Interrogation of all donors by sex did not result in any significantly enriched pathway. As this may be the result of age-dependent variation, functional analyses of sex-induced effect were evaluated within each age class (*Fig. 5D*). Most variable effect was observed within the L2 category (36-52 years old) 24h p.-s. with 156 DEG, enriching pathways related to activation or cell cycle as MYC targets, mTORC1 signaling, E2F targets, glycolysis or IL-2/STAT5 signaling in men compared to women, while IFN-α response was enriched in women. Similar results were outlined in L1 category (21-35 years old), with enrichment of E2F targets and G2M checkpoint. However, L3 category (53-72 years old) yielded the opposite trend with a negative enrichment score of activation-linked pathways. These data support that activation is strengthened in men compared to women in L1 and L2 categories. Assessment of stimulation effect outlined 5266 DEG when comparing 72h to 24h stimulation in women (*Supplementary Fig. 7A*) and showed functional enrichment of similar pathways, demonstrating upregulation of genes linked to activation and cell cycle, together with a downregulation of innate immunity (*Supplementary Fig. 7B*). Similar results were observed in men cells (data not shown). Since men samples clustered together regardless of age but women samples did not, the effect of age was further evaluated in women samples by comparing hallmark enrichments between each age category at 24h p.-s. (*Fig. 5E*). Comparison of L3 category with either L2 or L1 showed enrichment of E2F targets, G2M checkpoint, MYC targets, glycolysis or mTORC1 signaling, suggesting an enhanced activation potency in older women compared to younger ones. Comparison of L2 with L1 presented more variable results, with enrichment in L2 of E2F targets and G2M checkpoints, while mTORC1 signaling or IL-2/STAT5 signaling were enriched in L1.

Altogether, these results suggest that sex and age influenced cellular transcriptome of CD4+ T cells. We evidenced biased combined expression of paralogs on X and Y chromosomes by sex, as well as an enrichment of activation-linked pathways in donor categories most susceptible to HIV infection (men and older donors), suggesting that enhanced permissiveness to HIV is related to enhanced activation potency.

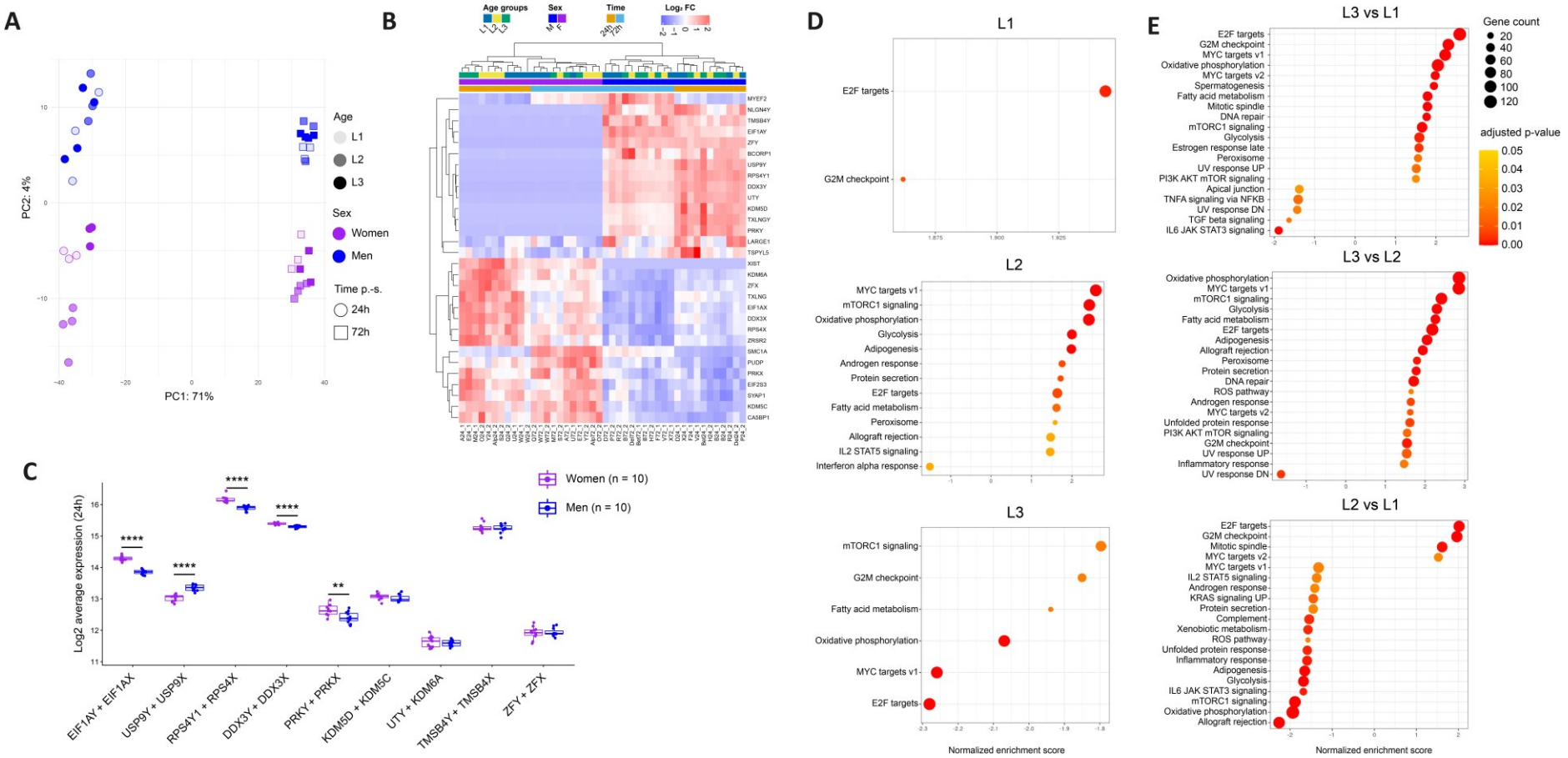

Figure 5: Identification of sex-specific gene expression and of sex and age impact on activation-linked pathways. (A) PCA plot with explained percentage of variance between cell sample transcriptomes. CD4 + T cells were stimulated for 24h (circles) or 72h (squares). Women samples are depicted in purple and men samples in blue. Age is represented by color intensity (22-35 years old in light shade (L1), 36-52 in medium shade (L2) and 53-72 in dark shade (L3)). (B) Top differentially expressed genes between men and women cells at 24h p.-s. The $\log_2$ FC of each gene compared to its average expression is represented in shades of blue to red. (C) Combined expression at 24h p.-s. of Y-linked genes and their X chromosome paralogs in men (in blue) and in women (in purple). Statistical differences were calculated by t-test. **** $p < 0.0001$, ** $p < 0.01$. (D, E) Hallmarks of gene set enrichments. P-values are represented by significance in orange to red shades. Gene count per pathway is represented by circle size. (D) Men compared to women at 24h p.-s. by age category. (E) Age comparisons in women at 24h p.-s. PCA, Principal Component Analysis; DEG, differentially expressed gene; p.-s., post-stimulation; FC, fold-change.

Discussion

HIV-infection success of CD4+ T cells was proven to differ between individuals for more than two decades, but so far most efforts focused on identifying cell features involved in permissiveness *per se* but lacked individual-related considerations, such as sex or age [25, 26]. In this study, we hypothesized that both factors could impact permissiveness to HIV in a CD4+ T cell activation kinetics. We thus first tracked activation levels and permissiveness phenotype differentially according to sex or age. In a second phase, we deciphered sex- and age-specific transcriptomic landscapes to identify gene correlates with cell permissiveness to HIV.

We isolated and stimulated primary CD4+ T cells from 20 HIV-negative blood donors over a 6-day (144h) period and infected them with HIV GKO dual reporter (EF-1α-mKO2 and LTR-GFP) pseudotyped with VSV-G (amphotropic), BaL (R5-tropic) or LAI (X4-tropic) envelopes. Consistent with previous reports, HIV infection success increased with time p.-s. [27]. In our experimental system, cells were most permissive between 24 and 72h p.-s., and kinetics were dependent on the viral envelope. Viral entry upon VSV-G pseudotyping was not limited by expression of HIV receptors and therefore reflects permissiveness dictated by the intracellular environment, while the use of BaL and LAI envelopes also relied on expression of HIV entry receptors. Our data showed that cell susceptibility kinetics to HIV GKO/LAI was similar to HIV GKO/VSV-G, which suggests that receptors exploited upon LAI-mediated entry were not limiting infection. Conversely, susceptibility kinetics to HIV GKO/BaL appeared shifted to a day earlier, suggesting that CCR5 low levels were a limiting factor, impairing efficient infection. Importantly, vectors harboring HIV envelopes displayed reduced infection rates compared to that harboring VSV-G envelope. In addition, HIV GKO lacks Nef, resulting in decreased uncoating efficiency upon infection with native HIV envelopes but not VSV-G [28].

Upon differential analysis of infection by sex, we showed that CD4+ T cells derived from men displayed an increased susceptibility to HIV within the most permissive 24-72h time window. Analysis performed *ex vivo* on cells derived from people living with HIV evidenced reduced HIV RNA synthesis in cells from women [12]. For the first time, our study enabled to recapitulate these findings in an *in vitro* infection model, suggesting that it can be the result of intrinsic cellular composition, without immune mediation, at least in part. As the size of the latent reservoir was estimated to be comparable between men and women, it would imply an enhanced HIV-killing of infected cells in men [12]. Thus, our study could not reproduce conclusions from the collaborations between Bosque and Planelles groups that did not find a sex-specific impact on the susceptibility to HIV in CD4+ T cells [29, 30]. However, some differences in the experimental design may explain these discrepancies. Indeed, while we used total fraction of CD4+ T cells, both studies used memory CD4+ T cells exclusively, potentially implying that the sex bias found in our study may not be imputed to the memory cell fraction. Our work evidenced a sex bias upon HIV infection mediated by VSV-G or LAI envelope, but not BaL. This could likely be explained by the reduced infection success by HIV GKO/BaL, as the peak of infection was 1.1% on average, and as the controlled expression of fluorescent reporters over time p.-i. showed that it was significantly higher in male cells

for the three entry modes. As for age, given the extent of immune-related changes in later life, it was possible to envision implications on HIV infection. Yet, studies on a direct impact of age on cellular susceptibility to HIV are still lacking, as only one decreasing association was observed between age and HIV replication rate in memory CD4+ T cells from women [30]. Our analysis outlined donors aged 50 years or older as displaying an increased susceptibility to HIV infection in the most permissive 24h-72h time window, significant only upon LAI-mediated HIV entry. Again, the low infection efficiency did not allow identifying a significant impact in the BaL setting. Similar to sex analysis, controlled expression of fluorescent reporters over time p.-i. resulted in significantly higher levels in older donor category upon entry mediated by both HIV envelopes. However, no effect of age was observed upon VSV-G entry, suggesting that age-dependent differences are related to gp120-induced signaling cascade.

Upon kinetics of TCR-mediated stimulation, we found a higher proportion of CD4+ T cells from men compared to women expressing CD69, CD25, PD-1, CTLA-4 and TIM-3, as well as higher expression of CD25, HLA-DR and PD-1 in donors aged 50 or more compared to younger ones, all of which are surface markers upregulated upon activation. In addition, we found positive correlations between kinetics of CD69, CTLA-4 and PD-1 relative expression and cell permissiveness to HIV with at least one of the three used viral reporters. These results suggest that higher permissiveness of cells derived from men or older donors is notably due to higher activation. Indeed, we showed that as activation progressed, innate immunity downregulated and transcriptional activity increased, likely explaining increasing HIV permissiveness. Importantly, a previous study found the opposite gender bias in activation, with female CD4+ T cells exhibiting higher CD69 expression [31]. We think that this outcome may originate from stimulation method, where phytohemagglutinin (PHA) was employed, while we used anti-CD3/CD28 and IL-2 in the present study. Given that the signaling transduced by the two stimulation methods are different, with PHA crosslinking CD3 without inducing CD28 costimulation, they could result in different outcomes. This supports that the stimulation method must be selected with care, as two methods can result in an opposite pattern.

Single-cell analysis with 23 subtype annotations of CD4+ T cell pool composition exhibited no sex-specific enrichment of any subpopulation, which suggests that the difference in permissiveness to HIV is not attributed to a specific subtype but rather to a cellular state. While previous studies evidenced higher levels of Th1 and Th2 in women and higher Th17 and Treg in men, our results did not recapitulate these findings [5]. However, this analysis may necessitate an increased number of donors in order to reveal a statistically significant tendency. This could also be the result of the stimulation method used, *i.e.* TCR-mediated in presence of IL-2, which affects subtype composition as compared to antigen-antigen presenting cell complex [32]. Switch of stimulation method might thus favor differentiation of specific subtypes and reveal sex bias in sc-RNA-Seq.

Transcriptomic analyses outlined a differential sex and age regulation in CD4+ T cells prior exposure to HIV, with DEG linked to sex chromosomes in men compared to women. To potentially compensate the absence of X- or Y-linked genes, most of the

genes identified in the present study harbored a paralog displaying a conserved function on the other sex chromosome [33]. Combined expression of both paralogs showed a sex bias in the average expression, with increased levels of EIF1AY/EIF1AX, DDX3Y/DDX3X, RPS4Y1/RPS4X and PRKY/PRKX in women. Interestingly, EIF1A, DDX3 and PRKX were demonstrated to enhance HIV replication, suggesting that their activity is not sufficient to counter the sex bias in HIV susceptibility [34-36]. Previous studies identified RPS4 as interfering with RRE in HIV and as associated with decreased hepatitis C virus replication, making it a potential HIV inhibitory factor [37, 38]. Conversely, USP9Y/USP9X levels were increased in men. A facilitating role was shown in gammaherpesvirus, but a putative interaction with HIV remains to be deciphered [39]. Our transcriptomic data also showed that donor categories displaying enhanced HIV susceptibility presented enriched cellular pathways linked to activation and cell cycle, which might explain higher permissiveness to HIV. Of note, upon sex comparison, we found enrichment of these pathways in L1 (22-35 years old) and L2 (36-52 years old) categories but not in L3 (53-72 years old). This suggests that sex bias in activation is linked to reproductive period in women, with hormone exposure participating in reducing activation in women, which no longer impacts it after menopause. Indeed, this hypothesis is supported by the fact that progesterone was recently shown to dampen activation in CD4+ T cells [40]. Comparison of L2 and L1 categories yielded variable results, suggesting that there is more variability within these categories, which is probably the result of differential hormonal regulation, that can be influenced by state of hormonal cycle and recent pregnancy. Future studies should consider steroid hormone in the role of cellular activation and permissiveness to HIV.

In conclusion, this study outlined the importance of considering sex and age of donor cells in HIV infection studies and identified novel genes potentially impacting cell permissiveness. Future work should further confirm the role of these genes in HIV replication and identify potential links between individual activation potency and HIV latency reactivation. Indeed, deciphering reactivation mechanisms might help improving the spectrum of latency reactivation strategies and thus purging the reservoir.

Methods

Ethics statement

All blood donors have provided written informed consent and all samples were anonymized.

Cell samples, isolation and culture

Peripheral Blood Mononuclear Cells (PBMCs) from HIV-negative blood donors were purified from whole blood samples by Ficoll gradient separation, using Leucosep tubes (Greiner, Kremsmünster, Austria) according to manufacturer's recommendations. Following purification, PBMCs were frozen in heat-inactivated Fetal Bovine Serum (HI-FBS) with 7.5% dimethyl sulfoxide (DMSO, Merck, Darmstadt, Germany) in liquid nitrogen in cryotubes (Thermo Fisher Scientific, Waltham, MA, USA) for long-term storage.

Primary CD4+ T cells were isolated from PBMCs by negative-selection and magnetic separation using EasySep Human CD4+ T Cell Isolation Kit (Stemcell Technologies, Vancouver, Canada) according to manufacturer's instructions. They were cultured at a concentration of 10^6 cells/mL in RPMI-1640 (Thermo Fisher Scientific) supplemented with 10% HI-FBS (Thermo Fisher Scientific) and 50 µg/mL gentamicin (Thermo Fisher Scientific) at 37°C, 5% CO_2. One day after purification, CD4+ T cells were stimulated in T25 flask for four days by adding 25 µL/mL ImmunoCult Human CD3/CD28 T Cell Activator (Stemcell Technologies) in medium supplemented with IL-2 [200 IU/mL] (R&D Systems, Minneapolis, MN, USA). After four days, culture medium was replaced by fresh medium supplemented with IL-2 [200 IU/mL] and cells were cultured for two more days.

Virus production and infection

HIV-based lentiviruses LTR-HIV-Δ-env-nefATG-csGFP-EF-1α-mKO2 (referred as HIV GKO) were produced by co-transfection of 5 million HEK293T per 10-cm dish with 7.5 µg of HIV GKO (gift from Eric Verdin, provided by Matthieu Perreau, Addgene #112234 [21]) and 2.5 µg of one envelope plasmid using jetPRIME transfection reagent (Polyplus-transfection, Illkirch, France) according to manufacturer's recommendations. Culture medium was replaced by fresh 293 Serum Free Medium III (Thermo Fisher Scientific) supplemented with glutamax (Thermo Fisher Scientific) 8 hours post-transfection. Viral particles were collected 48h post-transfection and filtered using 0.22 µm filter (Merck). Viral titers were measured by p24 immunoassay using INNOTEST HIV Antigen mAb (Fujirebio, Tokyo, Japan) according to manufacturer's instructions.

Alternative envelopes were used: VSV-G encoded by pMD2.G plasmid (gift from Didier Trono, Addgene #12259 [41]), the X4-tropic LAI envelope encoded by pCI-X4 plasmid (gift from Robert Siliciano [42]), or the R5-tropic BaL envelope cloned in pCl-X4 backbone. For this latter construct, the LAI *env* sequence in pCI-X4 was substituted by the one in pNL4-3-BaL *env* [43] through KpnI-BlpI (New England Biolabs, Ipswich, MA, USA) restriction cloning. Single-reporter HIV-based lentiviruses for flow cytometry compensation were constructed through SgrAI-XmaI and BlpI-HpaI (New England Biolabs) restriction cloning for deletion of GFP and mKO2, respectively.

Cell permissiveness to HIV was monitored by GFP and mKO2 expression of primary CD4+ T cells infected at 0h, 24h, 48h, 72h, 96h, 120h and 144h p.-s. and assessed by flow cytometry at 47h p.-i. Additionally, cells were infected at 24h p.-s. and further monitored by flow cytometry at 23h, 47h, 71h, 95h, 119h and 143h p.-i. Briefly, this was performed by exposing 100,000 cells to 30 ng p24 equivalent of HIV GKO/VSV-G, or 100 ng HIV GKO/BaL and HIV GKO/LAI, or mock treatment, in a volume of 110 µL in a 96-well U bottom plate. Infections were carried out in presence of 4 µg/mL polybrene (Merck) and spinoculation (1500 g, 90 min, 25°C). After that, cells were washed and resuspended at 10^6 cells/mL in R10 supplemented with IL-2 [200 IU/L] and incubated for 47h. Cells were fixed in 200 µL CellFix 1X (Becton Dickinson, Franklin Lakes, NJ, USA) to monitor GFP and mKO2 expression.

Cell surface marker staining

Cell surface marker expression was assessed using fluorophore-conjugated antibody staining on 50,000 primary CD4+ T cells at 0h, 24h, 48h, 72h, 96h, 120h and 144h p.-s. Antibodies were purchased from Biolegend and aim at measuring marker expression involved in HIV entry (CD4, CXCR4, CCR5), cell activation (CD69, CD25, HLA-DR) and cell immune checkpoint inhibition (PD-1, CTLA-4, TIM-3) (*Supplementary table 2*). Briefly, cells were washed once using FACS buffer (Phosphate-buffered saline (PBS, Bichsel, Interlaken, Switzerland); 5% HI-FBS; 2 mM Ethylenediaminetetraacetic acid (EDTA, Thermo Fisher Scientific)) and incubated with the different antibodies according to manufacturer's recommendations during 30 min at 4°C. Cells were then washed with FACS buffer and fixed in 150 µL CellFix 1X. Marker expression was assessed by flow cytometry.

Flow cytometry

Flow cytometry analysis of infected samples and antibody-stained samples were performed using Gallios machine on 10,000 events (Beckman Coulter, Brea, CA, USA; Flow Cytometry Facility, University of Lausanne). Infection success was measured on channels 1 (GFP) and 2 (mKO2), and surface marker expression on channels 2 (PE) and 6 (APC). All flow cytometry graphs and analyses were generated using FlowJo (v.10.7.1) software (Becton Dickinson).

Statistical analyses

Statistical analyses and graphical distributions were performed using GraphPad Prism (v.9.1.0) software (GraphPad Software, La Jolla, CA, USA). Kinetic comparisons were performed using parametric paired t-test. Area under curve (AUC) measurements were compared using two-way analysis of variance (ANOVA) with a false discovery rate (FDR) method of Benjamini and Hochberg. Correlation analyses were made based on linear regressions.

Sc-RNA-Seq library preparation and sequencing

Cells resuspended in PBS supplemented with 0.04% bovine serum albumin (BSA) were loaded into a Chromium Next GEM chip K with a target capture of 10,000 cells per sample. Gene expression (GEX) libraries were generated using Chromium Next GEM Single Cell 5' Reagent Kit v2 (10X Genomics, Pleasanton, CA, US) according to manufacturer's recommendations and were then sequenced using NovaSeq 6000 (Illumina, San Diego, CA, US) by paired-end 100 nucleotides dual indexing protocol in Lausanne Genomic Technologies Facility (LGTF).

Sc-RNA-Seq analysis

Matrixes of GEX reads were generated by alignment and read count using CellRanger (10X Genomics, v.7.1). They were then loaded into R (v.4.2.0) and analyzed using Seurat package (v4) [24]. Briefly, samples were filtered for poor quality (expressing less than 200 transcripts and displaying more than 15% mitochondrial genes). Samples were then normalized using SCTransform and mapped against reference for generation of uniform manifold approximation and projection (UMAP) visualization and determination of

subtype composition. Cell types were annotated with Seurat multimodal reference mapping (reference data set [24]), and with the R package singleR [44]. DICE [22] and Monaco [23] were used as references annotations.

Population RNA-Seq library preparation and sequencing

Total RNA was extracted from 500,000 cells stimulated for 24h or 72h using Quick-RNA Miniprep Kit (Zymo Research, Irvine, CA, US) according to manufacturer's recommendations. Libraries were prepared using Illumina stranded mRNA protocol and sequenced using NovaSeq 6000 by single-read 100 nucleotide protocol in LGTF.

Population RNA-Seq analysis

Quality control, trimming of quality sequences and sequencing adaptors, and read alignment were performed using nf-core/rnaseq (v.3.12.0) from the nf-core workflow collection [45]. The pipeline was executed with Nextflow (v.23.04.1) [46]. Counts and transcripts per million were estimated using Salmon (v.1.5.2) [47], and the human reference genome GRCh38. Lowly expressed genes, with an average expression per condition of less than one count per million were removed from all conditions with the filtered.data function from the NOIseq R package (v.2.36.0) [48]. Differential gene expression analyses were performed using DESeq2, edgeR and limma [49-51] and used threshold of $p < 0.01$ and Log_2 fold-change > 0.5. P-values were adjusted for multiple comparisons by Benjamini and Hochberg method. Differentially expressed genes were considered when identified as such by the three algorithms. The p-value represented is the largest observed. GSEA [52] was performed with the clusterProfiler R package (v.4.2.2) [53] with the following parameters minGSSize = 10, maxGSSize = 1000, eps = 0, pvalueCutoff = 0.05. Pathways with an adjusted p-value < 0.05 were deemed as significantly enriched. Hallmark gene set for GSEA was obtained from MSigDB (v.7.5.1). Gene sets signature scores were computed using GSVA R package (v.1.44.5) [54], and signature scores for each donor and for significantly enriched pathways were plotted as heatmaps.

References

1. Gantner, P., Buranapraditkun, S., Pagliuzza, A., . . . Chomont, N., *HIV rapidly targets a diverse pool of CD4(+) T cells to establish productive and latent infections.* Immunity, 2023. **56**(3): p. 653-668 e5.
2. Cavrois, M., Banerjee, T., Mukherjee, G., . . . Roan, N.R., *Mass Cytometric Analysis of HIV Entry, Replication, and Remodeling in Tissue CD4+ T Cells.* Cell Rep, 2017. **20**(4): p. 984-998.
3. Luo, X., Frouard, J., Zhang, G., . . . Greene, W.C., *Subsets of Tissue CD4 T Cells Display Different Susceptibilities to HIV Infection and Death: Analysis by CyTOF and Single Cell RNA-seq.* Front Immunol, 2022. **13**: p. 883420.
4. Rato, S., Rausell, A., Munoz, M., . . . Ciuffi, A., *Single-cell analysis identifies cellular markers of the HIV permissive cell.* PLoS Pathog, 2017. **13**(10): p. e1006678.
5. Klein, S.L. and Flanagan, K.L., *Sex differences in immune responses.* Nat Rev Immunol, 2016. **16**(10): p. 626-38.

6. Wilkinson, N.M., Chen, H.C., Lechner, M.G., and Su, M.A., *Sex Differences in Immunity.* Annu Rev Immunol, 2022. **40**: p. 75-94.
7. Jacobsen, H. and Klein, S.L., *Sex Differences in Immunity to Viral Infections.* Front Immunol, 2021. **12**: p. 720952.
8. Unaids. *Global HIV & AIDS statistics — Fact sheet*. 2022 09.02.2023]; Available from: https://www.unaids.org/en/resources/fact-sheet.
9. Patel, P., Borkowf, C.B., Brooks, J.T., . . . Mermin, J., *Estimating per-act HIV transmission risk: a systematic review.* AIDS, 2014. **28**(10): p. 1509-19.
10. Sterling, T.R., Vlahov, D., Astemborski, J., . . . Quinn, T.C., *Initial plasma HIV-1 RNA levels and progression to AIDS in women and men.* N Engl J Med, 2001. **344**(10): p. 720-5.
11. Farzadegan, H., Hoover, D.R., Astemborski, J., . . . Vlahov, D., *Sex differences in HIV-1 viral load and progression to AIDS.* Lancet, 1998. **352**(9139): p. 1510-4.
12. Scully, E.P., Gandhi, M., Johnston, R., . . . Deeks, S.G., *Sex-Based Differences in Human Immunodeficiency Virus Type 1 Reservoir Activity and Residual Immune Activation.* J Infect Dis, 2019. **219**(7): p. 1084-1094.
13. Meier, A., Chang, J.J., Chan, E.S., . . . Altfeld, M., *Sex differences in the Toll-like receptor-mediated response of plasmacytoid dendritic cells to HIV-1.* Nat Med, 2009. **15**(8): p. 955-9.
14. Chang, J.J., Woods, M., Lindsay, R.J., . . . Altfeld, M., *Higher expression of several interferon-stimulated genes in HIV-1-infected females after adjusting for the level of viral replication.* J Infect Dis, 2013. **208**(5): p. 830-8.
15. Das, B., Dobrowolski, C., Luttge, B., . . . Karn, J., *Estrogen receptor-1 is a key regulator of HIV-1 latency that imparts gender-specific restrictions on the latent reservoir.* Proc Natl Acad Sci U S A, 2018. **115**(33): p. E7795-E7804.
16. Gianella, S., Rawlings, S.A., Nakazawa, M., . . . Karn, J., *Sex differences in HIV Persistence and Reservoir Size during Aging.* Clin Infect Dis, 2021.
17. Ruel, T.D., Zanoni, B.C., Ssewanyana, I., . . . Feeney, M.E., *Sex differences in HIV RNA level and CD4 cell percentage during childhood.* Clin Infect Dis, 2011. **53**(6): p. 592-9.
18. Scully, E.P., *Sex Differences in HIV Infection.* Curr HIV/AIDS Rep, 2018. **15**(2): p. 136-146.
19. Zhang, H., Weyand, C.M., and Goronzy, J.J., *Hallmarks of the aging T-cell system.* FEBS J, 2021. **288**(24): p. 7123-7142.
20. Gabuzda, D., Jamieson, B.D., Collman, R.G., . . . Hunt, P.W., *Pathogenesis of Aging and Age-related Comorbidities in People with HIV: Highlights from the HIV ACTION Workshop.* Pathog Immun, 2020. **5**(1): p. 143-174.
21. Battivelli, E., Dahabieh, M.S., Abdel-Mohsen, M., . . . Verdin, E., *Distinct chromatin functional states correlate with HIV latency reactivation in infected primary CD4(+) T cells.* Elife, 2018. **7**.
22. Schmiedel, B.J., Gonzalez-Colin, C., Fajardo, V., . . . Vijayanand, P., *Single-cell eQTL analysis of activated T cell subsets reveals activation and cell type-dependent effects of disease-risk variants.* Sci Immunol, 2022. **7**(68): p. eabm2508.
23. Monaco, G., Lee, B., Xu, W., . . . Larbi, A., *RNA-Seq Signatures Normalized by mRNA Abundance Allow Absolute Deconvolution of Human Immune Cell Types.* Cell Rep, 2019. **26**(6): p. 1627-1640 e7.
24. Hao, Y., Hao, S., Andersen-Nissen, E., . . . Satija, R., *Integrated analysis of multimodal single-cell data.* Cell, 2021. **184**(13): p. 3573-3587 e29.

25. Ciuffi, A., Bleiber, G., Munoz, M., . . . Telenti, A., *Entry and transcription as key determinants of differences in CD4 T-cell permissiveness to human immunodeficiency virus type 1 infection.* J Virol, 2004. **78**(19): p. 10747-54.
26. Brandt, L., Cristinelli, S., and Ciuffi, A., *Single-Cell Analysis Reveals Heterogeneity of Virus Infection, Pathogenicity, and Host Responses: HIV as a Pioneering Example.* Annu Rev Virol, 2020. **7**(1): p. 333-350.
27. Oswald-Richter, K., Grill, S.M., Leelawong, M., and Unutmaz, D., *HIV infection of primary human T cells is determined by tunable thresholds of T cell activation.* Eur J Immunol, 2004. **34**(6): p. 1705-14.
28. Yu, D., Wang, W., Yoder, A., . . . Wu, Y., *The HIV envelope but not VSV glycoprotein is capable of mediating HIV latent infection of resting CD4 T cells.* PLoS Pathog, 2009. **5**(10): p. e1000633.
29. Szaniawski, M.A., Spivak, A.M., Bosque, A., and Planelles, V., *Sex Influences SAMHD1 Activity and Susceptibility to Human Immunodeficiency Virus-1 in Primary Human Macrophages.* J Infect Dis, 2019. **219**(5): p. 777-785.
30. Macedo, A.B., Resop, R.S., Martins, L.J., . . . Bosque, A., *Influence of Biological Sex, Age, and HIV Status in an In Vitro Primary Cell Model of HIV Latency Using a CXCR4 Tropic Virus.* AIDS Res Hum Retroviruses, 2018. **34**(9): p. 769-777.
31. Abdullah, M., Chai, P.S., Chong, M.Y., . . . Vidyadaran, S., *Gender effect on in vitro lymphocyte subset levels of healthy individuals.* Cell Immunol, 2012. **272**(2): p. 214-9.
32. Tan, C., Wei, L., Vistica, B.P., . . . Gery, I., *Phenotypes of Th lineages generated by the commonly used activation with anti-CD3/CD28 antibodies differ from those generated by the physiological activation with the specific antigen.* Cell Mol Immunol, 2014. **11**(3): p. 305-13.
33. Godfrey, A.K., Naqvi, S., Chmatal, L., . . . Page, D.C., *Quantitative analysis of Y-Chromosome gene expression across 36 human tissues.* Genome Res, 2020. **30**(6): p. 860-873.
34. Rawle, D.J., Li, D., Swedberg, J.E., . . . Harrich, D., *HIV-1 Uncoating and Reverse Transcription Require eEF1A Binding to Surface-Exposed Acidic Residues of the Reverse Transcriptase Thumb Domain.* mBio, 2018. **9**(2).
35. Frohlich, A., Rojas-Araya, B., Pereira-Montecinos, C., . . . Soto-Rifo, R., *DEAD-box RNA helicase DDX3 connects CRM1-dependent nuclear export and translation of the HIV-1 unspliced mRNA through its N-terminal domain.* Biochim Biophys Acta, 2016. **1859**(5): p. 719-30.
36. De Martini, W., Rahman, R., Ojegba, E., . . . Chang, S.L., *Kinases: Understanding Their Role in HIV Infection.* World J AIDS, 2019. **9**(3): p. 142-160.
37. Naji, S., Ambrus, G., Cimermancic, P., . . . Gerace, L., *Host cell interactome of HIV-1 Rev includes RNA helicases involved in multiple facets of virus production.* Mol Cell Proteomics, 2012. **11**(4): p. M111 015313.
38. Tai, A.W., Benita, Y., Peng, L.F., . . . Chung, R.T., *A functional genomic screen identifies cellular cofactors of hepatitis C virus replication.* Cell Host Microbe, 2009. **5**(3): p. 298-307.
39. Chappell, D.L., Sandhu, P.K., Wong, J.P., . . . Damania, B., *KSHV Viral Protein Kinase Interacts with USP9X to Modulate the Viral Lifecycle.* J Virol, 2023. **97**(3): p. e0176322.
40. Hellberg, S., Raffetseder, J., Rundquist, O., . . . Gustafsson, M., *Progesterone Dampens Immune Responses in In Vitro Activated CD4(+) T Cells and Affects Genes*

Associated With Autoimmune Diseases That Improve During Pregnancy. Front Immunol, 2021. **12**: p. 672168.
41. Naldini, L., Blomer, U., Gallay, P., . . . Trono, D., *In vivo gene delivery and stable transduction of nondividing cells by a lentiviral vector.* Science, 1996. **272**(5259): p. 263-7.
42. Yang, H.C., Xing, S., Shan, L., . . . Siliciano, R.F., *Small-molecule screening using a human primary cell model of HIV latency identifies compounds that reverse latency without cellular activation.* J Clin Invest, 2009. **119**(11): p. 3473-86.
43. Meylan, P.R., Baumgartner, M., Ciuffi, A., . . . Sahli, R., *The nef gene controls syncytium formation in primary human lymphocytes and macrophages infected by HIV type 1.* AIDS Res Hum Retroviruses, 1998. **14**(17): p. 1531-42.
44. Aran, D., Looney, A.P., Liu, L., . . . Bhattacharya, M., *Reference-based analysis of lung single-cell sequencing reveals a transitional profibrotic macrophage.* Nat Immunol, 2019. **20**(2): p. 163-172.
45. Ewels, P.A., Peltzer, A., Fillinger, S., . . . Nahnsen, S., *The nf-core framework for community-curated bioinformatics pipelines.* Nat Biotechnol, 2020. **38**(3): p. 276-278.
46. Di Tommaso, P., Chatzou, M., Floden, E.W., . . . Notredame, C., *Nextflow enables reproducible computational workflows.* Nat Biotechnol, 2017. **35**(4): p. 316-319.
47. Patro, R., Duggal, G., Love, M.I., . . . Kingsford, C., *Salmon provides fast and bias-aware quantification of transcript expression.* Nat Methods, 2017. **14**(4): p. 417-419.
48. Tarazona, S., Furio-Tari, P., Turra, D., . . . Conesa, A., *Data quality aware analysis of differential expression in RNA-seq with NOISeq R/Bioc package.* Nucleic Acids Res, 2015. **43**(21): p. e140.
49. Love, M.I., Huber, W., and Anders, S., *Moderated estimation of fold change and dispersion for RNA-seq data with DESeq2.* Genome Biol, 2014. **15**(12): p. 550.
50. Chen, Y., Lun, A.T., and Smyth, G.K., *From reads to genes to pathways: differential expression analysis of RNA-Seq experiments using Rsubread and the edgeR quasi-likelihood pipeline.* F1000Res, 2016. **5**: p. 1438.
51. Ritchie, M.E., Phipson, B., Wu, D., . . . Smyth, G.K., *limma powers differential expression analyses for RNA-sequencing and microarray studies.* Nucleic Acids Res, 2015. **43**(7): p. e47.
52. Subramanian, A., Tamayo, P., Mootha, V.K., . . . Mesirov, J.P., *Gene set enrichment analysis: a knowledge-based approach for interpreting genome-wide expression profiles.* Proc Natl Acad Sci U S A, 2005. **102**(43): p. 15545-50.
53. Yu, G., Wang, L.G., Han, Y., and He, Q.Y., *clusterProfiler: an R package for comparing biological themes among gene clusters.* OMICS, 2012. **16**(5): p. 284-7.
54. Hanzelmann, S., Castelo, R., and Guinney, J., *GSVA: gene set variation analysis for microarray and RNA-seq data.* BMC Bioinformatics, 2013. **14**: p. 7.

Supplementary material

Supplementary figures

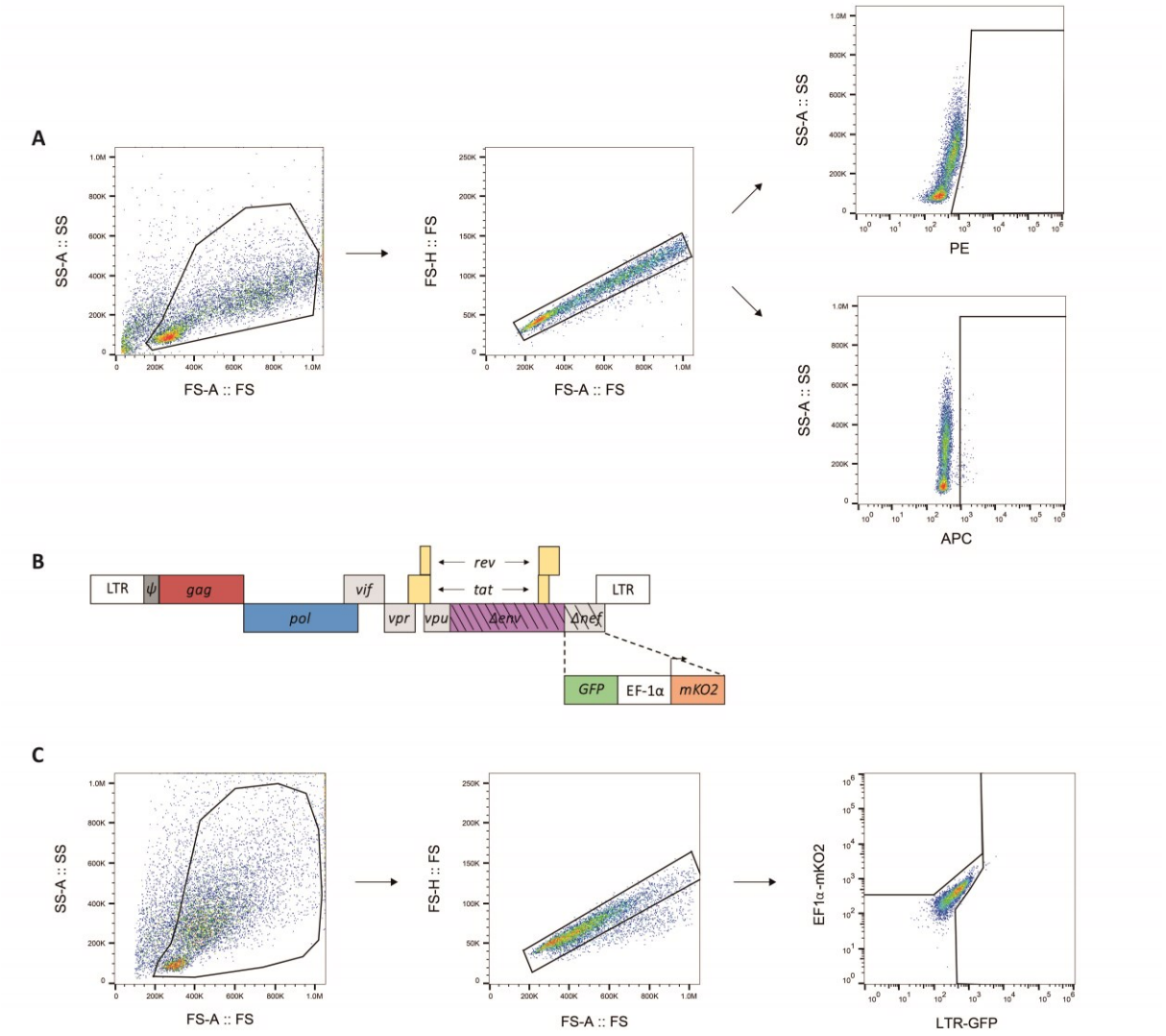

Supplementary Figure 1: Flow cytometry gating strategies and HIV GKO genomic structure. (A) Gating strategy for cell surface marker assessment. Living cells were gated on SS-A *vs* FS-A plot and single cells were selected on FS-H *vs* FS-A plot. Marker expression was assessed based on fluorochrome expression, *i.e.* PE or APC. (B) HIV GKO is a dual reporter expressing LTR-controlled GFP and EF1-α-controlled (constitutive) mKO2 in *nef* ORF and harboring deletion in *env*. (C) Gating strategy for infection monitoring. Living cells were gated on SS-A *vs* FS-A plot and single cells were selected on FS-H *vs* FS-A plot. Susceptible cells were measured based on mKO2 expression, permissive cells based on GFP expression and latent cells based on mKO2 expression and absence of GFP. SS, side scatter; FS, forward scatter; PE, phycoerythrin; APC, allophycocyanin.

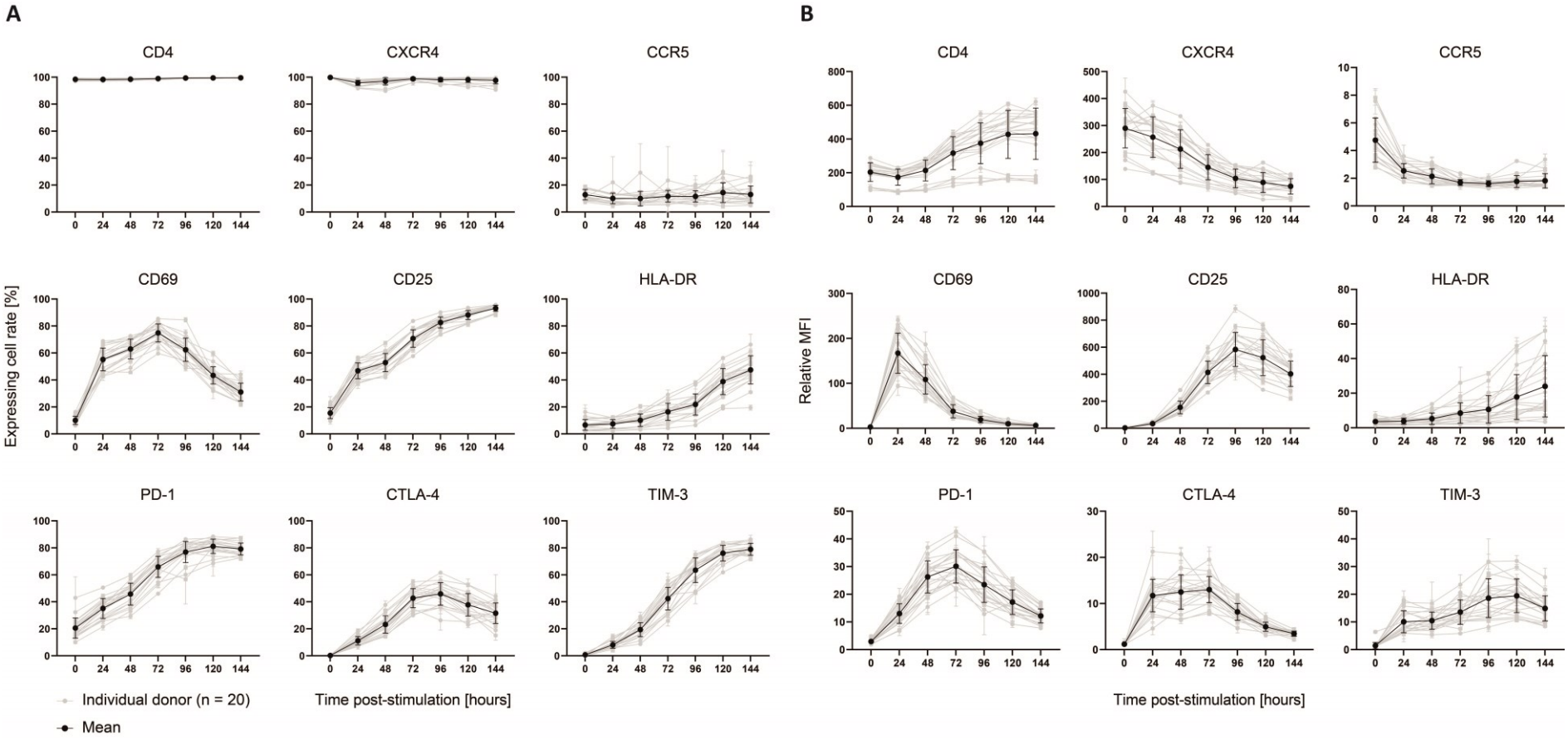

Supplementary Figure 2: Surface marker expression over time post-stimulation for HIV entry, activation markers and ICIs. Grey lines represent expression kinetics obtained for each individual donor and is the mean of biological duplicates. Black line represents the mean of all donors. Error bars represent the SD. (A) Proportion of expressing surface marker (B) Global expression level was assessed as relative MFI, normalized by the corresponding non-stained control. SD, standard deviation; MFI, Mean Fluorescence Intensity.

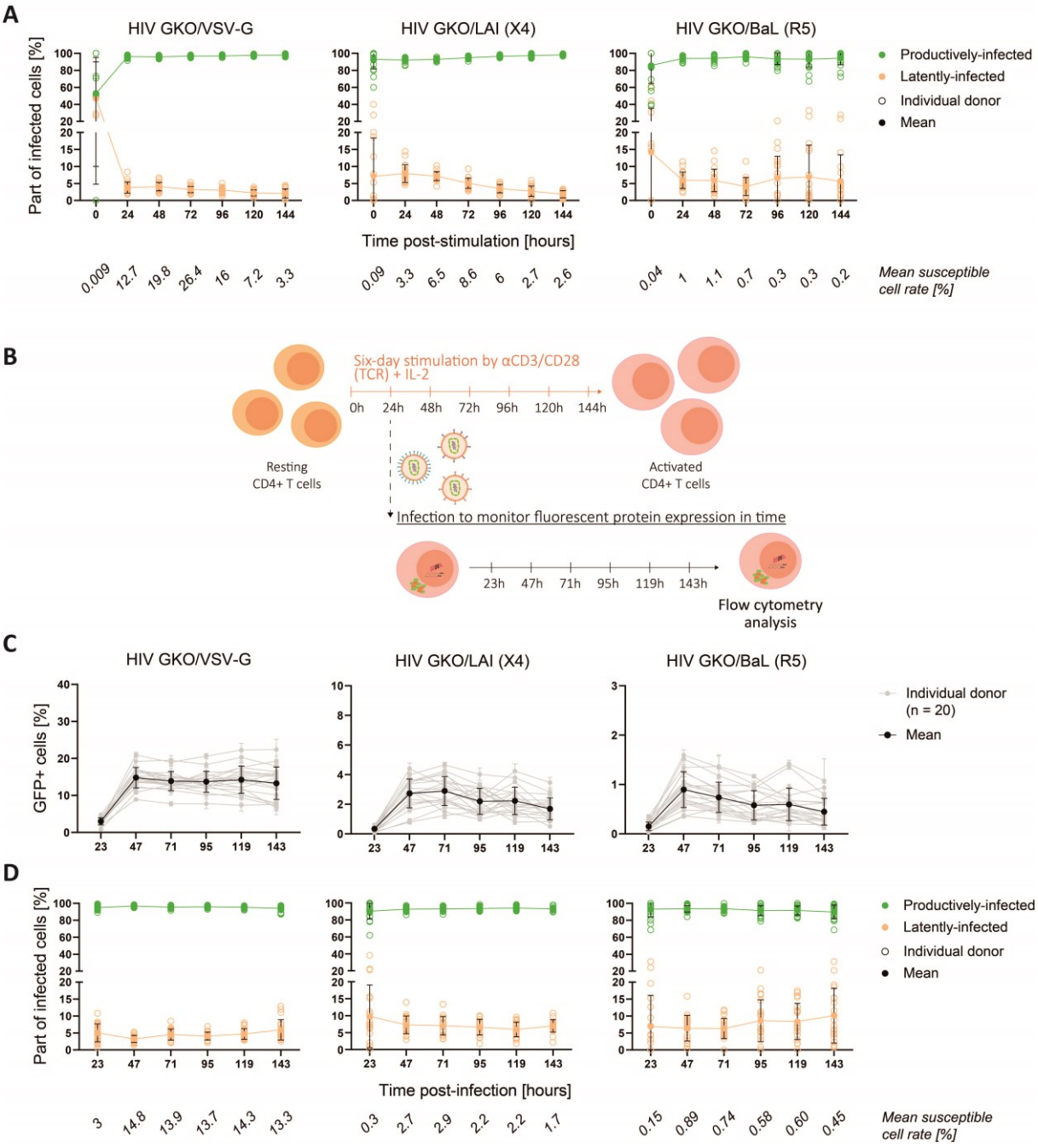

Supplementary Figure 3: HIV latent infection. Proportion of infected cells upon infection with HIV GKO vectors harboring distinctive envelopes (VSV-G, LAI (X4), BaL (R5)), and divided as productive infection (mKO2+ GFP+ cells; green) and latent infection (mKO2+ GFP-; orange). Dots represent mean of biological duplicates per individual donor and lines represents the mean of all donors. (A) Proportion of latently and productively infected cells over time p.-s. Cells were stimulated for 6 days and cells were infected each 24h. Levels of infection success, as measured by mKO2+ cells 47h p.-i., are indicated at the bottom of the graphs. (B) Experimental workflow used to assess GFP expression stability over time in mKO2+ infected cells. Resting CD4+ T cells were stimulated for 24h with anti-CD3/CD28 in presence of IL-2 and infected with the three HIV GKO reporters (VSVS-G, LAI (X4), BaL (R5)). mKO2 and GFP expression were measured by flow cytometry at 23h, 47h, 71h, 95h, 119h and 144h p.-i. (C) Stability of viral protein expression over time was assessed by rate of GFP+ cells. Grey lines represent infection kinetics obtained for each individual donor and are the mean of biological duplicates. Black line represents the mean of all donors. Error bars represent the SD. (D) Proportions of latently (GFP-) and productively (GFP+) infected cells in mKO2+ cells over time p.-i. The proportion of mKO2+ infected cells (i.e. susceptible cells) is indicated at the bottom of the graphs. p.-s., post-stimulation; p.-i., post-infection; SD, standard deviation.

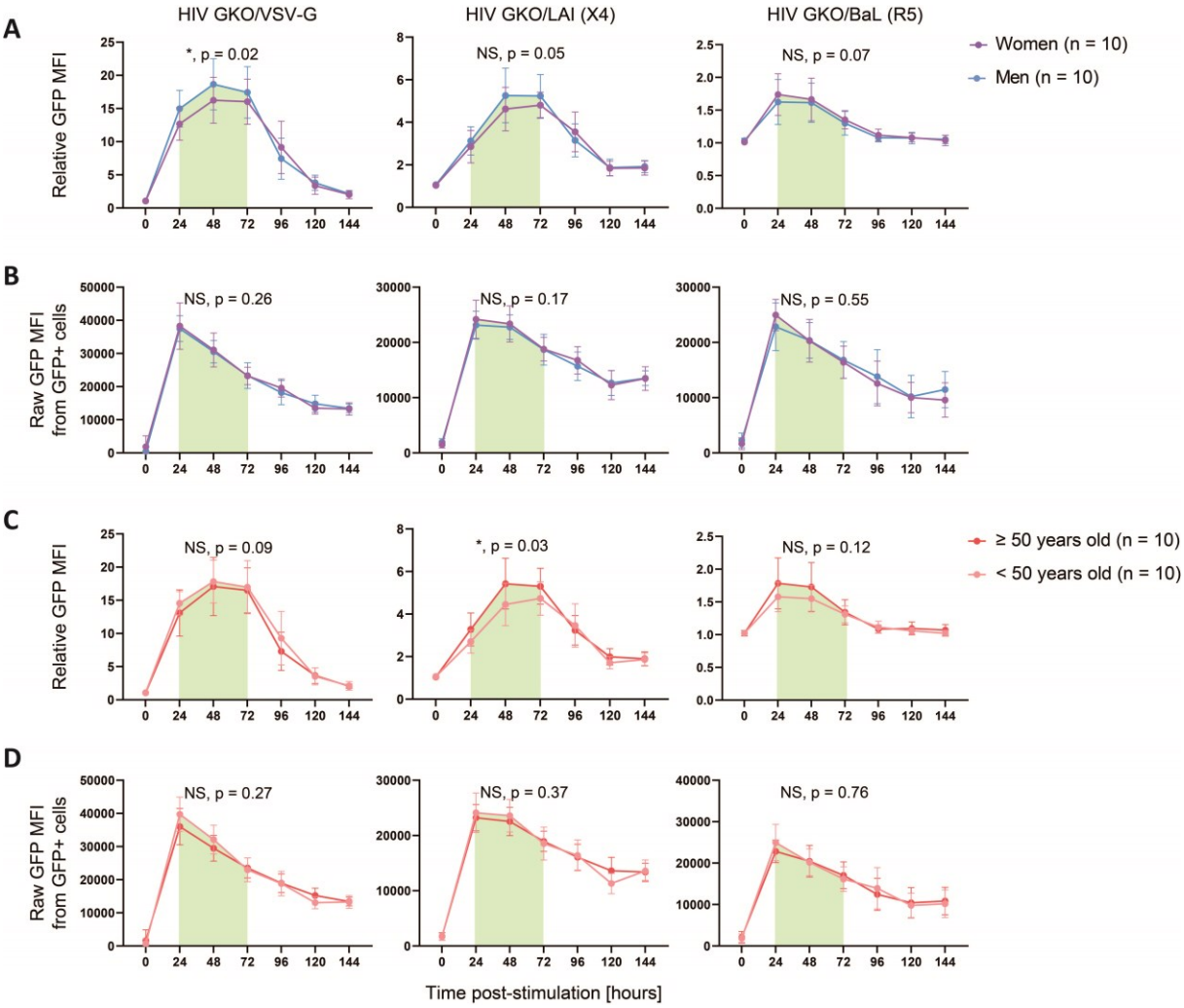

Supplementary Figure 4: Sex and age impact cell permissiveness to HIV infection at the global level but not at the intracellular one. Permissiveness to HIV over time p.-s. for the three HIV GKO reporters (VSV-G, LAI (X4), BaL (R5)), separated according to sex (women: purple; men: blue) (A, B) or according to age (<50 years old: pale orange; ≥50 years old: red) (C, D). Lines represent the mean of each category per time point. Error bars represent SD. Statistical differences were calculated between 24 and 72h p.-s. (indicated by the green box) using paired t-test. Global cell population permissiveness to HIV was assessed as relative GFP MFI, normalized by the corresponding mock-infected control (A, C) and intracellular permissiveness level was assessed by measuring the raw GFP MFI in GFP+ cells (B, D). * $p < 0.05$. p.-s., post-stimulation; SD, standard deviation; MFI, mean fluorescence intensity.

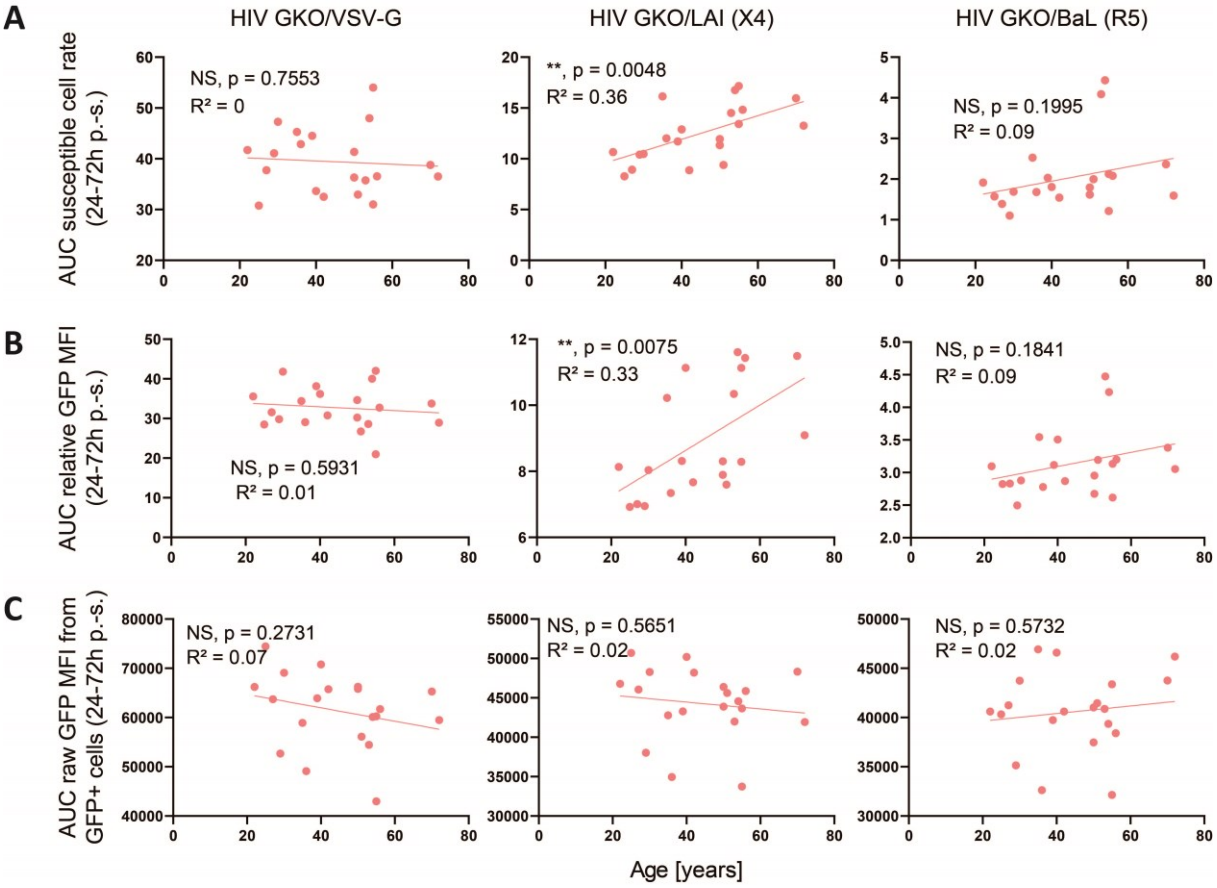

Supplementary Figure 5: Age correlates with HIV infection success upon LAI (X4)-mediated entry. HIV infection success is represented by AUC 24 and 72h p.-s of susceptible cell rate (A), global permissiveness to HIV reflected by GFP levels (B) and intracellular GFP levels (C). Each dot corresponds to the mean of biological duplicates for one donor. Correlation with donor age was calculated for the three HIV GKO vectors (VSV-G, LAI (X4), BaL (R5)) using linear regression. AUC, area under curve; p.-s. post-stimulation.

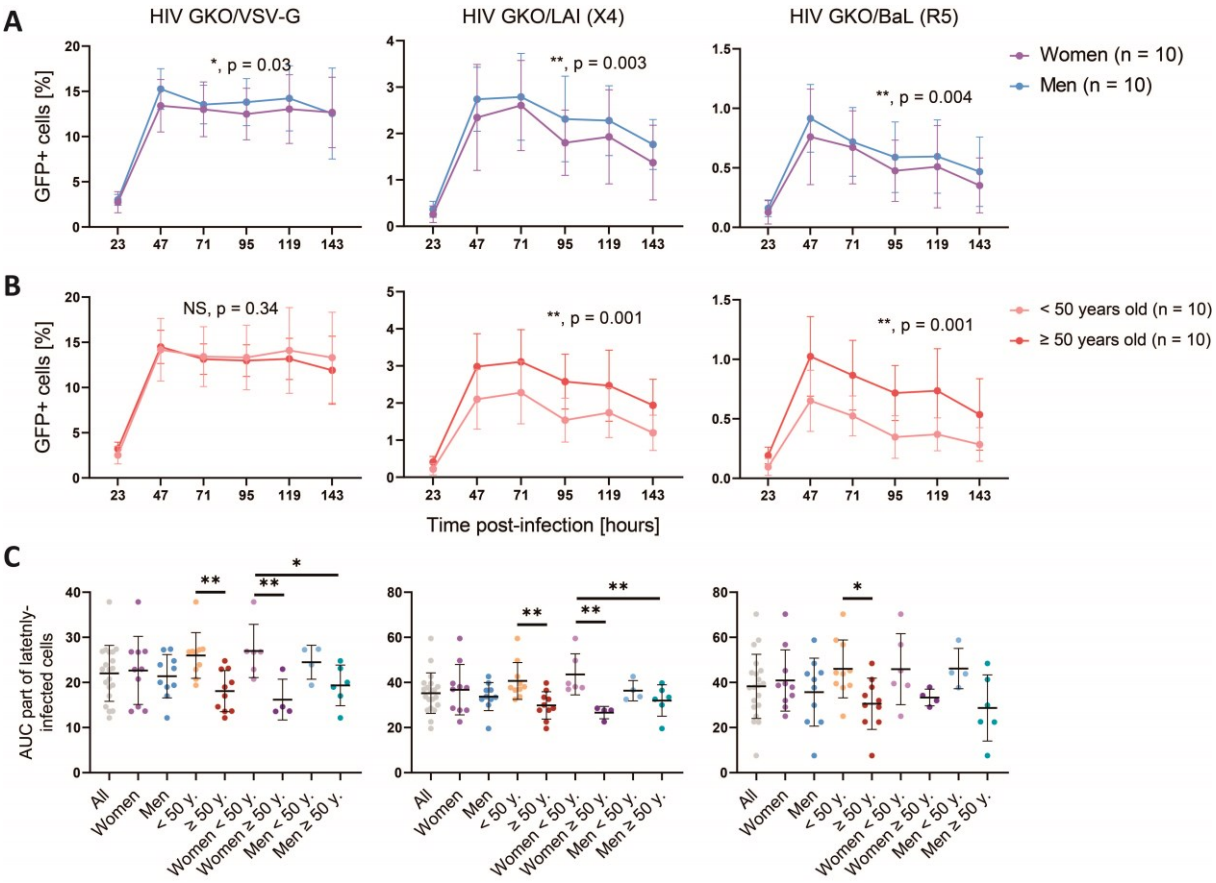

Supplementary Figure 6: Sex and age impact latency establishment over time post-infection. (A, B) Stability of the proportion of productively infected cells (GFP+) over time p.-i. upon infection with the three HIV GKO reporters (VSV-G, LAI (X4), BaL (R5)), according to sex (A) and age (B). Lines represent the mean of each category per time point. Error bars represent SD. Statistical differences were calculated using paired t-test. (C) Proportion of latently infected cells (mKO2+ GFP- over mKO2+ population), calculated as the AUC at the 24-72h p.-s. time window for each HIV GKO vector, in multiple donor categories. Each dot corresponds to the mean of biological duplicates of one donor. Statistical differences between sex and age were calculated by two-way ANOVA. * $p < 0.05$, ** $p < 0.01$. p.-i., post-infection; SD, standard deviation; AUC, area under curve; ANOVA, analysis of variance.

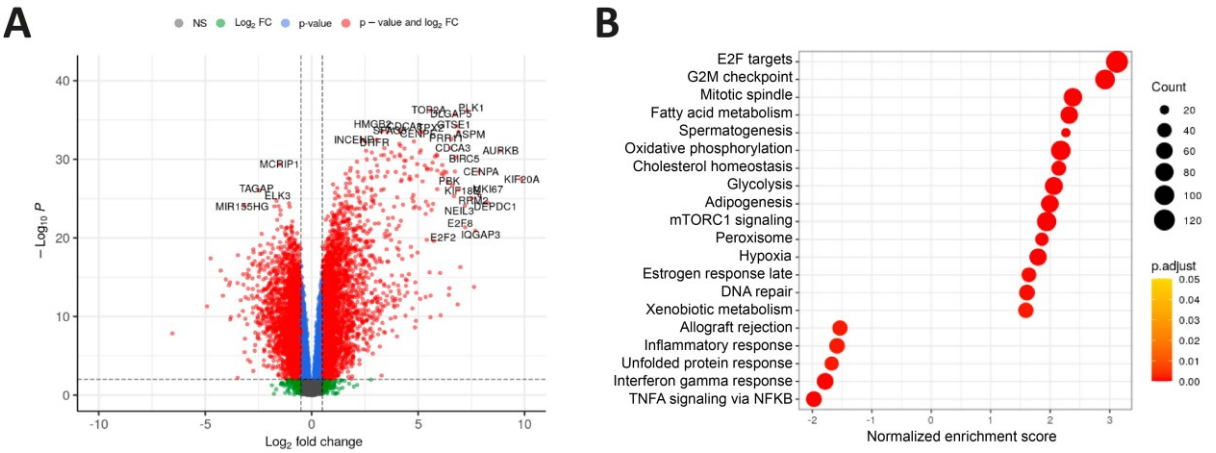

Supplementary Figure 7: Transcriptome impact of 72h vs 24h stimulation. (A) Volcano plot of DEG between 72h and 24h stimulation in women cell samples. Dashed lines represent cut-offs for identification of DGE ($Log_2FC > 0.5$ and $-Log_{10}\ p > 2$). Significantly enriched DGE are represented in red, significant *p*-value only in blue, significant Log FC only in green and non-significant genes in grey. (B) Hallmark enrichment score between 72h and 24h stimulation in women cell samples. *P*-values are represented by significance in orange to red shades. Gene count per pathway is represented by circle size. DGE, differentially expressed genes; FC, fold-change.

Supplementary tables

Supplementary table 1: Cell distribution by donor according to reference comparison and annotations. Raw cell counts and frequency distribution (percentage) over total population are represented for each comparison. Sex, age and total cell count are indicated for each donor. CTL, cytotoxic T lymphocyte; TCM, T cell memory; TEM, T effector memory; Treg, regulatory T cell; Th, T helper; Tfh, T follicular helper; M, male; F, female; y., years; freq., frequency.

Reference	Subset	Donor 1 (M, 29 y., 6601 cells)		Donor 2 (M, 36 y., 5802 cells)		Donor 3 (F, 25 y., 6288 cells)		Donor 4 (F, 39 y., 5878 cells)	
		Count	Freq.	Count	Freq.	Count	Freq.	Count	Freq.
Seurat	CTL	85	1.3	281	4.8	89	1.4	188	3.2
	CD4 Naive	337	5.1	500	8.6	460	7.3	646	11.0
	CD4 Proliferating	696	10.5	429	7.4	305	4.9	446	7.6
	CD4 TCM	4992	75.6	4084	70.4	4636	73.7	4198	71.4
	CD4 TEM	34	0.5	90	1.6	263	4.2	56	1.0
	Treg	457	6.9	418	7.2	535	8.5	344	5.9
Monaco	Follicular helper	243	3.7	413	7.1	268	4.3	415	7.1
	Naïve CD4	852	12.9	935	16.1	732	11.6	1133	19.3
	T regulatory	2044	31.0	1282	22.1	1595	25.4	1204	20.5
	Terminal effector CD4	141	2.1	297	5.1	121	1.9	232	3.9
	Th1	1193	18.1	725	12.5	808	12.8	884	15.0
	Th1/Th17	1647	25.0	1623	28.0	2171	34.5	1477	25.1
	Th17	233	3.5	289	5.0	293	4.7	227	3.9
	Th2	248	3.8	238	4.1	300	4.8	306	5.2
DICE	Memory Treg	447	6.8	436	7.5	546	8.7	409	7.0
	Naïve	239	3.6	380	6.5	142	2.3	465	7.9
	Naïve Treg	56	0.8	155	2.7	84	1.3	105	1.8
	Naïve stimulated	4946	74.9	3488	60.1	4410	70.1	3537	60.2
	Tfh	501	7.6	766	13.2	524	8.3	761	12.9
	Th1	164	2.5	272	4.7	242	3.8	317	5.4
	Th1/Th17	57	0.9	89	1.5	138	2.2	51	0.9
	Th17	111	1.7	136	2.3	131	2.1	99	1.7
	Th2	80	1.2	80	1.4	71	1.1	134	2.3

Supplementary table 2: Antibodies used for surface marker staining.

Target protein	Fluorophore	Host/Target Ig	Reference
CD4	APC	Rat IgG2b, κ	Biolegend, ref. 357407
CXCR4	PE	Mouse IgG2a, κ	Biolegend, ref. 306505
CCR5	PE	Rat IgG2b, κ	Biolegend, ref. 359105
CD69	PE	Mouse IgG1, κ	Biolegend, ref. 310905
CD25	APC	Mouse IgG1, κ	Biolegend, ref. 302609
HLA-DR	PE	Mouse IgG2a, κ	Biolegend, ref. 307606
PD-1	PE	Mouse IgG1, κ	Biolegend, ref. 329905
CTLA-4	APC	Mouse IgG1, κ	Biolegend, ref. 349907
TIM-3	APC	Mouse IgG1, κ	Biolegend, ref. 345011

B. Additional project: Single-cell analysis identified novel determinants of CD4+ T cell permissiveness to HIV

During my PhD, I contributed to an additional project aiming at finding cellular determinants of permissiveness to HIV using a single-cell approach. The manuscript for publication will be submitted after analysis of additional results. Results and discussion of current outcomes are enclosed hereafter. Additionally, the project resulted in the publication of a review article, equally enclosed.

Summary

This study aimed at investigating differences in permissiveness to HIV at the cellular level by single-cell RNA-Seq (sc-RNA-Seq). For this, we performed a 6-day activation kinetics to study the impact of activation on CD4+ T cell subset composition and correlated the results with HIV-based vector infection success as measured by flow cytometry. Cell heterogeneity and cell permissiveness were further investigated by sc-RNA-Seq on CD4+ T cells infected with a single-round VSV-G pseudotyped HIV vector and identified a 53-gene signature that can effectively predict resistant over permissive phenotype on a non-exposed population.

Contribution

- Conceptualization of experiments was performed in collaboration with AC and SC.
- Performing experiments: cell culture and infection, Chromium loading and library preparation were performed in collaboration with RM.
- Data analysis was carried out by PA.
- Writing was performed with AC.
- Figure design and formatting was performed with PA.

Current results are enclosed hereafter. The manuscript will be submitted for publication after analysis and incorporation of additional pending results.

Single-cell analysis identified novel determinants of CD4+ T cell permissiveness to HIV

Paolo Angelino[1,2], Ludivine Brandt[1], Raquel Martinez[1], Sara Cristinelli[1], Angela Ciuffi[1]

[1] *Institute of Microbiology, Lausanne University Hospital and University of Lausanne, Switzerland*
[2] *DS-facility, AGORA Cancer Research Center, Swiss Institute of Bioinformatics, Lausanne, Switzerland*

Abstract

HIV replication success is influenced by CD4+ T cell heterogeneity. Single-cell technologies allowed for cell subtype analysis and identification of cells displaying increased permissiveness to HIV. Nevertheless, a comprehensive list of host factors leading to a permissive or resistant phenotype is still lacking. Cellular activation plays a pivotal role in shaping a permissive state but requires further characterization following activation dynamics. Here, we explored the evolution of CD4+ T cell population composition over time upon T-cell receptor (TCR)-mediated activation using single-cell RNA-Seq (sc-RNA-Seq). We then further associated cell activation kinetics with cell permissiveness to HIV infection by flow cytometry using an HIV-encoded GFP reporter. Cells displaying the highest permissiveness phenotype were found between 48h to 96h post-stimulation when the abundance of activated/proliferating cells was the lowest. Detection of viral RNA in single cells revealed that all proliferating cells contained viral transcripts, reflecting successful HIV infection of these cells. In contrast, naïve, central memory and regulatory T cells were heterogeneously infected, displaying a mixture of infected (HIV RNA+) and non-infected (HIV RNA-) cells. Projection of transcriptomic signatures displayed by naïve, central memory and Treg cells on HIV non-exposed cells allowed inferring the transcriptomic profile of permissive cells. We finally identified a 53-gene signature efficiently predicting cell permissiveness or resistance to HIV. Further analysis of these genes revealed an antiviral role with genes enriched in virus response, innate immune response, and response to type I interferon and interferon-γ. Our study confirmed that cells non-permissive to HIV infection were displaying higher expression of genes involved in antiviral defense, thereby refining previous gene signatures. Further characterization of these 53 genes may lead to the identification of novel HIV restriction factors and help characterize reservoir cells.

Introduction

Human immunodeficiency virus type 1 (HIV-1, hereafter abbreviated HIV) infection requires expression of the CD4 major receptor, as well as a CCR5 or a CXCR4 co-receptor, for successful cell entry. However, multiple *in vivo* and *in vitro* studies revealed limited HIV infection success despite the presence of viral entry receptors [1-3]. Differences in infection outcome originate from the balance between multiple host cell factors displayed by a large diversity of CD4+ T cells, either favoring or restricting infection. Thus, cell heterogeneity results from a combination of (i) cell activation status, (ii) cell subtype and (iii) differentiation stage [4].

For the past decade, the advent of single-cell technologies revolutionized the understanding of HIV biology, enabling refined characterization of HIV infection [5]. A wide range of techniques allowing analysis of transcriptome, protein expression, chromatin accessibility, or TCR sequence are employed to further understand viral reservoir and reactivation, host response, or cellular permissiveness to HIV [6]. Notably, memory CD4+ T cells all support HIV entry in fusion assays, including central memory (Tcm), effector memory (Tem), terminally differentiated (Ttm), T follicular helper (Tfh) and regulatory T cells (Treg), as well as subtypes Th1, Th2 and Th17, with preferential targeting of Th2 and Th17 [7]. In acute infection phase, permissive cells were shown to be mostly composed of memory Th1 harboring high CCR5 expression in a recent *in vivo* study by Nicolas Chomont's group [8]. In addition to successful viral entry, the cellular environment has to be permissive to viral replication, with permissive cells displaying an activated or exhausted phenotype as well as a low type I interferon response [9, 10].

These studies largely contributed to the effort of refining the characterization of the cellular features required for successful HIV replication, nevertheless these findings do not enable discrimination of a permissive from a resistant cell. In addition, the process of cellular activation evolves with stimulation over time, affecting cellular environment. Therefore, understanding how cellular activation kinetics changes upon TCR-mediated stimulation, at the level of cellular population composition, as well as at intracellular environment, may help gather further insight into determinants impacting permissiveness to HIV.

In this study, we addressed how CD4+ T cell population composition evolved over TCR-mediated stimulation kinetics through parallel analysis of single-cell transcriptome (sc-RNA-Seq) and HIV infection success of a VSV-G pseudotyped HIV vector expressing GFP measured by flow cytometry. We found that cell subsets were differentially impacted by cell activation. Furthermore, our data revealed intra-subset heterogeneity with differential HIV RNA expression in naïve, Tcm and Treg. Finally, projection analysis of the permissive transcriptomic signature by k-nearest neighbors (k-NN) algorithm on HIV non-exposed cells allowed identifying a 53-gene-specific signature able to distinguish efficiently resistant and permissive cells. This predictive 53-gene signature is mainly involved in response to virus, innate immune response, and response to type I interferon and interferon-γ.

Results

Dynamic evolution of CD4+ T cell population composition upon TCR-mediated stimulation affects permissiveness to HIV

To determine how CD4+ T cell population composition changed with TCR-induced activation, we stimulated cells for a total of 144h and analyzed subpopulation composition by sc-RNA-Seq each day starting from 48h. We analyzed a total of 32,250 cells and mapped them against the Seurat reference to identify representation of six subtypes: cytotoxic T lymphocyte (CTL), naïve, effector cells (proliferating), Tcm, Tem and Treg (*Fig. 1A, Supplementary Table 1*) [11]. Analysis over time post-stimulation (p.-

s.) revealed a dynamic cell pool composition, differentially impacting cellular subsets (*Fig. 1B*). Naïve and Treg cell fraction decreased over time to the benefit of increasing proliferating cells that peaked at 120h with up to 71% of cells, consistent with cells being activated upon TCR-mediated stimulation. The Tcm population remained stable after stimulation and increased only at 144h, possibly indicating the evolution of proliferating cells to Tcm. Tem and CTL only accounted for less than 0.5% of the total CD4+ T cell population throughout activation, with very low counts, hindering reliable interpretation. In parallel, cells were infected with an HIV-based lentiviral vector harboring GFP expression as a constitutively expressed reporter, and pseudotyped with VSV-G (referred to as HIV_GFP/VSV-G), allowing assessment of cell permissiveness to viral infection by flow cytometry, corresponding to successful viral entry, integration, and expression (*Fig. 1C and D*). CD4+ T cells displayed the highest permissive state between 48 to 96h p.-s. (*Fig. 1C*). The relative GFP Mean Fluorescence Intensity (MFI) of the total cell population showed higher GFP expression at 48h p.-s., reflecting a most permissive state at this time (*Fig. 1D*). Interestingly, although activated and proliferating status is known to facilitate viral infection, it is not sufficient as shown at the 120h p.-s. timepoint, where 71.46% of proliferating cells are present, but only 34.5% of cells were productively infected. This suggests that cells at 120h (late activation stage) were poised to differentiate into Tcm and displayed a less permissive environment.

Overall, these data showed that CD4+ T cell pool composition is dynamic and evolves with activation, leading to changes in cell permissiveness to HIV. In this cell context, cells activated for 48h presented the most productive infection phenotype.

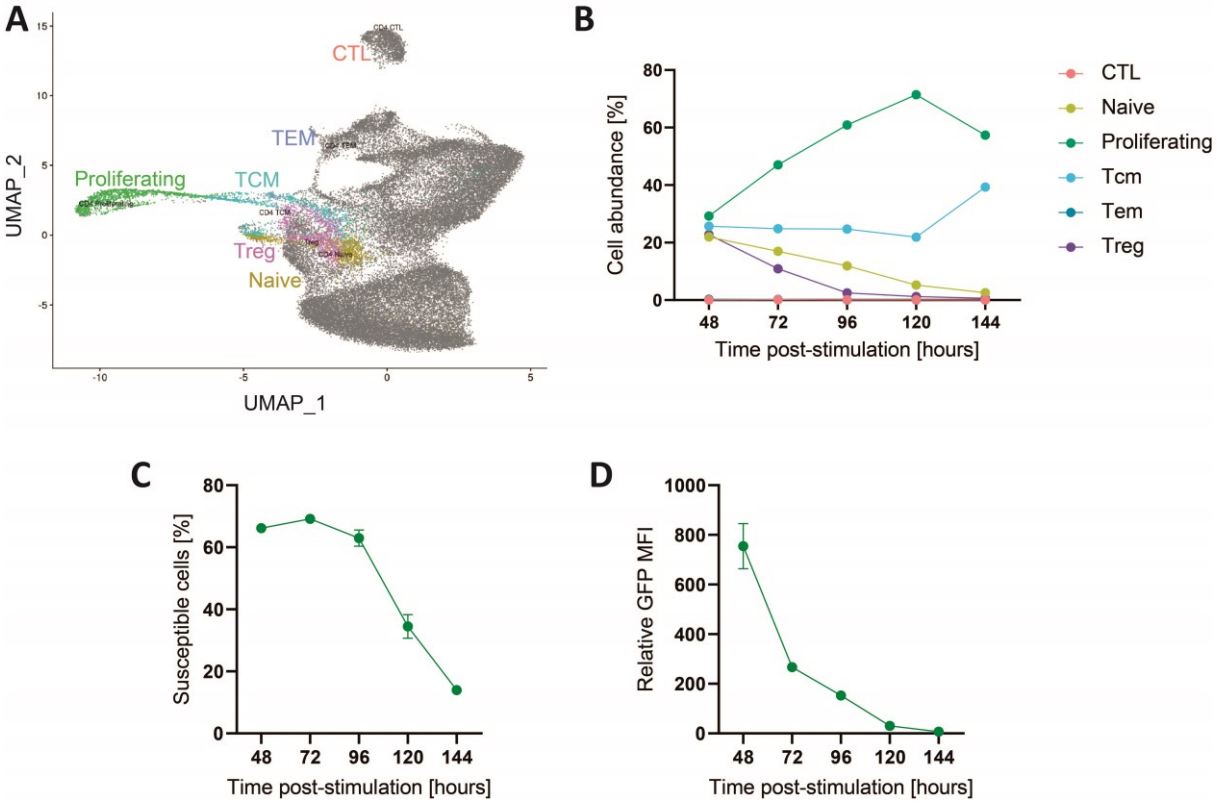

Figure 1: Dynamic evolution of CD4+ T cell population composition upon TCR-mediated stimulation affects permissiveness to HIV. (A) UMAP projection of activated CD4+ T cells (colored) on cell reference dataset (grey) by Hao *et al.* [11] allowed identifying CD4+ T cell subset of each single cell. (B) Cell subset abundance p.-s. (C, D) Cell permissiveness to HIV_GFP/VSV-G infection (green), assessed by viral GFP expression at 47h p.-i., and reported as the proportion of GFP-expressing cells and thus productively infected cells (C) or relative GFP MFI of the total cell population normalized by the corresponding mock-infected control, reflecting GFP expression intensity (D). Dots represent the mean of biological duplicates. Error bars represent SD. UMAP, uniform manifold approximation and projection; p.-s., post-stimulation; p.-i., post-infection; SD, standard deviation; MFI, mean fluorescence intensity; CTL, cytotoxic T lymphocyte; Tcm, T cell memory; Tem, T effector memory; Treg, regulatory T cell.

Naïve, Tcm and Treg display heterogeneous response to HIV infection

To investigate cellular features of permissiveness to HIV within CD4+ T cell subtypes, we used single-cell transcriptomics. CD4+ T cells were stimulated for 48h and infected with single-round HIV pseudotyped with VSV-G (HIV/VSV-G), and sc-RNA-Seq was performed 28h post-infection (p.-i.). HIV RNAs were detected and counted similarly to cellular transcripts, in each cell subtype (*Fig. 2A, Supplementary Table 2*). On a total of 3,342 HIV-exposed cells, 86% were HIV RNA+. Proliferating cells accounted for 73% of all HIV RNA+ cells, forming a homogeneous infection target (97% HIV RNA+). Conversely, naïve, Tcm and Treg exhibited 58.0%, 65.2% and 68.5% HIV RNA+ cells in respective subpopulations, suggesting that these cells were more heterogeneous in their permissiveness phenotype to HIV. To further explore the origin of this heterogeneity, HIV-exposed cells were computationally depleted from the proliferating subset, leaving 1,158 cells, most of which being Tcm (*Fig. 2B*). HIV RNA normalized counts were then analyzed in order to separate HIV-exposed cells in infected and thus permissive cells (HIV RNA+) and non-infected cells (HIV RNA-) (*Fig. 2C*).

These data outlined that the heterogeneity in permissiveness to HIV lied mostly in Tcm, naïve and Treg cell subsets and allowed further characterization of transcriptomic profiles by cell subtype in order to identify gene-specific signatures associated with the permissiveness phenotype.

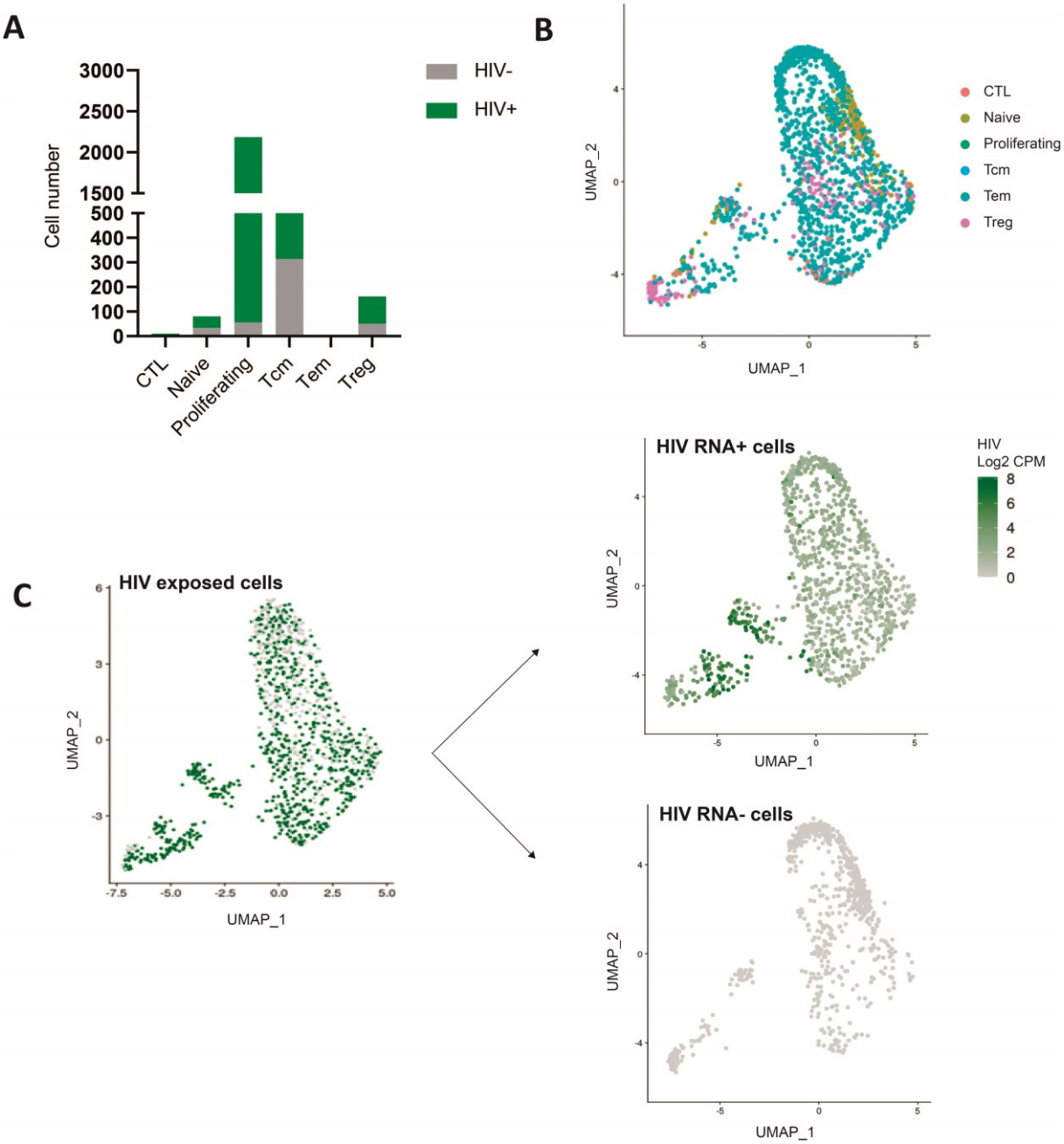

Figure 2: Naïve, Tcm and Treg display heterogeneous response to HIV infection. (A) Presence or absence of HIV RNA in each CD4+ T cell subset. Cell counts are divided in HIV RNA+ cells (green) and HIV RNA- cells (grey). (B) UMAP plot presenting cell subset distribution in HIV-exposed cells after depletion of proliferating cell subset. (C) Distribution of HIV RNA+ (green) and HIV RNA- (grey) cells in HIV-exposed cells. Plots were then further visualized concentrating on separated UMAP projections in HIV RNA+ cells (from 1 to 8 normalized counts; green), with RNA presence intensity presented as darker green shading (upper panel) and HIV RNA- cells (0 normalized counts; grey) (lower panel). UMAP, uniform manifold approximation and projection; Tcm, T cell memory; Treg, regulatory T cell; CTL, cytotoxic T lymphocyte; Tem, T effector memory; CPM, count per million.

Single-cell projection of HIV-exposed cells on non-exposed cells enables prediction of permissive and resistant phenotypes and identifies a corresponding 53-gene signature

The single transcriptomic profiles of infected (HIV RNA+, permissive) and non-infected (HIV RNA-, resistant) cells in HIV-exposed cells were projected on the 1,919 non-exposed cells. Each non-exposed single-cell was then predicted to be either permissive or resistant by similarity to the HIV-exposed cells using k-NN algorithm (*Fig. 3A*). This approach allowed for comparing the transcriptome of resistant cells to permissive cells, prior to HIV infection and thus HIV-induced alterations. Cell subtype annotation revealed a similar heterogeneity across predicted permissive or resistant cells in the HIV non-exposed cells compared to infected (HIV RNA+, permissive) and non-infected (HIV RNA-, resistant) cells in the HIV-exposed cells (*Supplementary Fig. 1A and B, Supplementary Table 3*). Differential gene expression (DGE) analysis between the two predicted cell phenotypes resulted in a 64-gene signature, that could be further separated into two major clusters (*Supplementary Table 4*). The first cluster contains 11 genes that were mostly downregulated in cells predicted to be resistant to HIV (top), while the second cluster with 53 genes showed a global upregulation in the inferred resistant cells (bottom) (*Fig. 3B*). Importantly, these gene lists were not associated with specific cellular subsets. The ability of the gene signature to efficiently discriminate between permissive and resistant cells can be assessed through comparison of global gene expression between the two cell phenotypes. Our data showed that the 53-gene signature expression score in predicted resistant cells was significantly higher than in predicted permissive cells, thereby indicating that this 53-gene signature could indeed be used to efficiently separate the two cell phenotypes (****, $p = 2 \times 10^{-83}$) (*Fig. 3C*). The use of the 64- or 11-gene signatures was also efficient in discriminating both phenotypes but presented higher *p*-values (*Supplementary Figure 2*). Functional analysis of the 53-gene signature by gene ontology-based over-representation analysis revealed significant enrichment of multiple antiviral pathways including response to virus, innate immune response, and response to type I interferon and interferon-γ (*Fig. 3D*). Thus, the higher expression of these genes in the inferred HIV resistant cells is consistent with a repressive cellular environment, which is mostly due to innate immunity.

Overall, our data identified a sophisticated gene signature that efficiently predicted HIV infection success within CD4+ T cell subsets thanks to their heterogeneity to HIV infection permissiveness.

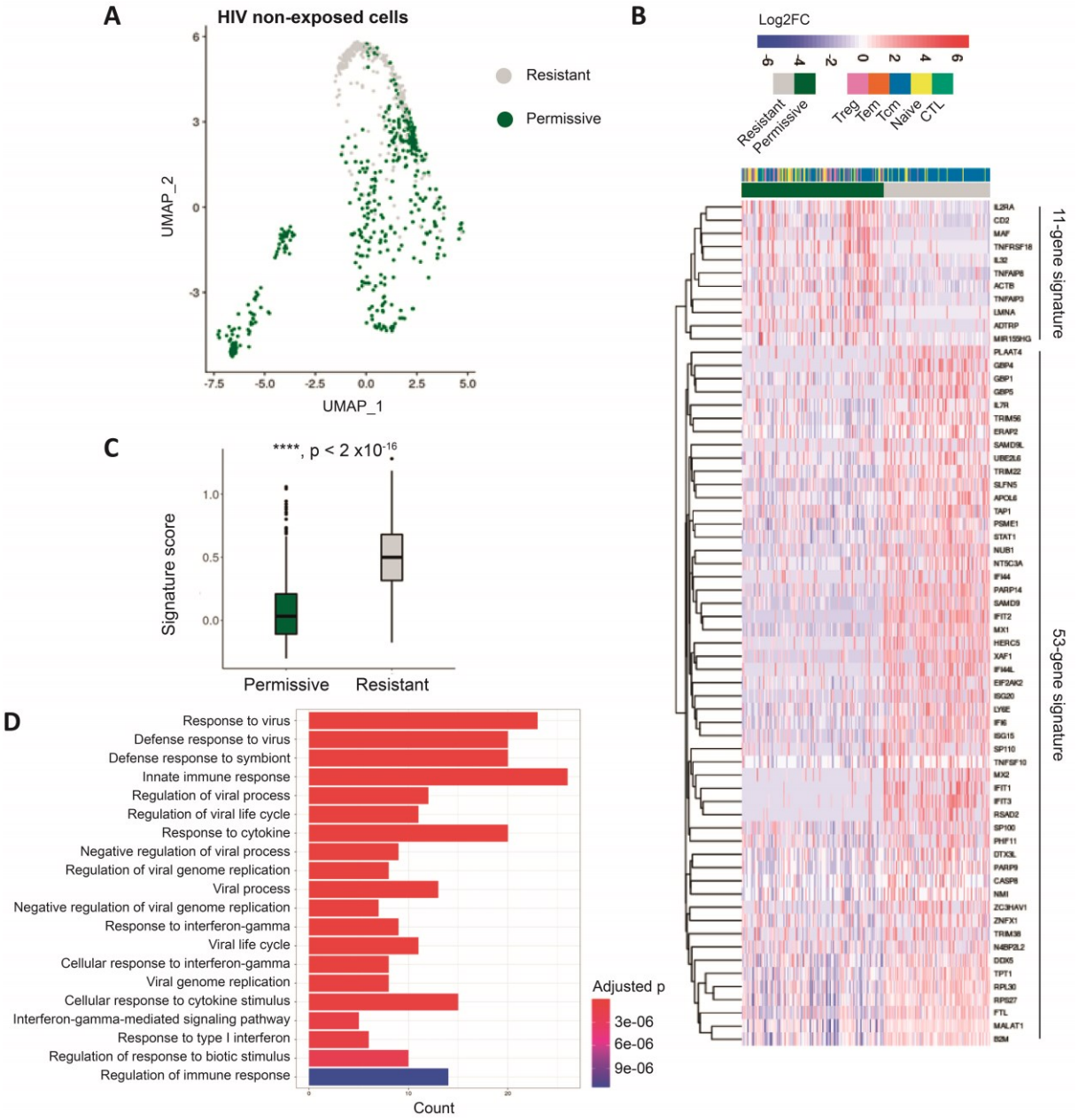

Figure 3: Single-cell projection of HIV-exposed cells on non-exposed cells enables prediction of permissive and resistant phenotypes and identifies a corresponding 53-gene signature. (A) UMAP projection of inferred phenotype of permissive and resistant cells in HIV non-exposed cells. (B) DEG between resistant (grey) and permissive (green) cell phenotype. Cell subsets are indicated on top. Upregulated (red) and downregulated (blue) genes are indicated. (C) Prediction score of permissive (green) and resistant (grey) using the 53-gene signature. Statistical significance was calculated using t-test. (D) Gene ontology-based ORA of the 53 DEG signature. Enriched pathways are represented by gene count per pathway and colored according to significance. UMAP, uniform manifold approximation and projection; DEG, differentially expressed genes; ORA, over-representation analysis.

53-gene signature validation in another blood donor efficiently predicts resistant over permissive cells

To evaluate the potential of the 53-gene signature in permissive or resistant cell prediction, we analyzed CD4+ T cells from an independent blood donor. We first assessed the 53-gene signature score within each cell subtype (*Fig. 4A*). Cells displaying

the lowest 53-gene expression score were proliferating cells, consistent with their highest permissiveness to HIV (97% HIV RNA+ cells in *Fig. 2A, Supplementary Table 2*). In contrast, naïve, Treg and Tcm displayed higher 53-gene expression scores, consistent with less permissive phenotypes. Furthermore, variations in the signature expression score reflect cell heterogeneity within each cell subpopulation, consistent with some cells being permissive and some cells being resistant. Uniform manifold approximation and projection (UMAP) single cell projections allow for the visual comparison between cell subtype distribution (*Fig. 4B*), predicted cell permissiveness phenotype (*Fig. 4C*), and the 53-gene signature expression score (*Fig. 4D*). Visual inspection confirms that cells from the same subset cluster together and that cell subset heterogeneity can be particularly observed in the Tcm subset, consistent with previous data.

Altogether, we showed that the 53-gene signature may likely be used to predict cell resistance or permissiveness to HIV in multiple cell subsets and multiple donors.

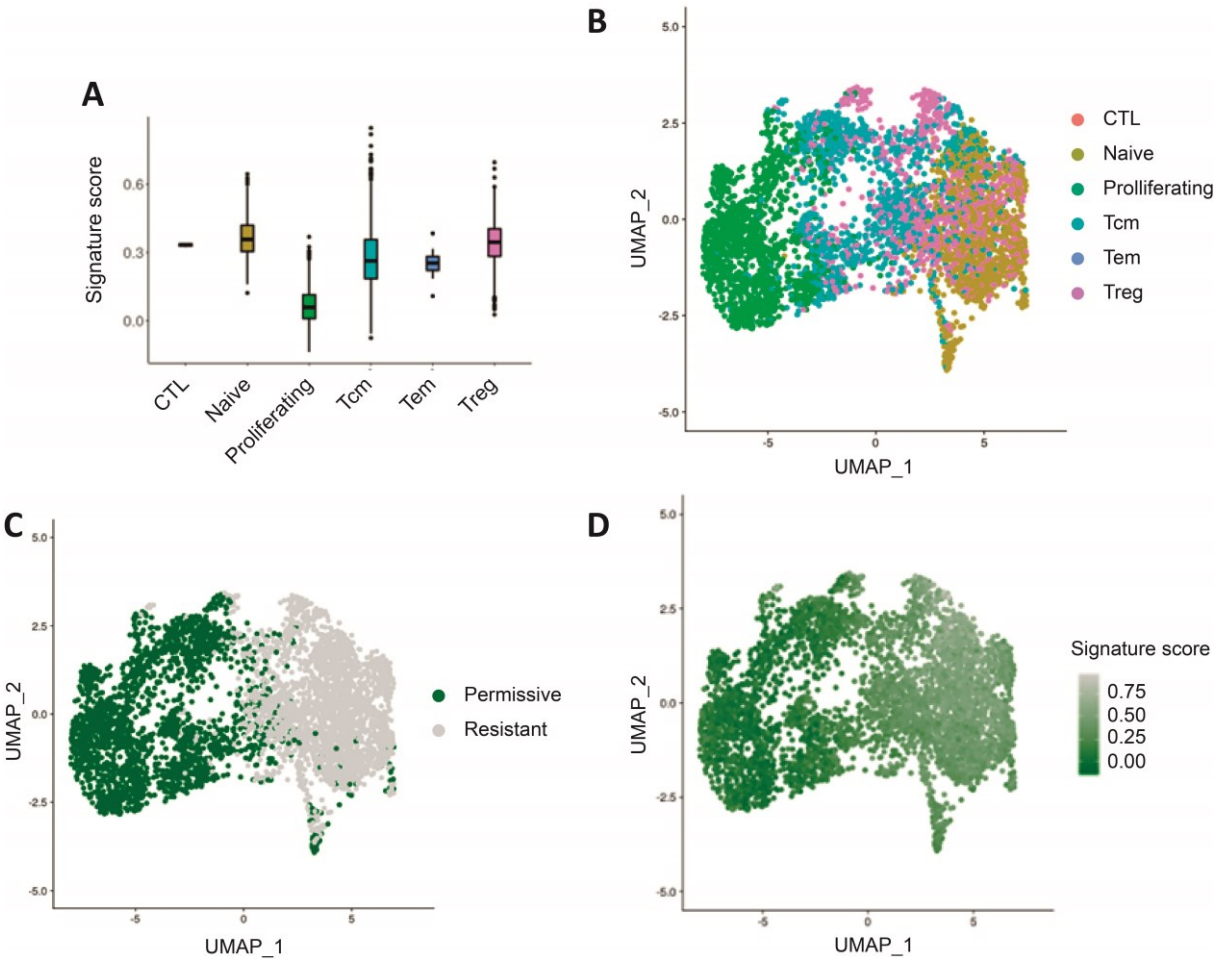

Figure 4: 53-gene signature validation in another blood donor efficiently predicts resistant over permissive cells. (A) 53-gene signature expression score in CD4+ T cell subsets from an independent blood donor. (B-D) UMAP visualization of CD4+ T cells according to annotated cell subsets (B), according to predicted cell phenotype in response to HIV infection (C), and according to the 53-gene expression score (green shading) (D). DEG, differentially expressed genes; UMAP, uniform manifold approximation and projection.

Discussion

In the past decade, single-cell analyses revolutionized the field of HIV, as many other fields, allowing studies on a variety of HIV-related topics, such as the characterization of latent cells, the latent cell heterogeneity upon reactivation, and cell permissiveness to HIV [5]. In this study, we addressed how CD4+ T cell subset composition affected permissiveness to HIV using sc-RNA-Seq and took advantage of cell heterogeneous response to HIV infection to identify a robust gene-signature associated with permissiveness phenotype.

We demonstrated by sc-RNA-Seq how cell activation impacted CD4+T cell distribution and evidenced that the abundance of activated/proliferating cells increased over time and represented the major subset identified at every time point. The remaining of the cells was mainly represented by Tcm, naïve and Treg. Our data showed that cell stimulation was efficient as most cells reached an activated and thus proliferating state over time. However, our results did not allow discriminating the cell subset origin of the proliferating cells based on single-cell transcriptome profiles, and we could thus only speculate the naïve and Treg origin based on the progressive decline of cell counts over time. Cell infection with a VSV-G pseudotyped HIV-based virus encoding a GFP reporter peaked between 48 and 96h p.-s., with an increased permissive cellular environment at 48h, as indicated by GFP intensity levels. At this moment, the proportion of proliferating, *i.e.* activated effector cells, was at its lowest and increased with time. In the future, HIV RNA production should be assessed in parallel to verify whether findings using GFP assessment can be recapitulated at the RNA level. Recently, Luo *et al.* investigated tissue CD4+ T cell susceptibility by CyTOF and observed preferential infection of CD4+ T cell memory subtypes and exhibition of an activated phenotype [10]. Our data showed that permissiveness to HIV is not reflected by the abundance of proliferating cells, suggesting that the cellular environment of these proliferating cells evolves in stimulation time. Future work should address the differences of cellular environment between stimulation times within the proliferating subtype to evidence molecular determinants of permissiveness. Moreover, including non-stimulated and 24h-stimulated cells should help track cellular origin to understand the initial cellular subtype of proliferating cells before stimulation. Previous studies evidenced preferential HIV fusion with Th2 and Th17 subsets *in vitro* [7] and increased productive infection of CCR5*high* memory Th1-like *in vivo* [8]. Our study does not recapitulate these findings, as Seurat annotation used in this study does not allow to identify the subtype composition. Other reference sets as DICE [12] or Monaco [13] could be used for cell annotation and thus provide a more complete profile of cell subtype evolution in stimulation time.

Upon infection of 48h-stimulated CD4+ T cells with a VSV-G-pseudotyped HIV and sc-RNA-Seq analysis, the majority of infected cells (HIV RNA+) were the proliferating cell subset, followed by Tcm subset, consistent with published data [7, 10]. Previous studies identified CTL and Tem as cells actively producing HIV RNA in antiretroviral therapy (ART)-treated patients [14, 15], and although we could detect the presence of HIV RNA in these cell types, we could not draw any reliable conclusion due to the rare amounts of cells detected in our experimental setup. This was expected as CTL only represent a small percentage of peripheral CD4+ T cells, therefore a sorting step would be required

prior to infection to further investigate them. As for Tem, their rarity might come from the use of a strong *in vitro* TCR stimulation, resulting in high activation of these cells, which would transfer them in the proliferating subset.

Except for proliferating cells, each cell subtype (naïve, Tcm and Treg) displayed heterogeneity in permissiveness to HIV. To further understand this cell heterogeneity, we removed proliferating cells and focused on these three subsets only. UMAP of HIV-exposed cells that were computationally depleted from proliferating subtype was projected on HIV non-exposed cells by starting with HIV RNA+ (infected, permissive) and HIV RNA- (non-infected, resistant) cells from HIV-exposed cells and using a k-NN approach, we predicted the permissiveness phenotype of HIV non-exposed cells and split them into resistant or permissive cells. Upon single-cell differential gene expression analysis, we identified a robust 53-gene signature that could efficiently discriminate cells according to their permissiveness to HIV. These genes were associated with antiviral response and were consistently upregulated in resistant cells and downregulated in permissive cells. This 53-gene signature presents a refined genetic signature compared to the 96-gene signature identified in a previous study from our lab [9]. The difference can originate from the experimental approach, as the sc-RNA-Seq methods and the number of cells analyzed were different, *i.e.* Fluidigm C1 (85 cells) *vs* 10X Genomics (1,158 cells). Although a distinct individual donor cell composition cannot be excluded as contributing to this difference, we showed that the 53-gene signature could also be used to predict resistance to HIV with cells isolated from a second donor. More interestingly, 12 genes were commonly identified in the two studies and both highlighted enrichment of genes globally involved in antiviral response, including proven HIV inhibitory factors, such as ISG15 [16], GBP5 [17] and SLFN5 [18]. The expression of this signature should be assessed in activation kinetics data to determine if it can explain the evolution of permissiveness over time. Further investigations using machine learning approaches on infection data should be used to evaluate the predictive accuracy of this 53-gene signature to identify cell permissiveness phenotype. Finally, the effect of these genes should be investigated *in vitro* to determine whether they correlate with permissiveness to HIV and to evaluate their impact on HIV replication by deletion/overexpression assays.

The identification of the 53-restrictive transcriptomic signature might be used to further understand innate immunity and HIV latency. Indeed, evaluation of each gene can help identify novel inhibitory mechanisms of HIV replication. Similarly, these genes could be further assessed in latently infected cells to explore mechanisms of persistence, as well as reactivation. Finally, further characterization of these 53 genes will be needed to examine their potential in HIV cure strategies.

Methods

Ethics statement

All blood donors have provided written informed consent and all samples were anonymized.

Cell samples, isolation and culture

Peripheral Blood Mononuclear Cells (PBMCs) from HIV-negative blood donors were purified from whole blood samples by Ficoll gradient separation, using Leucosep tubes (Greiner, Kremsmünster, Austria). Following purification, PBMCs were frozen in heat-inactivated Fetal Bovine Serum (HI-FBS) with 7.5% dimethyl sulfoxide (DMSO, Merck, Darmstadt, Germany) in liquid nitrogen in cryotubes (Thermo Fisher Scientific, Waltham, MA, USA) for long-term storage.

Primary CD4+ T cells were isolated from PBMCs by negative-selection and magnetic separation using EasySep Human CD4+ T Cell Isolation Kit (Stemcell Technologies, Vancouver, Canada) according to manufacturer's instructions. They were cultured at a concentration of 10^6 cells/mL in R10 culture medium, consisting in RPMI-1640 (Thermo Fisher Scientific) supplemented with 10% HI-FBS (Thermo Fisher Scientific) and 50 µg/mL gentamicin (Thermo Fisher Scientific) at 37°C, 5% CO_2. CD4+ T cells were stimulated by adding 25 µL/mL ImmunoCult Human CD3/CD28 T Cell Activator (Stemcell Technologies) supplemented with IL-2 [200 IU/mL] (R&D Systems, Minneapolis, MN, USA) for various time points.

Virus production and infection

HIV-based lentiviral vector (HIV_GFP/VSV-G) used for flow cytometry analyses was produced by co-transfection of 5 million HEK293T per 10-cm dish with 4 µg pSINcPPT-CMV-eGFP genomic plasmid [19], 4 µg psPAX2 Gag-Pol packaging plasmid (gift from Didier Trono, Addgene #12260 [19]) and 2 µg of pMD2.G VSV-G envelope (gift from Didier Trono, Addgene #12259 [19]) using jetPRIME transfection reagent (Polyplus-transfection, Illkirch, France) according to manufacturer's recommendations. Alternatively, single-round HIV reporter (HIV/VSV-G) used for single-cell infection assessment was produced by co-transfection with 7.5 µg pNL4-3ΔEnv-GFP (NIH AIDS Research and Reference Reagent program, Cat. #11100) and 2.5 µg of pMD2.G in similar conditions. Culture medium was replaced by fresh 293 Serum Free Medium III (Thermo Fisher Scientific) supplemented with glutamax (Thermo Fisher Scientific) 8 hours post-transfection. Viral particles were collected 48h post-transfection and filtered using 0.22 µm filter (Merck) (HIV_GFP/VSV-G) or on Centricon units (Merck) (HIV/VSV-G). Viral titers were measured by p24 immunoassay using INNOTEST HIV Antigen mAb (Fujirebio, Tokyo, Japan) according to manufacturer's instructions.

Permissiveness to HIV was monitored by GFP expression of primary CD4+ T cells infected at 48h, 72h, 96h, 120h and 144h p.-s. and assessed by flow cytometry 47h p.-i. Briefly, this was performed by exposing 100,000 cells to 30 ng HIV_GFP/VSV-G or mock treatment, in a volume of 110 µL in a 96-well U bottom plate. Alternatively, 1,000,000 cells 48h post-TCR stimulation were exposed to 1100 ng HIV/VSV-G or mock treatment, in a volume of 400 µL in a 14 mL polypropylene tube. Infections were carried out in presence of 4 µg/mL polybrene (Merck) and by spinoculation (1500 g, 90 min, 25°C). After that, cells were washed and resuspended at 10^6 cells/mL in R10 supplemented with IL-2 [200 IU/L] and incubated for 28 (HIV/VSV-G) or 47h (HIV_GFP/VSV-G). Cells were fixed in 200 µL CellFix 1X (Becton Dickinson, Franklin Lakes, NJ, USA) to monitor GFP expression by flow cytometry.

Flow cytometry

Flow cytometry analysis of infected samples were performed using Gallios machine on FL1 channel (Beckman Coulter, Brea, CA, USA; Flow Cytometry Facility, University of Lausanne). All flow cytometry graphs and analyses were generated using FlowJo (v.10.7.1) software (Becton Dickinson).

Sc-RNA-Seq library preparation and sequencing

Cell suspensions were loaded into a Chromium Next GEM chip G with a target capture of 10,000 cells per sample. Gene expression (GEX) libraries were generated using Chromium Next GEM Single Cell 3' Reagent Kit v3.1 (10X Genomics, Pleasanton, CA, US) according to manufacturer's recommendations and were then sequenced using NovaSeq 6000 (Illumina, San Diego, CA, US) by paired-end 100 nucleotides dual indexing protocol at Lausanne Genomic Technologies Facility (LGTF).

Sc-RNA-Seq analysis

GEX matrix reads were generated by alignment and read count using CellRanger (10X Genomics, v.7.1). They were then loaded into R (v.4.0.4) and analyzed using Seurat package (v4) [11]. Briefly, samples were filtered for poor quality (expressing less than 200 transcripts and displaying more than 15% mitochondrial genes). Samples were then normalized using SCTransform. Cell types were annotated with Seurat multimodal reference mapping (reference dataset [11]), and our datasets and Seurat reference were integrated for generating a common UMAP visualization [11]. Resistant and permissive cell labelling for non-exposed cells was achieved by similarity to exposed-infected and resistant cells. The similarity was computed by a k-NN algorithm in Seurat, on normalized datasets [20]. Signature scores on single cell expression data were computed with the AddModuleScore function from the Seurat package. This function implements the method described in by Tirosh *et al.* [21]. Statistical significance was calculated by non-parametric Wilcoxon t-test. Gene set enrichment analysis (GSEA) [22] was performed with the GSEA function from the clusterProfiler R package (version 4.2.2 [23]) with the following parameters: minGSSize = 10, maxGSSize = 1000, eps = 0, pvalueCutoff = 0.05. Pathways with an adjusted *p*-value < 0.05 were deemed as significantly enriched.

References

1. Whitney, J.B. and Brad Jones, R., *In Vitro and In Vivo Models of HIV Latency.* Adv Exp Med Biol, 2018. **1075**: p. 241-263.
2. Ciuffi, A., Bleiber, G., Munoz, M., . . . Telenti, A., *Entry and transcription as key determinants of differences in CD4 T-cell permissiveness to human immunodeficiency virus type 1 infection.* J Virol, 2004. **78**(19): p. 10747-54.
3. Rausell, A., Munoz, M., Martinez, R., . . . Ciuffi, A., *Innate immune defects in HIV permissive cell lines.* Retrovirology, 2016. **13**(1): p. 43.
4. Woodland, D.L. and Dutton, R.W., *Heterogeneity of CD4(+) and CD8(+) T cells.* Curr Opin Immunol, 2003. **15**(3): p. 336-42.

5. Brandt, L., Cristinelli, S., and Ciuffi, A., *Single-Cell Analysis Reveals Heterogeneity of Virus Infection, Pathogenicity, and Host Responses: HIV as a Pioneering Example.* Annu Rev Virol, 2020. **7**(1): p. 333-350.
6. Wong, M., Wei, Y., and Ho, Y.C., *Single-cell multiomic understanding of HIV-1 reservoir at epigenetic, transcriptional, and protein levels.* Curr Opin HIV AIDS, 2023. **18**(5): p. 246-256.
7. Cavrois, M., Banerjee, T., Mukherjee, G., . . . Roan, N.R., *Mass Cytometric Analysis of HIV Entry, Replication, and Remodeling in Tissue CD4+ T Cells.* Cell Rep, 2017. **20**(4): p. 984-998.
8. Gantner, P., Buranapraditkun, S., Pagliuzza, A., . . . Chomont, N., *HIV rapidly targets a diverse pool of CD4(+) T cells to establish productive and latent infections.* Immunity, 2023. **56**(3): p. 653-668 e5.
9. Rato, S., Rausell, A., Munoz, M., . . . Ciuffi, A., *Single-cell analysis identifies cellular markers of the HIV permissive cell.* PLoS Pathog, 2017. **13**(10): p. e1006678.
10. Luo, X., Frouard, J., Zhang, G., . . . Greene, W.C., *Subsets of Tissue CD4 T Cells Display Different Susceptibilities to HIV Infection and Death: Analysis by CyTOF and Single Cell RNA-seq.* Front Immunol, 2022. **13**: p. 883420.
11. Hao, Y., Hao, S., Andersen-Nissen, E., . . . Satija, R., *Integrated analysis of multimodal single-cell data.* Cell, 2021. **184**(13): p. 3573-3587 e29.
12. Schmiedel, B.J., Gonzalez-Colin, C., Fajardo, V., . . . Vijayanand, P., *Single-cell eQTL analysis of activated T cell subsets reveals activation and cell type-dependent effects of disease-risk variants.* Sci Immunol, 2022. **7**(68): p. eabm2508.
13. Monaco, G., Lee, B., Xu, W., . . . Larbi, A., *RNA-Seq Signatures Normalized by mRNA Abundance Allow Absolute Deconvolution of Human Immune Cell Types.* Cell Rep, 2019. **26**(6): p. 1627-1640 e7.
14. Grau-Exposito, J., Serra-Peinado, C., Miguel, L., . . . Buzon, M.J., *A Novel Single-Cell FISH-Flow Assay Identifies Effector Memory CD4(+) T cells as a Major Niche for HIV-1 Transcription in HIV-Infected Patients.* mBio, 2017. **8**(4).
15. Collora, J.A., Liu, R., Pinto-Santini, D., . . . Ho, Y.C., *Single-cell multiomics reveals persistence of HIV-1 in expanded cytotoxic T cell clones.* Immunity, 2022. **55**(6): p. 1013-1031 e7.
16. Jurczyszak, D., Manganaro, L., Buta, S., . . . Simon, V., *ISG15 deficiency restricts HIV-1 infection.* PLoS Pathog, 2022. **18**(3): p. e1010405.
17. Krapp, C., Hotter, D., Gawanbacht, A., . . . Kirchhoff, F., *Guanylate Binding Protein (GBP) 5 Is an Interferon-Inducible Inhibitor of HIV-1 Infectivity.* Cell Host Microbe, 2016. **19**(4): p. 504-14.
18. Ding, J., Wang, S., Wang, Z., . . . Cen, S., *Schlafen 5 suppresses human immunodeficiency virus type 1 transcription by commandeering cellular epigenetic machinery.* Nucleic Acids Res, 2022. **50**(11): p. 6137-6153.
19. Naldini, L., Blomer, U., Gallay, P., . . . Trono, D., *In vivo gene delivery and stable transduction of nondividing cells by a lentiviral vector.* Science, 1996. **272**(5259): p. 263-7.
20. Stuart, T., Butler, A., Hoffman, P., . . . Satija, R., *Comprehensive Integration of Single-Cell Data.* Cell, 2019. **177**(7): p. 1888-1902 e21.
21. Tirosh, I., Izar, B., Prakadan, S.M., . . . Garraway, L.A., *Dissecting the multicellular ecosystem of metastatic melanoma by single-cell RNA-seq.* Science, 2016. **352**(6282): p. 189-96.

22. Subramanian, A., Tamayo, P., Mootha, V.K., . . . Mesirov, J.P., *Gene set enrichment analysis: a knowledge-based approach for interpreting genome-wide expression profiles.* Proc Natl Acad Sci U S A, 2005. **102**(43): p. 15545-50.
23. Yu, G., Wang, L.G., Han, Y., and He, Q.Y., *clusterProfiler: an R package for comparing biological themes among gene clusters.* OMICS, 2012. **16**(5): p. 284-7.

Supplementary material

Supplementary Figures

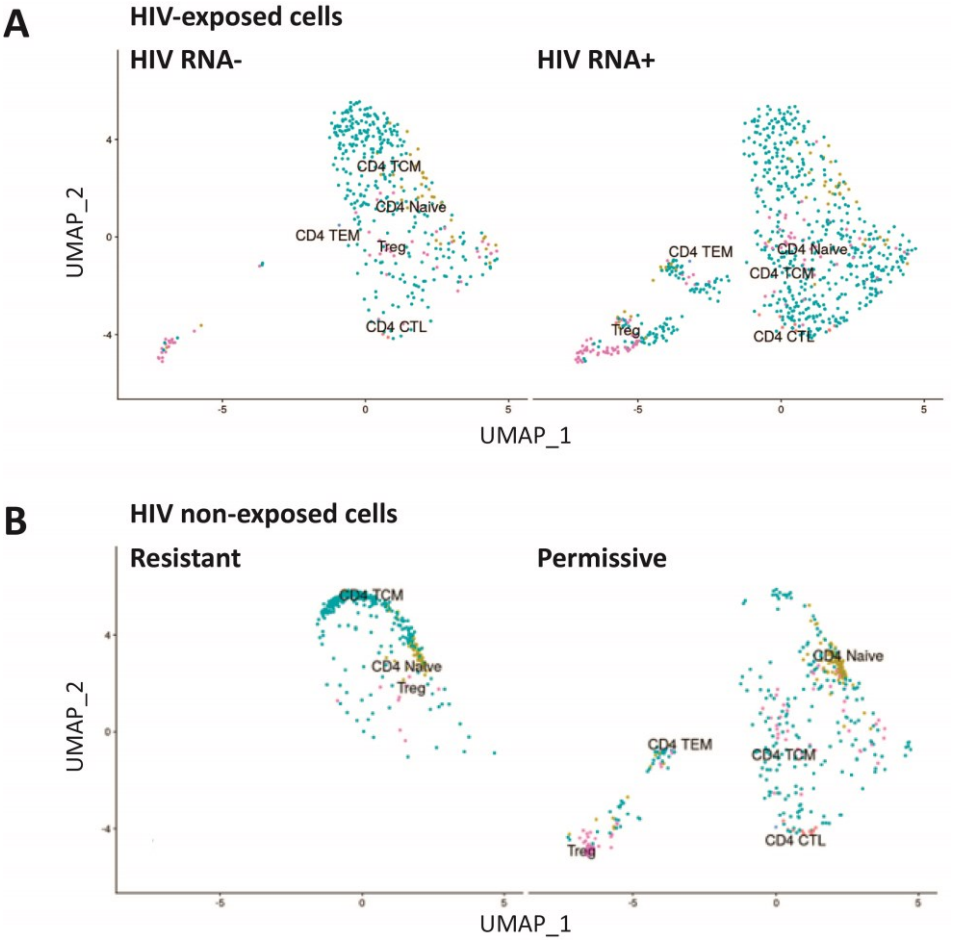

Supplementary Figure 1: UMAP cell subtype distribution. Cell subtype identification and distribution in HIV-exposed cells in HIV RNA- (left) and HIV RNA+ (right) cells (A), and in HIV non-exposed cells in predicted resistant (left) or permissive (right) cells. CTL, cytotoxic lymphocyte (red); TCM, T central memory (blue); TEM, T effector memory (dark blue); Treg, regulatory T cell (pink); Naïve, CD4+ Naïve T cells (kaki); UMAP, uniform manifold approximation and projection.

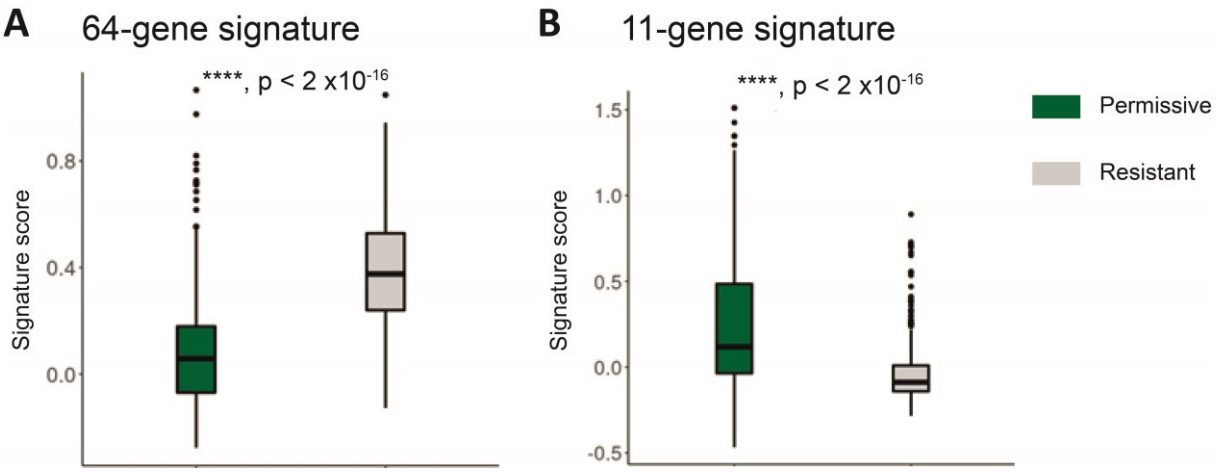

Supplementary Figure 2: Gene signature scores for prediction of permissive and resistant cell phenotype. Prediction score of permissive (green) and resistant (grey) using the total 64-gene signature (A) or the 11-gene signature downregulated in resistant cells (B). DEG, differentially expressed gene.

Supplementary Tables

Supplementary Table 1: Cell counts over time post-stimulation and annotated with Seurat. CTL, cytotoxic lymphocyte; Tcm, T central memory; Tem, T effector memory; Treg, regulatory T cell.

	48h	72h	96h	120h	144h
CD4 CTL	2 (0.04%)	4 (0.08%)	4 (0.07%)	5 (0.09%)	3 (0.05%)
CD4 Naïve	1,025 (21.99%)	832 (16.99%)	662 (11.87%)	295 (5.23%)	165 (2.59%)
CD4 Proliferating	1,362 (29.22%)	2,304 (47.04%)	3,396 (60.89%)	4,032 (71.46%)	3,655 (57.39%)
CD4 Tcm	1,199 (25.72%)	1,215 (24.81%)	1,376 (24.67%)	1,237 (21.92%)	2,502 (39.28%)
CD4 Tem	13 (0.28%)	10 (0.20%)	0 (0%)	3 (0.05%)	4 (0.06%)
Treg	1,060 (22.74%)	533 (10.88%)	139 (2.49%)	70 (1.24%)	40 (0.63%)
Total	4,661	4,898	5,577	5,642	6,369

Supplementary Table 2: Cell counts in the HIV-exposed cell sample as annotated with Seurat and separated according to HIV RNA detection in the sample. Percentages of resistant and permissive cells are indicated in parenthesis in function of total cells from each subtype. CTL, cytotoxic lymphocyte; Tcm, T central memory; Tem, T effector memory; Treg, regulatory T cell.

	Total cells	HIV RNA- cells (resistant)	HIV RNA+ cells (permissive)
CD4 CTL	10	2 (20%)	8 (80%)
CD4 Naïve	81	34 (42.0%)	47 (58.0%)
CD4 Proliferating	2,184	56 (2.6%)	2,128 (97.4%)
CD4 Tcm	903	314 (34.8%)	589 (65.2%)
CD4 Tem	2	1 (50%)	1 (50%)
Treg	162	51 (31.5%)	111 (68.5%)
Total	3,342	458 (13.7%)	2,884 (86.3%)

Supplementary Table 3: Cell counts in the HIV non-exposed cell sample as annotated with Seurat and separated according to predicted phenotype. Percentages of resistant and permissive cells are indicated in parenthesis in function of total cells from each subtype. CTL, cytotoxic lymphocyte; Tcm, T central memory; Tem, T effector memory; Treg, regulatory T cell.

	Total cells	Resistant	Permissive
CD4 CTL	10	0 (0%)	10 (2.0%)
CD4 Naïve	176	54 (14.6%)	122 (24.5%)
CD4 Tcm	554	307 (83.0%)	247 (49.6%)
CD4 Tem	4	0 (0%)	4 (0.8%)
Treg	124	9 (2.4%)	115 (0.8%)
Total	868	370	498

Supplementary Table 4: 64-gene signature differentially expressed between permissive and resistant cells.

Signature	Gene name	p-value	Average log_2FC	Expression frequency in permissive cells	Expression frequency in resistant cells	Adjusted p-value
53-gene signature	**IFIT2**	1.54E-63	-1.99	0.104	0.654	2.68E-59
	SAMD9	1.60E-55	-1.734	0.357	0.778	2.79E-51
	MX1	1.76E-47	-1.508	0.61	0.905	3.05E-43
	IFIT3	1.25E-40	-1.837	0.096	0.489	2.18E-36
	IFIT1	2.00E-36	-1.32	0.026	0.343	3.48E-32
	RSAD2	3.63E-36	-1.572	0.068	0.419	6.31E-32
	IFI6	7.43E-36	-1.154	0.6	0.873	1.29E-31
	ISG15	4.49E-35	-1.029	0.863	0.986	7.81E-31
	MALAT1	2.33E-33	-0.639	1	1	4.04E-29
	XAF1	4.96E-33	-1.351	0.249	0.603	8.61E-29
	RPL30	3.93E-32	-0.478	1	1	6.82E-28
	TPT1	1.90E-31	-0.589	1	1	3.30E-27
	FTL	1.24E-30	-0.642	1	1	2.15E-26
	NUB1	2.68E-29	-1.029	0.902	0.997	4.66E-25
	TRIM56	2.99E-27	-0.804	0.743	0.965	5.19E-23
	SLFN5	6.51E-27	-0.906	0.896	0.992	1.13E-22
	APOL6	3.39E-25	-0.873	0.765	0.954	5.88E-21
	RPS27	5.10E-25	-0.473	1	1	8.87E-21
	GBP1	2.29E-24	-0.901	0.729	0.938	3.98E-20
	B2M	2.89E-24	-0.468	1	1	5.02E-20
	MX2	4.36E-22	-1.092	0.086	0.341	7.58E-18
	DDX5	9.92E-21	-0.437	1	1	1.72E-16
	TRIM22	1.74E-20	-0.775	0.763	0.943	3.03E-16
	HERC5	6.34E-20	-1.087	0.171	0.422	1.10E-15
	PSME1	6.57E-20	-0.468	1	1	1.14E-15
	IFI44L	1.01E-19	-1.077	0.118	0.365	1.75E-15
	DTX3L	3.90E-18	-0.672	0.546	0.786	6.77E-14
	STAT1	1.05E-17	-0.506	0.982	1	1.82E-13
	PARP14	2.29E-17	-0.846	0.942	1	3.98E-13

	NT5C3A	2.63E-16	-0.652	0.783	0.935	4.56E-12
	PARP9	2.72E-16	-0.534	0.55	0.797	4.72E-12
	LY6E	8.55E-15	-0.536	0.966	1	1.48E-10
	TAP1	1.86E-14	-0.463	0.988	1	3.22E-10
	IFI44	1.98E-14	-0.838	0.127	0.324	3.44E-10
	ISG20	2.42E-13	-0.953	0.289	0.47	4.20E-09
	GBP5	2.61E-13	-0.962	0.175	0.373	4.54E-09
	GBP4	3.84E-13	-0.892	0.163	0.357	6.66E-09
	CASP8	4.16E-13	-0.511	0.687	0.892	7.22E-09
	ZC3HAV1	4.42E-13	-0.541	0.878	0.997	7.68E-09
	ERAP2	2.55E-12	-0.479	0.737	0.924	4.43E-08
	TRIM38	9.18E-12	-0.558	0.871	0.986	1.59E-07
	IL7R	9.82E-12	-0.478	0.753	0.965	1.71E-07
	NMI	3.65E-11	-0.431	0.765	0.941	6.34E-07
	UBE2L6	7.58E-11	-0.427	0.839	0.986	1.32E-06
	SP110	1.09E-10	-0.461	0.908	0.997	1.89E-06
	PLAAT4	2.08E-10	-0.645	0.157	0.338	3.61E-06
	TNFSF10	3.44E-10	-0.465	0.781	0.962	5.97E-06
	SP100	4.78E-10	-0.451	0.97	1	8.30E-06
	EIF2AK2	8.58E-10	-0.5	0.924	1	1.49E-05
	N4BP2L2	8.88E-10	-0.424	0.98	0.997	1.54E-05
	ZNFX1	1.78E-09	-0.429	0.775	0.938	3.09E-05
	PHF11	3.01E-08	-0.452	0.861	0.986	5.23E-04
	SAMD9L	7.20E-08	-0.71	0.213	0.346	1.25E-03
11-gene signature	**TNFAIP8**	9.82E-16	0.44	1	1	1.70E-11
	IL2RA	6.40E-14	0.646	1	1	1.11E-09
	CD2	2.23E-13	0.706	1	1	3.88E-09
	ACTB	3.42E-11	0.492	1	1	5.95E-07
	ADTRP	4.64E-10	0.489	0.317	0.135	8.07E-06
	TNFAIP3	5.50E-10	0.488	0.946	0.997	9.56E-06
	TNFRSF18	7.88E-10	0.728	0.934	0.992	1.37E-05
	LMNA	4.29E-09	0.502	0.932	0.997	7.44E-05
	IL32	4.96E-08	1.05	0.988	1	8.62E-04
	MAF	1.24E-07	1.195	0.912	0.997	2.15E-03
	MIR155HG	2.84E-07	0.549	0.988	1	4.93E-03

ANNUAL REVIEWS

Annual Review of Virology

Single-Cell Analysis Reveals Heterogeneity of Virus Infection, Pathogenicity, and Host Responses: HIV as a Pioneering Example

Ludivine Brandt,* Sara Cristinelli,* and Angela Ciuffi

Institute of Microbiology, Lausanne University Hospital, University of Lausanne, 1011 Lausanne, Switzerland; email: Angela.Ciuffi@chuv.ch

Annu. Rev. Virol. 2020. 7:333–50

The *Annual Review of Virology* is online at virology.annualreviews.org

https://doi.org/10.1146/annurev-virology-021820-102458

*These authors contributed equally to this article.

Keywords

single-cell, heterogeneity, HIV, permissiveness, latency, innate immunity, immunity

Abstract

While analyses of cell populations provide averaged information about viral infections, single-cell analyses offer individual consideration, thereby revealing a broad spectrum of diversity as well as identifying extreme phenotypes that can be exploited to further understand the complex virus-host interplay. Single-cell technologies applied in the context of human immunodeficiency virus (HIV) infection proved to be valuable tools to help uncover specific biomarkers as well as novel candidate players in virus-host interactions. This review aims at providing an updated overview of single-cell analyses in the field of HIV and acquired knowledge on HIV infection, latency, and host response. Although HIV is a pioneering example, similar single-cell approaches have proven to be valuable for elucidating the behavior and virus-host interplay in a range of other viruses.

1. INTRODUCTION

Analyses of populations are very useful as they provide a general picture of the infectiousness of a virus or the features of a viral disease, including clinical signs and progression. However, population analyses average multiple individual infection outcomes that vary according to host genetic, environmental, and viral factors. Indeed, individuals are genetically unique, displaying specific responses to viral infections, from resistance to susceptibility toward acquisition, from low to high viremia, from long-term nonprogression to rapid progression of the disease, or from absence of control to elite immune control (**Figure 1*a***). Extreme phenotypes are thus usually masked in the average bulk population. In order to understand the genetic bases of these variable individual responses toward human immunodeficiency virus (HIV) infection, the past two decades have included a focus on genome-wide association studies highlighting a major role of human leukocyte antigens (HLAs) and C-C chemokine receptor type 5 (CCR5) loci (1–4). These studies allowed researchers to identify specific gene variants involved in HIV pathogenesis at large and explain a maximum of ~30% of individual variation (5).

Similarly, individual cells also present variability toward HIV infection, despite mostly identical genetic content, except for HIV genome insertion, point mutations, or T cell receptor rearrangement (**Figure 1*b***). Therefore, infection success depends mostly on cell composition (with the spectrum of expressed gene products providing a favorable or restrictive environment for virus replication) and on the environment (extracellular milieu and interactions with neighboring cells). Improvement of technologies in the past decade has allowed for isolation and analysis at single-cell resolution, thereby providing tools to explore cell heterogeneity and identify gene products and cell biomarkers involved in specific HIV-related phenotypes (6). In this review we summarize the application of a wide range of such single-cell approaches and discuss examples of the integration of complementary results from different approaches. These results both illustrate powerful advances in understanding HIV replication and host interactions, and provide a useful example of the dramatic potential of emerging similar single-cell studies for other viruses.

2. SINGLE-CELL TECHNOLOGIES

Analyses at the single-cell level have traditionally used technologies with poor resolution, such as cell imaging or flow cytometry, providing limited information about the cell. The identification of the human genome sequence in the third millennium opened new perspectives to understand human and cell biology in a more comprehensive and genome-wide manner (7). Tang et al. (8) marked the second milestone and opened the way of single-cell technologies by publishing the first transcriptome-wide analysis of an individual cell by sequencing messenger RNAs (mRNAs) from a single mouse blastomer [single-cell RNA sequencing (scRNA-Seq)]. This analysis was the first step toward gathering a broader and more complete picture of the cell.

The study of individual cells is mainly a two-step process, requiring single-cell isolation on one hand and analysis of that cell at the molecular level on the other hand; these steps are briefly described here.

2.1. Single-Cell Isolation

The single-cell analysis workflow starts with sorting and isolating individual cells, which can be achieved using multiple approaches that diverge mainly in throughput and automation level (9–12). Limiting dilution of a cell suspension can be performed with conventional lab equipment; it is cost effective but labor intensive, resulting in a low cell throughput. Micromanipulation for manual cell picking or laser microdissection requires some specific equipment and results

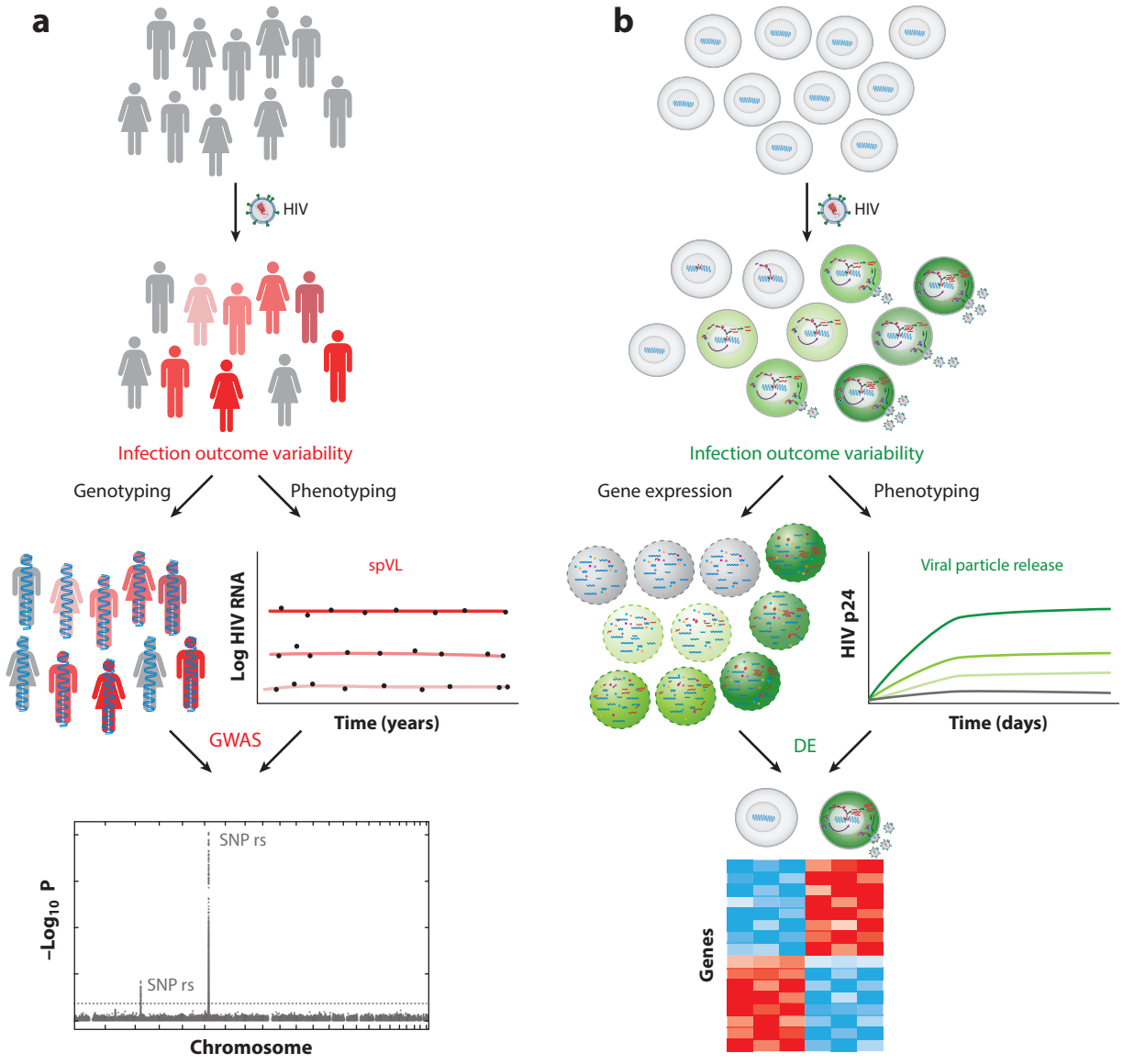

Figure 1

Exploring living heterogeneity as a tool to identify virus-host interactions. (*a*) Individuals are not equal toward HIV acquisition and HIV disease progression. Some people are resistant (*gray*), while other people are infected but are able to control viremia to undetectable or low levels, and hence they do not progress or progress slowly to disease (*light red*). In contrast, some people progress very rapidly to disease onset (*red*). Analysis of individual genotypes and correlation with a specific phenotype such as the spVL allow for GWASs and identification of gene variants that affect the phenotype outcome, either positively or negatively. (*b*) Individual cells are not equal toward HIV infection. Although almost genetically identical, cells from the same donor are not equally permissive to HIV infection, ranging from resistant cells (*gray*) to various levels of productive infection (*green shades*). Analysis of individual cellular content (RNA, protein, etc.) and correlation with a specific phenotype such as viral production allow for the identification of cellular proteins that affect the phenotypic outcome. Abbreviations: DE, differential expression; GWAS, genome-wide association study; HIV, human immunodeficiency virus; SNP rs, single-nucleotide polymorphism reference; spVL, set-point viral load.

usually in a low cell throughput. Fluorescence-activated cell sorting (FACS) allows single-cell sorting by flow cytometry using fluorescent reporters or antibody-based recognition of specific proteins. This approach can be coupled with automated single-cell dispensing, thereby increasing the cell throughput recovery. Although FACS can sort cells according to up to 18 colorimetric parameters, it requires pressurization to handle cells, which can induce damage. Novel devices have been recently developed, allowing automated single-cell sorting and dispensing based on a few parameters only but with lower pressure to minimize cell perturbation. Progress in microfluidics further allowed the development of well-based integrated circuits or droplet-based technologies to physically separate or encapsulate single cells, allowing for full automation and higher throughput. Further progress in nano- and picofluidics, combined with cell indexing and barcoding, further pushed forward the number of individual cells that can be isolated and analyzed. Thus, single-cell isolation techniques improved in the past decade, starting from one single cell isolated manually in 2009 to up to 100,000 cells isolated mechanically today (8, 11).

2.2. Single-Cell Analysis

Recent advances in molecular biology, such as sequencing technologies, allowed the development of methods supporting the study and characterization of individual cells. These methods include profiling of the genome (13–15), epigenome (16–18), transcriptome (6, 19–25), or proteome (26–28), and they can be used either alone or in combination (e.g., coupled analysis of RNA sequences with epigenetic modifications or protein abundance) (29–33) (**Figure 2**).

Although ideally single-cell analysis points toward integrated multi-omic analysis to gather the most complete picture of the single cell, the technology that is currently mostly used focuses on whole transcriptome analysis, as it can benefit from powerful high-throughput sequencing technologies and thus provide an extensive view of the RNA cell content (6, 11, 20, 29, 34, 35). In order to perform scRNA-Seq, the first barrier to overcome is the initial RNA material input. Indeed, a single cell contains between 1 and 50 pg RNA according to the cell type, which is not enough to perform RNA-Seq. To overcome this limitation, the RNA is first converted into complementary DNA (cDNA) and amplified before preparing sequencing libraries. Multiple methods exist for reverse transcription and cDNA library preparation, which differ mostly by three criteria: (*a*) full-length or 3′-end enrichment of RNA molecules such as switching mechanism at 5′ end of RNA template sequencing (Smart-Seq) and droplet-sequencing (Drop-Seq), respectively; (*b*) insertion or not of a unique molecular identifier (UMI) and a cell barcode; and (*c*) linear or exponential cDNA amplification followed by RNA-based library preparation or by tagmentation (reviewed in 11, 20, 21).

In a comparative study, Ziegenhain et al. (20) showed that full-length methods, i.e., covering the whole transcript but without UMIs or barcode, were more sensitive than multiplexed 3′-counting methods with UMIs. Indeed, using a cutoff of 1 million reads per cell, full-length based RNA-Seq allowed a median detection ranging from 7,572 to 9,138 genes, while the median detection of genes was generally lower for 3′-end based RNA-Seq samples, from 4,763 to 7,906 genes. Furthermore, pool analysis of 65 individual cells allowed detecting a total of ~17,000 to ~21,000 genes, similar to bulk RNA-Seq detection. Besides sensitivity, full-length methods are likely to be more appropriate for isoform analyses, alternative splicing, and single nucleotide polymorphism identification on a small size sample, while tag-based methods may be more adapted for gene expression quantification in a complex cell sample by allowing multiplexing and analysis of a larger number of cells at the same time.

Variability of gene expression across cells is very high, as 87% of genes are detected in only 1–2 single cells with a low level of expression (20). This single-cell transcriptome diversity has

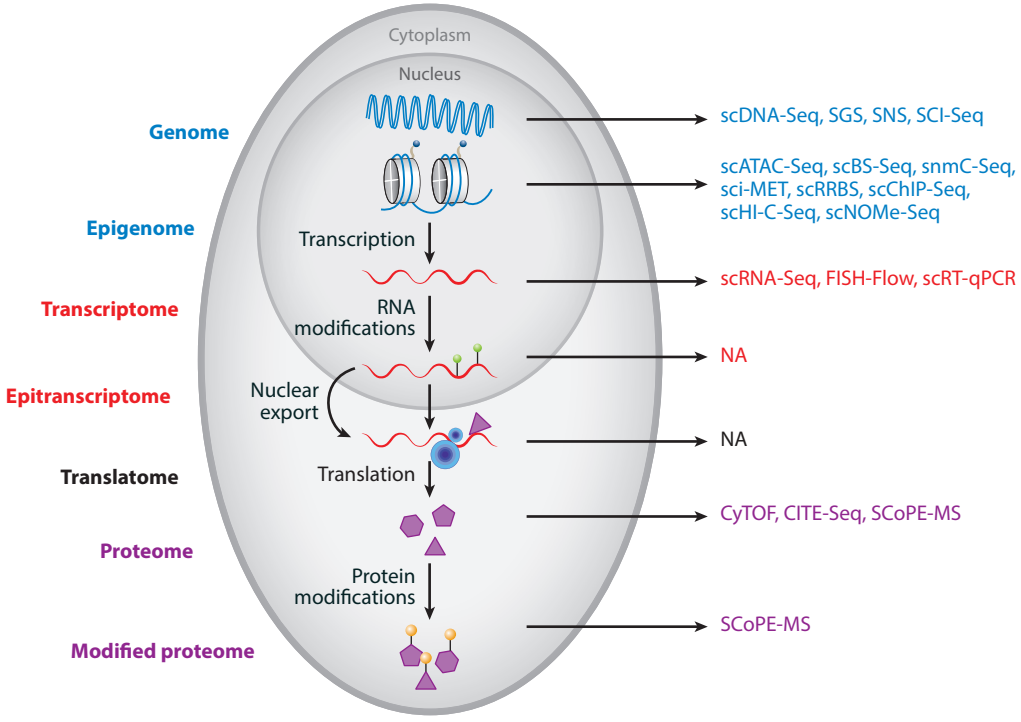

Figure 2

Single-cell technologies. Multiple single-cell methods have been developed in order to interrogate the various layers of the cell. The single-cell genome can be analyzed by single-cell DNA sequencing (scDNA-Seq), single-genome sequencing (SGS), short nascent DNA strand sequencing (SNS), and single-cell combinatorial indexed sequencing (SCI-Seq). The single-cell epigenome can be analyzed by single-cell assay for transposase-accessible chromatin followed by sequencing (scATAC-Seq), single-cell bisulfite conversion sequencing (scBS-Seq), single nucleus methylcytosine sequencing (snmC-Seq), single-cell combinatorial indexing for methylation analysis (sci-MET), single-cell reduced-representation bisulfite sequencing (scRRBS), single-cell chromatin immune-precipitation sequencing (scChIP-Seq), single-cell Hi-C sequencing (scHI-C-Seq), and single-cell nucleosome occupancy and methylome sequencing (scNOMe-Seq). The single-cell transcriptome can be explored by single-cell RNA sequencing (scRNA-Seq), fluorescence in situ hybridization coupled with flow cytometry (FISH-Flow), and single-cell reverse transcription followed by quantitative PCR (scRT-qPCR). Single-cell technologies to explore the epitranscriptome and translatome have not been developed yet. The study of the proteome at single-cell resolution can be performed by cytometry time-of-flight (CyTOF) and cellular indexing of transcriptomes and epitopes by sequencing (CITE-Seq). Single-cell proteomes and modified proteomes can be analyzed by single-cell proteomics by mass spectrometry (SCoPE-MS). Abbreviation: NA, not applicable.

two main origins: biological and technical. Cellular variability is due to variations in cell-specific expression programs (cell lineage, cell state) and stochastic gene expression. Technical variability is instead due to the incomplete capture of all cellular mRNAs and sequencing depth. Thus, the major challenge of scRNA-Seq is data analysis aimed at minimizing the technical variability, starting from barcode processing, read mapping to a genome or transcriptome reference, raw count matrix generation (gene/UMI counting), preprocessing, normalization, and differential expression analysis (36–38). In a recent study, Vieth et al. (37) evaluated multiple scRNA-Seq pipelines and identified library preparation protocols and normalization as having the greatest effect on the analysis quality. They further recommended analyzing UMI-containing scRNA-Seq data using genome mapping with GENCODE annotation and the splice-aware aligner STAR, preprocessing for gene dropout using SAVER imputation, normalization benefiting from spike-in inclusion and using scran with prior clustering, and differential expression testing using limma-trend (37).

Finally, scRNA-Seq data can be visualized in a two-dimensional plot upon dimensionality reduction, ranging from principal component analysis (PCA) plots for low complexity samples, to t-distributed stochastic neighbor embedding (t-SNE) plots for more complex samples, and more recently to the preferred and more comprehensive uniform manifold approximation and projection (UMAP) plots (38).

2.3. Single-Cell Limitations

Single-cell analyses offer ways to explore cellular heterogeneity per se, as well as cellular heterogeneity in response to a viral infection, providing unprecedented opportunities to identify novel players in the virus-host interplay (6). However, it is important to keep in mind the limitations associated with these technologies: technological restrictions, phenotype association, and possible time-lapse between the single-cell analysis and the phenotype.

Indeed, single-cell technologies are powerful but suffer from multiple technical constraints, such as the manipulation leading to single-cell isolation, the one-shot analysis of a number of limited molecules or parameters, and the technical sensitivity. Exploring the cell-omic content reveals cell heterogeneity but is poorly informative if it is not related to a specific phenotype for the analysis, which needs to be identified and measured as accurately as possible. Finally, it is important to consider the possible temporal gap between the time at which the single-cell analysis is performed and the time at which the associated phenotype is observed, as cell-omic content may change. Indeed, it is difficult to characterize the transcriptomic features of a permissive cell at the time of infection before knowing if the cell is indeed truly permissive and thus infected, for instance.

3. HETEROGENEOUS CELLS PROVIDE HETEROGENEOUS RESPONSES TO HIV

To date, in the field of HIV, single-cell technologies have been mostly used to identify specific gene signatures in the following topics: the cell permissiveness to HIV infection, the latent HIV-infected cell and its reactivation, and the control of HIV infection by immune cells (**Figure 3**). An overview of the main findings is summarized here.

3.1. HIV Permissiveness

Infection outcome is determined by the cell content and results from a balance between cellular players promoting or restricting HIV progression throughout the cell. To successfully replicate, HIV encodes 15 proteins, each of which is able to interact with a plethora of cellular proteins (39, 40). On one hand, HIV hijacks cellular factors, termed HIV dependency factors (HDFs), to favor its own replication (41). On the other hand, the cell possesses innate immune defenses, with HIV restriction factors and HIV inhibitory factors (HIFs), which are however often counteracted by HIV proteins (42–45). The identification of HDFs and HIFs informs on HIV life cycle but also provides novel opportunities for targeted antiviral development. Exploiting the cell heterogeneity toward HIV infection should help researchers gain more insights into HIV replication and the role of novel cellular factors.

$CD4^+$ T cell permissiveness to HIV infection can be observed using diverse approaches. Methodologies based on time-lapse microscopy, FACS, three-dimensional immuno-DNA fluorescence, and other visualization techniques provide many examples of cellular heterogeneity toward HIV infection, informing on many viral and kinetic features, such as time for early and late gene expression, nuclear location of proviruses, and viral RNA transcription, but without characterizing the permissive cell per se (46–56).

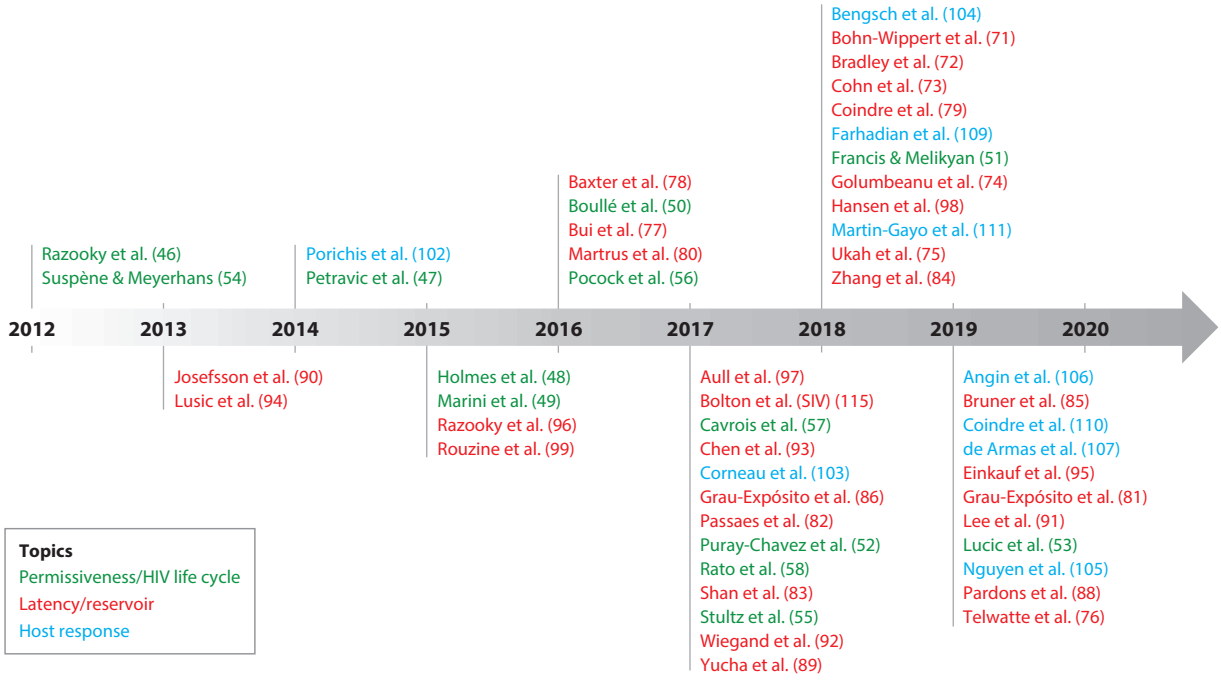

Figure 3

Timeline of human immunodeficiency virus (HIV) single-cell studies. In recent years, the number of studies using single-cell technologies has exponentially increased in the field of HIV, improving the knowledge of HIV life cycle and permissiveness (*green*), HIV latency and reservoir (*red*), and host immune response to HIV (*blue*).

Attempts at characterizing permissiveness were recently achieved by two studies using two different approaches (**Figure 4**). In a first study, Cavrois et al. (57) used mass cytometry or cytometry by time-of-flight (CyTOF) to investigate tonsillar $CD4^+$ T cell permissiveness using 38 parameters, aimed at identifying $CD4^+$ T cell subsets, activation status, and some receptors. They used a beta-lactamase (BlaM)-Vpr HIV virus encoding the murine heat stable antigen (HSA) as late reporter. The incorporation of BlaM-Vpr protein in the virion allows the rapid detection, within a 2-h time window, of viral entry upon virus fusion at the cell membrane, via intracellular cleavage of a fluorescent BlaM substrate, and subsequent sorting by FACS before CyTOF analysis. This analysis showed that HIV virions did not enter naïve $CD4^+$ T cells ($CD4^+CD45RA^+CD45RO^-$), likely due to low CCR5 expression, but entered all memory $CD4^+$ T cells ($CD4^+CD45RA^-CD45RO^+$) efficiently. In particular, virion fusion occurred more efficiently in Th2-like, Th17-like, and T regulatory cells. Cell permissiveness was then assessed by looking at virus-encoding HSA after 4 days of infection as a surrogate of successful viral expression. Although viruses entered all memory $CD4^+$ T cells, Th17-like ($CCR6^+CCR4^+$) and Tfh ($PD1^+CXCR5^+$) cells were more permissive to HIV replication and were further characterized by expression of CD69, CD38, PD1, CD57, and low CD127. In the second study, Rato et al. (58) used full-length scRNA-Seq to profile 166 $CD4^+$ T cells from two donors displaying opposite permissiveness phenotypes, correlating the transcriptome to cell surface protein expression and permissiveness. Their analysis identified highly permissive cells as expressing high levels of CD25, CD298, CD63, and CD317 and that were characterized at the transcriptome level by downregulation of innate immunity components such as genes involved in the type I interferon (IFN) pathway and certain other restriction factors.

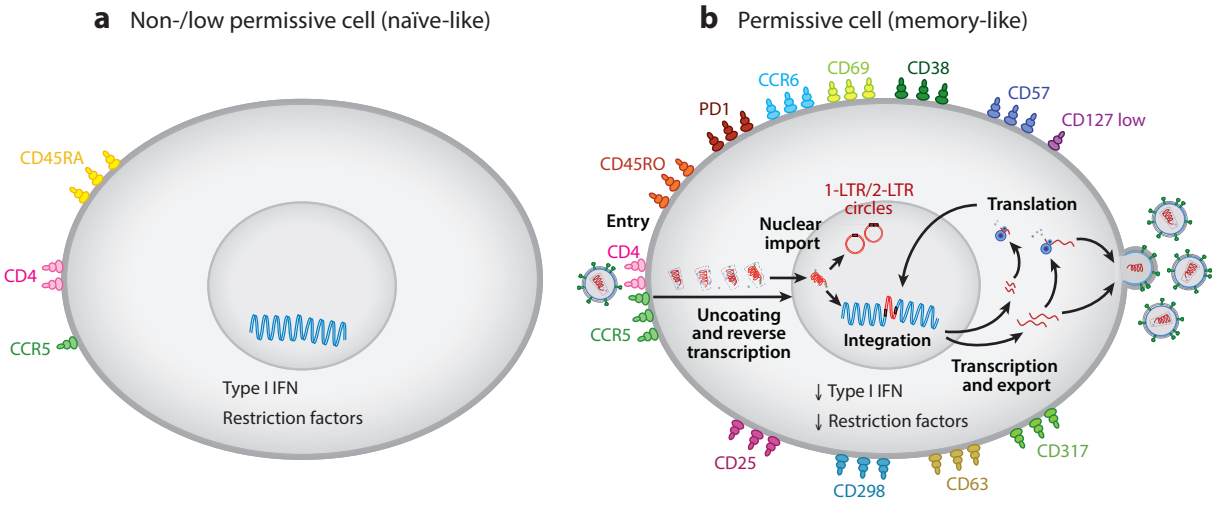

Figure 4

Determinants of human immunodeficiency virus (HIV) permissiveness. (*a*) Naïve CD4$^+$ T cells are mostly nonpermissive, mainly due to low C-C chemokine receptor (CCR) 5 expression. (*b*) In contrast, memory CD4$^+$ T cells are more permissive to HIV infection. However, Th17-like (CCR6$^+$CCR4$^+$) and Tfh (PD1$^+$CXCR5$^+$) cells expressing some activation markers (CD69, CD38), CD57, and low levels of CD127 (the interleukin-7 receptor) were shown to be the most permissive. Using another approach, CD4$^+$ T cells expressing high levels of CD25, CD298, CD63, and CD317 cell surface molecules corresponded to cells with impaired type I interferon (IFN) response and reduced expression of some HIV restriction factors, consistent with a permissive phenotype to HIV infection.

These studies are complementary and point toward an active cellular state and impaired immune response factors as determinants of HIV permissiveness.

3.2. HIV Pathogenicity: Latency Versus Reactivated or Productive Viral Expression

Although combined antiretroviral therapy (ART) allows efficiently stopping HIV disease progression, bringing plasma viremia to undetectable levels, it cannot completely get rid of the virus (59, 60). Indeed, upon ART cessation, the virus rebounds typically within 2–3 weeks, indicating the presence of a persistent viral reservoir (59–63). This reservoir is established very quickly upon virus transmission, within the first 2 to 3 days, and decays very slowly, thereby requiring life-long treatment for HIV$^+$ individuals and representing the major obstacle to an HIV cure (64–66). To date, the viral reservoir is characterized by the persistence of long-lived infected cells that contain an integrated copy of the viral genome and that are not eliminated, either because they reside in anatomical sanctuaries or because they are latent, i.e., with reduced viral protein expression and replication in these cells (67–70). Understanding all the features of this latent reservoir is thus considered to be essential in the development of targeted strategies aiming at its eradication (67–70).

The latent reservoir is very complex and heterogeneous as (*a*) the infected cell subset varies and thus differs in its transcriptomic and proteomic cell content, including naïve CD4$^+$ T cells, memory CD4$^+$ T cells (such as central or memory), or non-T cells (such as macrophages); (*b*) the cell state can vary, from resting to active or cycling status; and (*c*) the integration site of the HIV genome differs from one cell to another. This variability, in turn, affects the reactivation potential of latently infected cells, i.e., the potential for efficient induction of HIV gene product expression.

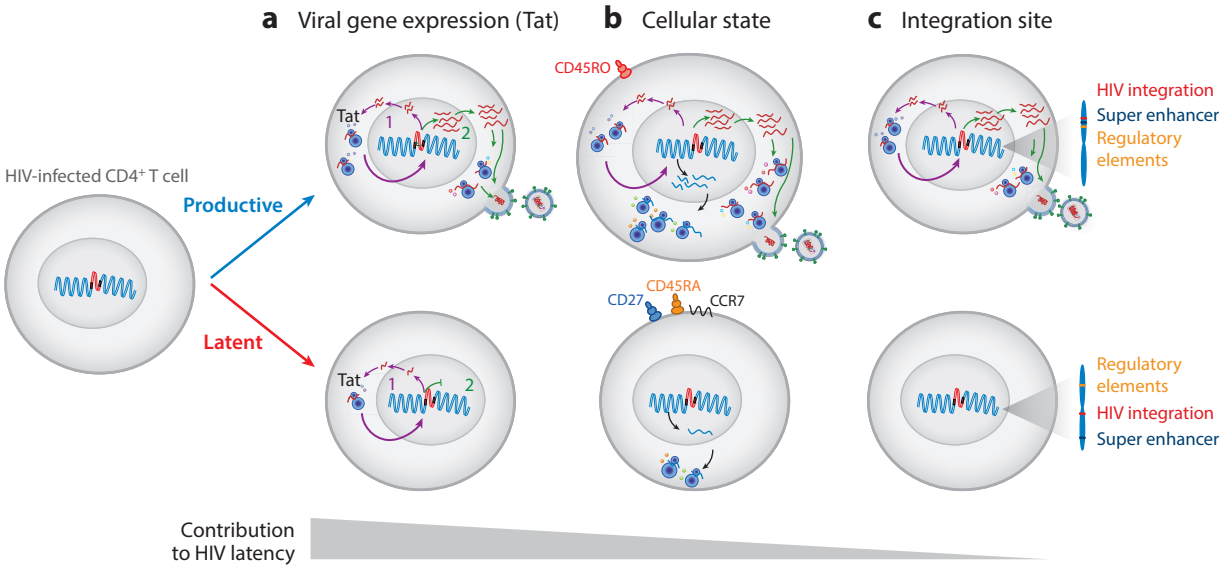

Figure 5

Relevant features of latently infected CD4$^+$ T cells. Human immunodeficiency virus (HIV)-infected CD4$^+$ T cells can be in either a productive or latent state. The cell fate can be influenced by three major contributors: (*a*) the expression level of the early viral Tat protein (*purple arrows*) that either can be insufficient to boost viral transcription (latent cell) or can successfully trigger the late phase of gene expression (*green arrows*) and allow viral particle production, (*b*) the cellular state of the cell can provide different cellular environments that can support and promote viral particle production or not, and (*c*) the provirus genomic context that can affect viral gene expression. Proviral insertions located close to super enhancers and certain other regulatory elements are more likely to be transcriptionally active. Abbreviation: CCR, C-C chemokine receptor.

Single-cell studies are thus instrumental to explore the heterogeneity of HIV latency establishment and reactivation. In particular, three aspects of virus-host interaction can be investigated with single-cell technologies: (*a*) host cell environment and genetic makeup, (*b*) the integration site location and nuclear location, and (*c*) viral gene expression (**Figure 5**).

Single-cell transcriptomic analyses were used to profile latent cells, characterizing cell heterogeneity and the associated transcriptional environment (71–76). Bradley et al. (72) used a primary cell latency model and analyzed a total of 4,206 latent CD4$^+$ T cells from three donors. They compared cellular transcriptomes of GFP^{high} vRNA^{high} cells versus GFP^{neg} vRNA^{low} bona fide latent cells and found 89 upregulated transcripts and 42 downregulated transcripts. Genes upregulated in the GFP^{high} vRNA^{high} productive population were consistent with an activated T cell state (CD25, OX40L, GITR) while the GFP^{neg} vRNA^{low} population was enriched in markers consistent with a naïve (Tn) or central memory (Tcm) phenotype (CCR7, CXCR4, CD62L, CD127).

One strategy to overcome latency consists of reactivating virus expression to purge the viral reservoir. Latency reversal agents (LRAs) can reactivate only a limited fraction of latently infected cells, confirming some degree of heterogeneity in the latent cell population. Golumbeanu et al. (74) explored transcriptional heterogeneity of 224 latently infected cells upon different reactivation conditions using scRNA-Seq in a primary cell latency model. They identified a 134-gene signature characterizing the inducible latent cell, showing enrichment for metabolism. Consistent with this, Bohn-Wippert et al. (71) and Cohn et al. (73) showed that cell size and cellular metabolic activity positively correlated with reactivation potential of latently infected cells, e.g.,

large and metabolically active cells were more prone to reactivation (71, 72, 74). Furthermore, scRNA-Seq analysis of latent or phytohaemagglutinin-reactivated $CD4^+$ T cells isolated from HIV-1^+ blood donors revealed enrichment for gene ontology immune system functions (73).

Single-cell flow-based and single-cell RT-qPCR techniques were extensively used to explore correlation between T cell subsets and latency reactivation potential (77–86). Overall, these studies suggested that cells displaying an effector memory (Tem) or transition memory (Ttm) phenotype were a niche for transcriptional and translational competent reservoirs (81, 87–89). Furthermore, LRA-mediated HIV reactivation was shown to be heterogeneous, acting by either increasing transcription from active cells or increasing the number of transcriptionally active cells (89). An in-depth investigation of multiple LRAs and their ability to reactivate latently infected cells isolated from ART-treated HIV^+ individuals showed that only 2.6% of HIV-1 latent proviruses were completely reactivated upon LRA stimulation (81). Moreover, they showed that different drugs had different effects according to the T cell subset, i.e., Panobinostat successfully reactivated HIV in Tcm cells only while Romidepsin affected all memory subsets.

Nevertheless, all these studies pointed out a similar observation: Only a fraction of cells were efficiently reactivated, regardless of the T cell subset or cellular environment, indicating that other factors, such as proviral DNA integrity, integration site, or stochasticity, likely also contribute to latency establishment.

Several studies took advantage of full-length single-genome sequences to explore the implication of provirus DNA and its integration site location in latency (90–92). These studies described that the majority of latently infected cells contain only one provirus and that HIV proviruses identified in different cell subsets and in different anatomical sites were genetically similar, potentially suggesting clonality from a common progenitor ancestor. Furthermore, Wiegand et al. (92) investigated the proportion of transcriptionally active cells in 3 ART-treated HIV^+ individuals. They performed cell-associated HIV RNA and DNA single-genome sequencing (CARD-SGS) and found out that 7% of proviruses expressed HIV RNA, ranging from 1 to 62 HIV molecules/cell (median of 1).

Integration site location, considered at the level of both chromosomal context and nuclear topology, can contribute to HIV latency (93–95). Chen et al. (93) used a single virus tracking technique (Barcoded HIV ensembles, or B-HIVE) to show that integration sites close to enhancers resulted in higher provirus expression levels. Although comparison of HIV integration site location between latently and productively infected cells did not reveal any difference, distance from enhancers was on average two times further for latent proviruses, indicating an effect of integration site location on provirus expression (93). These findings were confirmed by Einkauf et al. (95), who used Matched Integration Site and Proviral Sequencing (MIP-Seq) to investigate integration site location and proviral sequence at sc level in 3 ART-treated patients. They observed that intact proviruses were enriched in non-genic regions and found in the opposite orientation with respect to host genes.

HIV genome position within the nucleus can also affect gene expression. Indeed, HIV proviruses colocalized within nuclear bodies in latently infected cells, and such colocalization was lost upon LRA reactivation (94).

Viral transcription, hence viral reactivation, is highly dependent on the HIV transactivator of transcription, Tat. Indeed, accumulation of Tat boosts viral transcription and favors viral production.

Studies of the efficiency of viral expression benefited from fluorescence reporter-based single-cell techniques, identifying two major determinants of latent or productive cell fate: (*a*) initial determination of basal level of Tat expression due to stochasticity and Tat accumulation and

(*b*) direct Tat-mediated effect on viral transcription (92, 96–98). In case of low Tat amounts, viral gene expression depends mainly on the cellular gene expression context. In contrast, high Tat levels triggered a positive feedback loop where virus expression is maintained even in case of cellular reversion to a resting stage, suggesting that the Tat feedback loop dictated HIV expression, overcoming the cellular state influence (96, 98).

Altogether, Tat expression, host cell environment, and integration site location can all affect viral gene expression to various degrees.

Latency has often been perceived as an evolutionary mistake; however, Rouzine et al. (99) used advanced modeling strategies to show that latency gives an evolutionary advantage to lentiviruses by facilitating the spread in target-cell-poor environment (i.e., mucosa) and increasing survival of the virus.

3.3. Host Response to HIV: Immune Control from Immune Cells

As mentioned in **Figure 1*a***, individuals do not respond equally toward HIV infection. This can be due to differential $CD4^+$ T cell susceptibility to HIV infection but also to differential immune control capacity potentially involving a variety of immune cells, including $CD8^+$ T cells, dendritic cells (DCs), $CD4^+$ T helper cells, and B cells (100, 101). Efficient immune response against viral infection can be characterized by antiviral signaling molecules (IFNs, cytokines, or chemokines), antibody production, and cytotoxic response. A minority of HIV^+ individuals, named elite controllers (ECs), are able to control HIV infection and preserve their immune functions. However, HIV overtakes the immune response in most HIV^+ individuals (normal/rapid progressors), leading to exhaustion and depletion of the immune system (102–111) (**Figure 6**).

Single-cell analysis of 96 subset-specific genes was performed on 1,440 individual $CD8^+$ Tcm cells isolated from controllers or ART-treated progressors and revealed opposite patterns of gene expression (106). $CD8^+$ Tcm cells isolated from HIV controllers displayed overexpression of effector function genes (*GZMB*, *GZK*, *CCL3*, *CCL3L1*, *XCL1*), survival genes (*CD69*, *KLRD1*), CTL-induced apoptosis genes (*FASLG*, *TNF*, *TRAIL*), and *IFNB*. Furthermore, these cells were able to use energy sources (i.e., fatty acids) other than glucose. In contrast, $CD8^+$ Tcm cells isolated from ART-treated progressors displayed increased activation, increased exhaustion (*LAG3*) increased glycolysis and dependence on glucose as the sole energy source, and increased expression of IFN-stimulated genes (*MX1*, *OAS1*). Of note, glucose dependency can be inhibited upon IL-15 exposure and downregulation of the REPIN-1 transcription factor, responsible for downregulation of glucose transport.

Upon analysis of HIV-infected peripheral blood mononuclear cells from three ECs, a subset of myeloid dendritic cells (mDCs) displaying an antiviral state was identified and further characterized by scRNA-Seq (111). These antiviral mDCs were characterized by high expression of PD-L1 and CD64, by the ability to stimulate IFNγ response, and by degranulation markers (LAMP1/CD107a, TNFα) from autologous $CD8^+$ T cells. This antiviral mDC profile can be stimulated by TLR3 and poly:IC. Moreover, Coindre et al. (110) used CyTOF to characterize monocytes and DCs from blood myeloid cells. They identified that specific classical dendritic cell (cDC) clusters, expressing high levels of $CD1c^+$, CD32b, and HLA-DR, can be associated with elite control.

Chronic infection leads to immune cell exhaustion, resulting in functional defects and expression of inhibitory receptors, that can be investigated by CyTOF analysis (104). HIV-induced $CD8^+$ T cell exhaustion is characterized by the expression of inhibitory receptors, such as PD-1 and TIGIT. These cell surface receptors are increased in $CD27^+/CD45RA^-$ effector memory

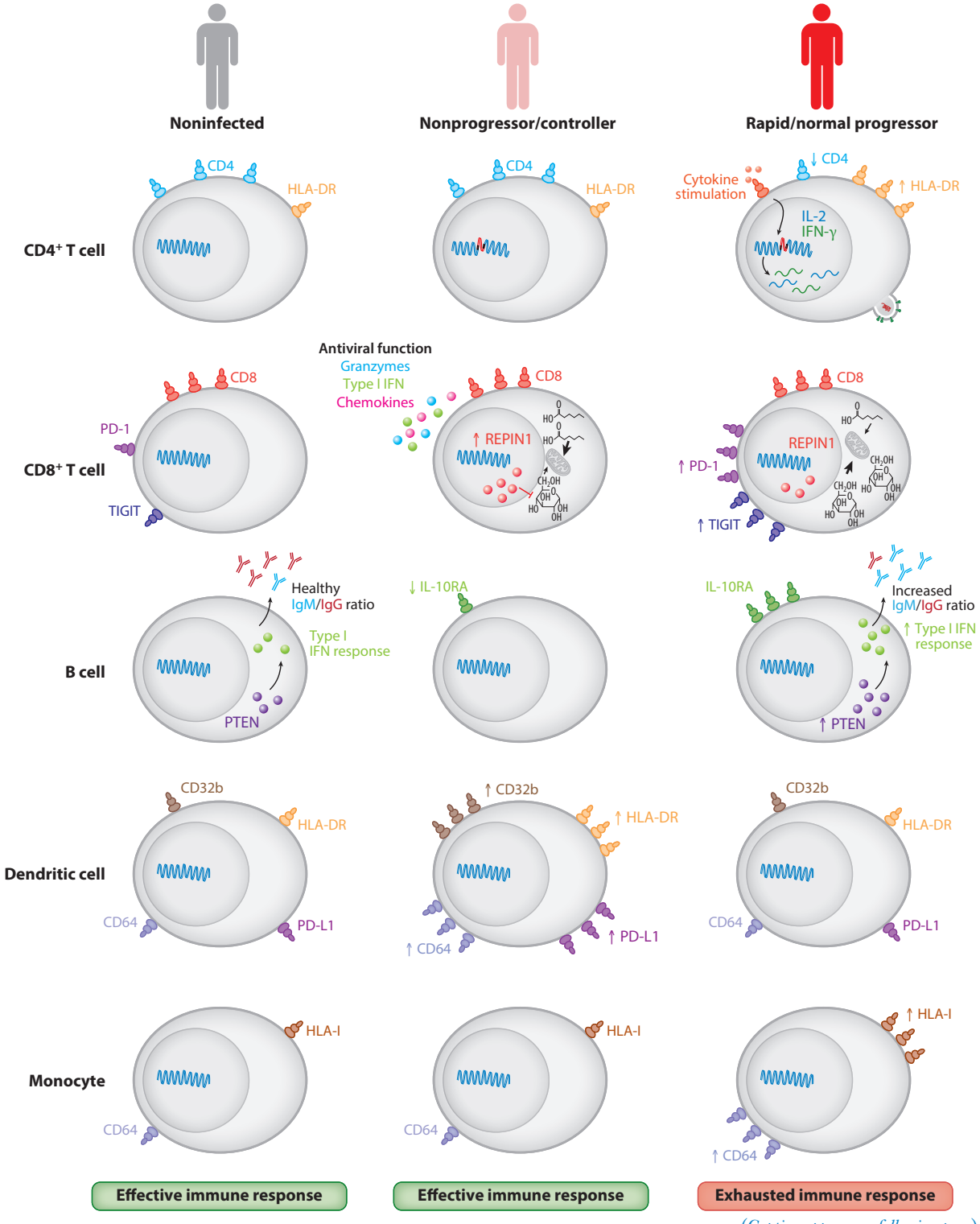

(*Caption appears on following page*)

Figure 6 (*Figure appears on preceding page*)

Host immune control of human immunodeficiency virus (HIV). Comparative single-cell analyses on immune cells derived from noninfected individuals (*gray*), controller/nonprogressor HIV$^+$ individuals (*light red*), and rapid/normal progressors (*red*). Single-cell analyses were performed on only two sample subsets at a time, either noninfected individuals versus normal/rapid progressors or controllers/nonprogressors versus normal/rapid progressors. Thus, the absence of a specific marker in a sample subset panel without indication reflects a lack of available data or information in the literature. Immune cells isolated from noninfected individuals or HIV controllers/nonprogressors displayed effective immune response, while cells isolated from rapid or normal progressors showed an exhausted phenotype. Abbreviations: HLA, human leukocyte antigen; IFN, interferon; IgM/IgG, immunoglobulin M to immunoglobulin G.

CD8$^+$ T cells. In contrast, CD8$^+$ T cell function is preserved in ECs and is associated with inhibitory receptor downregulation, cytolytic molecule downregulation, and cytokine upregulation, which are typical of a functional memory phenotype with a poor but potent cytotoxic activity (105).

Most HIV pathogenesis studies focus on T cells, as they are the main targets of HIV. However, despite not being infected by HIV, B cells' function can be altered in the presence of HIV-infected cells. Indeed, upon H1N1 vaccination, single-cell reverse transcription PCR highlighted an immunoglobulin G to immunoglobulin M production switch in HIV-infected individuals but not in healthy donors (107). This impairment in antibody response is likely the result of the enhanced IFN-I response, leading to B cell exhaustion. Thus, it is tempting to think that restoring B cell function could partially contribute to antibody-mediated control of HIV infection.

4. CONCLUDING REMARKS AND PERSPECTIVES

Single-cell analyses provide the unprecedented opportunity to study one cell at a time, one layer at a time, and one phenotype at a time. Further integrating additional layers using single-cell multi-omics technologies should allow advancing one step forward to a more comprehensive picture of the HIV-infected cell and of host immune control. The analysis of cell heterogeneity toward HIV infection has the potential to identify novel cellular players affecting HIV replication, either promoting or inhibiting it. In addition, analysis of host immune control should help uncover the molecular determinants leading to successful control. Thus, single-cell analyses should provide further cues on HIV replication as well as pave the way for novel targeted therapeutic interventions.

Moreover, these HIV studies provide useful and valuable models to be extended to other viruses. Such single-cell studies are being pursued with a growing number of viruses for varied purposes, especially in the realm of single-cell RNA sequencing (e.g., 112–115). The many examples outlined here for HIV show the rich potential for developing and fruitfully integrating a broad array of diverse single-cell studies in order to fully characterize the replication and host interactions of essentially all viruses and exploit these results to improve virus control.

DISCLOSURE STATEMENT

The authors are not aware of any affiliations, memberships, funding, or financial holdings that might be perceived as affecting the objectivity of this review.

ACKNOWLEDGMENTS

S.C., L.B., and A.C. acknowledge support from the Swiss National Science Foundation SNF 314730-188877. Apologies are extended to the many investigators whose work was omitted due to space limitations.

LITERATURE CITED

1. Telenti A, Goldstein DB. 2006. Genomics meets HIV-1. *Nat. Rev. Microbiol.* 4:865–73
2. Fellay J, Shianna KV, Ge D, Colombo S, Ledergerber B, et al. 2007. A whole-genome association study of major determinants for host control of HIV-1. *Science* 317:944–47
3. McLaren PJ, Carrington M. 2015. The impact of host genetic variation on infection with HIV-1. *Nat. Immunol.* 16:577–83
4. Bartha I, McLaren PJ, Ciuffi A, Fellay J, Telenti A. 2014. GuavaH: a compendium of host genomic data in HIV biology and disease. *Retrovirology* 11:6
5. Bartha I, McLaren PJ, Brumme C, Harrigan R, Telenti A, Fellay J. 2017. Estimating the respective contributions of human and viral genetic variation to HIV control. *PLOS Comput. Biol.* 13:e1005339
6. Cristinelli S, Ciuffi A. 2018. The use of single-cell RNA-Seq to understand virus-host interactions. *Curr. Opin. Virol.* 29:39–50
7. Venter JC, Adams MD, Myers EW, Li PW, Mural RJ, et al. 2001. The sequence of the human genome. *Science* 291:1304–51
8. Tang F, Barbacioru C, Wang Y, Nordman E, Lee C, et al. 2009. mRNA-Seq whole-transcriptome analysis of a single cell. *Nat. Methods* 6:377–82
9. Gross A, Schoendube J, Zimmermann S, Steeb M, Zengerle R, Koltay P. 2015. Technologies for single-cell isolation. *Int. J. Mol. Sci.* 16:16897–919
10. Mincarelli L, Lister A, Lipscombe J, Macaulay IC. 2018. Defining cell identity with single-cell omics. *Proteomics* 18:e1700312
11. Svensson V, Vento-Tormo R, Teichmann SA. 2018. Exponential scaling of single-cell RNA-seq in the past decade. *Nat. Protoc.* 13:599–604
12. Hu P, Zhang W, Xin H, Deng G. 2016. Single cell isolation and analysis. *Front. Cell Dev. Biol.* 4:116
13. Tanay A, Regev A. 2017. Scaling single-cell genomics from phenomenology to mechanism. *Nature* 541:331–38
14. Gawad C, Koh W, Quake SR. 2016. Single-cell genome sequencing: current state of the science. *Nat. Rev. Genet.* 17:175–88
15. Vitak SA, Torkenczy KA, Rosenkrantz JL, Fields AJ, Christiansen L, et al. 2017. Sequencing thousands of single-cell genomes with combinatorial indexing. *Nat. Methods* 14:302–8
16. Wen L, Tang F. 2018. Single cell epigenome sequencing technologies. *Mol. Aspects Med.* 59:62–69
17. Mulqueen RM, Pokholok D, Norberg SJ, Torkenczy KA, Fields AJ, et al. 2018. Highly scalable generation of DNA methylation profiles in single cells. *Nat. Biotechnol.* 36:428–31
18. Karemaker ID, Vermeulen M. 2018. Single-cell DNA methylation profiling: technologies and biological applications. *Trends Biotechnol.* 36:952–65
19. Kanter I, Kalisky T. 2015. Single cell transcriptomics: methods and applications. *Front. Oncol.* 5:53
20. Ziegenhain C, Vieth B, Parekh S, Reinius B, Guillaumet-Adkins A, et al. 2017. Comparative analysis of single-cell RNA sequencing methods. *Mol. Cell* 65:631–43
21. Kulkarni A, Anderson AG, Merullo DP, Konopka G. 2019. Beyond bulk: a review of single cell transcriptomics methodologies and applications. *Curr. Opin. Biotechnol.* 58:129–36
22. Cao J, Packer JS, Ramani V, Cusanovich DA, Huynh C, et al. 2017. Comprehensive single-cell transcriptional profiling of a multicellular organism. *Science* 357:661–67
23. Rosenberg AB, Roco CM, Muscat RA, Kuchina A, Sample P, et al. 2018. Single-cell profiling of the developing mouse brain and spinal cord with split-pool barcoding. *Science* 360:176–82
24. Chen KH, Boettiger AN, Moffitt JR, Wang S, Zhuang X. 2015. Spatially resolved, highly multiplexed RNA profiling in single cells. *Science* 348:aaa6090
25. Kolodziejczyk AA, Lonnberg T. 2018. Global and targeted approaches to single-cell transcriptome characterization. *Brief Funct. Genom.* 17:209–19
26. Wu M, Singh AK. 2012. Single-cell protein analysis. *Curr. Opin. Biotechnol.* 23:83–88
27. Su Y, Shi Q, Wei W. 2017. Single cell proteomics in biomedicine: high-dimensional data acquisition, visualization, and analysis. *Proteomics* 17:1600267
28. Levy E, Slavov N. 2018. Single cell protein analysis for systems biology. *Essays Biochem.* 62:595–605

29. Macaulay IC, Ponting CP, Voet T. 2017. Single-cell multiomics: multiple measurements from single cells. *Trends Genet*. 33:155–68
30. Stuart T, Satija R. 2019. Integrative single-cell analysis. *Nat. Rev. Genet.* 20:257–72
31. Chen W, Li S, Kulkarni AS, Huang L, Cao J, et al. 2020. Single cell omics: from assay design to biomedical application. *Biotechnol. J.* 15:e1900262
32. Angermueller C, Clark SJ, Lee HJ, Macaulay IC, Teng MJ, et al. 2016. Parallel single-cell sequencing links transcriptional and epigenetic heterogeneity. *Nat. Methods* 13:229–32
33. Hu Y, Huang K, An Q, Du G, Hu G, et al. 2016. Simultaneous profiling of transcriptome and DNA methylome from a single cell. *Genome Biol*. 17:88
34. Bock C, Farlik M, Sheffield NC. 2016. Multi-omics of single cells: strategies and applications. *Trends Biotechnol*. 34:605–8
35. Hu Y, An Q, Sheu K, Trejo B, Fan S, Guo Y. 2018. Single cell multi-omics technology: methodology and application. *Front. Cell Dev. Biol.* 6:28
36. Ziegenhain C, Vieth B, Parekh S, Hellmann I, Enard W. 2018. Quantitative single-cell transcriptomics. *Brief Funct. Genom.* 17:220–32
37. Vieth B, Parekh S, Ziegenhain C, Enard W, Hellmann I. 2019. A systematic evaluation of single cell RNA-seq analysis pipelines. *Nat. Commun.* 10:4667
38. Choi YH, Kim JK. 2019. Dissecting cellular heterogeneity using single-cell RNA sequencing. *Mol. Cells* 42:189–99
39. van Dijk D, Ertaylan G, Boucher CA, Sloot PM. 2010. Identifying potential survival strategies of HIV-1 through virus-host protein interaction networks. *BMC Syst. Biol.* 4:96
40. Ptak RG, Fu W, Sanders-Beer BE, Dickerson JE, Pinney JW, et al. 2008. Cataloguing the HIV type 1 human protein interaction network. *AIDS Res. Hum. Retroviruses* 24:1497–502
41. Bushman FD, Malani N, Fernandes J, D'Orso I, Cagney G, et al. 2009. Host cell factors in HIV replication: meta-analysis of genome-wide studies. *PLOS Pathog*. 5:e1000437
42. Yin X, Langer S, Zhang Z, Herbert KM, Yoh S, et al. 2020. Sensor sensibility—HIV-1 and the innate immune response. *Cells* 9:254
43. Schoggins JW. 2019. Interferon-stimulated genes: What do they all do? *Annu. Rev. Virol.* 6:567–84
44. Bergantz L, Subra F, Deprez E, Delelis O, Richetta C. 2019. Interplay between intrinsic and innate immunity during HIV infection. *Cells* 8:922
45. Sauter D, Kirchhoff F. 2019. Key viral adaptations preceding the AIDS pandemic. *Cell Host Microbe* 25:27–38
46. Razooky BS, Gutierrez E, Terry VH, Spina CA, Groisman A, Weinberger LS. 2012. Microwell devices with finger-like channels for long-term imaging of HIV-1 expression kinetics in primary human lymphocytes. *Lab. Chip* 12:4305–12
47. Petravic J, Ellenberg P, Chan ML, Paukovics G, Smyth RP, et al. 2014. Intracellular dynamics of HIV infection. *J. Virol.* 88:1113–24
48. Holmes M, Zhang F, Bieniasz PD. 2015. Single-cell and single-cycle analysis of HIV-1 replication. *PLOS Pathog*. 11:e1004961
49. Marini B, Kertesz-Farkas A, Ali H, Lucic B, Lisek K, et al. 2015. Nuclear architecture dictates HIV-1 integration site selection. *Nature* 521:227–31
50. Boullé M, Muller TG, Dahling S, Ganga Y, Jackson L, et al. 2016. HIV cell-to-cell spread results in earlier onset of viral gene expression by multiple infections per cell. *PLOS Pathog*. 12:e1005964
51. Francis AC, Melikyan GB. 2018. Single HIV-1 imaging reveals progression of infection through CA-dependent steps of docking at the nuclear pore, uncoating, and nuclear transport. *Cell Host Microbe* 23:536–48
52. Puray-Chavez M, Tedbury PR, Huber AD, Ukah OB, Yapo V, et al. 2017. Multiplex single-cell visualization of nucleic acids and protein during HIV infection. *Nat. Commun.* 8:1882
53. Lucic B, Chen HC, Kuzman M, Zorita E, Wegner J, et al. 2019. Spatially clustered loci with multiple enhancers are frequent targets of HIV-1 integration. *Nat. Commun.* 10:4059
54. Suspène R, Meyerhans A. 2012. Quantification of unintegrated HIV-1 DNA at the single cell level in vivo. *PLOS ONE* 7(5):e36246

55. Stultz RD, Cenker JJ, McDonald D. 2017. Imaging HIV-1 genomic DNA from entry through productive infection. *J. Virol.* 91(9):e00034-17
56. Pocock GM, Zimdars LL, Yuan M, Eliceiri KW, Ahlquist P, Sherer NM. 2016. Diverse activities of viral *cis*-acting RNA regulatory elements revealed using multicolor, long-term, single-cell imaging. *Mol. Biol. Cell* 28(3):476–86
57. Cavrois M, Banerjee T, Mukherjee G, Raman N, Hussien R, et al. 2017. Mass cytometric analysis of HIV entry, replication, and remodeling in tissue $CD4^+$ T cells. *Cell Rep*. 20:984–98
58. Rato S, Rausell A, Munoz M, Telenti A, Ciuffi A. 2017. Single-cell analysis identifies cellular markers of the HIV permissive cell. *PLOS Pathog*. 13:e1006678
59. Durand CM, Blankson JN, Siliciano RF. 2012. Developing strategies for HIV-1 eradication. *Trends Immunol*. 33:554–62
60. Spivak AM, Planelles V. 2016. HIV-1 eradication: early trials (and tribulations). *Trends Mol. Med.* 22:10–27
61. Rothenberger MK, Keele BF, Wietgrefe SW, Fletcher CV, Beilman GJ, et al. 2015. Large number of rebounding/founder HIV variants emerge from multifocal infection in lymphatic tissues after treatment interruption. *PNAS* 112:E1126–34
62. Colby DJ, Trautmann L, Pinyakorn S, Leyre L, Pagliuzza A, et al. 2018. Rapid HIV RNA rebound after antiretroviral treatment interruption in persons durably suppressed in Fiebig I acute HIV infection. *Nat. Med.* 24:923–26
63. Van Lint C, Bouchat S, Marcello A. 2013. HIV-1 transcription and latency: an update. *Retrovirology* 10:67
64. Whitney JB, Hill AL, Sanisetty S, Penaloza-MacMaster P, Liu J, et al. 2014. Rapid seeding of the viral reservoir prior to SIV viraemia in rhesus monkeys. *Nature* 512:74–77
65. Whitney JB, Lim SY, Osuna CE, Kublin JL, Chen E, et al. 2018. Prevention of SIVmac251 reservoir seeding in rhesus monkeys by early antiretroviral therapy. *Nat. Commun.* 9:5429
66. Bachmann N, von Siebenthal C, Vongrad V, Turk T, Neumann K, et al. 2019. Determinants of HIV-1 reservoir size and long-term dynamics during suppressive ART. *Nat. Commun.* 10:3193
67. Falcinelli SD, Ceriani C, Margolis DM, Archin NM. 2019. New frontiers in measuring and characterizing the HIV reservoir. *Front. Microbiol.* 10:2878
68. Pitman MC, Lau JSY, McMahon JH, Lewin SR. 2018. Barriers and strategies to achieve a cure for HIV. *Lancet HIV* 5:e317–28
69. Sengupta S, Siliciano RF. 2018. Targeting the latent reservoir for HIV-1. *Immunity* 48:872–95
70. Ait-Ammar A, Kula A, Darcis G, Verdikt R, De Wit S, et al. 2019. Current status of latency reversing agents facing the heterogeneity of HIV-1 cellular and tissue reservoirs. *Front. Microbiol.* 10:3060
71. Bohn-Wippert K, Tevonian EN, Lu Y, Huang MY, Megaridis MR, Dar RD. 2018. Cell size-based decision-making of a viral gene circuit. *Cell Rep*. 25:3844–57
72. Bradley T, Ferrari G, Haynes BF, Margolis DM, Browne EP. 2018. Single-cell analysis of quiescent HIV infection reveals host transcriptional profiles that regulate proviral latency. *Cell Rep*. 25:107–17
73. Cohn LB, da Silva IT, Valieris R, Huang AS, Lorenzi JCC, et al. 2018. Clonal $CD4^+$ T cells in the HIV-1 latent reservoir display a distinct gene profile upon reactivation. *Nat. Med.* 24:604–9
74. Golumbeanu M, Cristinelli S, Rato S, Munoz M, Cavassini M, et al. 2018. Single-cell RNA-Seq reveals transcriptional heterogeneity in latent and reactivated HIV-infected cells. *Cell Rep*. 23:942–50
75. Ukah OB, Puray-Chavez M, Tedbury PR, Herschhorn A, Sodroski JG, Sarafianos SG. 2018. Visualization of HIV-1 RNA transcription from integrated HIV-1 DNA in reactivated latently infected cells. *Viruses* 10:534
76. Telwatte S, Morón-López S, Aran D, Kim P, Hsieh C, et al. 2019. Heterogeneity in HIV and cellular transcription profiles in cell line models of latent and productive infection: implications for HIV latency. *Retrovirology* 16(1):32
77. Bui JK, Mellors JW, Cillo AR. 2016. HIV-1 virion production from single inducible proviruses following T-cell activation ex vivo. *J. Virol.* 90(3):1673–76
78. Baxter AE, Niessl J, Fromentin R, Richard J, Porichis F, et al. 2016. Single-cell characterization of viral translation-competent reservoirs in HIV-infected individuals. *Cell Host Microbe* 20(3):368–80

79. Coindre S, Tchitchek N, Alaoui L, Vaslin B, Bourgeois C, et al. 2018. Mass cytometry analysis reveals the landscape and dynamics of CD32a$^+$ CD4$^+$ T cells from early HIV infection to effective cART. *Front. Immunol.* 9:1217
80. Martrus G, Niehrs A, Cornelis R, Rechtien A, García-Beltran W, et al. 2016. Kinetics of HIV-1 latency reversal quantified on the single-cell level using a novel flow-based technique. *J. Virol.* 90(20):9018–28
81. Grau-Expósito J, Luque-Ballesteros L, Navarro J, Curran A, Burgos J, et al. 2019. Latency reversal agents affect differently the latent reservoir present in distinct CD4$^+$ T subpopulations. *PLOS Pathog.* 15:e1007991
82. Passaes CP, Bruel T, Decalf J, David A, Angin M, et al. 2017. Ultrasensitive HIV-1 p24 assay detects single infected cells and differences in reservoir induction by latency reversal agents. *J. Virol.* 91(6):e02296-16
83. Shan L, Deng K, Gao H, Xing S, Capoferri AA, et al. 2017. Transcriptional reprogramming during effector-to-memory transition renders CD4$^+$ T cells permissive for latent HIV-1 infection. *Immunity* 47(4):766–75
84. Zhang W, Svensson Akusjärvi S, Sönnerborg A, Neogi U. 2018. Characterization of inducible transcription and translation-competent HIV-1 using the RNAscope ISH technology at a single-cell resolution. *Front. Microbiol.* 9:2358
85. Bruner KM, Wang Z, Simonetti FR, Bender AM, Kwon KJ, et al. 2019. A quantitative approach for measuring the reservoir of latent HIV-1 proviruses. *Nature* 566(7742):120–25
86. Grau-Expósito J, Serra-Peinado C, Miguel L, Navarro J, Curran A, et al. 2017. A novel single-cell FISH-flow assay identifies effector memory CD4$^+$ T cells as a major niche for HIV-1 transcription in HIV-infected patients. *mBio* 8(4):e00876-17
87. Bushman FD, Craigie R. 1990. Sequence requirements for integration of Moloney murine leukemia virus DNA in vitro. *J. Virol.* 64:5645–48
88. Pardons M, Baxter AE, Massanella M, Pagliuzza A, Fromentin R, et al. 2019. Single-cell characterization and quantification of translation-competent viral reservoirs in treated and untreated HIV infection. *PLOS Pathog.* 15:e1007619
89. Yucha RW, Hobbs KS, Hanhauser E, Hogan LE, Nieves W, et al. 2017. High-throughput characterization of HIV-1 reservoir reactivation using a single-cell-in-droplet PCR assay. *EBioMedicine* 20:217–29
90. Josefsson L, Palmer S, Faria NR, Lemey P, Casazza J, et al. 2013. Single cell analysis of lymph node tissue from HIV-1 infected patients reveals that the majority of CD4$^+$ T-cells contain one HIV-1 DNA molecule. *PLOS Pathog.* 9(6):e1003432
91. Lee GQ, Reddy K, Einkauf KB, Gounder K, Chevalier JM, et al. 2019. HIV-1 DNA sequence diversity and evolution during acute subtype C infection. *Nat. Commun.* 10(1):2737
92. Wiegand A, Spindler J, Hong FF, Shao W, Cyktor JC, et al. 2017. Single-cell analysis of HIV-1 transcriptional activity reveals expression of proviruses in expanded clones during ART. *PNAS* 114:E3659–68
93. Chen HC, Martinez JP, Zorita E, Meyerhans A, Filion GJ. 2017. Position effects influence HIV latency reversal. *Nat. Struct. Mol. Biol.* 24:47–54
94. Lusic M, Marini B, Ali H, Lucic B, Luzzati R, Giacca M. 2013. Proximity to PML nuclear bodies regulates HIV-1 latency in CD4$^+$ T cells. *Cell Host Microbe* 13:665–77
95. Einkauf KB, Lee GQ, Gao C, Sharaf R, Sun X, et al. 2019. Intact HIV-1 proviruses accumulate at distinct chromosomal positions during prolonged antiretroviral therapy. *J. Clin. Invest.* 129(3):988–98
96. Razooky BS, Pai A, Aull K, Rouzine IM, Weinberger LS. 2015. A hardwired HIV latency program. *Cell* 160:990–1001
97. Aull KH, Tanner EJ, Thomson M, Weinberger LS. 2017. Transient thresholding: a mechanism enabling noncooperative transcriptional circuitry to form a switch. *Biophys. J.* 112:2428–38
98. Hansen MMK, Wen WY, Ingerman E, Razooky BS, Thompson CE, et al. 2018. A post-transcriptional feedback mechanism for noise suppression and fate stabilization. *Cell* 173:1609–21
99. Rouzine IM, Weinberger AD, Weinberger LS. 2015. An evolutionary role for HIV latency in enhancing viral transmission. *Cell* 160(5):1002–12
100. Walker BD, Yu XG. 2013. Unravelling the mechanisms of durable control of HIV-1. *Nat. Rev. Immunol.* 13:487–98

101. McBrien JB, Kumar NA, Silvestri G. 2018. Mechanisms of $CD8^+$ T cell-mediated suppression of HIV/SIV replication. *Eur. J. Immunol.* 48:898–914
102. Porichis F, Hart MG, Griesbeck M, Everett HL, Hassan M, et al. 2014. High-throughput detection of miRNAs and gene-specific mRNA at the single-cell level by flow cytometry. *Nat. Commun.* 5:5641
103. Corneau A, Cosma A, Even S, Katlama C, Le Grand R, et al. 2017. Comprehensive mass cytometry analysis of cell cycle, activation, and coinhibitory receptors expression in CD4 T cells from healthy and HIV-infected individuals. *Cytometry B Clin. Cytom.* 92:21–32
104. Bengsch B, Ohtani T, Khan O, Setty M, Manne S, et al. 2018. Epigenomic-guided mass cytometry profiling reveals disease-specific features of exhausted CD8 T cells. *Immunity* 48:1029–45
105. Nguyen S, Deleage C, Darko S, Ransier A, Truong DP, et al. 2019. Elite control of HIV is associated with distinct functional and transcriptional signatures in lymphoid tissue $CD8^+$ T cells. *Sci. Transl. Med.* 11(523):eaax4077
106. Angin M, Volant S, Passaes C, Lecuroux C, Monceaux V, et al. 2019. Metabolic plasticity of HIV-specific $CD8^+$ T cells is associated with enhanced antiviral potential and natural control of HIV-1 infection. *Nat. Metab.* 1:704–16
107. de Armas LR, Pallikkuth S, Pan L, Rinaldi S, Cotugno N, et al. 2019. Single cell profiling reveals PTEN overexpression in influenza-specific B cells in aging HIV-infected individuals on anti-retroviral therapy. *Sci. Rep.* 9:2482
108. Han Q, Bradley T, Williams WB, Cain DW, Montefiori DC, et al. 2020. Neonatal rhesus macaques have distinct immune cell transcriptional profiles following HIV envelope immunization. *Cell Rep.* 30:1553–69
109. Farhadian SF, Mehta SS, Zografou C, Robertson K, Price RW, et al. 2018. Single-cell RNA sequencing reveals microglia-like cells in cerebrospinal fluid during virologically suppressed HIV. *JCI Insight* 3:e121718
110. Coindre S, Tchitchek N, Alaoui L, Vaslin B, Bourgeois C, et al. 2019. Mass cytometry analysis reveals complex cell-state modifications of blood myeloid cells during HIV infection. *Front. Immunol.* 10:2677
111. Martin-Gayo E, Cole MB, Kolb KE, Ouyang Z, Cronin J, et al. 2018. A reproducibility-based computational framework identifies an inducible, enhanced antiviral state in dendritic cells from HIV-1 elite controllers. *Genome Biol.* 19:10
112. Zanini F, Robinson ML, Croote D, Sahoo MK, Sanz AM, et al. 2018. Virus-inclusive single-cell RNA sequencing reveals the molecular signature of progression to severe dengue. *PNAS* 115(52):E12363–69
113. Wyler E, Franke V, Menegatti J, Kocks C, Boltengagen A, et al. 2019. Single-cell RNA-sequencing of herpes simplex virus 1-infected cells connects NRF2 activation to an antiviral program. *Nat. Commun.* 10:4878
114. Zhang J, Liu J, Yuan Y, Huang F, Ma R, et al. 2020. Two waves of pro-inflammatory factors are released during the influenza A virus (IAV)-driven pulmonary immunopathogenesis. *PLOS Pathog.* 16(2):e1008334
115. Bolton DL, McGinnis K, Finak G, Chattopadhyay P, Gottardo R, et al. 2017. Combined single-cell quantitation of host and SIV genes and proteins ex vivo reveals host-pathogen interactions in individual cells. *PLOS Pathog.* 13(6):e1006445

IV. Conclusion and perspectives

Research on HIV-host interplay within the last decades led to a better perception of HIV life cycle and to the development of specialized inhibitors, improving life quality and expectancy of people living with HIV. However, current ART does not eliminate HIV, which persists in reservoirs. Thus, research efforts must be pursued in order to find a sterilizing cure, or at least reach long-term viral suppression in absence of ART. This can only be achieved by further deciphering HIV replication and latency mechanisms. In this context, a better perception of the permissive cellular landscape, necessary for successful replication, should also help better understanding the viral reservoirs, which is essential for developing efficient latency reactivation or block and lock strategies.

One major obstacle to HIV cure resides in the large heterogeneity of HIV-infected cells and thus the variety of persistence or latency mechanisms, rendering difficult to target them with a one-for-all approach. The advent of single-cell technologies helped investigating cell heterogeneity related to various phenotypes. They allowed finer perception of the cellular proteins involved in HIV life cycle and enabled identifying rare cell types, so far masked in population-based analyses. Heterogeneity can be further fueled by differences in immune cell distribution, which can be further influenced by sex and age. It is noteworthy to highlight that these parameters were overlooked in most past studies. Indeed, the importance of considering women independently from men in clinical studies was only established in 2015, with introduction of novel policies by the National Institutes of Health (US). In this work, we aimed at further investigating cell heterogeneity at the cell and individual levels, as well as in response to HIV infection, using conventional and novel single-cell technologies, in order to identify novel players involved in HIV replication.

Our first strategy was to investigate evolution of *in vitro* cellular permissiveness to HIV within donors of both sexes and various ages through activation kinetics. We observed that cells derived from men and donors aged 50 years or more were more susceptible to HIV infection, and that this phenotype was associated with cellular activation-related pathways. Further experiments will be required to validate these results and notably investigate the role of sex hormones, by controlling their levels at the time of blood sampling. Our second strategy took advantage of sc-RNA-Seq to refine the association between permissiveness to HIV and cellular activation. We characterized cell distribution changes over time p.-s. as well as differences in productive HIV infection. Finally, we identified a 53-gene signature of which expression level could predict cell permissiveness phenotype and thus infection success.

Evidence provided by the first strategy allows pursuing the project using different approaches. First, genes identified as putative novel players in HIV replication should be investigated *in vitro* to characterize their role in the replication cycle. Differentially expressed sex-linked paralogs may be studied by generating single and double knockouts (KO) in primary CD4+ T cells derived from men and women donors (*Fig. 12A*). This could be achieved by transfection of Cas9 and either one gRNA targeting one paralog, or a combination of two gRNAs targeting both paralogs at the same time. HIV infection success using HIV GKO vector could then be compared between KO and wild-

type (WT) cells by flow cytometry, in order to determine whether infection is enhanced or reduced upon KO, and whether these genes play a role in higher HIV susceptibility of male cells. For example, increased USP9 expression was shown to facilitate gammaherpesvirus replication [229] and might thus also facilitate HIV replication, as USP9 was also shown to be expressed at higher levels in male cells. Second, we hypothesize that cellular activation potency is linked to viral latency reactivation efficiency. This may be investigated upon establishment of latent infection in primary CD4+ T cells from men and women of various age, followed by viral reactivation using immune checkpoint inhibitor blockade for example (*Fig. 12B*). Reactivation efficiency may then be assessed by both RT-qPCR and flow cytometry to discriminate viral reactivation occurring only at transcript level or also at protein level. Observation of higher HIV reactivation in cells from men and older donors would imply that activation potency is linked to HIV reactivation efficiency. Furthermore, data presented in this thesis may be refined by performing additional analyses. First, HIV infection data obtained by flow cytometry may be compared with transcriptomic data from each donor cells to find putative genes of which expression correlates with infection success, first in all donors, then by considering sex and age (*Fig. 12C*). Next, although single-cell analysis did not identify a sex bias in CD4+ T cell subtype composition between men and women, gene expression profiles may be further analyzed according to sex within each cell subtype to investigate putative transcript differences (*Fig. 12D*). In particular, we may focus and investigate genes related to activation and immunity: indeed, higher expression of genes related to activation combined with a downregulation of immunity may explain the higher susceptibility of male cells, which might be subtype-dependent. Finally, the expression of the 53-HIV resistance gene signature identified in our second project may be further exploited and used to interrogate our single-cell data to investigate whether its expression is enriched in one or several subtypes from female cells, which may be consistent with a higher resistance to HIV (*Fig. 12E*). In addition, the 53-gene signature may also be assessed in bulk RNA-Seq data to investigate whether an enrichment can be found in women and younger donor cells, thereby explaining their reduced susceptibility. Similarly, this may also be verified using the refined 12-gene signature that was commonly identified between this study and Rato *et al.* [85].

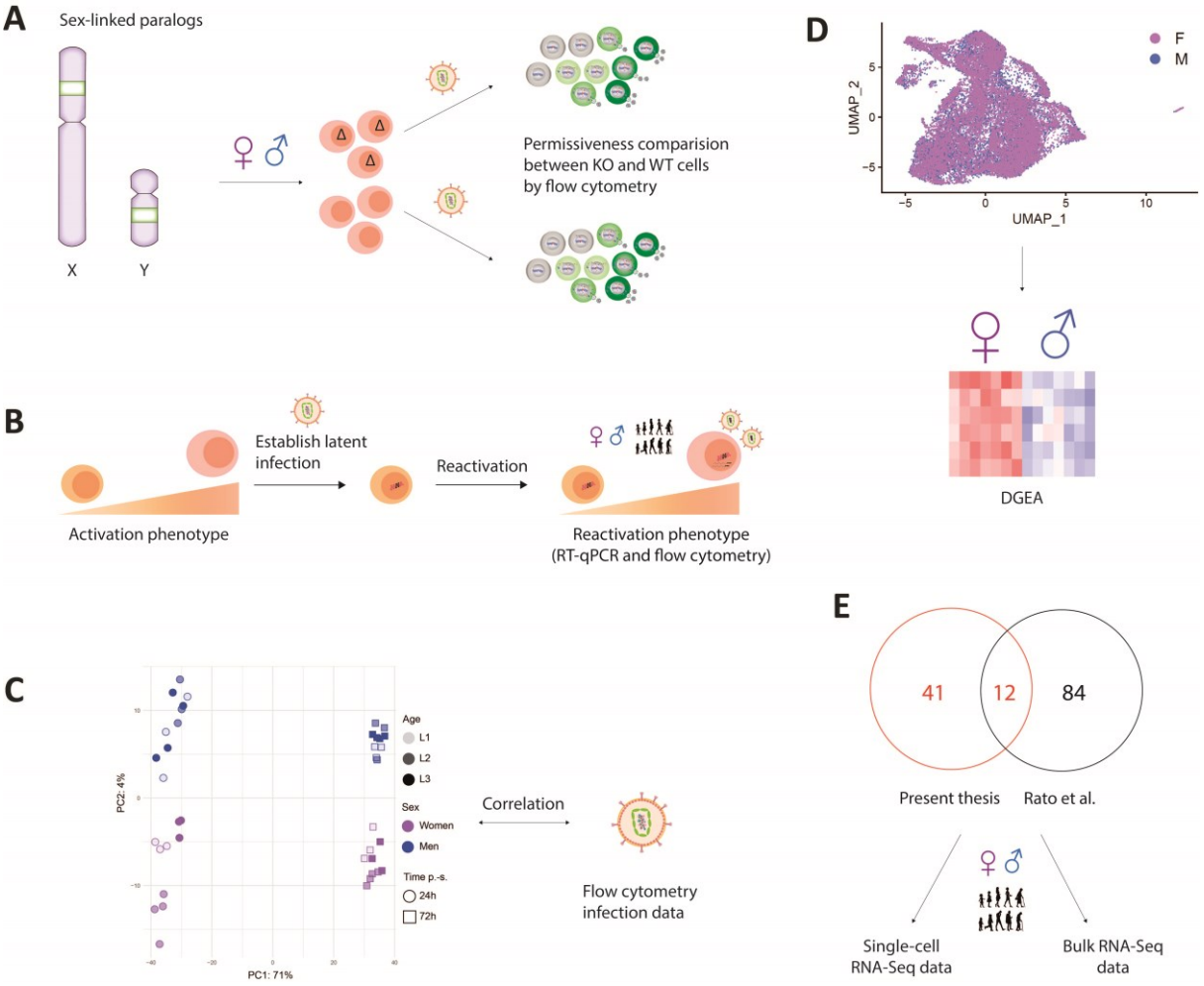

Figure 12: Possible studies to further investigate candidates involved in sex and age-related determinants of HIV permissiveness. (A) Pairs of sex-linked paralogs may be knocked out and infected by HIV to further investigate their impact on HIV replication efficiency. (B) HIV latent infection may be established and then reactivated, allowing correlating cell activation potency to HIV reactivation efficiency, using RT-qPCR and flow cytometry measurements. The influence of sex and age on reactivation efficiency may thus be considered. (C) Flow cytometry data of HIV-infected cells may be correlated with transcriptomic data to highlight putative genes linked with infection success. (D) Single-cell data may be further analyzed to identify sex-associated DEG within CD4+ T cell subtypes. (E) Expression of 53- or refined 12-gene signatures may be assessed in both single-cell and bulk RNA-Seq data to determine a putative bias according to sex and/or age. KO, knock out; WT, wild-type; DGEA, differential gene expression analysis; DEG, differentially expressed genes.

Future work enabled by results from our second sc-RNA-Seq study may include further characterization of the 12-gene signature overexpressed in cells poorly permissive to HIV, and commonly identified between this thesis and Rato *et al.* [85]. This could be achieved by a similar approach than the one described to study the sex-linked paralogs, *i.e.* knocking-out the expression of these gene candidates by CRISPR-Cas9 (*Fig. 13A*). So far, an HIV inhibitory function was described for three of them (*i.e.* ISG15 [230], GBP5 [82] and SLFN5 [231]). By contrast, limited information is available on the putative HIV inhibition mechanism of the nine remaining gene candidates (*i.e.* IFIT2, SAMD9, MX1, IFIT3, RSAD2, XAF1, IFI44L, ISG20 and SAMD9L). Furthermore, we performed a detailed stimulation kinetics over six days, and used sc-RNA-Seq to analyze the transcriptome of single cells before exposure to HIV, and then upon mock- and HIV GKO/BaL-infection every 24 hours. These data have yet to be processed and analyzed, but they will allow investigating further transcriptional features of cell subtype distribution and temporal

evolution of the intracellular environment, and how these may impact HIV infection (*Fig. 13B*). This should allow characterizing the cellular landscape upon stimulation and therefore identifying cellular subtypes and factors responsible for increased cell susceptibility and permissiveness to HIV in early stimulation. Finally, enrichment of the 53- and 12-gene signatures may be assessed overt time, upon stimulation and mock or HIV infection (*Fig. 13C*). Putative enrichment of these candidate genes before stimulation or long after stimulation might explain the reduced susceptibility and permissiveness to HIV.

Overall, the present thesis brought further evidence that addressing cell and individual-linked heterogeneity may help refining our understanding of HIV biology. We are convinced that a comprehensive characterization of permissive cells linked to cellular activation might pinpoint novel players involved in viral latency and reactivation potency, and ultimately lead to opportunities for specific reservoir targeting strategies.

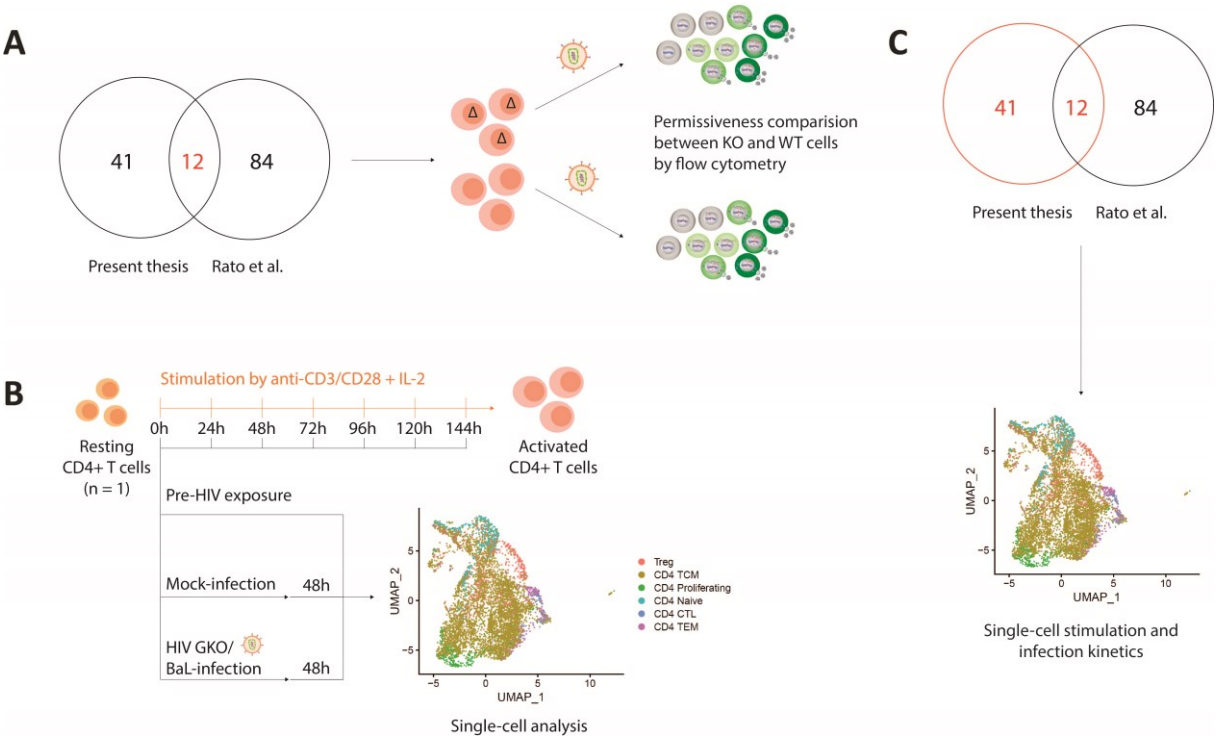

Figure 13: Future work using single-cell studies to further investigate candidates involved in HIV permissiveness. (A) The 12-commonly identified genes between this project and Rato *et al.* [85] may be knocked out and their impact may be investigated upon assessment of permissiveness to HIV replication. (B) Single-cell data following stimulation and infection kinetics may be analyzed over a six-day period in order to assess gene expression profile evolution. (C) Expression of the 53- or refined 12-gene signature may be interrogated over time, upon cell stimulation and infection. KO, knock out; WT, wild-type.

V. References

1. Centers for Disease, C., *Kaposi's sarcoma and Pneumocystis pneumonia among homosexual men--New York City and California.* MMWR Morb Mortal Wkly Rep, 1981. **30**(25): p. 305-8.
2. Gottlieb, M.S., Schroff, R., Schanker, H.M., . . . Saxon, A., *Pneumocystis carinii pneumonia and mucosal candidiasis in previously healthy homosexual men: evidence of a new acquired cellular immunodeficiency.* N Engl J Med, 1981. **305**(24): p. 1425-31.
3. Siegal, F.P., Lopez, C., Hammer, G.S., . . . Armstrong, D., *Severe acquired immunodeficiency in male homosexuals, manifested by chronic perianal ulcerative herpes simplex lesions.* N Engl J Med, 1981. **305**(24): p. 1439-44.
4. Durack, D.T., *Opportunistic infections and Kaposi's sarcoma in homosexual men.* N Engl J Med, 1981. **305**(24): p. 1465-7.
5. Masur, H., Michelis, M.A., Greene, J.B., . . . Cunningham-Rundles, S., *An outbreak of community-acquired Pneumocystis carinii pneumonia: initial manifestation of cellular immune dysfunction.* N Engl J Med, 1981. **305**(24): p. 1431-8.
6. Centers for Disease, C., *Update on acquired immune deficiency syndrome (AIDS)--United States.* MMWR Morb Mortal Wkly Rep, 1982. **31**(37): p. 507-8, 513-4.
7. Barre-Sinoussi, F., Chermann, J.C., Rey, F., . . . Montagnier, L., *Isolation of a T-lymphotropic retrovirus from a patient at risk for acquired immune deficiency syndrome (AIDS).* Science, 1983. **220**(4599): p. 868-71.
8. Gallo, R.C., Sarin, P.S., Gelmann, E.P., . . . Popovic, M., *Isolation of human T-cell leukemia virus in acquired immune deficiency syndrome (AIDS).* Science, 1983. **220**(4599): p. 865-7.
9. Levy, J.A., Hoffman, A.D., Kramer, S.M., . . . Oshiro, L.S., *Isolation of lymphocytopathic retroviruses from San Francisco patients with AIDS.* Science, 1984. **225**(4664): p. 840-2.
10. Coffin, J., Haase, A., Levy, J.A., . . . Weiss, R., *Human immunodeficiency viruses.* Science, 1986. **232**(4751): p. 697.
11. Unaids. *Global HIV & AIDS statistics — Fact sheet*. 2022 09.02.2023]; Available from: https://www.unaids.org/en/resources/fact-sheet.
12. Shaw, G.M. and Hunter, E., *HIV transmission.* Cold Spring Harb Perspect Med, 2012. **2**(11).
13. Jin, F., Jansson, J., Law, M., . . . Wilson, D.P., *Per-contact probability of HIV transmission in homosexual men in Sydney in the era of HAART.* AIDS, 2010. **24**(6): p. 907-13.
14. Gonzalez, S.M., Aguilar-Jimenez, W., Su, R.C., and Rugeles, M.T., *Mucosa: Key Interactions Determining Sexual Transmission of the HIV Infection.* Front Immunol, 2019. **10**: p. 144.
15. Hudgens, M.G., Longini, I.M., Jr., Vanichseni, S., . . . Mastro, T.D., *Subtype-specific transmission probabilities for human immunodeficiency virus type 1 among injecting drug users in Bangkok, Thailand.* Am J Epidemiol, 2002. **155**(2): p. 159-68.
16. Volmink, J. and Marais, B., *HIV: mother-to-child transmission.* BMJ Clin Evid, 2008. **2008**.
17. Xu, H., Wang, X., and Veazey, R.S., *Mucosal immunology of HIV infection.* Immunol Rev, 2013. **254**(1): p. 10-33.

18. Botting, R.A., Rana, H., Bertram, K.M., . . . Harman, A.N., *Langerhans cells and sexual transmission of HIV and HSV.* Rev Med Virol, 2017. **27**(2).
19. Pantaleo, G., Graziosi, C., and Fauci, A.S., *The immunopathogenesis of human immunodeficiency virus infection.* N Engl J Med, 1993. **328**(5): p. 327-35.
20. Wu, L. and KewalRamani, V.N., *Dendritic-cell interactions with HIV: infection and viral dissemination.* Nat Rev Immunol, 2006. **6**(11): p. 859-68.
21. An, P. and Winkler, C.A., *Host genes associated with HIV/AIDS: advances in gene discovery.* Trends Genet, 2010. **26**(3): p. 119-31.
22. Looney, D., Ma, A., and Johns, S., *HIV Therapy—The State of ART*, in *The Future of HIV-1 Therapeutics: Resistance Is Futile?*, B.E. Torbett, D.S. Goodsell, and D.D. Richman, Editors. 2015, Springer International Publishing: Cham. p. 1-29.
23. Volberding, P.A. and Deeks, S.G., *Antiretroviral therapy and management of HIV infection.* Lancet, 2010. **376**(9734): p. 49-62.
24. Menendez-Arias, L. and Delgado, R., *Update and latest advances in antiretroviral therapy.* Trends Pharmacol Sci, 2022. **43**(1): p. 16-29.
25. Unaids. *Global AIDS Strategy 2021-2026 - End Inequalities. End AIDS.* 2021 [cited 09.02.2023; Available from: https://www.unaids.org/en/Global-AIDS-Strategy-2021-2026.
26. Unaids. *2025 AIDS targets*. 2021 09.02.2023]; Available from: https://www.unaids.org/en/topics/2025_target_setting.
27. Kapoor, A.K. and Padival, S., *HIV-2 Infection*, in *StatPearls*. 2023: Treasure Island (FL).
28. Hemelaar, J., *The origin and diversity of the HIV-1 pandemic.* Trends Mol Med, 2012. **18**(3): p. 182-92.
29. Bbosa, N., Kaleebu, P., and Ssemwanga, D., *HIV subtype diversity worldwide.* Curr Opin HIV AIDS, 2019. **14**(3): p. 153-160.
30. Gholizadeh, Z., Iqbal, M.S., Li, R., and Romerio, F., *The HIV-1 Antisense Gene ASP: The New Kid on the Block.* Vaccines (Basel), 2021. **9**(5).
31. Turner, B.G. and Summers, M.F., *Structural biology of HIV.* J Mol Biol, 1999. **285**(1): p. 1-32.
32. Strebel, K., *HIV accessory proteins versus host restriction factors.* Curr Opin Virol, 2013. **3**(6): p. 692-9.
33. Zhang, J. and Crumpacker, C., *HIV UTR, LTR, and Epigenetic Immunity.* Viruses, 2022. **14**(5).
34. Chamanian, M., Purzycka, K.J., Wille, P.T., . . . Arts, E.J., *A cis-acting element in retroviral genomic RNA links Gag-Pol ribosomal frameshifting to selective viral RNA encapsidation.* Cell Host Microbe, 2013. **13**(2): p. 181-92.
35. Simon, V. and Ho, D.D., *HIV-1 dynamics in vivo: implications for therapy.* Nat Rev Microbiol, 2003. **1**(3): p. 181-90.
36. Hu, W.S. and Hughes, S.H., *HIV-1 reverse transcription.* Cold Spring Harb Perspect Med, 2012. **2**(10).
37. Arhel, N., *Revisiting HIV-1 uncoating.* Retrovirology, 2010. **7**: p. 96.
38. Scoca, V. and Di Nunzio, F., *The HIV-1 Capsid: From Structural Component to Key Factor for Host Nuclear Invasion.* Viruses, 2021. **13**(2).
39. Shen, Q., Wu, C., Freniere, C., . . . Xiong, Y., *Nuclear Import of HIV-1.* Viruses, 2021. **13**(11).
40. Karn, J. and Stoltzfus, C.M., *Transcriptional and posttranscriptional regulation of HIV-1 gene expression.* Cold Spring Harb Perspect Med, 2012. **2**(2): p. a006916.

41. Nguyen Quang, N., Goudey, S., Segeral, E., . . . Gallois-Montbrun, S., *Dynamic nanopore long-read sequencing analysis of HIV-1 splicing events during the early steps of infection.* Retrovirology, 2020. **17**(1): p. 25.
42. Ferguson, M.R., Rojo, D.R., von Lindern, J.J., and O'Brien, W.A., *HIV-1 replication cycle.* Clin Lab Med, 2002. **22**(3): p. 611-35.
43. Mohammadi, P., Desfarges, S., Bartha, I., . . . Ciuffi, A., *24 hours in the life of HIV-1 in a T cell line.* PLoS Pathog, 2013. **9**(1): p. e1003161.
44. Wilen, C.B., Tilton, J.C., and Doms, R.W., *HIV: Cell Binding and Entry.* Cold Spring Harbor Perspectives in Medicine, 2012. **2**(8).
45. Hartley, O., Klasse, P.J., Sattentau, Q.J., and Moore, J.P., *V3: HIV's switch-hitter.* AIDS Res Hum Retroviruses, 2005. **21**(2): p. 171-89.
46. Pastore, C., Ramos, A., and Mosier, D.E., *Intrinsic obstacles to human immunodeficiency virus type 1 coreceptor switching.* J Virol, 2004. **78**(14): p. 7565-74.
47. Lee, B., Sharron, M., Montaner, L.J., . . . Doms, R.W., *Quantification of CD4, CCR5, and CXCR4 levels on lymphocyte subsets, dendritic cells, and differentially conditioned monocyte-derived macrophages.* Proc Natl Acad Sci U S A, 1999. **96**(9): p. 5215-20.
48. Yandrapally, S., Mohareer, K., Arekuti, G., . . . Banerjee, S., *HIV co-receptor-tropism: cellular and molecular events behind the enigmatic co-receptor switching.* Crit Rev Microbiol, 2021. **47**(4): p. 499-516.
49. Iliopoulou, M., Nolan, R., Alvarez, L., . . . Padilla-Parra, S., *A dynamic three-step mechanism drives the HIV-1 pre-fusion reaction.* Nat Struct Mol Biol, 2018. **25**(9): p. 814-822.
50. Pollakis, G. and Paxton, W.A., *Use of (alternative) coreceptors for HIV entry.* Curr Opin HIV AIDS, 2012. **7**(5): p. 440-9.
51. Parrish, N.F., Gao, F., Li, H., . . . Hahn, B.H., *Phenotypic properties of transmitted founder HIV-1.* Proc Natl Acad Sci U S A, 2013. **110**(17): p. 6626-33.
52. Iyer, S.S., Bibollet-Ruche, F., Sherrill-Mix, S., . . . Hahn, B.H., *Resistance to type 1 interferons is a major determinant of HIV-1 transmission fitness.* Proc Natl Acad Sci U S A, 2017. **114**(4): p. E590-E599.
53. Deeks, S.G., Overbaugh, J., Phillips, A., and Buchbinder, S., *HIV infection.* Nat Rev Dis Primers, 2015. **1**: p. 15035.
54. Koppensteiner, H., Brack-Werner, R., and Schindler, M., *Macrophages and their relevance in Human Immunodeficiency Virus Type I infection.* Retrovirology, 2012. **9**: p. 82.
55. Sheppard, H.W., Celum, C., Michael, N.L., . . . Buchbinder, S.P., *HIV-1 infection in individuals with the CCR5-Delta32/Delta32 genotype: acquisition of syncytium-inducing virus at seroconversion.* J Acquir Immune Defic Syndr, 2002. **29**(3): p. 307-13.
56. Margolis, L. and Shattock, R., *Selective transmission of CCR5-utilizing HIV-1: the 'gatekeeper' problem resolved?* Nat Rev Microbiol, 2006. **4**(4): p. 312-7.
57. Lusso, P., Earl, P.L., Sironi, F., . . . Burastero, S.E., *Cryptic nature of a conserved, CD4-inducible V3 loop neutralization epitope in the native envelope glycoprotein oligomer of CCR5-restricted, but not CXCR4-using, primary human immunodeficiency virus type 1 strains.* J Virol, 2005. **79**(11): p. 6957-68.
58. Connor, R.I., Sheridan, K.E., Ceradini, D., . . . Landau, N.R., *Change in coreceptor use correlates with disease progression in HIV-1--infected individuals.* J Exp Med, 1997. **185**(4): p. 621-8.

59. Sarabia, I. and Bosque, A., *HIV-1 Latency and Latency Reversal: Does Subtype Matter?* Viruses-Basel, 2019. **11**(12).
60. Joseph, S.B. and Swanstrom, R., *The evolution of HIV-1 entry phenotypes as a guide to changing target cells.* J Leukoc Biol, 2018. **103**(3): p. 421-431.
61. Connell, B.J., Hermans, L.E., Wensing, A.M.J., . . . Nijhuis, M., *Immune activation correlates with and predicts CXCR4 co-receptor tropism switch in HIV-1 infection.* Sci Rep, 2020. **10**(1): p. 15866.
62. Cicala, C., Arthos, J., Martinelli, E., . . . Fauci, A.S., *R5 and X4 HIV envelopes induce distinct gene expression profiles in primary peripheral blood mononuclear cells.* Proc Natl Acad Sci U S A, 2006. **103**(10): p. 3746-51.
63. Sirois, M., Robitaille, L., Sasik, R., . . . Corbeil, J., *R5 and X4 HIV viruses differentially modulate host gene expression in resting CD4+ T cells.* AIDS Res Hum Retroviruses, 2008. **24**(3): p. 485-93.
64. Jones, K.L., Roche, M., Gantier, M.P., . . . Mak, J., *X4 and R5 HIV-1 have distinct post-entry requirements for uracil DNA glycosylase during infection of primary cells.* J Biol Chem, 2010. **285**(24): p. 18603-14.
65. Saez-Cirion, A., Versmisse, P., Truong, L.X., . . . Pancino, G., *Persistent resistance to HIV-1 infection in CD4 T cells from exposed uninfected Vietnamese individuals is mediated by entry and post-entry blocks.* Retrovirology, 2006. **3**: p. 81.
66. Oswald-Richter, K., Grill, S.M., Leelawong, M., . . . Unutmaz, D., *Identification of a CCR5-expressing T cell subset that is resistant to R5-tropic HIV infection.* PLoS Pathog, 2007. **3**(4): p. e58.
67. Este, J.A. and Telenti, A., *HIV entry inhibitors.* Lancet, 2007. **370**(9581): p. 81-8.
68. Colomer-Lluch, M., Ruiz, A., Moris, A., and Prado, J.G., *Restriction Factors: From Intrinsic Viral Restriction to Shaping Cellular Immunity Against HIV-1.* Front Immunol, 2018. **9**: p. 2876.
69. Harris, R.S., Bishop, K.N., Sheehy, A.M., . . . Malim, M.H., *DNA deamination mediates innate immunity to retroviral infection.* Cell, 2003. **113**(6): p. 803-9.
70. Sheehy, A.M., Gaddis, N.C., and Malim, M.H., *The antiretroviral enzyme APOBEC3G is degraded by the proteasome in response to HIV-1 Vif.* Nat Med, 2003. **9**(11): p. 1404-7.
71. Goldstone, D.C., Ennis-Adeniran, V., Hedden, J.J., . . . Webb, M., *HIV-1 restriction factor SAMHD1 is a deoxynucleoside triphosphate triphosphohydrolase.* Nature, 2011. **480**(7377): p. 379-82.
72. Van Damme, N., Goff, D., Katsura, C., . . . Guatelli, J., *The interferon-induced protein BST-2 restricts HIV-1 release and is downregulated from the cell surface by the viral Vpu protein.* Cell Host Microbe, 2008. **3**(4): p. 245-52.
73. Stremlau, M., Perron, M., Lee, M., . . . Sodroski, J., *Specific recognition and accelerated uncoating of retroviral capsids by the TRIM5alpha restriction factor.* Proc Natl Acad Sci U S A, 2006. **103**(14): p. 5514-9.
74. Lee, W.J., Fu, R.M., Liang, C., and Sloan, R.D., *IFITM proteins inhibit HIV-1 protein synthesis.* Sci Rep, 2018. **8**(1): p. 14551.
75. Usami, Y., Wu, Y., and Gottlinger, H.G., *SERINC3 and SERINC5 restrict HIV-1 infectivity and are counteracted by Nef.* Nature, 2015. **526**(7572): p. 218-23.
76. Kane, M., Yadav, S.S., Bitzegeio, J., . . . Bieniasz, P.D., *MX2 is an interferon-induced inhibitor of HIV-1 infection.* Nature, 2013. **502**(7472): p. 563-6.
77. Zhu, Y., Chen, G., Lv, F., . . . Gao, G., *Zinc-finger antiviral protein inhibits HIV-1 infection by selectively targeting multiply spliced viral mRNAs for degradation.* Proc Natl Acad Sci U S A, 2011. **108**(38): p. 15834-9.

78. Zhang, Y., Lu, J., and Liu, X., *MARCH2 is upregulated in HIV-1 infection and inhibits HIV-1 production through envelope protein translocation or degradation.* Virology, 2018. **518**: p. 293-300.
79. Tada, T., Zhang, Y., Koyama, T., . . . Tokunaga, K., *MARCH8 inhibits HIV-1 infection by reducing virion incorporation of envelope glycoproteins.* Nat Med, 2015. **21**(12): p. 1502-7.
80. Li, M., Kao, E., Gao, X., . . . David, M., *Codon-usage-based inhibition of HIV protein synthesis by human schlafen 11.* Nature, 2012. **491**(7422): p. 125-8.
81. Zhou, T., Frabutt, D.A., Moremen, K.W., and Zheng, Y.H., *ERManI (Endoplasmic Reticulum Class I alpha-Mannosidase) Is Required for HIV-1 Envelope Glycoprotein Degradation via Endoplasmic Reticulum-associated Protein Degradation Pathway.* J Biol Chem, 2015. **290**(36): p. 22184-92.
82. Krapp, C., Hotter, D., Gawanbacht, A., . . . Kirchhoff, F., *Guanylate Binding Protein (GBP) 5 Is an Interferon-Inducible Inhibitor of HIV-1 Infectivity.* Cell Host Microbe, 2016. **19**(4): p. 504-14.
83. Lubow, J., Virgilio, M.C., Merlino, M., . . . Collins, K.L., *Mannose receptor is an HIV restriction factor counteracted by Vpr in macrophages.* Elife, 2020. **9**.
84. Rausell, A., Munoz, M., Martinez, R., . . . Ciuffi, A., *Innate immune defects in HIV permissive cell lines.* Retrovirology, 2016. **13**(1): p. 43.
85. Rato, S., Rausell, A., Munoz, M., . . . Ciuffi, A., *Single-cell analysis identifies cellular markers of the HIV permissive cell.* PLoS Pathog, 2017. **13**(10): p. e1006678.
86. Golumbeanu, M., Cristinelli, S., Rato, S., . . . Ciuffi, A., *Single-Cell RNA-Seq Reveals Transcriptional Heterogeneity in Latent and Reactivated HIV-Infected Cells.* Cell Reports, 2018. **23**(4): p. 942-950.
87. Luckheeram, R.V., Zhou, R., Verma, A.D., and Xia, B., *CD4(+)T cells: differentiation and functions.* Clin Dev Immunol, 2012. **2012**: p. 925135.
88. Farber, D.L., Yudanin, N.A., and Restifo, N.P., *Human memory T cells: generation, compartmentalization and homeostasis.* Nature Reviews Immunology, 2014. **14**(1): p. 24-35.
89. Bhattacharyya, N.D. and Feng, C.G., *Regulation of T Helper Cell Fate by TCR Signal Strength.* Front Immunol, 2020. **11**: p. 624.
90. Pennock, N.D., White, J.T., Cross, E.W., . . . Kedl, R.M., *T cell responses: naive to memory and everything in between.* Adv Physiol Educ, 2013. **37**(4): p. 273-83.
91. Fazilleau, N., McHeyzer-Williams, L.J., Rosen, H., and McHeyzer-Williams, M.G., *The function of follicular helper T cells is regulated by the strength of T cell antigen receptor binding.* Nat Immunol, 2009. **10**(4): p. 375-84.
92. Brogdon, J.L., Leitenberg, D., and Bottomly, K., *The potency of TCR signaling differentially regulates NFATc/p activity and early IL-4 transcription in naive CD4+ T cells.* J Immunol, 2002. **168**(8): p. 3825-32.
93. Reddy, M., Eirikis, E., Davis, C., . . . Prabhakar, U., *Comparative analysis of lymphocyte activation marker expression and cytokine secretion profile in stimulated human peripheral blood mononuclear cell cultures: an in vitro model to monitor cellular immune function.* J Immunol Methods, 2004. **293**(1-2): p. 127-42.
94. Cibrian, D. and Sanchez-Madrid, F., *CD69: from activation marker to metabolic gatekeeper.* Eur J Immunol, 2017. **47**(6): p. 946-953.
95. Ross, S.H. and Cantrell, D.A., *Signaling and Function of Interleukin-2 in T Lymphocytes.* Annu Rev Immunol, 2018. **36**: p. 411-433.

96. Saraiva, D.P., Azeredo-Lopes, S., Antunes, A., . . . Cabral, M.G., *Expression of HLA-DR in Cytotoxic T Lymphocytes: A Validated Predictive Biomarker and a Potential Therapeutic Strategy in Breast Cancer.* Cancers (Basel), 2021. **13**(15).
97. Boussiotis, V.A., *Molecular and Biochemical Aspects of the PD-1 Checkpoint Pathway.* N Engl J Med, 2016. **375**(18): p. 1767-1778.
98. Harjunpaa, H. and Guillerey, C., *TIGIT as an emerging immune checkpoint.* Clin Exp Immunol, 2020. **200**(2): p. 108-119.
99. Acharya, N., Sabatos-Peyton, C., and Anderson, A.C., *Tim-3 finds its place in the cancer immunotherapy landscape.* J Immunother Cancer, 2020. **8**(1).
100. Jiang, Q., Yang, G.C., Xiao, F., . . . Cui, D.W., *Role of Th22 Cells in the Pathogenesis of Autoimmune Diseases.* Frontiers in Immunology, 2021. **12**.
101. Takeuchi, A. and Saito, T., *CD4 CTL, a Cytotoxic Subset of CD4(+) T Cells, Their Differentiation and Function.* Front Immunol, 2017. **8**: p. 194.
102. Wong, M.T., Ong, D.E., Lim, F.S., . . . Newell, E.W., *A High-Dimensional Atlas of Human T Cell Diversity Reveals Tissue-Specific Trafficking and Cytokine Signatures.* Immunity, 2016. **45**(2): p. 442-56.
103. Gattinoni, L., Speiser, D.E., Lichterfeld, M., and Bonini, C., *T memory stem cells in health and disease.* Nat Med, 2017. **23**(1): p. 18-27.
104. Ruterbusch, M., Pruner, K.B., Shehata, L., and Pepper, M., *In Vivo CD4(+) T Cell Differentiation and Function: Revisiting the Th1/Th2 Paradigm.* Annu Rev Immunol, 2020. **38**: p. 705-725.
105. Ando, M., Ito, M., Srirat, T., . . . Yoshimura, A., *Memory T cell, exhaustion, and tumor immunity.* Immunol Med, 2020. **43**(1): p. 1-9.
106. Fenwick, C., Joo, V., Jacquier, P., . . . Pantaleo, G., *T-cell exhaustion in HIV infection.* Immunol Rev, 2019. **292**(1): p. 149-163.
107. Cavrois, M., Banerjee, T., Mukherjee, G., . . . Roan, N.R., *Mass Cytometric Analysis of HIV Entry, Replication, and Remodeling in Tissue CD4+ T Cells.* Cell Rep, 2017. **20**(4): p. 984-998.
108. Fromentin, R., DaFonseca, S., Costiniuk, C.T., . . . Chomont, N., *PD-1 blockade potentiates HIV latency reversal ex vivo in CD4(+) T cells from ART-suppressed individuals.* Nat Commun, 2019. **10**(1): p. 814.
109. Hurst, J., Hoffmann, M., Pace, M., . . . Frater, J., *Immunological biomarkers predict HIV-1 viral rebound after treatment interruption.* Nat Commun, 2015. **6**: p. 8495.
110. Fromentin, R., Bakeman, W., Lawani, M.B., . . . Chomont, N., *CD4+ T Cells Expressing PD-1, TIGIT and LAG-3 Contribute to HIV Persistence during ART.* PLoS Pathog, 2016. **12**(7): p. e1005761.
111. Boyer, Z. and Palmer, S., *Targeting Immune Checkpoint Molecules to Eliminate Latent HIV.* Front Immunol, 2018. **9**: p. 2339.
112. McGary, C.S., Deleage, C., Harper, J., . . . Paiardini, M., *CTLA-4(+)PD-1(-) Memory CD4(+) T Cells Critically Contribute to Viral Persistence in Antiretroviral Therapy-Suppressed, SIV-Infected Rhesus Macaques.* Immunity, 2017. **47**(4): p. 776-788 e5.
113. Brandt, L., Cristinelli, S., and Ciuffi, A., *Single-Cell Analysis Reveals Heterogeneity of Virus Infection, Pathogenicity, and Host Responses: HIV as a Pioneering Example.* Annu Rev Virol, 2020. **7**(1): p. 333-350.
114. Klein, S.L. and Flanagan, K.L., *Sex differences in immune responses.* Nat Rev Immunol, 2016. **16**(10): p. 626-38.
115. Wilkinson, N.M., Chen, H.C., Lechner, M.G., and Su, M.A., *Sex Differences in Immunity.* Annu Rev Immunol, 2022. **40**: p. 75-94.

116. Jacobsen, H. and Klein, S.L., *Sex Differences in Immunity to Viral Infections.* Front Immunol, 2021. **12**: p. 720952.
117. Jacobson, D.L., Gange, S.J., Rose, N.R., and Graham, N.M., *Epidemiology and estimated population burden of selected autoimmune diseases in the United States.* Clin Immunol Immunopathol, 1997. **84**(3): p. 223-43.
118. Cook, M.B., Dawsey, S.M., Freedman, N.D., . . . McGlynn, K.A., *Sex disparities in cancer incidence by period and age.* Cancer Epidemiol Biomarkers Prev, 2009. **18**(4): p. 1174-82.
119. Giefing-Kroll, C., Berger, P., Lepperdinger, G., and Grubeck-Loebenstein, B., *How sex and age affect immune responses, susceptibility to infections, and response to vaccination.* Aging Cell, 2015. **14**(3): p. 309-21.
120. Arruvito, L., Giulianelli, S., Flores, A.C., . . . Fainboim, L., *NK cells expressing a progesterone receptor are susceptible to progesterone-induced apoptosis.* J Immunol, 2008. **180**(8): p. 5746-53.
121. Dunn, S.E., Ousman, S.S., Sobel, R.A., . . . Steinman, L., *Peroxisome proliferator-activated receptor (PPAR)alpha expression in T cells mediates gender differences in development of T cell-mediated autoimmunity.* J Exp Med, 2007. **204**(2): p. 321-30.
122. Casimir, G.J., Heldenbergh, F., Hanssens, L., . . . Duchateau, J., *Gender differences and inflammation: an in vitro model of blood cells stimulation in prepubescent children.* J Inflamm (Lond), 2010. **7**: p. 28.
123. Carrel, L. and Willard, H.F., *X-inactivation profile reveals extensive variability in X-linked gene expression in females.* Nature, 2005. **434**(7031): p. 400-4.
124. Lee, B.W., Yap, H.K., Chew, F.T., . . . Seah, C.C., *Age- and sex-related changes in lymphocyte subpopulations of healthy Asian subjects: from birth to adulthood.* Cytometry, 1996. **26**(1): p. 8-15.
125. Lisse, I.M., Aaby, P., Whittle, H., . . . Christensen, L.B., *T-lymphocyte subsets in West African children: impact of age, sex, and season.* J Pediatr, 1997. **130**(1): p. 77-85.
126. Uppal, S.S., Verma, S., and Dhot, P.S., *Normal values of CD4 and CD8 lymphocyte subsets in healthy indian adults and the effects of sex, age, ethnicity, and smoking.* Cytometry B Clin Cytom, 2003. **52**(1): p. 32-6.
127. Abdullah, M., Chai, P.S., Chong, M.Y., . . . Vidyadaran, S., *Gender effect on in vitro lymphocyte subset levels of healthy individuals.* Cell Immunol, 2012. **272**(2): p. 214-9.
128. Huang, Z., Chen, B., Liu, X., . . . Su, W., *Effects of sex and aging on the immune cell landscape as assessed by single-cell transcriptomic analysis.* Proc Natl Acad Sci U S A, 2021. **118**(33).
129. Taneja, V., *Sex Hormones Determine Immune Response.* Front Immunol, 2018. **9**: p. 1931.
130. Zhang, H., Weyand, C.M., and Goronzy, J.J., *Hallmarks of the aging T-cell system.* FEBS J, 2021. **288**(24): p. 7123-7142.
131. Ligotti, M.E., Aiello, A., Accardi, G., . . . Candore, G., *Analysis of T and NK cell subsets in the Sicilian population from young to supercentenarian: The role of age and gender.* Clin Exp Immunol, 2021. **205**(2): p. 198-212.
132. Nikolich-Zugich, J., *The twilight of immunity: emerging concepts in aging of the immune system.* Nat Immunol, 2018. **19**(1): p. 10-19.
133. Clave, E., Araujo, I.L., Alanio, C., . . . Milieu Interieur, C., *Human thymopoiesis is influenced by a common genetic variant within the TCRA-TCRD locus.* Sci Transl Med, 2018. **10**(457).

134. Li, G., Yu, M., Lee, W.W., . . . Goronzy, J.J., *Decline in miR-181a expression with age impairs T cell receptor sensitivity by increasing DUSP6 activity.* Nat Med, 2012. **18**(10): p. 1518-24.
135. Kim, C., Hu, B., Jadhav, R.R., . . . Goronzy, J.J., *Activation of miR-21-Regulated Pathways in Immune Aging Selects against Signatures Characteristic of Memory T Cells.* Cell Rep, 2018. **25**(8): p. 2148-2162 e5.
136. Zhang, H., Jadhav, R.R., Cao, W., . . . Goronzy, J.J., *Aging-associated HELIOS deficiency in naive CD4(+) T cells alters chromatin remodeling and promotes effector cell responses.* Nat Immunol, 2023. **24**(1): p. 96-109.
137. Marquez, E.J., Chung, C.H., Marches, R., . . . Ucar, D., *Sexual-dimorphism in human immune system aging.* Nat Commun, 2020. **11**(1): p. 751.
138. Hu, B., Jadhav, R.R., Gustafson, C.E., . . . Goronzy, J.J., *Distinct Age-Related Epigenetic Signatures in CD4 and CD8 T Cells.* Front Immunol, 2020. **11**: p. 585168.
139. Botafogo, V., Perez-Andres, M., Jara-Acevedo, M., . . . Orfao, A., *Age Distribution of Multiple Functionally Relevant Subsets of CD4+ T Cells in Human Blood Using a Standardized and Validated 14-Color EuroFlow Immune Monitoring Tube.* Front Immunol, 2020. **11**: p. 166.
140. Patel, P., Borkowf, C.B., Brooks, J.T., . . . Mermin, J., *Estimating per-act HIV transmission risk: a systematic review.* AIDS, 2014. **28**(10): p. 1509-19.
141. Scully, E.P., *Sex Differences in HIV Infection.* Curr HIV/AIDS Rep, 2018. **15**(2): p. 136-146.
142. Byrne, E.H., Anahtar, M.N., Cohen, K.E., . . . Kwon, D.S., *Association between injectable progestin-only contraceptives and HIV acquisition and HIV target cell frequency in the female genital tract in South African women: a prospective cohort study.* Lancet Infect Dis, 2016. **16**(4): p. 441-8.
143. Sterling, T.R., Vlahov, D., Astemborski, J., . . . Quinn, T.C., *Initial plasma HIV-1 RNA levels and progression to AIDS in women and men.* N Engl J Med, 2001. **344**(10): p. 720-5.
144. Farzadegan, H., Hoover, D.R., Astemborski, J., . . . Vlahov, D., *Sex differences in HIV-1 viral load and progression to AIDS.* Lancet, 1998. **352**(9139): p. 1510-4.
145. Parsa, N., Zaheri, P.M., Hewitt, R.G., . . . Wallin, L., *The rapid CD4 + T-lymphocyte decline and human immunodeficiency virus progression in females compared to males.* Sci Rep, 2020. **10**(1): p. 16816.
146. Scully, E.P., Gandhi, M., Johnston, R., . . . Deeks, S.G., *Sex-Based Differences in Human Immunodeficiency Virus Type 1 Reservoir Activity and Residual Immune Activation.* J Infect Dis, 2019. **219**(7): p. 1084-1094.
147. Meier, A., Chang, J.J., Chan, E.S., . . . Altfeld, M., *Sex differences in the Toll-like receptor-mediated response of plasmacytoid dendritic cells to HIV-1.* Nat Med, 2009. **15**(8): p. 955-9.
148. Chang, J.J., Woods, M., Lindsay, R.J., . . . Altfeld, M., *Higher expression of several interferon-stimulated genes in HIV-1-infected females after adjusting for the level of viral replication.* J Infect Dis, 2013. **208**(5): p. 830-8.
149. Szaniawski, M.A., Spivak, A.M., Bosque, A., and Planelles, V., *Sex Influences SAMHD1 Activity and Susceptibility to Human Immunodeficiency Virus-1 in Primary Human Macrophages.* J Infect Dis, 2019. **219**(5): p. 777-785.
150. Das, B., Dobrowolski, C., Luttge, B., . . . Karn, J., *Estrogen receptor-1 is a key regulator of HIV-1 latency that imparts gender-specific restrictions on the latent reservoir.* Proc Natl Acad Sci U S A, 2018. **115**(33): p. E7795-E7804.

151. Gianella, S., Rawlings, S.A., Nakazawa, M., . . . Karn, J., *Sex differences in HIV Persistence and Reservoir Size during Aging.* Clin Infect Dis, 2021.
152. Ruel, T.D., Zanoni, B.C., Ssewanyana, I., . . . Feeney, M.E., *Sex differences in HIV RNA level and CD4 cell percentage during childhood.* Clin Infect Dis, 2011. **53**(6): p. 592-9.
153. Sorci, G. and Faivre, B., *Age-dependent virulence of human pathogens.* PLoS Pathog, 2022. **18**(9): p. e1010866.
154. Gabuzda, D., Jamieson, B.D., Collman, R.G., . . . Hunt, P.W., *Pathogenesis of Aging and Age-related Comorbidities in People with HIV: Highlights from the HIV ACTION Workshop.* Pathog Immun, 2020. **5**(1): p. 143-174.
155. Wen, L., Li, G., Huang, T., . . . Chen, Z.J., *Single-cell technologies: From research to application.* Innovation (Camb), 2022. **3**(6): p. 100342.
156. Tang, F., Barbacioru, C., Wang, Y., . . . Surani, M.A., *mRNA-Seq whole-transcriptome analysis of a single cell.* Nat Methods, 2009. **6**(5): p. 377-82.
157. Islam, S., Kjallquist, U., Moliner, A., . . . Linnarsson, S., *Characterization of the single-cell transcriptional landscape by highly multiplex RNA-seq.* Genome Res, 2011. **21**(7): p. 1160-7.
158. Jaitin, D.A., Kenigsberg, E., Keren-Shaul, H., . . . Amit, I., *Massively parallel single-cell RNA-seq for marker-free decomposition of tissues into cell types.* Science, 2014. **343**(6172): p. 776-9.
159. Macosko, E.Z., Basu, A., Satija, R., . . . McCarroll, S.A., *Highly Parallel Genome-wide Expression Profiling of Individual Cells Using Nanoliter Droplets.* Cell, 2015. **161**(5): p. 1202-1214.
160. Ramskold, D., Luo, S., Wang, Y.C., . . . Sandberg, R., *Full-length mRNA-Seq from single-cell levels of RNA and individual circulating tumor cells.* Nat Biotechnol, 2012. **30**(8): p. 777-82.
161. Picelli, S., Faridani, O.R., Bjorklund, A.K., . . . Sandberg, R., *Full-length RNA-seq from single cells using Smart-seq2.* Nat Protoc, 2014. **9**(1): p. 171-81.
162. Wang, X., He, Y., Zhang, Q., . . . Zhang, Z., *Direct Comparative Analyses of 10X Genomics Chromium and Smart-seq2.* Genomics Proteomics Bioinformatics, 2021. **19**(2): p. 253-266.
163. Jovic, D., Liang, X., Zeng, H., . . . Luo, Y., *Single-cell RNA sequencing technologies and applications: A brief overview.* Clin Transl Med, 2022. **12**(3): p. e694.
164. Flynn, E., Almonte-Loya, A., and Fragiadakis, G.K., *Single-Cell Multiomics.* Annu Rev Biomed Data Sci, 2023.
165. Macaulay, I.C., Haerty, W., Kumar, P., . . . Voet, T., *G&T-seq: parallel sequencing of single-cell genomes and transcriptomes.* Nat Methods, 2015. **12**(6): p. 519-22.
166. Dey, S.S., Kester, L., Spanjaard, B., . . . van Oudenaarden, A., *Integrated genome and transcriptome sequencing of the same cell.* Nat Biotechnol, 2015. **33**(3): p. 285-289.
167. Buenrostro, J.D., Wu, B., Litzenburger, U.M., . . . Greenleaf, W.J., *Single-cell chromatin accessibility reveals principles of regulatory variation.* Nature, 2015. **523**(7561): p. 486-90.
168. Bartosovic, M., Kabbe, M., and Castelo-Branco, G., *Single-cell CUT&Tag profiles histone modifications and transcription factors in complex tissues.* Nat Biotechnol, 2021. **39**(7): p. 825-835.
169. Smallwood, S.A., Lee, H.J., Angermueller, C., . . . Kelsey, G., *Single-cell genome-wide bisulfite sequencing for assessing epigenetic heterogeneity.* Nat Methods, 2014. **11**(8): p. 817-820.

170. Ma, S., Zhang, B., LaFave, L.M., . . . Buenrostro, J.D., *Chromatin Potential Identified by Shared Single-Cell Profiling of RNA and Chromatin.* Cell, 2020. **183**(4): p. 1103-1116 e20.
171. Bendall, S.C., Simonds, E.F., Qiu, P., . . . Nolan, G.P., *Single-cell mass cytometry of differential immune and drug responses across a human hematopoietic continuum.* Science, 2011. **332**(6030): p. 687-96.
172. Stoeckius, M., Hafemeister, C., Stephenson, W., . . . Smibert, P., *Simultaneous epitope and transcriptome measurement in single cells.* Nat Methods, 2017. **14**(9): p. 865-868.
173. Wang, X.M., Zhang, J.Y., Xing, X., . . . Wang, F.S., *Global transcriptomic characterization of T cells in individuals with chronic HIV-1 infection.* Cell Discov, 2022. **8**(1): p. 29.
174. Collora, J.A., Liu, R., Pinto-Santini, D., . . . Ho, Y.C., *Single-cell multiomics reveals persistence of HIV-1 in expanded cytotoxic T cell clones.* Immunity, 2022. **55**(6): p. 1013-1031 e7.
175. Freeman, T.L., Zhao, C., Schrode, N., . . . Swartz, T.H., *HIV-1 activates oxidative phosphorylation in infected CD4 T cells in a human tonsil explant model.* Front Immunol, 2023. **14**: p. 1172938.
176. Dufour, C., Richard, C., Pardons, M., . . . Chomont, N., *Phenotypic characterization of single CD4+ T cells harboring genetically intact and inducible HIV genomes.* Nat Commun, 2023. **14**(1): p. 1115.
177. Sun, W., Gao, C., Hartana, C.A., . . . Lichterfeld, M., *Phenotypic signatures of immune selection in HIV-1 reservoir cells.* Nature, 2023. **614**(7947): p. 309-317.
178. Weymar, G.H.J., Bar-On, Y., Oliveira, T.Y., . . . Nussenzweig, M.C., *Distinct gene expression by expanded clones of quiescent memory CD4(+) T cells harboring intact latent HIV-1 proviruses.* Cell Rep, 2022. **40**(10): p. 111311.
179. Pardons, M., Baxter, A.E., Massanella, M., . . . Chomont, N., *Single-cell characterization and quantification of translation-competent viral reservoirs in treated and untreated HIV infection.* PLoS Pathog, 2019. **15**(2): p. e1007619.
180. Cole, B., Lambrechts, L., Gantner, P., . . . Vandekerckhove, L., *In-depth single-cell analysis of translation-competent HIV-1 reservoirs identifies cellular sources of plasma viremia.* Nat Commun, 2021. **12**(1): p. 3727.
181. Gantner, P., Pagliuzza, A., Pardons, M., . . . Chomont, N., *Single-cell TCR sequencing reveals phenotypically diverse clonally expanded cells harboring inducible HIV proviruses during ART.* Nat Commun, 2020. **11**(1): p. 4089.
182. Grau-Exposito, J., Serra-Peinado, C., Miguel, L., . . . Buzon, M.J., *A Novel Single-Cell FISH-Flow Assay Identifies Effector Memory CD4(+) T cells as a Major Niche for HIV-1 Transcription in HIV-Infected Patients.* mBio, 2017. **8**(4).
183. Cortes-Llanos, B., Jain, V., Volkheimer, A., . . . Allbritton, N.L., *Automated microarray for single-cell sorting and collection of lymphocytes following HIV reactivation.* bioRxiv, 2023.
184. Sannier, G., Dube, M., Dufour, C., . . . Kaufmann, D.E., *Combined single-cell transcriptional, translational, and genomic profiling reveals HIV-1 reservoir diversity.* Cell Rep, 2021. **36**(9): p. 109643.
185. Yucha, R.W., Hobbs, K.S., Hanhauser, E., . . . Henrich, T.J., *High-throughput Characterization of HIV-1 Reservoir Reactivation Using a Single-Cell-in-Droplet PCR Assay.* EBioMedicine, 2017. **20**: p. 217-229.

186. Ramirez, N.P., Lee, J., Zheng, Y., . . . D'Orso, I., *ADAP1 promotes latent HIV-1 reactivation by selectively tuning KRAS-ERK-AP-1 T cell signaling-transcriptional axis.* Nat Commun, 2022. **13**(1): p. 1109.
187. de Armas, L.R., Gavegnano, C., Pallikkuth, S., . . . Pahwa, S., *The Effect of JAK1/2 Inhibitors on HIV Reservoir Using Primary Lymphoid Cell Model of HIV Latency.* Front Immunol, 2021. **12**: p. 720697.
188. Bradley, T., Ferrari, G., Haynes, B.F., . . . Browne, E.P., *Single-Cell Analysis of Quiescent HIV Infection Reveals Host Transcriptional Profiles that Regulate Proviral Latency.* Cell Rep, 2018. **25**(1): p. 107-117 e3.
189. Otte, F., Zhang, Y., Spagnuolo, J., . . . Swiss, H.I.V.C.S., *Revealing viral and cellular dynamics of HIV-1 at the single-cell level during early treatment periods.* Cell Rep Methods, 2023. **3**(6): p. 100485.
190. Collora, J.A. and Ho, Y.C., *Integration site-dependent HIV-1 promoter activity shapes host chromatin conformation.* Genome Res, 2023.
191. Gantner, P., Buranapraditkun, S., Pagliuzza, A., . . . Chomont, N., *HIV rapidly targets a diverse pool of CD4(+) T cells to establish productive and latent infections.* Immunity, 2023. **56**(3): p. 653-668 e5.
192. Ma, T., McGregor, M., Giron, L., . . . Roan, N.R., *Single-cell glycomics analysis by CyTOF-Lec reveals glycan features defining cells differentially susceptible to HIV.* Elife, 2022. **11**.
193. Luo, X., Frouard, J., Zhang, G., . . . Greene, W.C., *Subsets of Tissue CD4 T Cells Display Different Susceptibilities to HIV Infection and Death: Analysis by CyTOF and Single Cell RNA-seq.* Front Immunol, 2022. **13**: p. 883420.
194. Dahabieh, M.S., Battivelli, E., and Verdin, E., *Understanding HIV latency: the road to an HIV cure.* Annu Rev Med, 2015. **66**: p. 407-21.
195. Ho, D.D., Neumann, A.U., Perelson, A.S., . . . Markowitz, M., *Rapid turnover of plasma virions and CD4 lymphocytes in HIV-1 infection.* Nature, 1995. **373**(6510): p. 123-6.
196. Finzi, D., Hermankova, M., Pierson, T., . . . Siliciano, R.F., *Identification of a reservoir for HIV-1 in patients on highly active antiretroviral therapy.* Science, 1997. **278**(5341): p. 1295-300.
197. Chomont, N., El-Far, M., Ancuta, P., . . . Sekaly, R.P., *HIV reservoir size and persistence are driven by T cell survival and homeostatic proliferation.* Nat Med, 2009. **15**(8): p. 893-900.
198. Fromentin, R. and Chomont, N., *HIV persistence in subsets of CD4+ T cells: 50 shades of reservoirs.* Semin Immunol, 2021. **51**: p. 101438.
199. Buzon, M.J., Sun, H., Li, C., . . . Lichterfeld, M., *HIV-1 persistence in CD4+ T cells with stem cell-like properties.* Nat Med, 2014. **20**(2): p. 139-42.
200. Wong, M.E., Jaworowski, A., and Hearps, A.C., *The HIV Reservoir in Monocytes and Macrophages.* Front Immunol, 2019. **10**: p. 1435.
201. Kandathil, A.J., Sugawara, S., and Balagopal, A., *Are T cells the only HIV-1 reservoir?* Retrovirology, 2016. **13**(1): p. 86.
202. Banga, R., Procopio, F.A., Noto, A., . . . Perreau, M., *PD-1(+) and follicular helper T cells are responsible for persistent HIV-1 transcription in treated aviremic individuals.* Nat Med, 2016. **22**(7): p. 754-61.
203. Chun, T.W., Nickle, D.C., Justement, J.S., . . . Fauci, A.S., *Persistence of HIV in gut-associated lymphoid tissue despite long-term antiretroviral therapy.* J Infect Dis, 2008. **197**(5): p. 714-20.

204. Dufour, C., Gantner, P., Fromentin, R., and Chomont, N., *The multifaceted nature of HIV latency.* J Clin Invest, 2020. **130**(7): p. 3381-3390.
205. Perreau, M., Savoye, A.L., De Crignis, E., . . . Pantaleo, G., *Follicular helper T cells serve as the major CD4 T cell compartment for HIV-1 infection, replication, and production.* J Exp Med, 2013. **210**(1): p. 143-56.
206. Fukazawa, Y., Lum, R., Okoye, A.A., . . . Picker, L.J., *B cell follicle sanctuary permits persistent productive simian immunodeficiency virus infection in elite controllers.* Nat Med, 2015. **21**(2): p. 132-9.
207. Ho, Y.C., Shan, L., Hosmane, N.N., . . . Siliciano, R.F., *Replication-competent noninduced proviruses in the latent reservoir increase barrier to HIV-1 cure.* Cell, 2013. **155**(3): p. 540-51.
208. Lee, G.Q., Orlova-Fink, N., Einkauf, K., . . . Lichterfeld, M., *Clonal expansion of genome-intact HIV-1 in functionally polarized Th1 CD4+ T cells.* J Clin Invest, 2017. **127**(7): p. 2689-2696.
209. Lassen, K.G., Bailey, J.R., and Siliciano, R.F., *Analysis of human immunodeficiency virus type 1 transcriptional elongation in resting CD4+ T cells in vivo.* J Virol, 2004. **78**(17): p. 9105-14.
210. Elsheikh, M.M., Tang, Y., Li, D., and Jiang, G., *Deep latency: A new insight into a functional HIV cure.* EBioMedicine, 2019. **45**: p. 624-629.
211. Cohn, L.B., Chomont, N., and Deeks, S.G., *The Biology of the HIV-1 Latent Reservoir and Implications for Cure Strategies.* Cell Host Microbe, 2020. **27**(4): p. 519-530.
212. Ciuffi, A., Llano, M., Poeschla, E., . . . Bushman, F., *A role for LEDGF/p75 in targeting HIV DNA integration.* Nat Med, 2005. **11**(12): p. 1287-9.
213. Singh, P.K., Bedwell, G.J., and Engelman, A.N., *Spatial and Genomic Correlates of HIV-1 Integration Site Targeting.* Cells, 2022. **11**(4).
214. Einkauf, K.B., Lee, G.Q., Gao, C., . . . Lichterfeld, M., *Intact HIV-1 proviruses accumulate at distinct chromosomal positions during prolonged antiretroviral therapy.* J Clin Invest, 2019. **129**(3): p. 988-998.
215. Han, Y., Lin, Y.B., An, W., . . . Siliciano, R.F., *Orientation-dependent regulation of integrated HIV-1 expression by host gene transcriptional readthrough.* Cell Host Microbe, 2008. **4**(2): p. 134-46.
216. Chen, B.K., Feinberg, M.B., and Baltimore, D., *The kappaB sites in the human immunodeficiency virus type 1 long terminal repeat enhance virus replication yet are not absolutely required for viral growth.* J Virol, 1997. **71**(7): p. 5495-504.
217. Barboric, M., Nissen, R.M., Kanazawa, S., . . . Peterlin, B.M., *NF-kappaB binds P-TEFb to stimulate transcriptional elongation by RNA polymerase II.* Mol Cell, 2001. **8**(2): p. 327-37.
218. Yukl, S.A., Kaiser, P., Kim, P., . . . Wong, J.K., *HIV latency in isolated patient CD4(+) T cells may be due to blocks in HIV transcriptional elongation, completion, and splicing.* Sci Transl Med, 2018. **10**(430).
219. Lassen, K.G., Ramyar, K.X., Bailey, J.R., . . . Siliciano, R.F., *Nuclear retention of multiply spliced HIV-1 RNA in resting CD4+ T cells.* PLoS Pathog, 2006. **2**(7): p. e68.
220. Chiang, K., Liu, H., and Rice, A.P., *miR-132 enhances HIV-1 replication.* Virology, 2013. **438**(1): p. 1-4.
221. Huang, J., Wang, F., Argyris, E., . . . Zhang, H., *Cellular microRNAs contribute to HIV-1 latency in resting primary CD4+ T lymphocytes.* Nat Med, 2007. **13**(10): p. 1241-7.

222. Ahluwalia, J.K., Khan, S.Z., Soni, K., . . . Brahmachari, S.K., *Human cellular microRNA hsa-miR-29a interferes with viral nef protein expression and HIV-1 replication.* Retrovirology, 2008. **5**: p. 117.
223. Prins, J.M., Jurriaans, S., van Praag, R.M., . . . Lange, J.M., *Immuno-activation with anti-CD3 and recombinant human IL-2 in HIV-1-infected patients on potent antiretroviral therapy.* AIDS, 1999. **13**(17): p. 2405-10.
224. Sadowski, I. and Hashemi, F.B., *Strategies to eradicate HIV from infected patients: elimination of latent provirus reservoirs.* Cell Mol Life Sci, 2019. **76**(18): p. 3583-3600.
225. Ait-Ammar, A., Kula, A., Darcis, G., . . . Van Lint, C., *Current Status of Latency Reversing Agents Facing the Heterogeneity of HIV-1 Cellular and Tissue Reservoirs.* Front Microbiol, 2019. **10**: p. 3060.
226. Grau-Exposito, J., Luque-Ballesteros, L., Navarro, J., . . . Buzon, M.J., *Latency reversal agents affect differently the latent reservoir present in distinct CD4+ T subpopulations.* PLoS Pathog, 2019. **15**(8): p. e1007991.
227. Vansant, G., Bruggemans, A., Janssens, J., and Debyser, Z., *Block-And-Lock Strategies to Cure HIV Infection.* Viruses, 2020. **12**(1).
228. Murray, A.J., Kwon, K.J., Farber, D.L., and Siliciano, R.F., *The Latent Reservoir for HIV-1: How Immunologic Memory and Clonal Expansion Contribute to HIV-1 Persistence.* J Immunol, 2016. **197**(2): p. 407-17.
229. Chappell, D.L., Sandhu, P.K., Wong, J.P., . . . Damania, B., KSHV Viral Protein Kinase Interacts with USP9X to Modulate the Viral Lifecycle. J Virol, 2023. **97**(3): p. e0176322.
230. Jurczyszak, D., Manganaro, L., Buta, S., . . . Simon, V., ISG15 deficiency restricts HIV-1 infection. PLoS Pathog, 2022. **18**(3): p. e1010405.
231. Ding, J., Wang, S., Wang, Z., . . . Cen, S., Schlafen 5 suppresses human immunodeficiency virus type 1 transcription by commandeering cellular epigenetic machinery. Nucleic Acids Res, 2022. **50**(11): p. 6137-6153.